FLEXIBLE FORMWORK:

A TEXTILE-CENTRIC APPROACH

LUCY FLIEGER

TUDelft

Flexible Formwork: A Textile-Centric Approach

Investigating pattern influence on the deformation behavior of weft-knitted textile formworks under hydrostatic loading

Lucy Flieger
Master Thesis Research
5680387

MSc in Architecture, Urbanism, and Building Sciences
Building Technology Track

Mentors
Dr. Stijn Brancart
Dr. Mariana Popescu

Delft University of Technology
Faculty of Architecture and the Built Environment

20 June 2024

TUDelft

Abstract

Traditional methods of building with concrete are materially wasteful, highly polluting, and often structurally inefficient. The vast global consumption of concrete plays a large role in the construction industry's negative effects on the environment, necessitating a significant change in the way we design and build with concrete. The fluid properties of concrete combined with the flexibility of knit textile formwork makes it possible to shape concrete into complex, innovative structures that drastically reduce material consumption and waste. KnitCrete, which employs CNC-knitted textiles as flexible formwork for casting with concrete, has demonstrated the extraordinary potential of this technology to efficiently fabricate complex geometries without the need for costly, time-consuming rigid molds.

The objective of this research is to develop a pattern-specific knowledge base to support the future design of innovative architectural forms and structures using CNC-knit textile formwork. Through three main parts, the research approach investigates the implications of pattern selection on the behavior of the resulting concrete forms. The study employs a combination of information-based and inspiration-based design research methodologies. In the first phase, a comprehensive pattern repository is developed which catalogues relevant information for 21 different knit patterns. In the second phase, rigorous testing of each pattern under hydrostatic loading is performed and a deformation analysis is performed. The third phase involves an exploration of pattern combinations, informed by the information gathered in phases one and two, which demonstrates the potential of this technology to create complex or double curved geometries.

Key findings reveal that pattern selection significantly influences the structural and aesthetic properties of the resulting concrete forms. The comparison between warp and weft properties highlights distinct behaviors under hydrostatic loading with significant implications for flexible formwork design. Challenges in the precise calibration of combined patterns and controlling deformation during casting underscore the complexity of implementing CNC-knit formwork. Contributions to this field include advancements in understanding knit textile behavior, a replicable research approach, and interdisciplinary connections between textile engineering, material studies, and architectural design. In summary, this research lays a robust groundwork for future research and design in the field of CNC-knit textile formwork with a specific focus on knit pattern behavior.

Acknowledgments

Content

1.0 Introduction

1.1 Context

Flexible formwork is an innovative building technology that uses structural membranes as the main facing material for concrete molds (Veenendaal et al., 2011). In contrast to traditional rigid formwork, which involves high material volume and waste, flexible formwork is a light, efficient, and cost-effective solution for fabricating concrete forms. The use of this technology opens up new structural, architectural, and manufacturing possibilities through physically simple means (Hawkins et al., 2016). Various iterations of flexible formwork have been used in architecture and infrastructure since antiquity. However, interest in this technology has expanded in recent years due to increased pressure to make building construction more sustainable. Specifically, the use of CNC-knit textiles as flexible formwork membranes has gained traction as various researchers have demonstrated the potential of CNC-knit textile formwork to create complex concrete forms efficiently and with little waste. In combination with considerable material savings, CNC-knit flexible formwork presents opportunities for structural and architectural design innovation as well as cost reduction and time savings.

1.2 Problem Statement and Research Questions

Traditional methods of building with concrete are wasteful, polluting, and often structurally inefficient. Despite the amorphous properties of concrete, we force it into rigid formworks that in turn produce heavy, orthogonal elements. Alternatively, flexible formwork makes it possible to shape concrete into complex forms that exploit its structural capacities and align more closely with the natural force flows in the material. Although significant research has been conducted into the potential role of CNC-knit textiles as flexible formwork, more effort is required to understand how different knit patterns affect the physical behavior of a textile membrane under hydrostatic loading from wet concrete. This aspect of the research will support a more precise and informed design process for creating building elements from CNC-knit flexible formwork. Further, the reusability of CNC-knit formwork membranes has not been examined in great detail. Understanding the impact of the knit pattern on a textile formwork's reusability is essential to developing this technology's potential as a low-waste and low-material construction practice.

The main research questions include:

1. (General) How can the use of CNC-knit textiles as flexible formwork improve the way we build with concrete for architectural applications and shift the construction industry towards lighter and more sustainable structures?

2. (Specific) How do different knit patterns influence the physical behavior of a CNC-knit textile mold and therefore the formal properties of the hardened concrete element?

3. What is the impact of the knit pattern on the potential reuse of a CNC-knit textile formwork?

4. What is the potential of pattern combinations to facilitate the intentional design of innovative building / architectural components?

1.3 Thesis Methodology

The primary aim of this research is to develop a pattern-specific knowledge base that documents the physical behavior of knitted textiles under concrete loading. This data can support a more informed and precise design process for creating new and innovative flexibly formed architectural elements or structures. To address the research questions, this study combines information-based and inspiration-based design research, the former of which is built on the results of investigation, analysis and planning, while the latter is built on experimentation, ambiguity, and surprise (Sanders, 2005). Phases 1 and 2 represent the more technical aspect of the research where knit patterns are developed and tested for deformation using physical prototyping. This approach contributes to the development of a specific knowledge base that is relevant to the design of flexibly formed elements. A more theoretical, exploratory approach is taken in Phase 3 which uses data collected in Phases 1 and 2 to combine patterns in various forms. This phase represents inspiration-based design research because there is no particular objective of the forms produced other than to demonstrate what is possible. The three phases form a research for design approach, where relevant scientific and technological information is gathered and applied to prototypes to facilitate or inform future designs (Stappers & Giaccardi, 2014).

Literature Review

The literature review presents flexible formwork technology in terms of what types of building elements can be formed using this method. This includes both knitted and non-knitted textiles and foregrounds CNC knitting technology and delves into certain aspects such as pattern creation, stitch types, and current advancements. The analysis makes connections between mold typologies and the resulting forms and identifies certain trends. This positions the research to support phase 3, where exploratory pattern combinations are tested to understand what kinds of forms can be created with this technology.

Phase 1: Pattern Repository

The research approach in Phase 1 negotiates theoretical information (computer-based knitting patterns) and the realities of physical prototypes (knitted swatches). The pattern repository creates the foundational data by cataloguing 21 knit patterns by pattern name, image, yarn type, and motive. The patterns are extracted from knitting standards and subsequently translated to Model 9 software. All pattern swatches are knitted on a Steiger 9 flatbed weft knitting machine. The aim of the pattern repository is two-fold: first, to generate 21 appropriately sized cruciform samples for casting and second, to develop a basic understanding of pattern behavior. The calibration-based process developed during this phase extends throughout the research.

Phase 2: Concrete Loading Tests and Curvature Analysis

The research approach of Phase 2 combines information gathering through physical prototyping with theoretical analysis. First, all 21 pattern samples are tested under hydrostatic loading to study the amount of deformation and the degree of adhesion between the textile and the concrete. The experiment methodology involves pre-tensioning each textile on a frame applying concrete, and allowing it to freely deform under gravity. The theoretical analysis component of this phase is facilitated by 3D scanning the cast shapes and extracting the principal curvatures. The curvature analysis approach is predicated on the difference between the warp versus weft properties and relies on the structural concept of stiffness to create comparisons.

Phase 3: Pattern Combination

The experimental approach taken in Phase 3 relies entirely on the data produced in Phases 1 and 2. Carefully selected patterns are combined into specific shapes to demonstrate the design possibilities of this technology. While some combinations are inspired by existing shell structures, others are simply experimental. Certain principles extracted from the literature review guide the nature of the combinations, with a focus on arches, vaults, and shells.

Conclusion and Reflection

Finally, the conclusion and reflection analyze the results of the research, focusing on advantages and disadvantages, relevant findings, and answers to the research questions. The reflection positions this research in the broader context of flexible formwork and identifies pertinent contributions and future work.
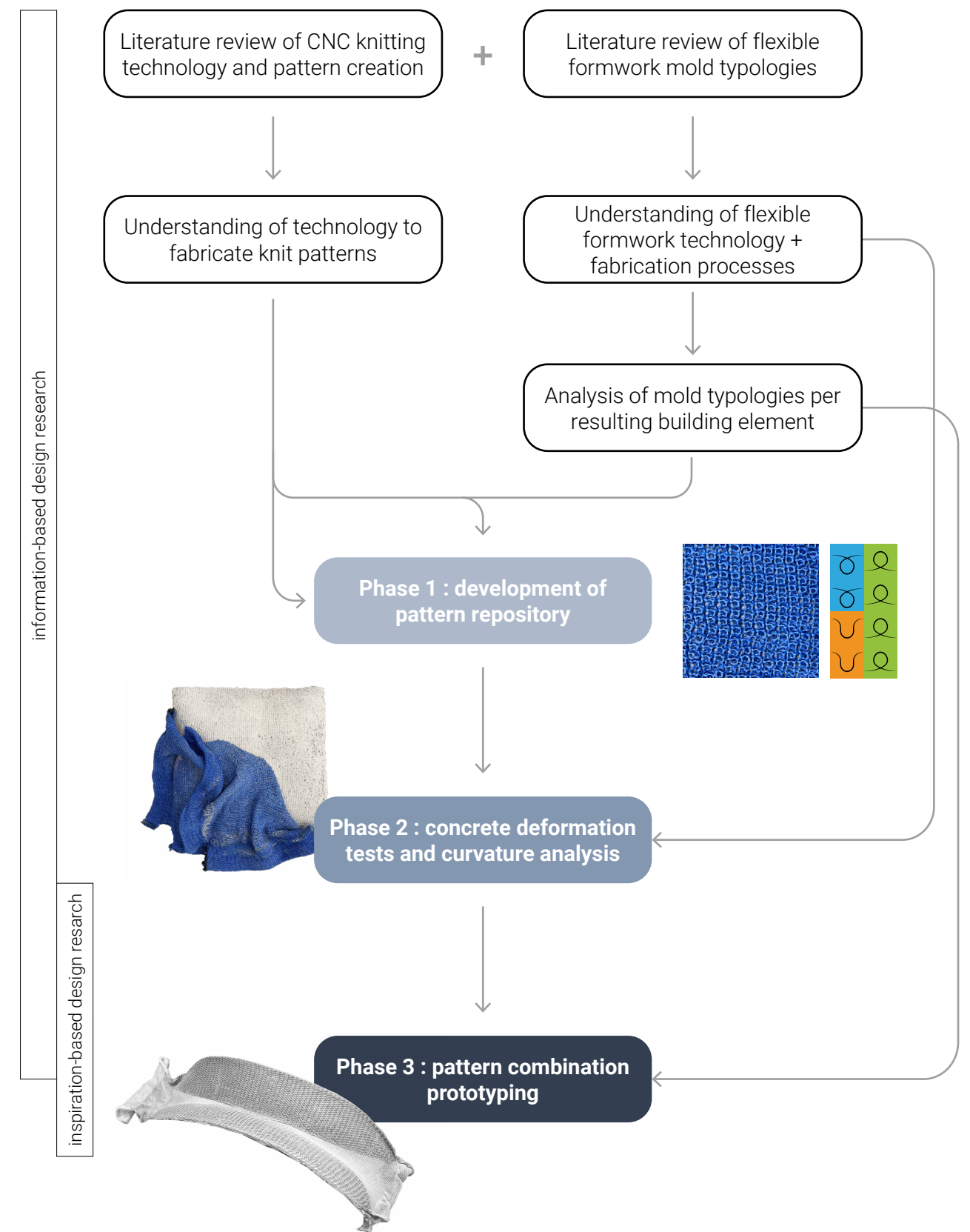

Figure 1. Methodology workflow chart.

1.4 Relevance of CNC-Knit Flexible Formwork

This section will describe the advantages CNC-knit flexible formwork in the contexts of sustainability, structural and architectural design innovation, and material/cost/time savings. The particular benefits of knit fabrics will also be discussed along with a brief explanation of CNC knitting. Finally, barriers to the adoption of this technology in mainstream construction practices will be identified.

1.4.1 Sustainability

Concrete is the world's most used building material. It derives popularity from its broad availability, low cost, familiarity, as well as durability and material strength (Flatt et al., 2012). In 2020, the global volume of concrete was estimated to be 14.0 billion m^3, while another 4.2 billion tons of cement were produced in the same year (*About Cement & Concrete*, 2023). The production of concrete, specifically cement, is resource intensive and highly polluting. In 2022, cement and concrete manufacture accounted for approximately 7% of global carbon emissions (Owen-Burge, 2022). The most recent Global Status Report for Buildings and Construction (United Nations Environment Programme, 2022) defines a primary goal of replacing of concrete with less-carbon intensive materials, but notes that a rapid increase in global urban densification indicates that the production of concrete will continue to rise. In lieu of a complete elimination of concrete from buildings and construction, architects and engineers must instead adapt their methods to design more materially efficient elements, and in turn, constructors must adopt new building practices.

1.4.2 Structural and Architectural Design Innovation

The standard concrete element is generally orthogonal and of uniform cross section. Despite engineering and design conventions that prioritize uniformity, the distribution of forces in even the most simple structures is almost always non-uniform (Hawkins et al., 2016). These standards lead to the overuse of material and reduced structural efficiency. Figure 2 illustrates a comparison between a traditional reinforced concrete floor and a funicular arched concrete floor with applied loads. The term 'funicular' refers to a loading situation where only compressive stresses are present (Faber, 1963); the ideal loading condition for concrete. The solid floor resists loads through bending, but the arched floor resists loads through compression action only: loads are transferred vertically to the supports, while
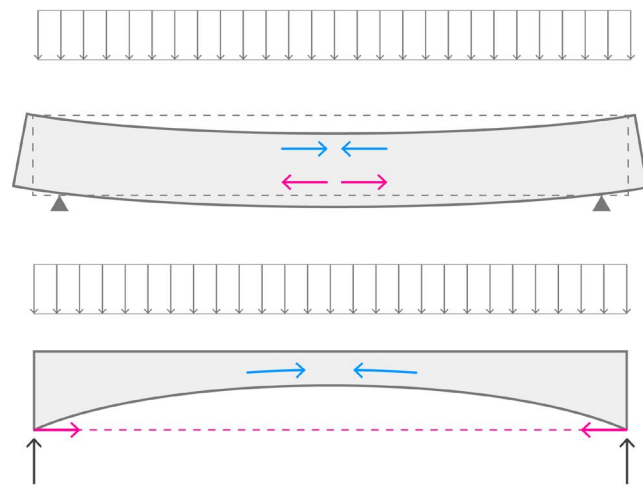
Figure 2. Comparison of solid concrete floor (left) to an arched concrete floor (right) under identical uniformly distributed loading. Adapted from Block et al., 2020.

the horizontal component is resolved by a tension tie. In the corresponding study performed by the Block Research Group, the arched floor was found to save 70% of material (Block et al., 2020). The specific funicular design of the arched floor exploits concrete's compressive capacity and eliminates the need for steel reinforcement.

Funicular forms greatly reduce the structural volume of an element by placing material only where required due to their ability to uniformly distribute applied loads (Block et al., 2020). Also known as skin-resistant structures, these forms gain strength as a direct result of the curvature and corrugation of their surfaces whose thickness is always small compared to their span (Nervi, 1956). Architects and engineers have experimented with these forms throughout history, but their construction remains complex and expensive. CNC-knit flexible formworks offer a promising solution. Unlike woven textiles which require cutting and shaping, knitted textiles support the fabrication double-curved geometries in one piece through local variation in length and width and geometric variation at a per-stitch scale (Lee et al., 2021). The unique cooperation of funicular forms, CNC-knit textiles, and the material capacity of concrete was first observed through the development of KnitCrete (M. A. Popescu, 2019). KnitCrete is a flexible formwork technology that uses tensioned or draped weft-knitted textiles as the shaping element for casting concrete structures (M. A. Popescu, 2019). Recent examples including the KnitCrete Bridge (M. Popescu et al., 2018), the KnitCandela pavilion (M. Popescu et al., 2020), and the KnitNervi pavilion (Scheder-Bieschin, Bodea, Popescu, Mele, et al., 2023), all funicular concrete shell prototypes, demonstrate the structural and architectural potential CNC-knit formwork.
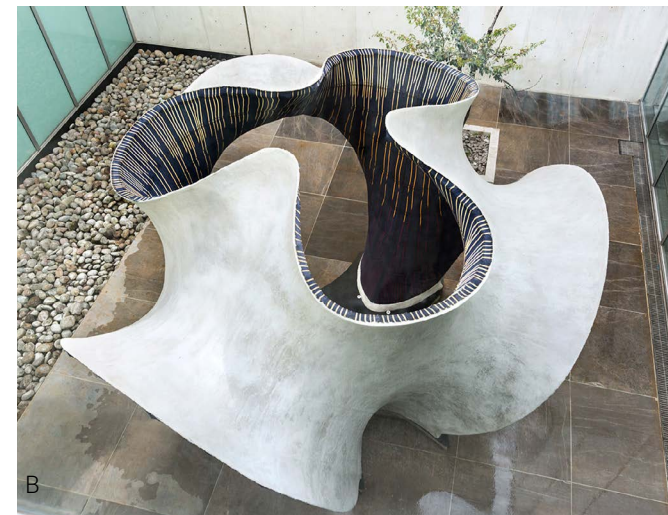
Figure 3. Various CNC knit formwork prototypes. (A) Concrete shell bridge (Source: Block Research Group), (B) KnitCandela Pavilion (Source: Zaha Hadid Architects), (C) KnitNervi Pavilion (Source: Block Research Group)

1.4.3 CNC Knitting

The use of CNC-knit textiles as architectural materials is still in its infancy (Tamke et al., 2020). Although it has been explored through tensile membranes and flexible formwork, this technology has been primarily restricted to the garment industry. Knitted textiles can be distinguished from woven textiles, which have historically dominated architectural applications, by the structural principles which inform their design (Nawab et al., 2017). Weaving creates a two-dimensional fabric by interlacing vertical warp yarns with horizontal weft yarns, while knitting involves the interlacing of one or more continuous yarns to create interconnected loops (Nader et al., 2021).
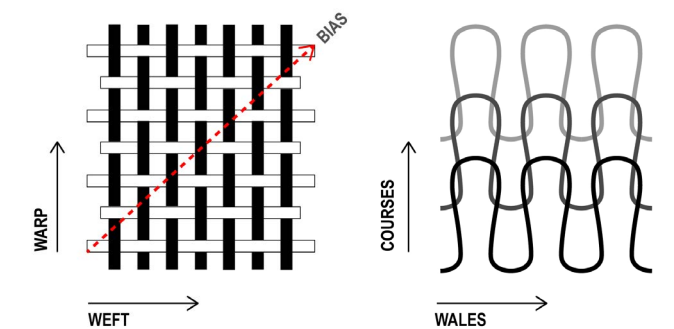
Woven fabrics are limited in their two-dimensionality, orthogonality, and restricted deformation along the bias (diagonal axis), while knitted textiles can be locally shaped and customized at a per-stitch scale to form three-dimensional elements in one piece. Knitting can be further described as a process by which bespoke materials are developed in direct response to user application-driven design criteria (M. Thomsen & Hicks, 2008). A simple example would be a knitted garment shaped to the human body, while a more complex application would be
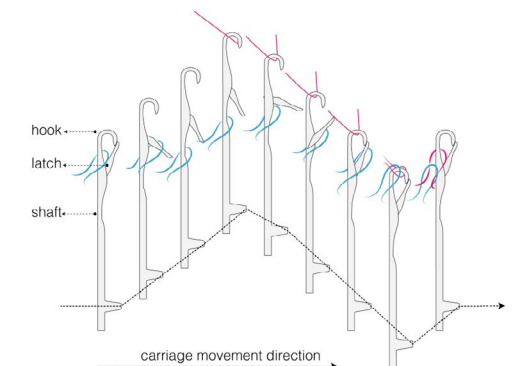
a knit structural membrane engineered to resist complex loading situations. On a flat-bed CNC weft-knitting machine, yarns are passed over an array of needles facing each other which pull the yarns through the loops created in the previous pass, forming new loops (Figure 5). The machine takes instruction from a knitting pattern represented as a bitmap, where each pixel represents one needle operation. The knit pattern is essentially a set of structural decisions which inform the textile's physical properties. CNC knitting in particular allows the user to combine the inherent three-dimensionality of knitting with the possibility to locally embed specific materials and parametrically modify patterns (Nader et al., 2021).

Figure 4. Knitting vs. Weaving. Adapted from Ahlquist, 2015.

Figure 5. Needle movement performed by CNC knitting machine to form a new loop. (M.A. Popescu, 2019)

1.4.4 Material, Cost, and Time Savings

Using traditional methods, the cost, time, and material required to create complex forms with concrete is immense. Even in standard cast-in-place projects, the material and labor for building concrete formwork accounts for 35-60% of the total project cost (Kreiger et al., 2019). Construction images from the 1950s-60s of works by Felix Candela and Eero Saarinen reveal the enormous amount of rigid formwork (and therefore time and cost) required to realize these shells.

More recent examples demonstrate the lack of advancement in mainstream construction practices. The Rolex Learning Center by SANAA, completed in 2010, required a staggering 7,500 square meters of shuttering, 1,500 individually customized wooden boxes, and 10,000 different cleats (*Rolex Learning*

A

B

C
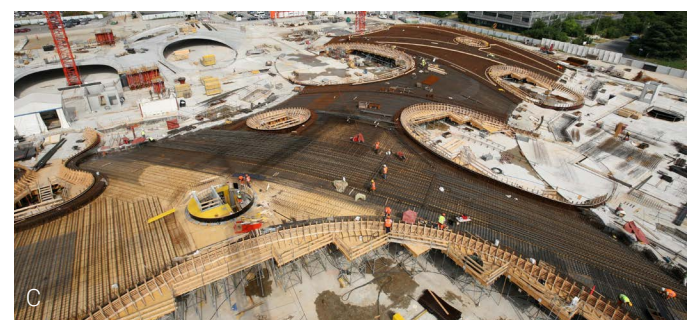
Figure 6. (A) Construction of the TWA Terminal by Eero Saarinen, 1962 (Source: Architect Magazine), (B) Construction of the Chapel del Palmira by Felix Candela, 1958 (Source: Alexander Eisenschmidt/ArchDaily), (C) Construction of the Rolex Learning Center by SANA

Figure 7. Construction of the NEST HiLo prototype. (Source: Block Research Group)

Center | SANAA, n.d.). The construction of the NEST HiLo project at EMPA in Dübendorf, Switzerland, stands in stark contrast to previous shell structures. The roof was constructed with a cable-net formwork with fabric shuttering that deforms under the weight of wet concrete to assume the desired shape of the double-curved surface (Block et al., 2017). The conceptual difference between the construction process of NEST HiLo and traditionally fabricated concrete shells is demonstrated in Figure 8.
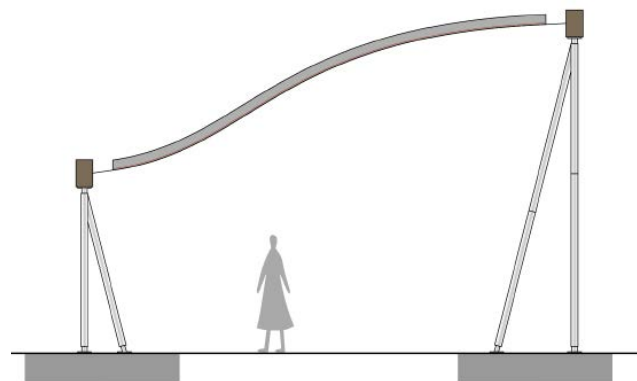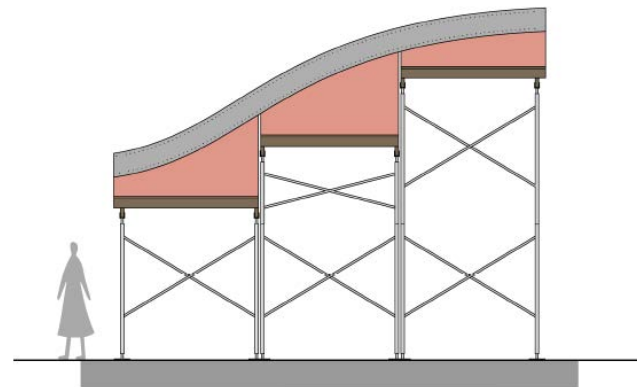

Figure 8. Rigid vs. flexible formwork systems. (M.A. Popescu, 2019)

As demonstrated through NEST HiLo, there is a significant reduction of material when flexible formwork techniques are used. This can be explained through two key structural principles: principles (West, 2017):

1. Flexible membranes resist forces in pure tension, which is more efficient than how rigid molds resist forces through bending.

2. Rigid molds require a high degree of stiffness and therefore necessitate material of much greater volume and weight.

Essentially, while heavy, rigid molds fight against deflection under hydrostatic pressure from wet concrete, flexible molds use those forces to assume the most efficient shape possible. This technology leads to a significant reduction of material, cost, and time during the construction process, and also 'naturally' produces the most structurally efficient form of concrete for the given loading situation, as it is able to assume this shape under gravity loading without much restriction.

In some studies, researchers have quantified certain material, cost, and time savings of flexible formwork systems. The textile used in KnitCandela weighed only 25kg, cost 230 EUR, and took only 36 hours to fabricate (M. A. Popescu, 2019). Another study which used flexible formwork to produce a variable section beam showed a 21.89% reduction in material use as compared to an equivalent prismatic beam. The study also showed a 49.2% reduction in construction cost (Acharekar & Savoikar, 2019). Some researchers have also demonstrated the ease with which textile formwork can be transported. Figure 9 shows examples where flexible formwork

textiles were transported to site in checked luggage, as compared to the traditional flatbed truck transporting rigid formwork. Although these examples present small-scale works, these savings benefits could have a major impact on larger-scale construction.

1.4.5 Barriers to Adoption

The construction industry is notoriously slow to adopt novel building techniques. In describing his work almost 70 years ago, Pier Luigi Nervi noted, "...all these promising developments are made possible by the progressive liberation of reinforced concrete from the fetters of wooden forms...until these bonds are totally removed, the architecture of concrete structures is bound to be...an architecture of wooden planks" (Nervi, 1956). Evidently, typical methods of building with concrete have not changed significantly. For the architect or engineer, it is easier to design and analyze orthogonal, prismatic forms. For the builder, rigid formworks are easy to work with because they are standardized and simple to quantify in terms of cost and time. Flexible formwork does not yet share these qualities. In terms of reuse, rigid formwork is more likely to produce multiple identical elements than a flexible textile mold, making standardization difficult.

A

B

C

Figure 9. Transportation of textile formwork vs. transportation of rigid formwork. (A) Textile formwork used in KnitCandela being vacuum-compressed for transport in checked luggage (Source: Block Research Group), (B) Luggage used to transport 13 building-scale column formworks (Source: Mark West / C.A.S.T), (C) Typical transport of rigid formwork (Source: Southern Cross Crane)

2.0 State-of-the-Art

This chapter provides an overview of flexible formwork applications. It also addresses CNC-knit pattern generation techniques, and makes connections between mold typologies and building elements. Section 2.1 addresses the latest advancements in CNC knitting technology in architecture beyond flexible formwork. Section 2.2 introduces current computational methods of creating patterns for CNC knitting. Section 2.3 provides a brief overview of flexible formwork throughout history. Section 2.4 draws connections between flexible mold typologies and specific building elements. Section 2.5 provides a summary discussion in the context of the thesis research questions.
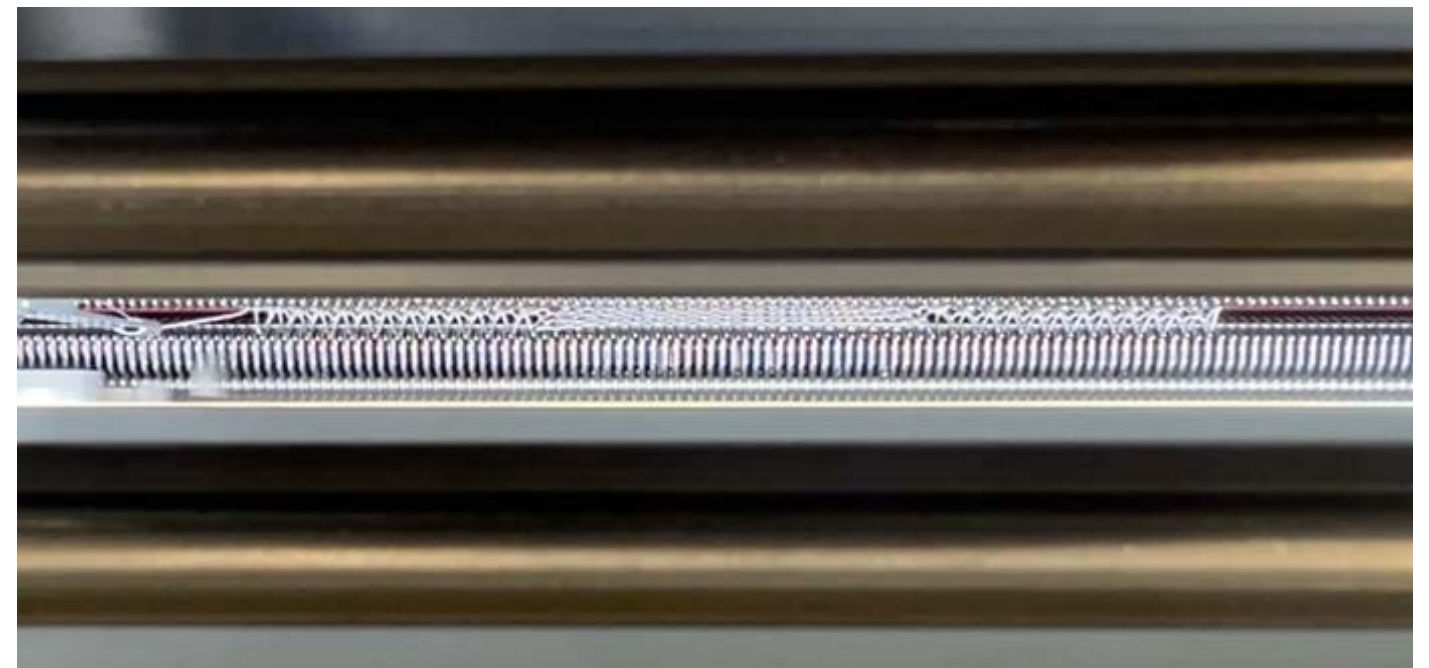
Figure 10. TU Delft CNC knitting machine producing a knit textile.

2.1 Recent Advancements of CNC Knitting in Architecture

The use of CNC-knit textiles as architectural materials has been explored primarily through small-scale tensile structures. The inherent flexibility of knit fabric, the ability to integrate shaping and detailing, and the variation of knit structure at a fiber scale (Tamke et al., 2020) makes this technology particularly suited to the formal complexity of double-curved tensile membranes. Two research projects completed at CITA, Isoropia and Hybrid Tower, demonstrated this potential and provided important knowledge about the influence of knit patterns.

Hybrid Tower (Figure 11), an experimental pavilion constructed in Portugal, explored flexibility at a material and structural level using CNC-knit membranes and bent compression rods (M. R. Thomsen et al., 2015). The guiding structural concept prioritized reducing stiffness through adaptability and minimizing material use by allowing for deformation. These principles relate closely to those noted by various authors in describing the benefits of flexible formwork, where stiff, rigid molds are replaced by flexible membranes which adapt to hydrostatic loads instead of resisting. Further, the pattern design of the membrane embedded four key functionalities: diagonal pockets to receive compression rods, structurally supported perforations for seams, custom shaping, and local reinforcement at the edges (M. R. Thomsen et al., 2015). Although initial tests showed that a piquet lacoste knit pattern was structurally sufficient, the fabrication of the final membrane was done on a

larger CNC knitting machine, resulting in a material with much higher elasticity, geometry, and behavior. This discrepancy is likely due to a difference in machine gauge and demonstrates the domino effect of stitch properties on the physical behavior of a textile.

Isoropia, the Danish pavilion constructed for the 2018 Venice Biennale, was a 35-meter bending-active textile hybrid structure. It used 41 discrete CNC-knit patches and glass fiber rods to form an undulating surface that morphs from canopy to vault (Tamke et al., 2020). During prototyping, various knit patterns were tested for physical performance. Initial tests revealed that a piquet lacoste pattern produced a fabric that was too tight to achieve the desired three-dimensionality of the vaults, so an alternative piquet pattern was introduced (Tamke et al., 2020). A tubular jersey pattern was used for double surface channels, while an interlock pattern was used for reinforcement sections and holes (Tamke et al., 2016). The knit surfaces also contained pattern variation to control movement. It was noted in this study that special attention should be paid to the interaction of knit structure, geometry, surface detailing, and tension stability to maximize mechanical performance. Over a total project time of only 4.5 months, Isoropia used CNC-knitting to demonstrate a fabrication technique which allowed direct programming of material behavior for the grading and design of a double-curved tensile structure (Tamke et al., 2020).

Multiple small-scale prototypes developed at

Figure 11. (A) Hybrid Tower (Source: Anders Ingvartsen/ArchDaily), (B) Knit patterns used in the Hybrid Tower textile (Source: CITA/ArchDaily)
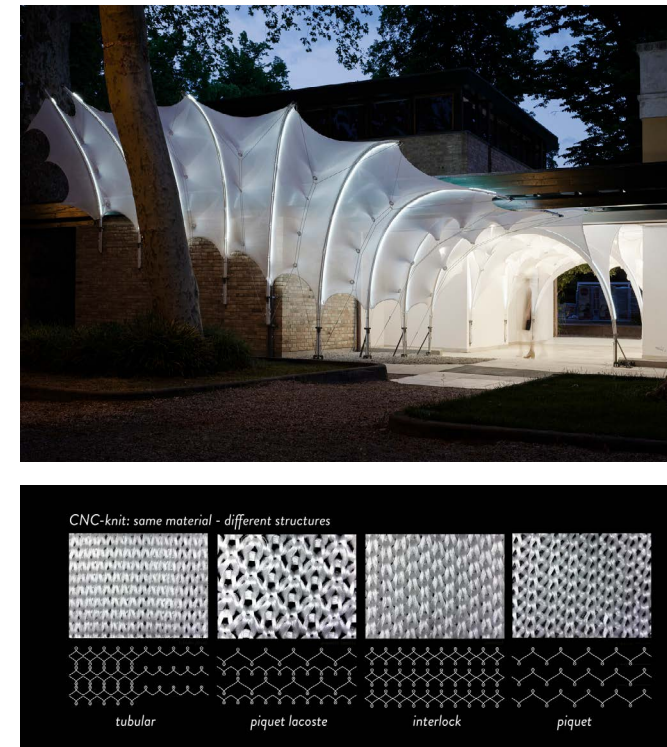

Figure 12. (Top) Completed Isoropia pavilion (Source: Anders Ingvartsen / ArchDaily), (Bottom) Patterns: tubular, piquet lacoste, interlock, piquet (Source: CITA/ArchDaily)

Taubman College (University of Michigan) used CNC-knit textiles to develop enhanced spatial experiences and placed strong emphasis on pattern manipulation. The Semi-Toroidal Textile Hybrid (Ahlquist, 2016) used varying stitch structures, including dropped stitches at the boundaries of the textile which allowed it to expand up to 2.7 times its circumference (Figure 13) . This study also noted that increased stitch density produces a self-forming textile, while the compactness of stitches embeds a compressive capacity especially in fabric with hexagonal patterning. The Mobius Rib-Knit prototype utilized a rib-knit structure to create an inherently elastic fabric, noting that the differentiation of stitches formed on the front or back of the needle bed creates a weighted bias which causes the textile to recoil (Ahlquist, 2016). The ribbed pattern was calibrated to the results of a spring-based simulation of the desired tensile form, resulting in a variable ribbing pattern resembling tree branches. It was also noted that a ribbed knit pattern creates a highly elastic fabric with inelastic yarn. The StretchPLAY prototype, designed as an interactive play space, was required to respond to both internal stresses and applied loads by users. The seamless textile utilized a dense structure and short stitch length to add compressive capacity to resist deformation, and short rows (shaping) to tune its response to tensile stress.
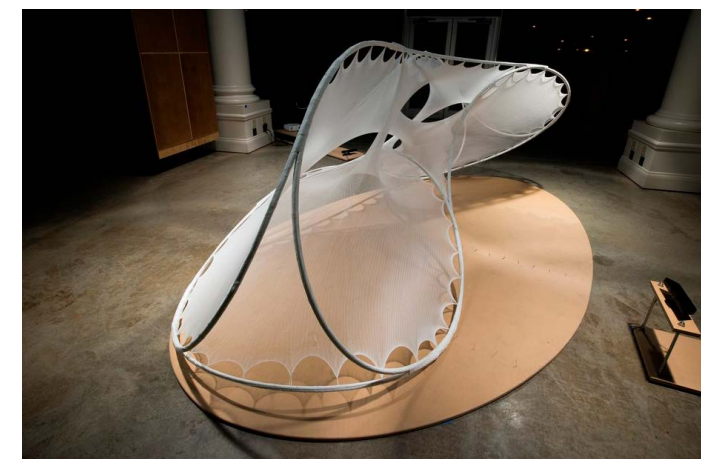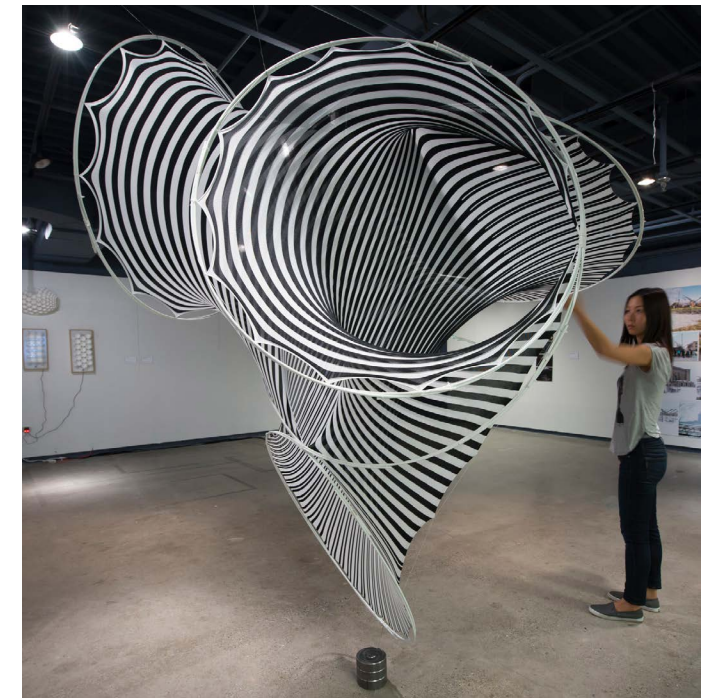

Figure 13. (From top to bottom) Semi-Toroidal Textile Hybrid, Mobius Rib-Knit Prototype, stretchPLAY prototype (Source (all): Sean Ahlquist / Lab for Material Architectures)

2.2 Computational Workflows for Pattern Creation

Knitting is an inherently computational process. Traditionally, knitting patterns were described using a set of repetitive written instructions or using a gridded chart where each cell refers to an individual needle operation. The design of knitting patterns, especially for complex shapes, is a time-consuming process requiring unique knowledge of knitting logic and stitch behavior. As a result, computational workflows have been developed which support automated pattern generation for complex forms, outputting bitmap files that can be interpreted by a CNC knitting machine. In discussing the results of their studies, multiple authors equate the importance of developing an integrative computational design method for pattern creation to the overall form of the final result.

The Knitted Composites Tower (Liu et al., 2021) and the Isoropia pavilion (Tamke et al., 2020) used similar computational workflows to generate knitting patterns for complex forms (Figure 14). Both authors noted key challenges including: (1) the pattern must respond to 3D geometry while obeying knitting logic and (2) the ideal combination of stitch structures must be determined. Both workflows relied on Grasshopper algorithms and generally followed these steps: (1) flatten 3D geometry through projection or mesh relaxation, (2) definition of pattern zones and stitch structures, (3) color key assignment, (4) non-uniform scaling, (5) export of bitmap file to CNC machine.

In the 7-meter Knitted Composites Tower, a spiraling anticlastic surface, the double-sided tuck pattern was chosen as the predominant stitch structure.

This allowed for interlocking or separation of the two sides of the fabric at random. However, it was noted that while a uniform stitch parameter input was used in the algorithm, the physical prototype showed that different stitch structures of the same input size differ considerably in shape when stretched. The authors noted that this resulted in redundant stitches which caused wrinkles in the fabric. In the Isoropia project, the authors noted the importance of frequent prototyping to calibrate the workflow to more precisely predict the behavior of the resulting fabric (Tamke et al., 2020). They also used 3D scanning to document the impact of various patterns and knit structures. Both projects addressed discrepancies between computer-generated algorithms and the resulting physical prototypes, revealing the need for more detailed information about the impact of knit patterns on textile behavior.

The computational workflows of the Knitted Composites Tower and Isoropia rely on unrolling and mesh relaxation of 3D surfaces to approximate non-developable surfaces. However, this approach does not fully solve non-developable surfaces and relies on the flexibility of the knitted textiles to achieve the desired shape (M. A. Popescu, 2019). The computational workflow developed in conjunction with KnitCrete proposes a different strategy which uses geometric descriptions, surface topology, loop geometry, and course direction. The functionality of the workflow, titled compas_knit, was developed in Python but interacts with Rhino 3DM as the user-input environment. The workflow follows three basic steps: (1) course generation through contouring of input geometry and definition of weft direction based on loop height, (2) loop generation and calculation

of loops per course, and (3) knit pattern generation of 3D graph to 2D bitmap pattern. Opportunities for making design changes and checks for knitting logic/connectivity are also integrated. This particular approach allows for significant control by the user in a visual interface and a more accurate realization of non-developable forms. Similarly to the aforementioned workflows, compas_knit also requires calibration between the digital pattern and the actual stretched loop parameters (M. A. Popescu, 2019).

The workflows presented in this section described three computational workflows for generating knitting patterns for complex forms. While varied, all share common challenges including: the accurate translation of 3D forms to 2D patterns, creating design flexibility while maintaining a connection to the CNC machine, and notably, understanding the geometric discrepancies between a computer-generated pattern and a knitted textile. Knitted textiles are difficult to simulate due to the vast number of stitches in a textile that are individually subjected to internal and external forces as well as multiple degrees of freedom (Anishchenko, 2023). Recent research focused on yarn-level modeling of knitted textiles which produced visual representations of knit textile deformation under loading (Anishchenko, 2023). The extent of this research suggests the importance of developing a greater understanding of stitch structures and knit patterns as they relate to the physical behavior of knit textiles.

2.3 Flexible Formwork throughout History

Flexible formwork is not a new building technology. Although its use can be connected to ancient

reed-centering practices for vault construction as described by Vitruvius (*The Project Gutenberg eBook of Ten Books on Architecture, by Vitruvius.*, n.d.), the technology was formally invented during the Industrial Revolution (Veenendaal et al., 2011). Beginning with Gustav Lilienthal's proposal for a fireproof ceiling (Lilienthal, 1899), various flexible formwork systems were patented throughout the 1900s. These inventions included flexibly formed funicular arches (Warrenne, 1952), hypar shells (Kersavage, 1975), façade panels (Fisac, 1975), beams, columns, floor systems (Warrenne, 1934), and even a proposal for an entire building (Parker, 1971).

Most of these systems relied on permeable woven textiles, namely Hessian, a vegetable fiber that is not particularly strong nor suited to reuse due to high adhesion (West, 2017). Others relied on impermeable and translucent plastic sheets such as polyethylene, which allowed for easy removal and visibility during pouring (Fisac, 1975). More recent work by Mark West/C.A.S.T. and Japanese architect Kenzo Unno includes flexibly formed beams, columns, shells, and wall panels, all of which relied on woven geotextiles. Woven geotextiles were chosen for these explorations due to their low cost, durability, lack of adhesion to concrete, and reuse potential. Although some of these systems were deployed at a large scale, notably flexibly-formed façade panels by Miguel Fisac as well as pneumatic concrete shell homes by various architects, none have become integrated into standard construction practices. Despite differences in technique and output, almost all of the aforementioned patents, the specifics of which will be discussed in the following section, cite a common goal of developing simple, economic construction methods for complex forms
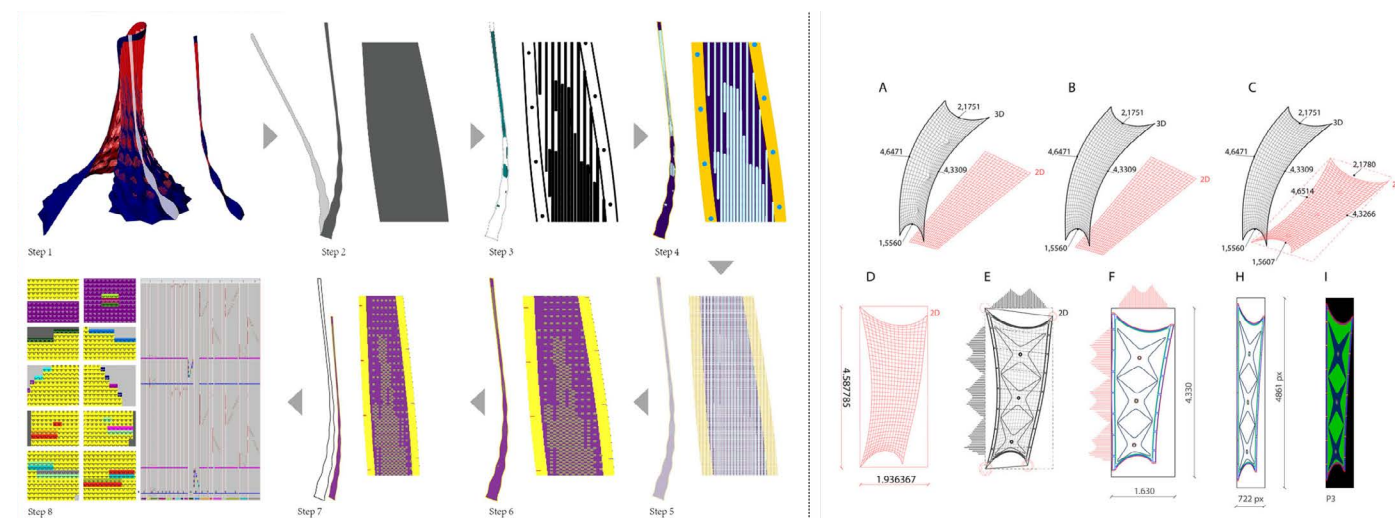

Figure 14. (A) Knitted Composites Tower pattern creation workflow (Liu et al., 2021), (B) Isoropia pattern creation workflow (Tamke et al., 2020)
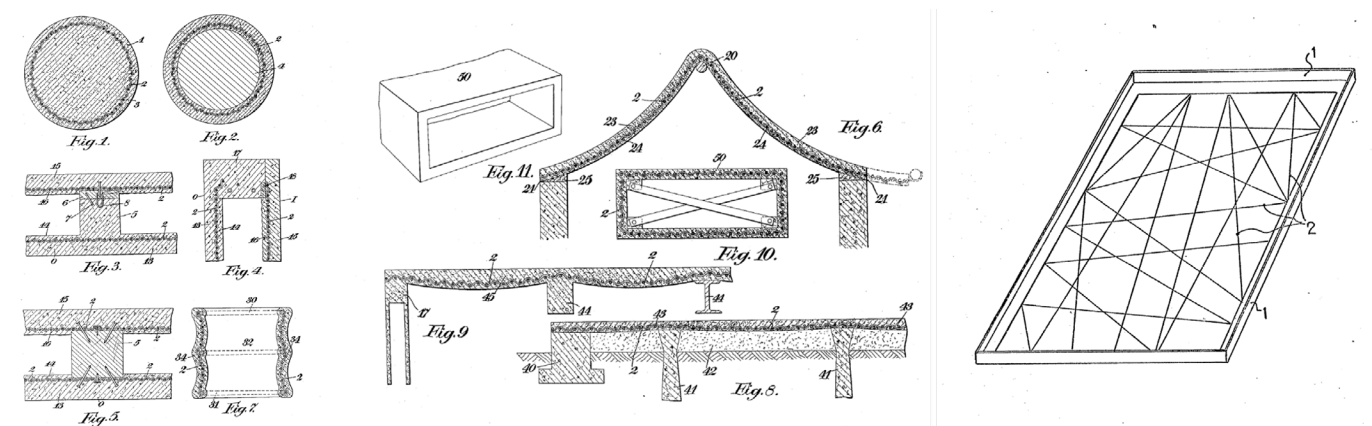

Figure 15. (A) Patented designs for a variety of flexibly formed building elements using Hessian (Warrenne, 1934), (B) Patented design for a flexible mold for a facade panel where a plastic textile is stretched over taught wires and allowed to bulge through under load from wet concrete (Fisac, 1975)

that minimize material use and construction time.

2.4 Fabrication of Building Elements per Mold Typologies

Hawkins et al. (2016) provides a comprehensive itemization of notable flexible formwork developments per mold typology and building element. Using the same conceptual organization, this section provides a more detailed discussion of selected examples. It also expands the list to include research conducted after 2016, notably projects that used CNC-knit textiles as flexible formwork membranes.

Figure 16 introduces a distinction between the two basic mold typologies (filled and surface molds) and the resulting building elements produced under specific loading conditions. In filled molds, wet concrete applies hydrostatic loads as it is poured, which causes the membrane to assume the most efficient geometry required to resist the load (Hawkins et al., 2016). Alternatively, surface molds use a single membrane on which concrete is sprayed or applied. Some key considerations for both filled and surface molds include the flexibility/stiffness of the textile membrane, permeability and capillary action, and the complexity of the rigging system. Further distinctions can be made based on the specific role and fate of the textile itself. A textile membrane falls into one of these categories:

Sacrificial: Textile membrane is removed following casting, but damage incurred during the removal process prevents reuse.

Reusable: Textile membrane is removed following casting and is able to be reused.

Stay-in-Place (formwork only): Textile membrane stays in place following casting but does not provide structural reinforcement to the final form.

Stay-in-Place (formwork + structural): Textile membrane stays in place following casting and provides structural reinforcement to the final form.

It is important to note that most examples of flexible formwork presented in this section rely on woven geotextiles, which have traditionally dominated flexible formwork construction. Knit textiles have been less popular for flexible formwork likely due to their high elasticity and deformation, permeability, and general unpredictability. This is especially true for filled molds; however, a recent patent application (NG et al., 2023) describes a filled-mold technique that uses CNC-knit textiles to cast solid complex forms and specifically notes the advantages of CNC-knit textiles over woven textiles. In differentiating the proposed technique, the patent authors note that the knitted membrane is not imbibed with a stiffening agent and instead utilizes the dynamic interaction of hydrostatic pressure and restraint.

2.4.1 Filled Molds
Columns and Branching Structures

A column mold can be described as a vertical, cylindrical tube that is laterally braced and filled with concrete from above (West, 2017). Typically, flexibly formed columns use either a continuous piece of
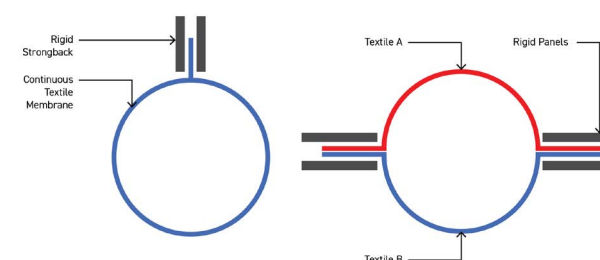
Figure 17. Typical mold setups for flexibly formed columns.

fabric that is attached at the ends, or two pieces of fabric which are held together by rigid panels.

During the pouring process, tension develops non-uniformly in the membrane as the wet concrete pushes against it; the highest tension forces naturally occur at the bottom of the column mold.

Key considerations for column molds include: (1) the prevention of material aggregation at the base, (2) the height and diameter of the column as it relates to the amount of pressure on the membrane, and (3) the extent of scaffolding required to support the mold during the pouring process. For any filled molds, but especially those of columns, the tension forces applied to the membrane impact the material qualities of the concrete because water and air are forced through openings in the material which strengthens the concrete and improves surface quality.

Many examples of flexibly formed columns exist, the most basic of which is the Fast-Tube developed by Fab-Form industries, which consists of a seamed polyethylene fabric that is clamped between a strongback (Fearn, 2024). Wet concrete is poured into the textile tube which has been placed around a reinforcement cage resting directly on the building foundation. Mark West / C.A.S.T. conducted multiple projects exploring flexibly formed columns with variable cross sections. These prototypes used clamped single textile molds and double-textile membranes sandwiched between rigid panels, titled "bulge-wall" column molds (West, 2017). Using the bulge-wall method, branching and scissor forms were explored as well as surface texturing using concentric layers of differing textiles.
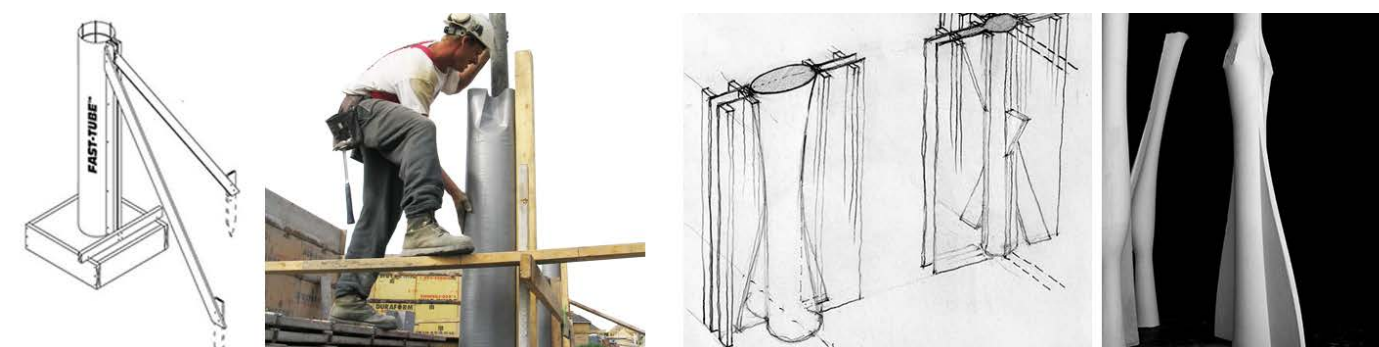

Figure 18. (A) Fast-Tube column fabrication (Source: Fab-Form Industries), (B) Bulge-Wall column fabrication method (Source: Mark West / C.A.S.T.)

Figure 19. Various flexibly formed columns produced by Mark West / C.A.S.T. using the bulge-wall method. (Source (all): Mark West / C.A.S.T.)

STRESS CONDITION	FILLED MOLDS	SURFACE MOLDS	TEXTILE ROLE/FATE
no pre-stress (fully supported)	foundation	canal liner	stay-in-place (formwork only)
no pre-stress (self-stressing)	floor/ceiling	catenary arch	stay-in-place (formwork only)
	beams	hollow floor/ceiling	stay-in-place (structural reinforcement)
			re-usable
	columns		sacrifical
bi-axial or multi-axial stress (pre-stressed)	walls + facade panels	complex shells	stay-in-place (formwork only)
			stay-in-place (structual)
			re-usable
			sacrifical

Figure 16. Taxonomy of fabric formwork mold typologies, resulting building elements, and the role/fate of the formwork textile post-casting. Adapted from Veenendaal et al., 2011 and Hawkins et al., 2016)

Figure 20. Six dart columns with corresponding tailored fabric formwork patterns (Milne et al., 2015)
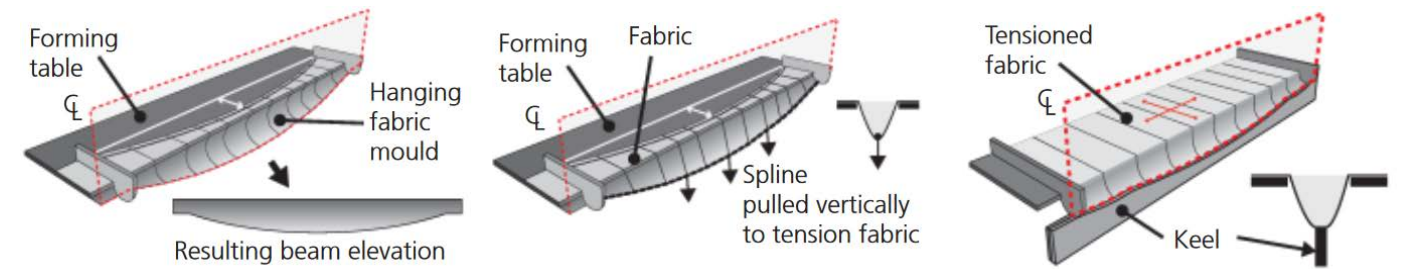

Figure 22. Three basic mold typologies designated for flexibly forming beams and trusses. From left to right: hanging mold, spline mold, keel mold (Orr et al., 2014)
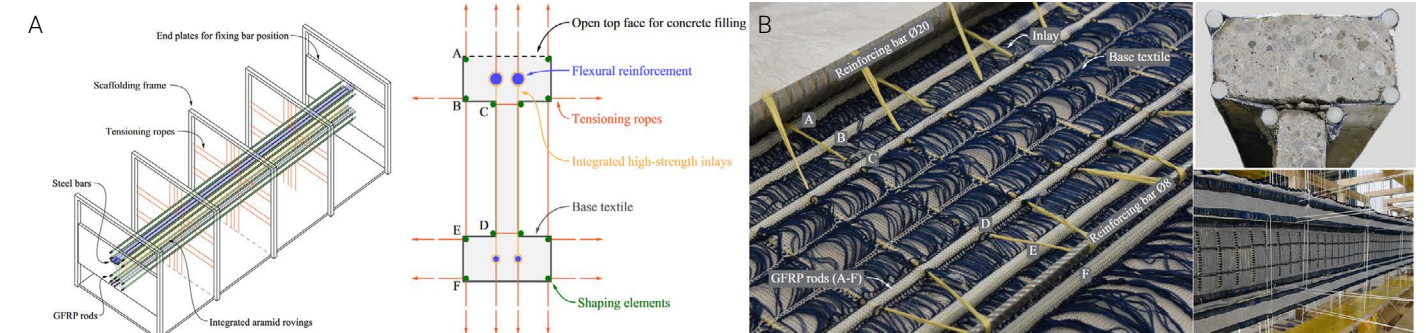

Figure 23. Flexibly formed I-beam by Lee et al., 2023 (A) Diagram of mold setup, (B) Construction of prototype (Source (all): Lee et al., 2023)

Other prototypes such as the Dart Columns constructed at the University of Edinburgh explored the effects of integral textile restraint on the form and expression of cast columns (Milne et al., 2015). Six different flexible membranes of differing dart arrangement were tested and cast as filled molds and showed the importance of membrane design on the final form assumed by the hardened concrete. The fabrication of these prototypes is especially interesting due to the use of darting, which is essentially the custom shaping of rectangular sheets of fabric often used in garment construction. While this process required cutting and sewing, similar manipulations could be performed on a CNC knitting machine within one piece of fabric.

Beams

Flexibly formed beams tend to share a unique goal of structural optimization through cross-section variation (Hawkins et al., 2016). The geometry of a form-active element follows the forces applied to it, which suggests that the most efficient shape of a beam would be a direct response to its parabolic distribution of bending moment (Pedreschi, 2011). A prototype developed by Mark West / C.A.S.T. for a

uniformly loaded, double-cantilevered beam used a pre-tensioned geotextile membrane that was shaped and filled to produce a variable cross-section beam that follows its bending moment curves (West, 2017).

Figure 22 demonstrates three basic subcategories of filled molds specifically designated for beams and trusses which include hanging molds, spline molds, and keel molds (Orr et al., 2014). Versions of these molds were used by Mark West/C.A.S.T. to produce additional prototypes which explored varying profiles and opening placements. The research field of structurally optimized beams through cross section variation is vast and beyond the scope of this thesis, but it is important to note that flexible formwork presents one of the few viable fabrication methods to produce these forms. A more recent study by (Lee et al., 2023) demonstrated a different approach to flexibly formed beams by integrating a CNC weft knitted textile reinforcement, allowing for the placement of custom features to guide shaping rods and other reinforcing elements. The research tested four versions of an I-profile section beam, where the cross-sections were created by folding a flat textile into the desired shape guided by bending-active

rods and tensioned ropes in a scaffolding frame. The pattern configurations of the knit textile played a role beyond shape determination, and included considerations of adhesion and structural capacity. Various patterns were tested for strength and concrete adhesion in a previous study by the same authors. Another important distinction is that the flexible formwork is intended to stay in place and become an integral part of the element's structural performance.

Floor/Ceiling Systems

Floor/ceiling systems represent some of the earliest experiments involving flexible formwork. Nearly identical patents for flexibly formed floor/ceiling systems were filed in 1899 (Lilienthal, 1899) and 1937 (Farrar et al., 1937). Both methods describe spreading Hessian fabric of limited permeability over parallel beams with sufficient slack, covering the fabric with wire mesh, and subsequently pouring concrete. Both note the simplicity, material

savings, economic benefits, and lack of skilled labor required for this construction method. A later patent filed in 1971 (Figure 25) proposed a building-scale application of this system by considering a floor/ceiling as an extended beam (Parker, 1971). The author describes a fabrication method for creating elongated concrete members "without formwork," a process in which textile sheets are spread over belts hung between steel beams, covered with wire mesh (to eliminate the need for steel reinforcement), and poured in place. A 20% reduction in material as compared to a prismatic shaped is also noted in a broader discussion of improved structural efficiency and construction cost/time savings. More recent examples of flexibly formed floor/ceiling systems are fairly limited. Various prototypes including a fabric-formed slab cantilever (Araya, 2014) and a fabric formed precast slab (C.A.S.T., 2010), demonstrate novel geometric expressions and connections to other building elements.

Figure 21. Prototype for a beam whose shape follows the curve of its bending moment by Mark West / C.A.S.T. (Source: Mark West / C.A.S.T.)
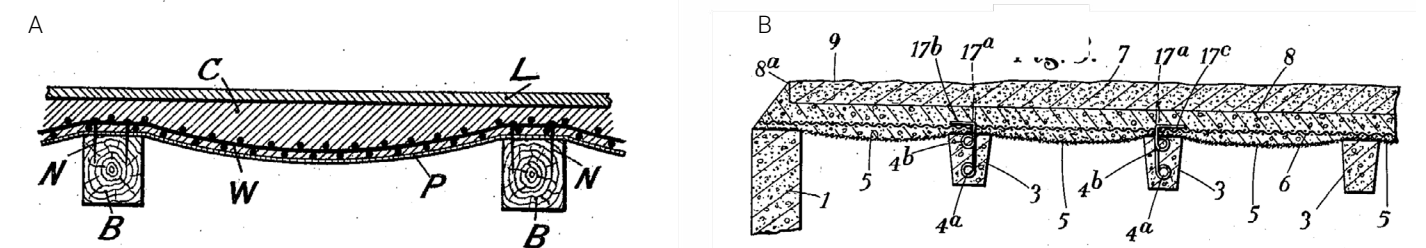

Figure 24. (A) Fireproof ceiling by Gustav Lilienthal (Lilienthal, 1899), (B) Floor system by Dennis Farrar (Farrar et al., 1937)
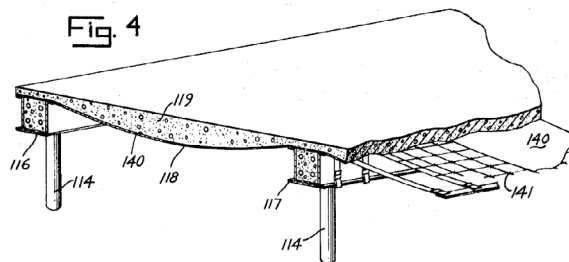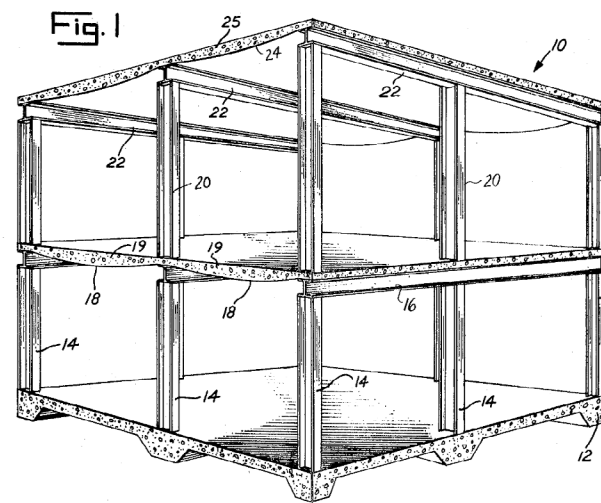
Figure 25. Patented drawings of a flexibly formed building showing completed structural system and enlarged cross section of a single floor plate (Parker, 1971)

Walls

The basic concepts behind flexibly formed walls can be clearly demonstrated through the work of Japanese architect Kenzo Unno. Unno uses two basic methods: the frame method or the quilt-point method (Figure 26). In the frame method, netting is stretched along the inside surface of a stud wall, and concrete is poured from above. The quilt-point method uses two layers of textile that are laterally restrained by wall form-ties.

Like column construction, flexibly formed wall molds develop considerable hydrostatic pressure at the base of the formwork, which necessitates a system or pattern of horizontal restraints to limit the outward bulging of the fabric (West, 2017). Translucent geotextiles are often used during construction so the level of concrete can be observed. In addition to cast-in-place walls, Unno also developed a pre-fabricated panel essentially a structurally insulated panel or SIP, (Figure 27a) which is installed without concrete and poured on site. Photographs of various projects by Unno in Japan (Figure 27b) demonstrate the application of this technology at the scale of an entire building.

Figure 26. Flexibly formed walls by Kenzo Unno. (A) Frame Method, (B) Quilt-Point Method, (C) Partially filled quilt-point mold (Source (all): Kenzo Unno)

Figure 27. (A) Structurally Insulated panel with incorporated flexible formwork (B) Various residential projects in Japan with flexibly formed concrete walls (Source (all): Kenzo Unno)

2.4.2 Surface Molds

Of the many potential applications of flexible formwork, the construction of flexibly-formed shell structures stands out as particularly innovative due to the notoriously difficult traditional methods used in building complex forms with rigid formwork. Although the term 'shell structures' is broad, the following sections establish these distinctions of mold typologies:

Textile membranes which are hung, sometimes flipped following hardening (arches, vaults)

Textile membranes which are stretched over a rigid frame (hyperbolic paraboloids)

Textile membranes which are pre-tensioned with ropes and scaffolding (non-developable surfaces)

Hung Molds

When a flexible membrane is hung and its ends allowed to deform freely under gravity, it assumes the form of a catenary arch. When loaded with concrete, the membrane will deform to the shape of its own resistance in pure tension (West, 2017). As tension and compression are geometric opposites, a catenary arch can be inverted to obtain a compression-only (funicular) loading condition (Jiang et al., 2018), the ideal situation for concrete.
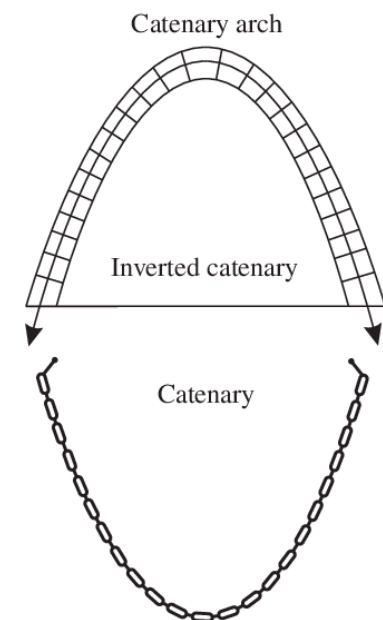
Figure 28. Diagram of a catenary arch and its inverted counterpart (Coll et al., 2014)

Multiple prototypes developed by Mark West/ C.A.S.T. demonstrate this concept clearly. In a prototype for a funicular barrel vault mold (Figure 29), a hanging fabric sheet was sprayed with GFRC and later inverted.

Figure 29. Hanging mold construction and flipped hardened element. (Source: Mark West / C.A.S.T.)

Another prototype for a "flayed beam" (Figure 30) shows a similar method applied to the formation of a doubly-curved surface, where a flexible membrane was hung over a specifically designed scaffolding, coated in GFRC by hand, and finally inverted.

Figure 30. Prototype for a "flayed beam" being cast on a hung mold (Source: Mark West / C.A.S.T.)

A third prototype for a funicular thin-shell floor panel (Figure 31) followed a similar process and demonstrated its potential for aggregation in a larger system.
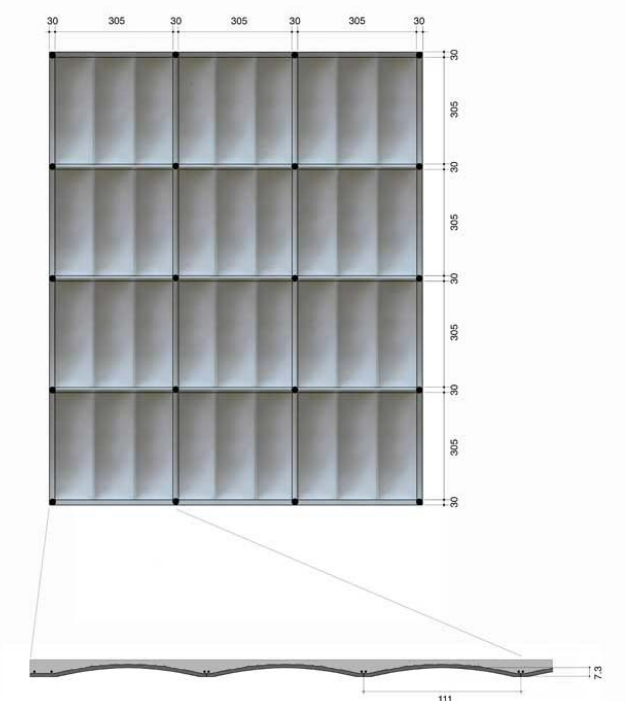
Figure 31. Prototype for a thin-shell funicular floor system fabricated on a hung mold (Source: Mark West / C.A.S.T.)
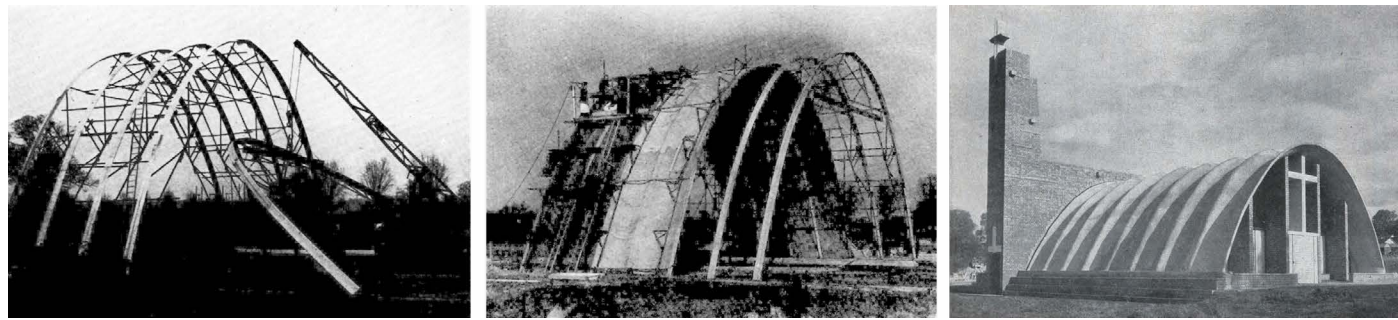
Figure 32. (A & B) Construction of a Ctesiphon shell (Source: Waller & Aston, 1953), (C) Completed Ctesiphon shell for Christ the King Church, Bristol (Source: Archidave / Flickr)

James Waller, who patented the 'Ctesiphon' system for flexibly-formed catenary arches, noted that "engineers are frequently unkind in their treatment of concrete, impolitely disregarding its aversion to tensile stress" (Waller & Aston, 1953). Inspired by the Great Arch of Ctesiphon in Baghdad, Waller designed and fabricated a series of ribbed catenary arches that were formed by bracing a series of ribs together and stretching vegetable fabric between them. Cement paste was then applied in multiple coats, allowing the fabric to adopt a natural catenary sag (Faber, 1963). The inclusion of ribbing was essential to achieving the required stiffness while maintaining a thin shell of ¾ to 1 ½ inches (approx. 2cm to 4cm) where spans ranged from 20 to 40 feet (approx. 6 to 12 meters). As a result, steel reinforcement was not required. This particular example actually represents a combination of two previously specified distinctions because both rigid frames and hung textile membranes are utilized.

Rigid Frames

A related prototype to the Ctesiphon shells was constructed at the University of Edinburgh (Figure 33) where two rigid catenary arches of identical span but differing height were fabricated with plywood and connected via a stretched fabric (Pedreschi, 2011). Thin layers of concrete were applied directly to the fabric, creating a gaussian vault upon hardening.

With some exceptions, most flexibly formed shells that involve stretching fabric over a rigid frame result in hyperbolic paraboloids. A 1975 patent (Kersavage, 1975) describes a process whereby individual strips of woven fabric are stretched over a rigid wood frame, secured by nails, and coated with cement paste. Later built works by George Nez / TSC Global relied on an identical method which was employed to construct about 20 hypar roof structures around the world, most of which were fabricated over the course of a few and with local unskilled labor (Figure 34). Compared to the construction of hypar shells of

Felix Candela with rigid formwork as noted in section 1.4.4, this method represents a much simpler and materially efficient system.
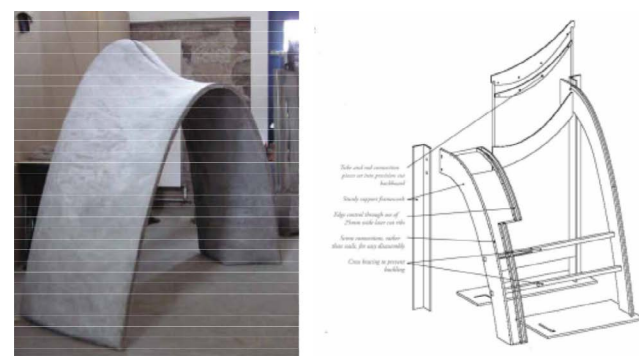
Figure 33. Rigid frame setup to cast a concrete gaussian vault and the hardened element (Pedreschi, 2011)
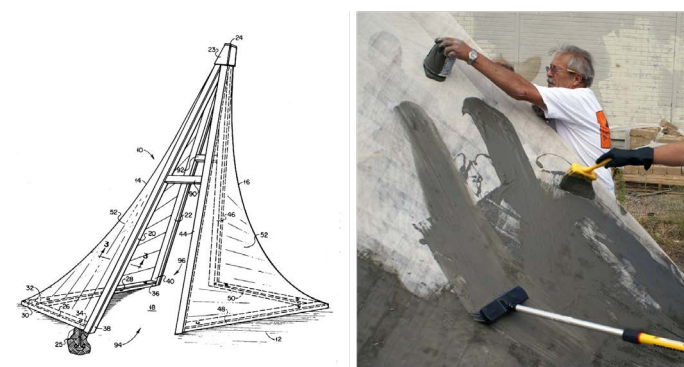
Figure 34. Diagram from a 1975 patent for flexible formwork using a rigid frame (Kersavage, 1975), (B) Construction of a hypar roof shell using textiles stretched over a rigid frame (Source: TSC Global), (C) Completed flexibly-formed hypar roof shells by George Nez (Source: TSC Global)

Pre-Tensioned or Pre-Formed

Textile membranes which are pre-tensioned to a specific shape can be assumed to share the same or highly similar geometry to that of the desired hardened form. Pre-tensioning of a rectangular, flat textile creates distortions known as buckles, which are typically prevented through cutting and shaping. Further, tensioned fabric alone is limited to anticlastic geometries, but can take on a wider range of shapes when combined with bending active systems or other components (M. Popescu et al., 2018). Although experiments using pre-tensioned flat textiles have been conducted, this section will address research specifically focused on the use of pre-tensioned CNC knit textile membranes whose resulting forms include non-developable and/or doubly curved surfaces.

A prototype developed at ETH Zurich (M. Popescu et al., 2018) used a CNC knit textile as stay-in-place formwork to construct a small-scale lightweight bridge (Figure 35).
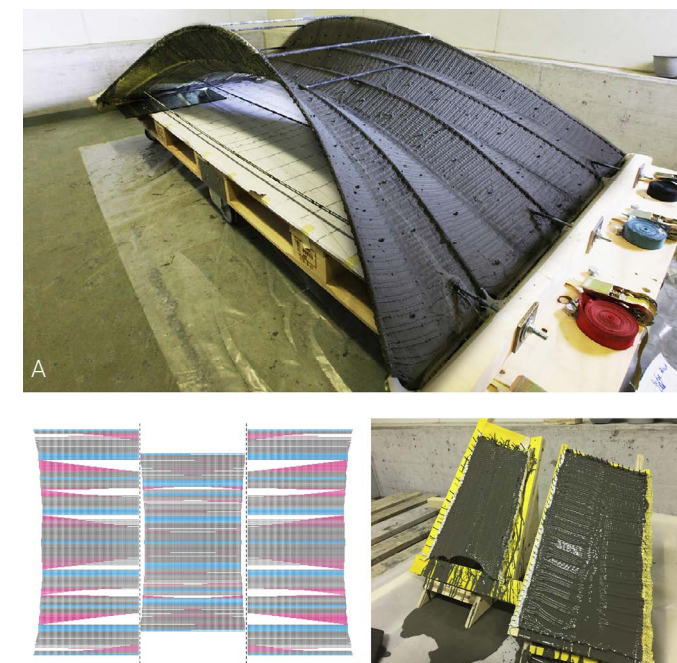
Figure 35. Construction of the concrete shell bridge prototype after a cement paste coating was applied (B) Knitting patterns used to fabricate the bridge alongside cement coating tests of different knit pattern swatches (Source (all): Popescu et al., 2018)

The textile, which was knit in three separate pieces, contained integrated elements to receive bending and ribbon elements used to tension the textile into the desired shape. Each piece was shaped to take on a doubly-curved form when stressed appropriately. Further, the development and calibration of the knitting pattern was a focus of the research and involved multiple cement coating

tests to determine the physical behavior adhesion capabilities of different stitch structures (Figure 33). Following tensioning, cement paste was applied directly to the textile in multiple steps to control deformation, which was measured by observing nodal deformations.

Subsequent research expanded on the technique, referred to as KnitCrete, that was initially developed in the concrete shell bridge prototype. The KnitCandela project used a knitted formwork that was tensioned by a timber and steel scaffolding frame to achieve the desired double-curved concrete shell.Through an iterative design process, a CNC knit technical textile was developed and fabricated as 4 discrete strips shaped specifically by the knit pattern to take on complex forms. The textile included the following features: (1) double layering for aesthetic and technical sides, (2) pockets for the insertion of inflatables, (3) varied loop sizes and densities, (4) channels for inserting tensioning cables, (5) seaming strategies, and (6) edge detailing (M. Popescu et al., 2021). Once the textile was tensioned and coated with cement paste, concrete was cast onto the stiffened textile and the pockets were deflated. Following the removal of scaffolding, the textile remained in place. The relatively simple and efficient construction process of the double curved form was made possible through the carefully designed cooperation of the CNC knit textile and the tensioning system.
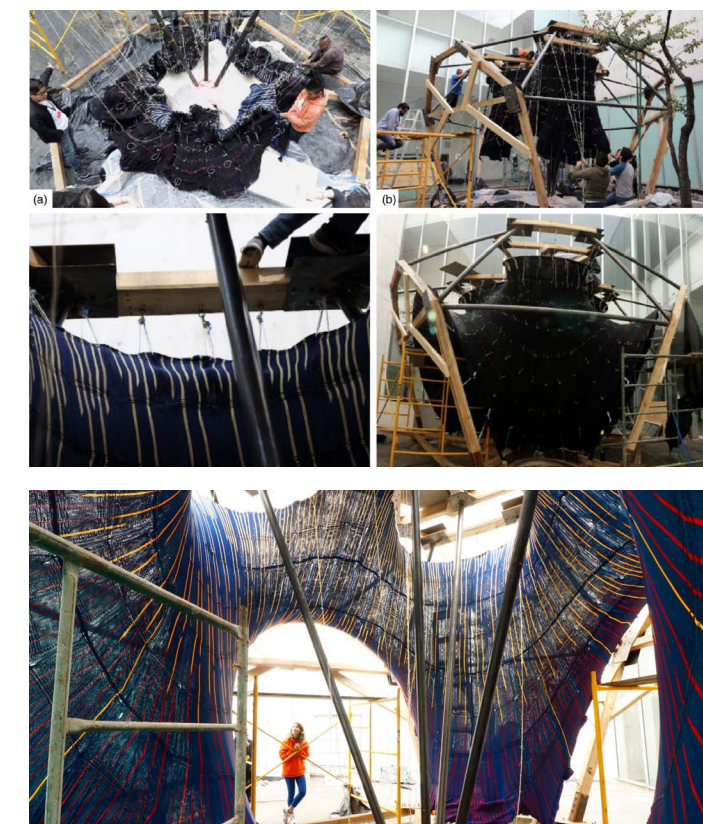

Figure 36. KnitCandela construction (Source: Popescu et al., 2021)
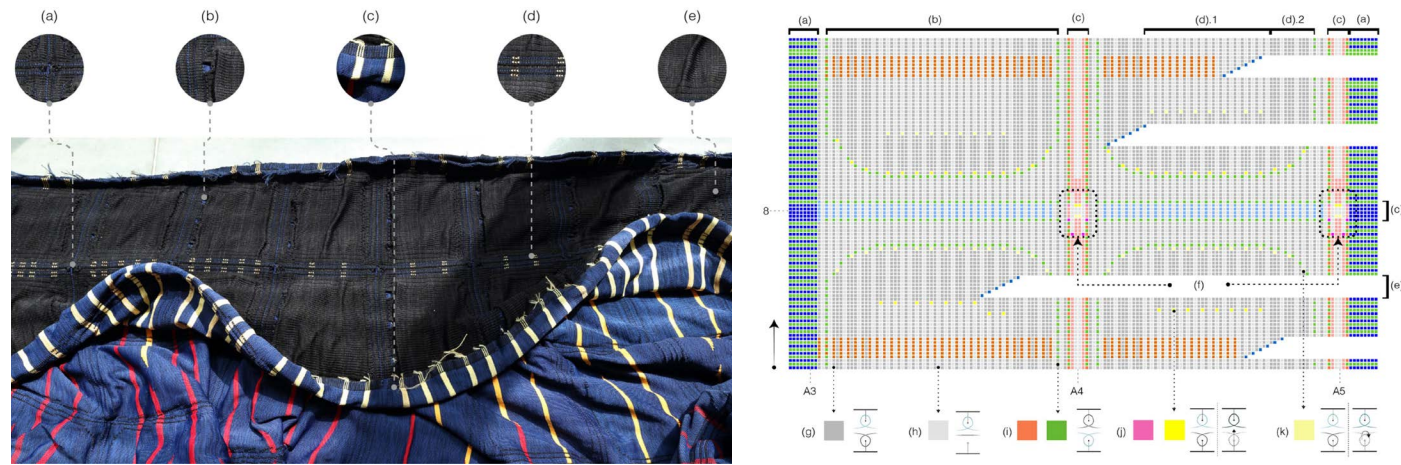
Figure 37. (A) Enlarged detail of the KnitCandela technical textile and its various functionalities, (B) Fragment of the knitting pattern used for KnitCandela (Image Source (all): Popescu et al., 2021)

The KnitNervi pavilion, constructed at MAXXI in Rome, Italy, expanded on the research developed by KnitCandela. The design and fabrication of KnitNervi proposed a method for creating a ribbed funicular concrete skeleton shell (Scheder-Bieschin, Bodea, Popescu, Van Mele, et al., 2023). Whereas the formwork system of KnitCandela relied on the textile membrane almost exclusively, KnitNervi used a steel bending active grid shell that serves both as formwork and integrated reinforcement encased by CNC knit textile shuttering. Another important distinction is the method of concrete application: instead of being applied directly to the surface of a textile, KnitNervi proposes that concrete is poured into a series of triangular ribs which are formed with rebar wrapped by a CNC knit textile. Single-layer knit panels fill the negative space between the ribs but do not perform structurally. Although concrete was not applied in the final structure, physical prototypes were created to show feasibility. Overall, the proposed system demonstrated an efficient method for fabricating concrete structures of bespoke double-curved geometries (Scheder-Bieschin, Bodea, Popescu, Van Mele, et al., 2023).

2.5 Summary and Discussion

Section 2.0 presented a state-of-the-art review of CNC knitting and flexible formwork as both discrete and cooperative fields of research. With particular focus on patterning and textile behavior, recent applications of CNC knitting beyond flexible formwork were discussed along with computational workflows for pattern creation. Further, the use of flexible formwork throughout history provided context for a broader discussion of flexible formwork fabrication as it relates to mold typologies and resulting building elements. A distinction was made between filled molds and surface molds which supported a review of flexibly formed building elements including columns, beams/trusses, floor/ceiling systems, walls, and shell structures as they relate mold typologies. Within surface molds and shell structures, further distinctions were established between hung, stretched, and pre-tensioned flexible membranes with a particular focus on research involving CNC knitted membranes. A brief discussion also addressed the differences between (non-structural) stay-in-place membranes, (structural) integrated reinforcement membranes,
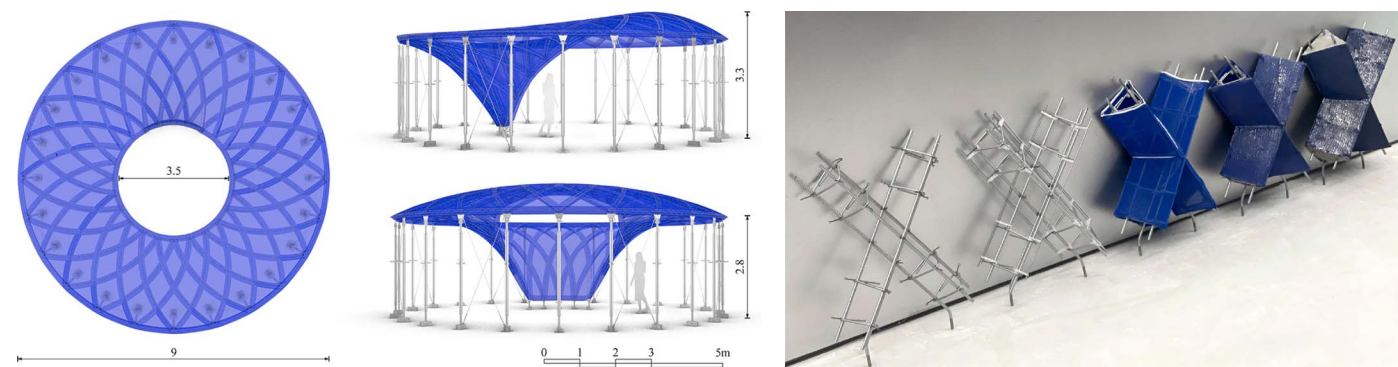
reusable membranes, and single-use / sacrificial membranes.

From the literature review, two key themes emerge which require more research: the impact of different knitting patterns on the physical behavior of a textile formwork membrane as well as its potential for reuse.

2.5.1 Patterns
The physical behavior of knitted textiles is currently difficult to simulate or predict, and limited resources exist which clearly define the impact of specific patterns, or a combination of patterns, on a textile under hydrostatic loading. Due to this unpredictability, the use of CNC knitted textiles as flexible formwork has been generally limited until the recent development of KnitCrete (M. A. Popescu, 2019). The research in this thesis will support the emerging field of CNC knitted flexible formwork by developing a greater knowledge base of pattern-influenced behavior that can be applied towards the creation of concrete building elements.

2.5.2 Reusability
Regardless of the physical properties of a textile, the reuse of flexible formwork presents challenges. As demonstrated in various prototypes discussed in Section 2.4, the knit pattern has a significant impact on a textile membrane's adhesion to concrete. In all of these prototypes, the textile was intended to stay in place, making strong adhesion essential. It was also demonstrated that more textured patterning allowed for greater control when pouring concrete directly onto the tensioned surface. There is extremely limited published research in which CNC knit textile formwork is removed from a hardened element and even less regarding reuse. This research will contribute to this currently limited knowledge base.

Certain qualities of flexible formwork which make it so appealing as a construction method also present a challenge of replicability. The likelihood that a reusable rigid mold will produce the same element multiple times is much higher than if a flexible mold were used. In a study where replicability was studied using flexible formwork, the authors noted, "…it may seem that the self-organizing nature of fabric-formed concrete might be at odds with the need for precision. However, the most important issue is to ensure accuracy where it is needed" (Pedreschi, 2011). The corresponding prototypes (Figure 39) demonstrate a series of variable columns, where the shafts were formed with flexible membranes, but the connections were vacuum-formed with a rigid

plastic insert to control accuracy and fit.

This prototype suggests a methodology for standardizing flexibly formed elements by rigidly constraining material only where absolutely necessary.

Figure 39. Flexibly formed columns where connections were strategically formed with rigid plastic molds to facilitate easy aggregation (Pedreschi, 2011)

Figure 38. (A) Plan and elevation diagrams of KnitNervi, (B) Prototypes demonstrating the feasibility of the proposed construction system (Source (all): Scheder-Bieschin et al., 2023)
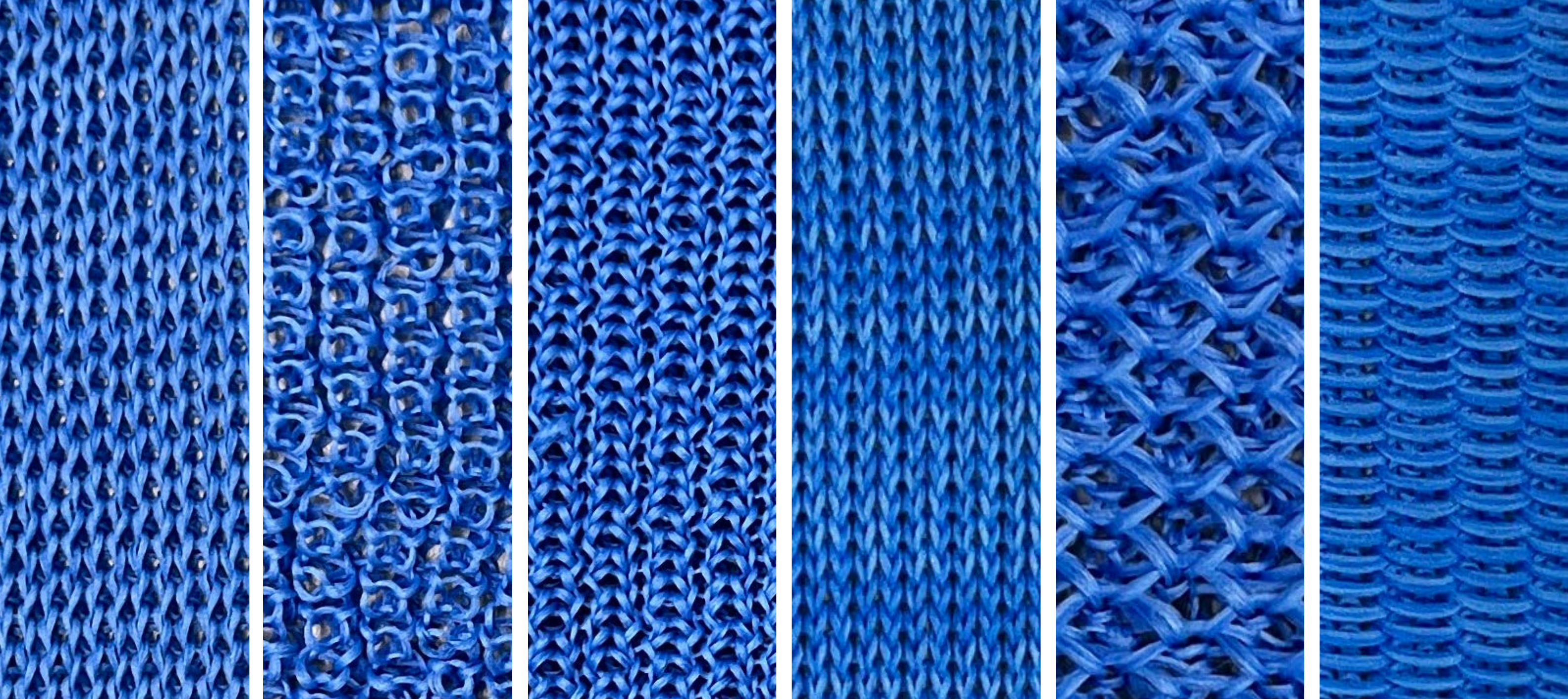
3.0 Pattern Repository

This chapter documents the various knit patterns that were selected for testing. The patterns were chosen from various sources, notably (Anishchenko, 2023). Most patterns included in this section can be considered standard in the context of knitting, as they are represented consistently across multiple sources and in ISO standards. The patterns can be categorized into three groups: 1-bed 1-yarn patterns, 2-bed, 1-yarn patterns, and 2-bed 2-yarn patterns. These classifications refer to the side or sides of the needle bed of the CNC knitting machine on which each pattern is knitted.

To facilitate comparison, all patterns were initially knit with 4 polyester yarns held together and sized to form a 300x300mm square testing sample within a cruciform shape. Pattern gauge/sizing was calibrated by knitting smaller samples of equal stitch count whose actual measurements, along with target dimensions, were input into an automatic stitch calculator developed in Excel. The gauging process revealed insights into the patterns' physical characteristics which will be discussed later in this chapter. Test samples were also knit using a recycled PET yarn to understand how changing the yarn type affects a pattern's gauge.

The patterns extracted from the literature review were translated to a Python script which produces bitmap files for Model9 software which supports the Steiger 9 CNC knitting machine. Within the Model9 software, these patterns were adapted to a cruciform shape to accommodate rods and weights for casting.

It should be noted that this repository and the pattern-specific information therein considers only one or two yarn types. Gauge, size, elasticity, among other factors would likely differ considerably were the yarn type to be altered, but it is also likely that certain global trends and relationships would remain consistent between patterns. This work therefore represents a replicable method for pattern comparison that would require further calibration for different yarn types.

3.1 Pattern Documentation & Motives

All patterns were photographed in an identical setup to visually preserve the size and textural differences between the patterns. Each pattern is numbered, identified, and accompanied by their motive, which refers to the repeated sequence of knitted stitches that create the pattern. The following key represents all relevant stitch actions:

Knit Front Knit Back Tuck Front Tuck Back Float Front/Back

Knit Front and Transfer to Back and vice versa

Knit back (Y1) front (Y2) Knit back (Y2) front (Y1)
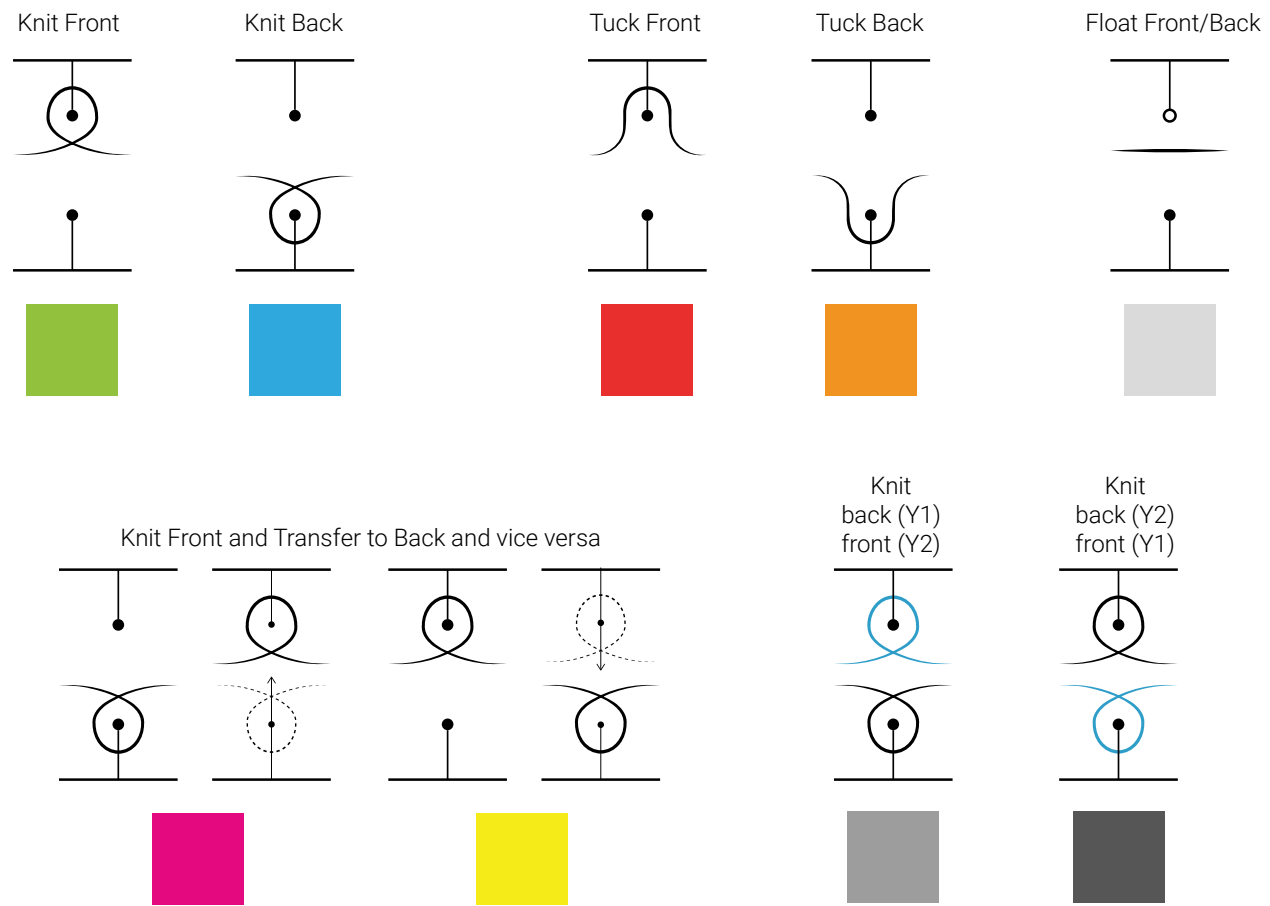
Figure 40. Partial stitch key adapted from M.A. Popescu, 2019. This key represents a small subset of the numerous stitch movements that the Steiger 9 machine is capable of performing.

2 Needle Beds, 1 Yarn

1. Milano
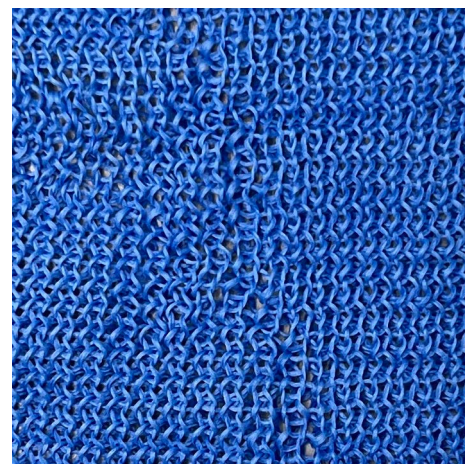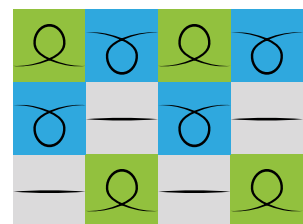
Front
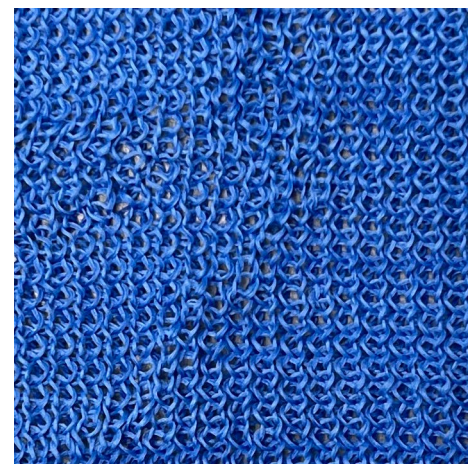
Back

2. Half Milano
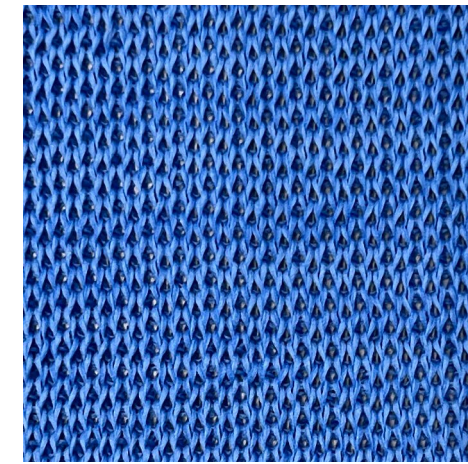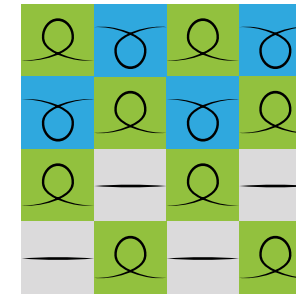
Front
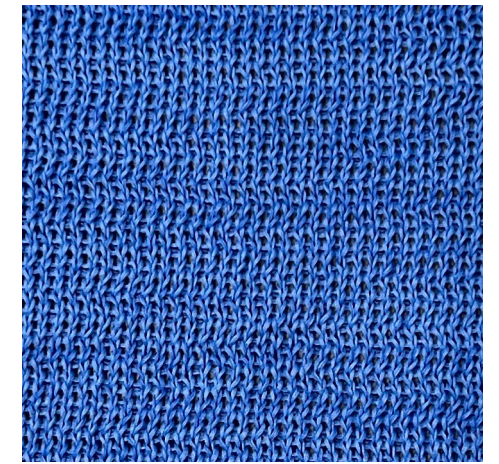
Back

3. Rib Ripple
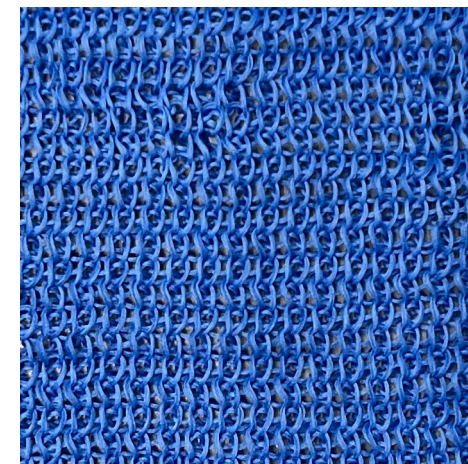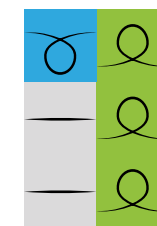
Front

Back

4. Double Half Cardigan
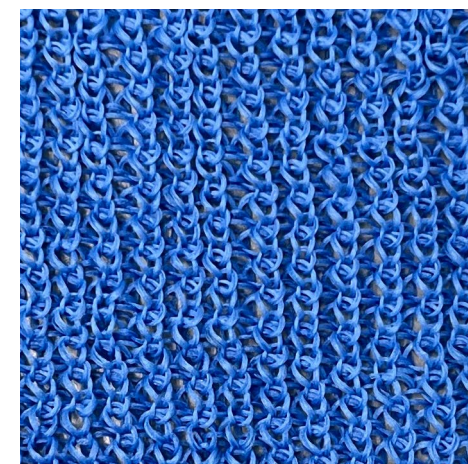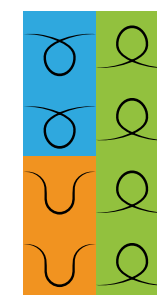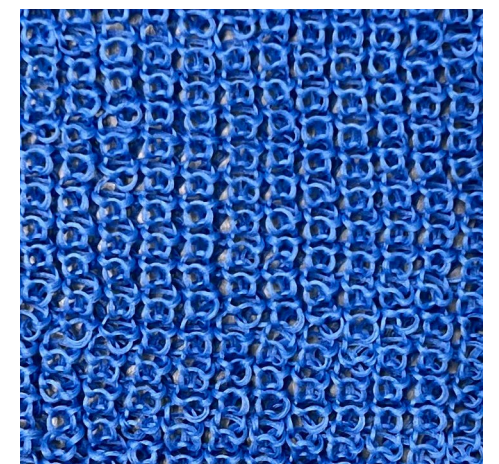
Front

Back

5. Half Cardigan

Front

Back

6. 2x2 Rib

Front

Back

7. Ripple Cardigan

Front

Back

8. Cardigan

Front

Back

1 Needle Bed, 1 Yarn

9. Crepe
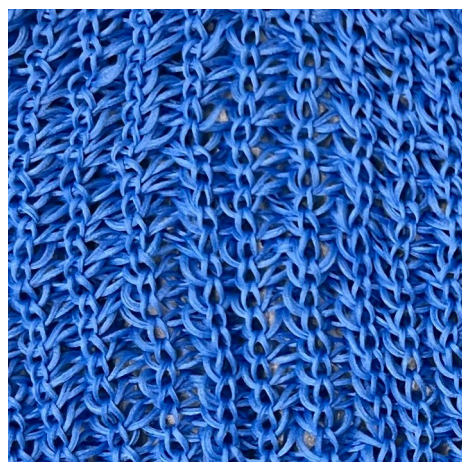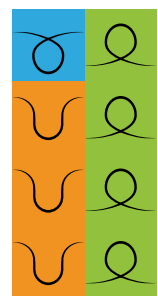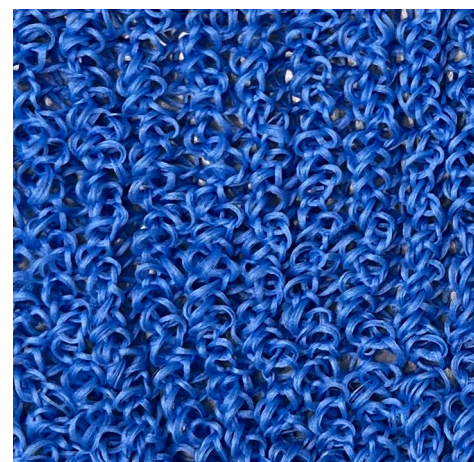
Front

Back

10. Cross-Miss
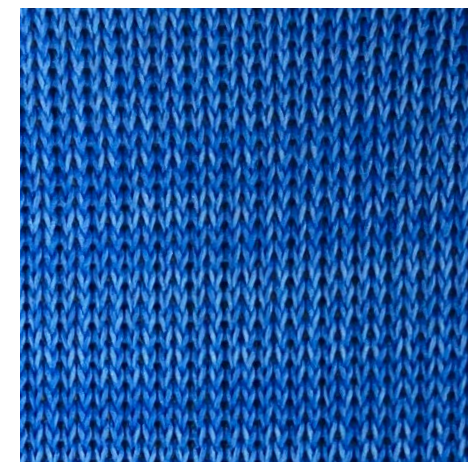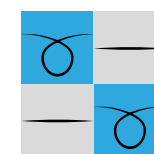
Front
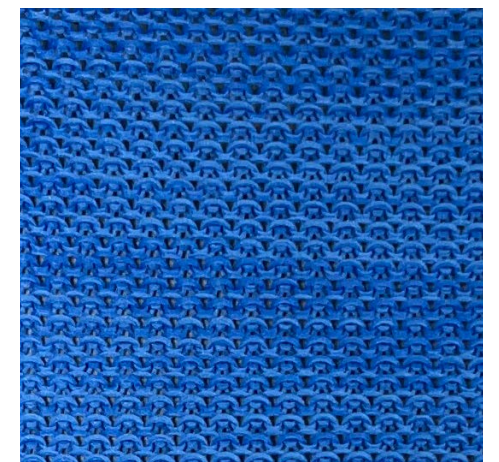
Back

11. Double Cross-Miss
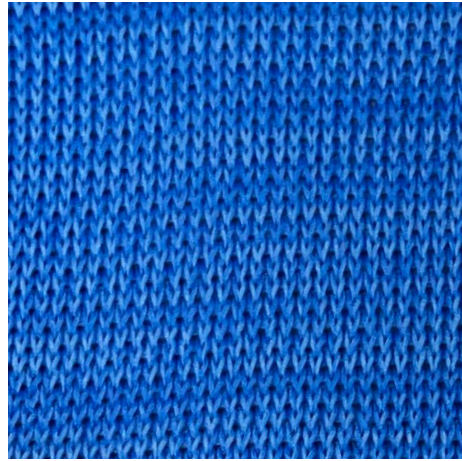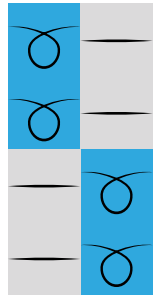
Front
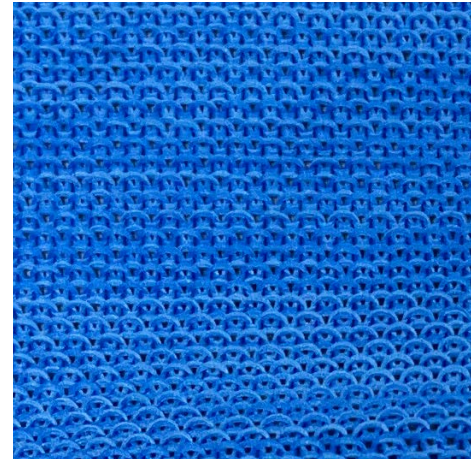
Back

14. Mock Rib
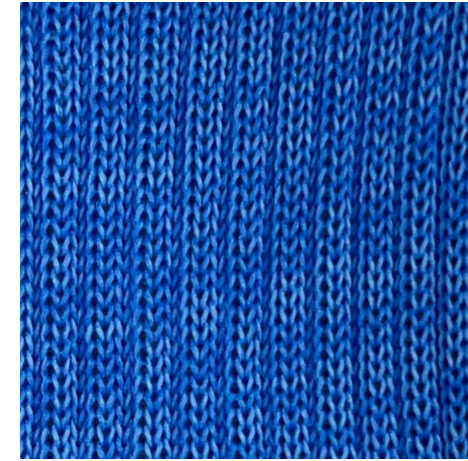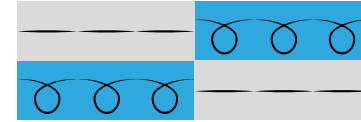
Front
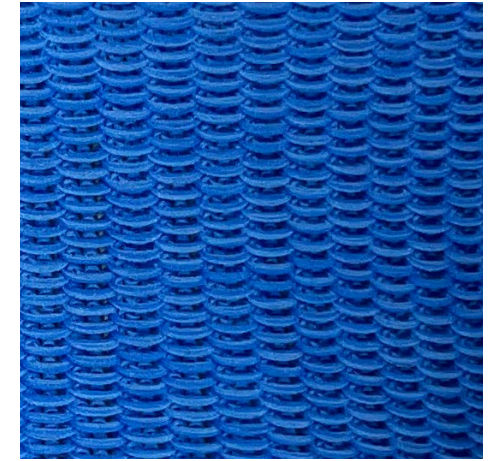
Back
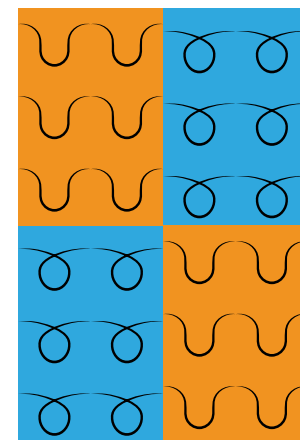
12. Double Lacoste
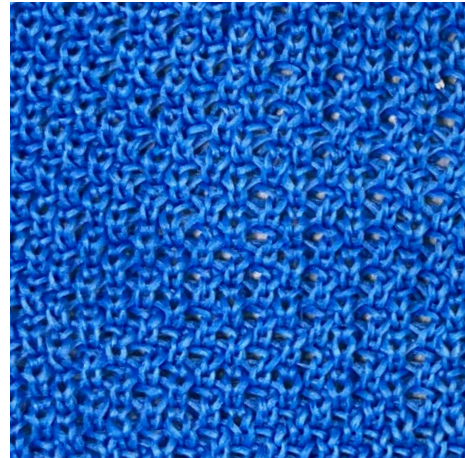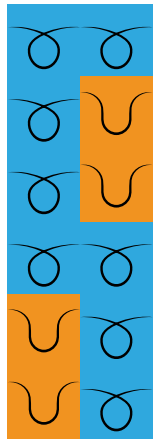
Front
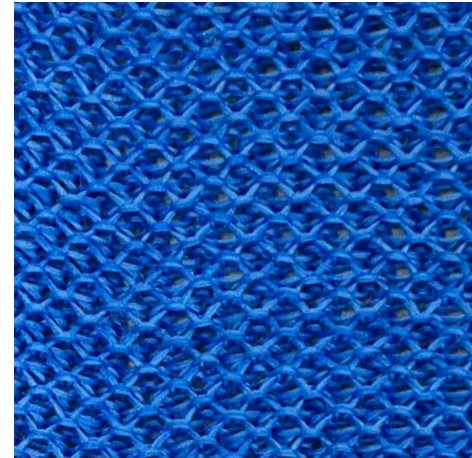
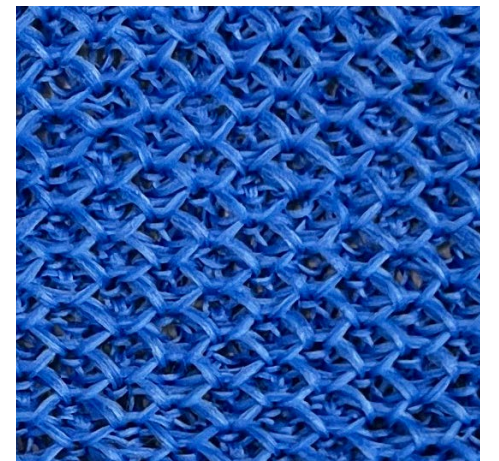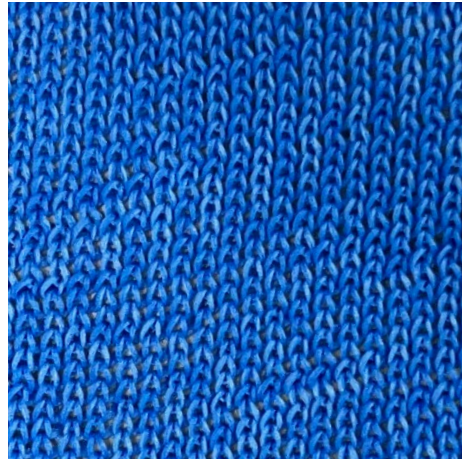Back

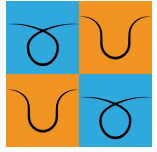## 15. Polo Pique
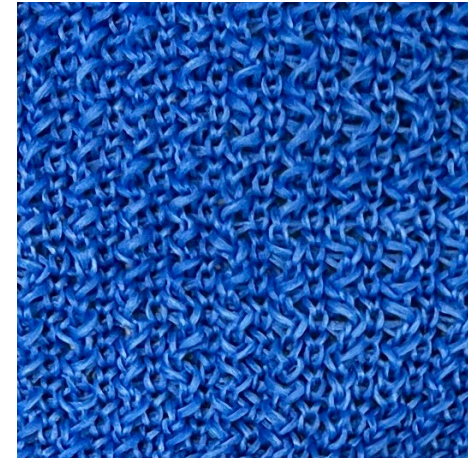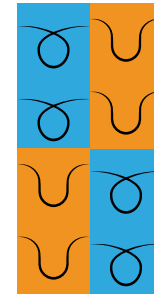
Front
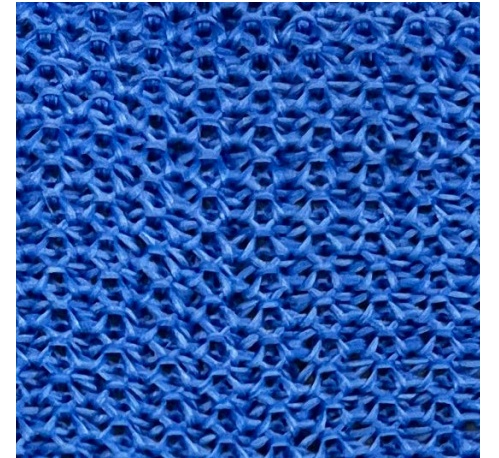
Back

13. Long Tuck Stripe
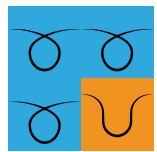
Front
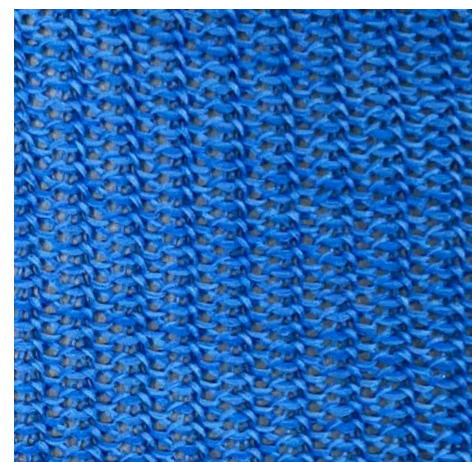
Back

16. Popcorn
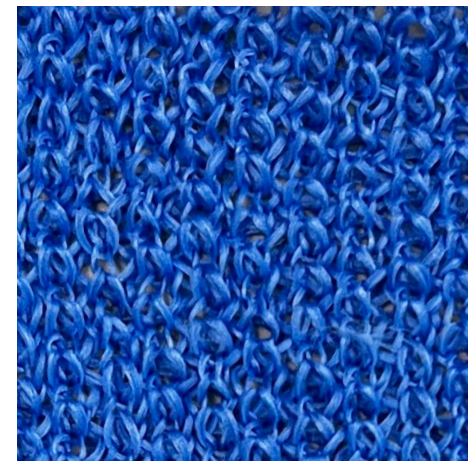
Front

Back

17. Single Cross Tuck
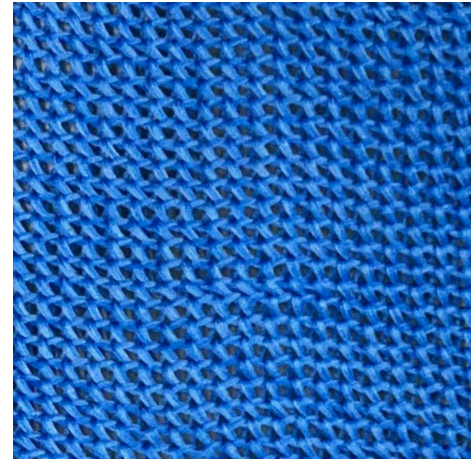
Front	Back

18. Twill Effect
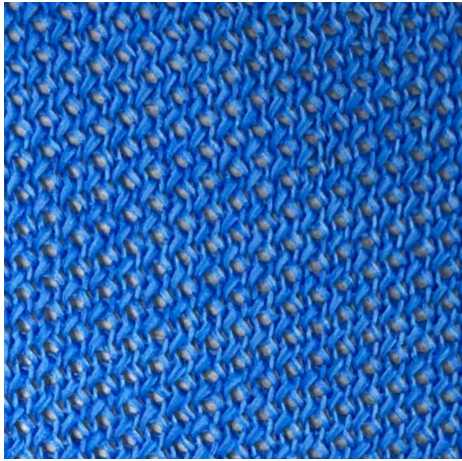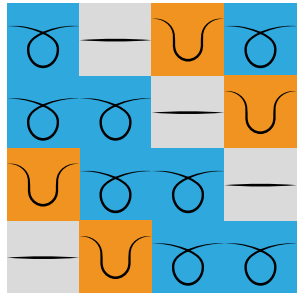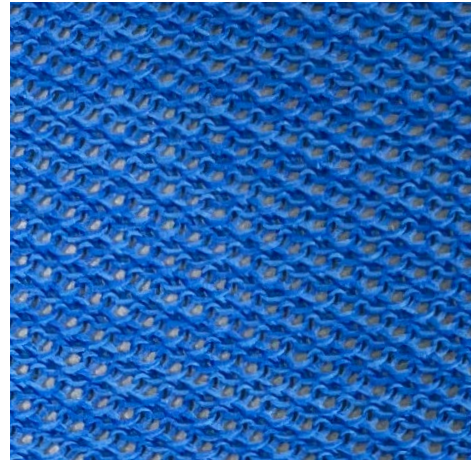
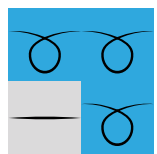| Front	Back

19. Weft Lock

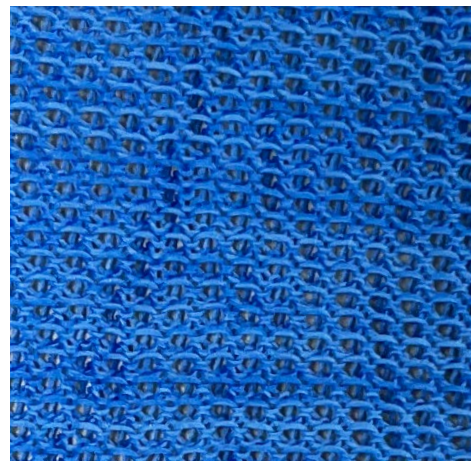| Front	Back

Figure 41. Initial gauge sample knitted to study multiple 1-Bed patterns.

3.2 Pattern Creation with Python and Model9

The Steiger 9 flat-bed weft CNC knitting machine relies on Model9 software to produce readable patterns for knitting. While there are multiple ways to create patterns using Model9, a standard approach is to generate a bitmap file in a different program that can be interpreted in Model9, where each pixel of the bitmap represents a specific needle action. At the outset of developing the pattern repository, a Python script was created to quickly generate bitmap patterns based on a list of written instructions. This exercise was also helpful to visualize and better understand the patterns selected from the literature review. Essentially, the script defines various knitting patterns, organizes them into categories, and generates bitmap files (and optionally PDFs). The script employs the following workflow:
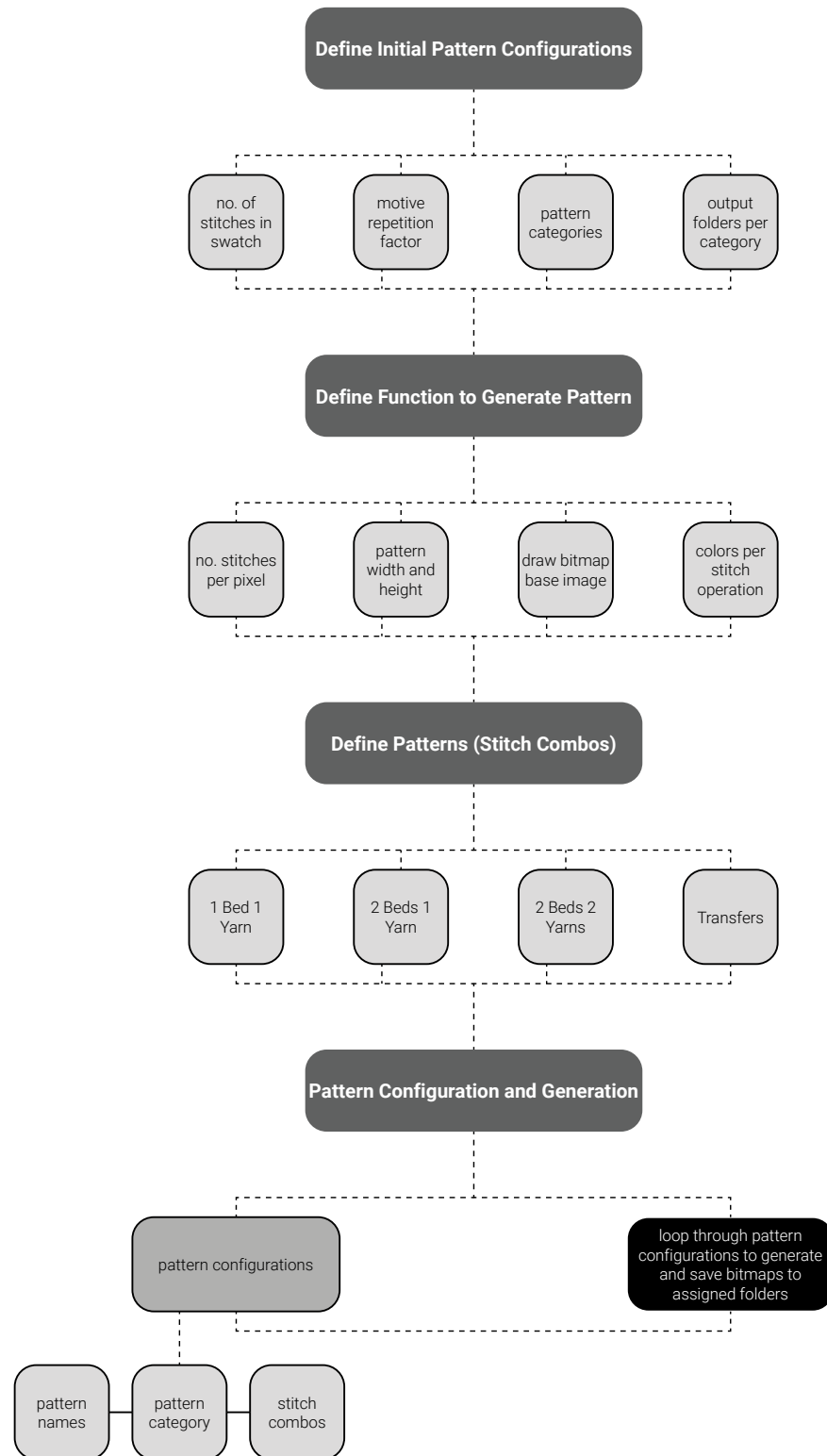

Figure 42. Workflow diagram demonstrating the Python script developed to quickly produce bitmap patterns for testing.

The result of the script is a series of bitmaps (saved in their designated folders by category) which are ready for import to Model9. Figure 40 shows an example of one of the bitmaps produced along with the list and function used to generate it.


```
twill_effect = [

    ['KF', 'FL', 'TF', 'KF'],

    ['KF', 'KF', 'FL','TF'],

    ['TF', 'KF', 'KF', 'FL'],

    ['FL', 'TF', 'KF', 'KF']

]

twill_effect = [item * (double_
repeat //2) for item in twill_
effect]
```
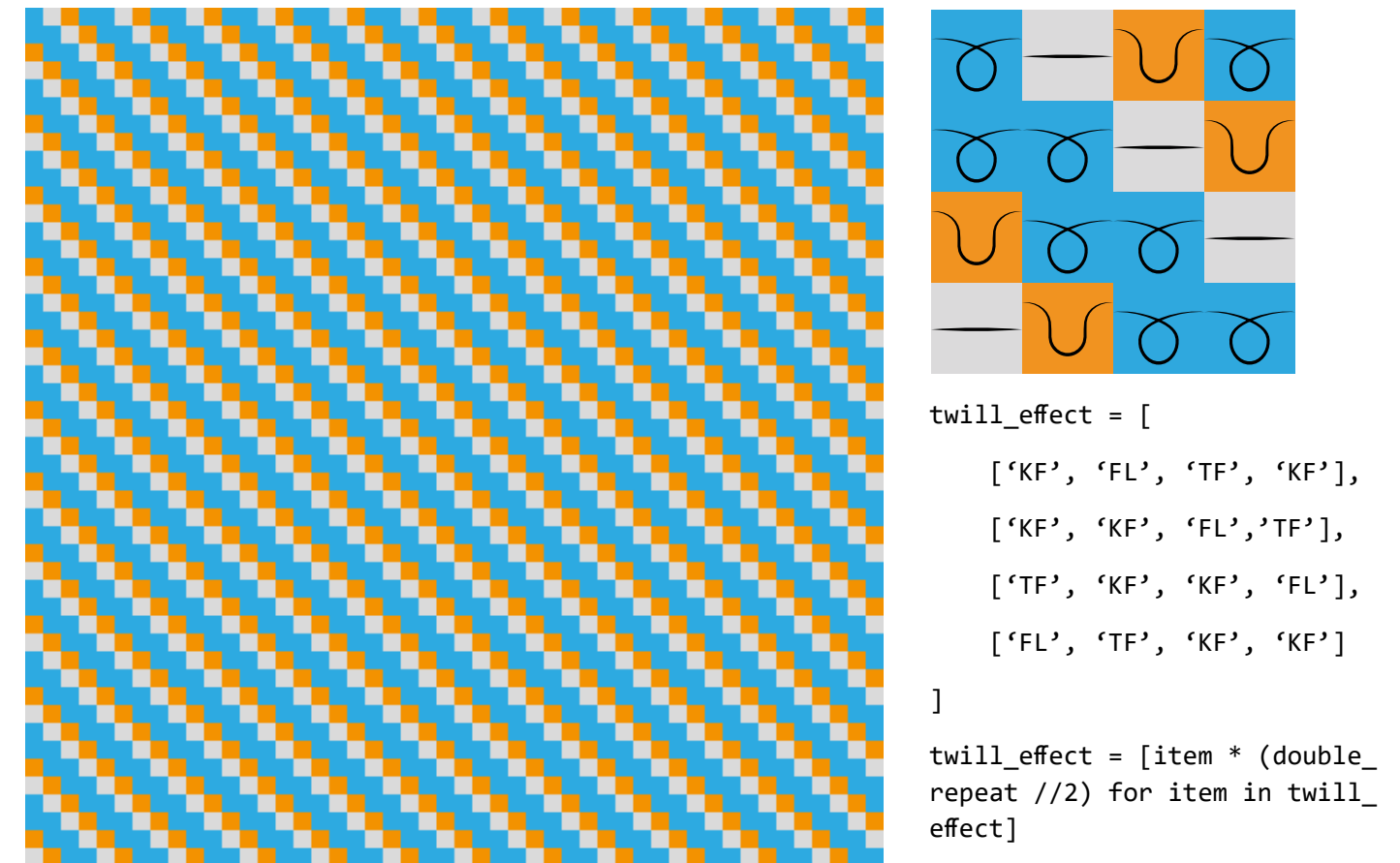
Figure 43. (Left) Complete Twill Effect bitmap pattern generated by the Python script. (Right) Repetitive sequence and list used within the script to generate the bitmap image. Double_repeat refers to the amount of times the pattern motive should be repeated to create the desired number of stitches in the X and Y direction.

In Model9, the user imports the bitmap and manually assigns a specific stitch operation to each color to define the motive. Once the motive is defined, the user can assign it to any region using a fill tool, making it easy to apply a complete pattern to a shape defined in Model9.
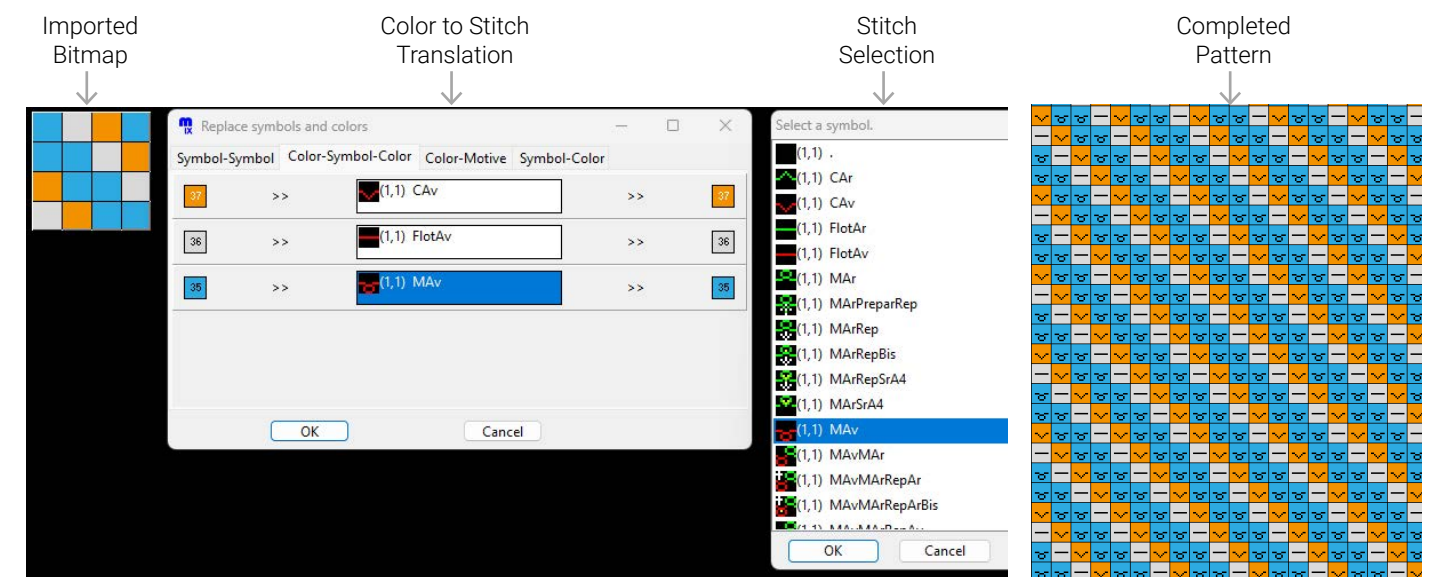

Figure 44. Translation of bitmap pattern to knitting pattern within Model9.

3.3 Pattern Gauge Calibration

In both hand knitting and machine knitting, the term 'pattern gauge' refers to the number of stitches per unit of measurement in a knitted textile measured at rest with no forces applied in either direction. Gauge is affected foremost by the pattern and stitch composition itself, but also by the yarn type, machine gauge, and tension, among other factors. Every pattern has a different gauge, resulting in different sized textiles despite a consistent stitch count. To support a uniform comparison of the patterns, two strategies were considered. The first strategy proposed knitting all samples with the same stitch count at a size large enough to accommodate the 300x300mm testing area on the casting frame. Using this method, it was difficult to predict the size of the knitted textile and whether it could accommodate the casting frame. Instead, a different method was developed in which the pattern gauge was measured and scaled to predict the number of stitches required in the X and Y direction (weft and warp direction), so that all knitted samples (regardless of stitch count) would measure 300x300mm. This method followed these steps:

1. Create Model9 .eds files of each pattern measuring 120x120 stitches.

2. Knit all 120x120 pattern swatches.

3. Measure actual dimensions (mm) of each swatch in the X and Y direction.

4. Input actual measurements into Excel formula sheet.

5. Excel formula sheet automatically generates the required number of stitches for each pattern to achieve a 300x300mm knitted square.

	Target Width (W) mm	Target Height (H) mm	Target Tab Width (W) mm	Target Tab Height (H) mm	4 yarns polyester
	300	240	60	60	
	Square Stitch Count (Gauge)				
	120	*do not adjust*			
Pattern #	Pattern Name	Measured Width (W) mm	Measured Height (H) mm	Adjusted Stitch Count (W)	Adjusted Stitch Count (H)
1	MILANO	240	140	150	206
2	HALF MILANO	250	100	144	288
3	RIB RIPPLE	205	160	176	180
4	DOUBLE HALF CARDIGAN	325	135	111	213
5	HALF CARDIGAN	320	85	113	339
6	2X2 RIB	180	225	200	128
7	RIPPLE CARDIGAN	390	85	92	339
8	CARDIGAN	230	150	157	192

Figure 45. Excerpt from Excel formula sheet developed to calculate number of stitches required in the X (weft) and Y direction (wrap) using actual pattern measurements from 120x120 sample. The formula multiplies the knitted stitch count by the target width or height and divides the result by the actual measured width or height. The target height is set to 240mm to accommodate the cruciform shape of the piece. The tabs knitted at either end account for the difference and help to form a complete 300x300mm square.

This method provided a reliable and straightforward way to produce samples of approximately the same size. More calibration and physical testing could be done to achieve more precise dimensions, but the degree of accuracy required for the casting experiments was sufficient using this method. The first set of gauge tests described was performed using 4 strands of polyester yarn. A second set of gauge tests was also performed

using a recycled PET yarn to demonstrate how changing the yarn type affects the gauge calculations. This also showed that the formula sheet could be applied to various yarn types or other changing conditions so long as physical testing and calibration is performed.

Figure 46. Group of 2-bed cruciform samples prepared using the described gauging method.
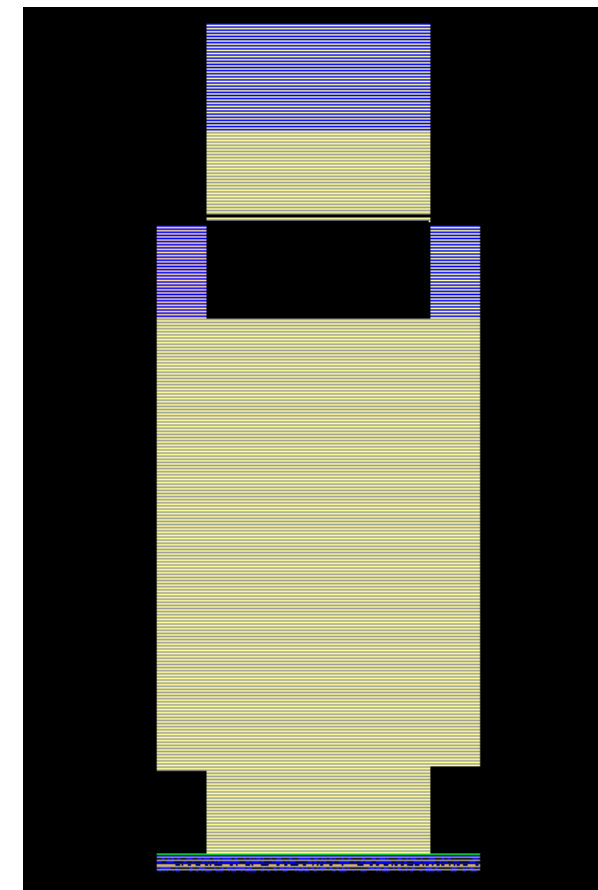

Figure 47. Example of a knit pattern for a cruciform sample in Model 9 software.

Figure 48. Double Half Cardigan cruciform sample being fitted to the casting frame during the guage calibration process. Some samples were knit multiple times to achieve precise dimensioning.

01 Milano
265mm x 135mm

02 Half Milano
300mm x 90mm

01 Milano
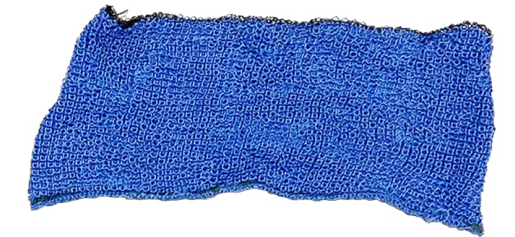240mm x 140mm

02 Half Milano
250mm x 100mm

03 Rib Ripple
240mm x 145 mm

04 Double Half Cardigan
350mm x 110mm

03 Rib Ripple
205mm x 160mm

04 Double Half Cardigan
325mm x 135mm

05 Half Cardigan
340mm x 70mm

06 2x2 Rib
180mm x 150mm

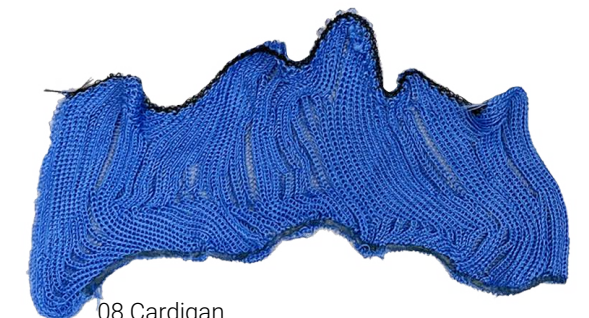05 Half Cardigan
320mm x 85mm

06 2x2 Rib
180mm x 225mm

07 Ripple Cardigan
360mm x 85mm

08 Cardigan
260mm x 125mm

07 Ripple Cardigan
390mm x 85mm

08 Cardigan
230mm x 150mm

Figure 49. 2-Bed pattern gauge samples (120x120 stitches) with actual measured dimensions. (Left) Recycled PET Yarn samples (Right) 4-strand polyester yarn samples.

09 Crepe
320mm x 120mm

10 Cross-Miss
250mm x 110mm

11 Double Cross-Miss
250mm x 110mm

12 Double Lacoste
410mm x 70mm

13 Long Tuck Stripe
390mm x 145mm

14 Mock Rib
225mm x 90mm

15 Polo Pique
410mm x 80mm

16 Popcorn
360mm x 90mm

17 Single Cross Tuck
380mm x 125mm

18 Twill Effect
380mm x 70mm

19 Weft Lock
240mm x 150mm
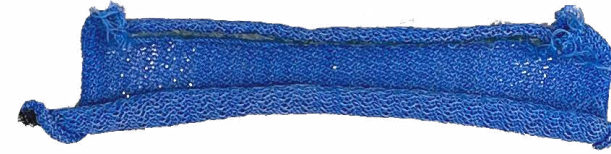
09 Crepe
340mm x 130mm

10 Cross-Miss
200mm x 135mm

11 Double Cross-Miss
215mm x 115mm

12 Double Lacoste
330mm x 90mm

13 Long Tuck Stripe
335mm x 120mm

14 Mock Rib
180mm x 115mm

15 Polo Pique
350mm x 90mm

16 Popcorn
310mm x 100mm

17 Single Cross Tuck
360mm x 110mm

18 Twill Effect
330mm x 110mm

19 Weft Lock
220mm x 145mm

Figure 50. 1-Bed pattern gauge samples (120x120 stitches) with actual measured dimensions. (Left) Recycled PET Yarn samples (Right) 4-strand polyester yarn samples.

3.4 Discussion of Results: Initial Comparison and Analysis of Knit Patterns

The method used to determine the pattern gauges was initially developed to fabricate identically sized swatches of different patterns, but it also allowed for ratio-based comparisons which relate to the physical qualities of the knit patterns. From the data gathered during pattern gauging process, certain conclusions can be drawn about the physical properties of the textiles as they relate to weft/warp stitch count ratio and total stitch magnitude.
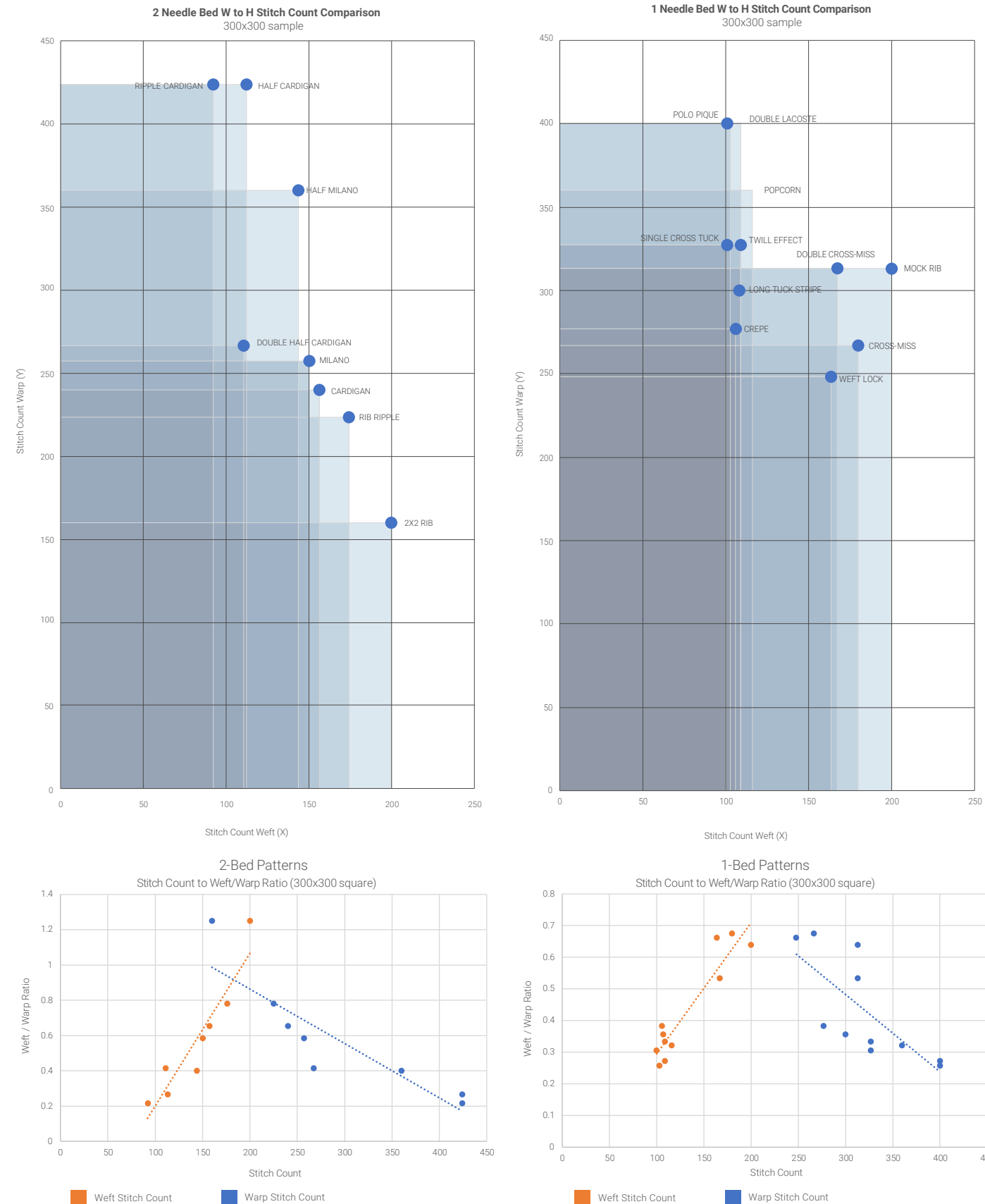
Figure 51. (Top Left) Scatter plot of 2-bed pattern charting the weft (x) to warp (y) stitch count ratios. (Bottom Left) Scatter plot of 2-bed pattern weft/warp ratios showing the positive and negative relationships between the weft and warp stitch count to the weft/warp ratio. (Top and Bottom Right) Same as described for 1-bed patterns.

When given a consistent stitch count of a 120x120 square, all patterns produced knit textiles whose X (weft) and (Y) warp dimensions were different. This indicates that the knitted textile has different physical properties in the weft and warp direction. Using the formula sheet, the following tables were generated to understand the weft and warp stitch counts required to produce a 300x300mm square along with the corresponding weft/warp ratios. From these tables, it can be inferred that the greater the numerical distance from the calculated weft/warp ratio to 1.0, the greater the dimensional discrepancy between the weft and warp edge lengths. Further, it was observed that a higher ratio tends to produce a narrower and taller fabric, while a lower ratio results in a wider and shorter fabric. The charts in Figure 51 visualize the relationship between the weft and warp stitch counts to the resulting weft/warp ratios, demonstrating that higher warp stitch counts indicate lower ratios, while higher weft stitch counts indicate higher ratios. Based on qualitative assessment, it was also observed that patterns with lower ratios, therefore greater discrepancy between the weft and warp stitch counts, showed a more pronounced difference between the amount of stretch in the weft and warp directions. Most patterns across both yarn types with a ratio below 1.0 showed more stretch in the warp direction than in the weft. Patterns with a ratio closer to 1.0 showed less difference in the amount of stretch in both directions, and patterns with a ratio above 1.0 showed more stretch in the weft direction. From observations of the selected pattern group used in this research, it can be inferred that lower ratios (higher warp stitch counts) tend to indicate greater stretch in the warp direction, while higher ratios (higher weft stitch counts) tend to indicate either less discrepancy between in the stretch in the weft and warp directions or greater stretch in the weft direction.

(A) Ripple Cardigan at rest.

(B) Ripple Cardigan stretches from 5cm to approx. 10cm in the weft direction.

(C) Ripple Cardigan stretches from 5cm to approx. 12cm in the weft direction.

(D) 2X2 Rib at rest.

(F) 2x2 Rib stretches from 5cm to approx. 20cm in the weft direction.

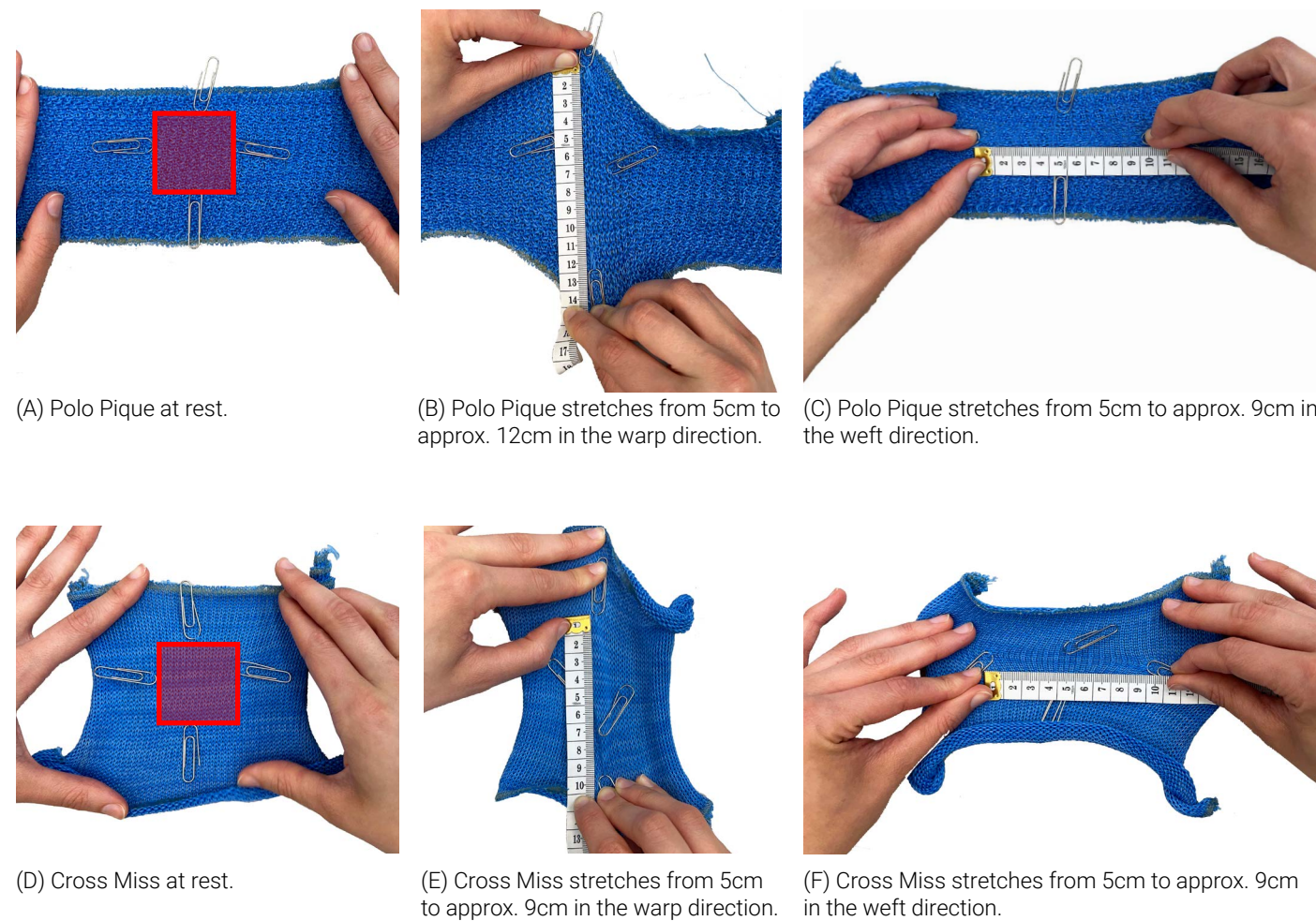(E) 2x2 Rib stretches from 5cm to approx. 10.5cm in the warp direction.

Figure 52. Of the 2-Bed pattern group, Ripple Cardigan and 2x2 Rib maintain the lowest and highest weft/warp ratios of 0.22 and 1.25 respectively. In these images, both textiles were stretched to their perceived maximum point in the weft (and warp direction within a 5x5cm area marked by pins. It is evident that Ripple Cardigan stretches more in the warp direction than in the weft, and 2x2 Rib stretches more in the weft direction than in the warp.

However, there are notable exceptions. In the polyester knit group, all but one pattern, 2x2 Rib, produced ratios below 1.0, indicating that, in general, more stitches are required in the warp direction than in the weft direction to produce a 300mm knitted square. As noted in section 2.1, ribbed patterns produce a highly elastic fabric with a weighted bias formed on both sides of the needle bed that causes the textile to recoil, differentiating it from other pattern structures. It is possible that other patterns not tested in this research would produce ratios at or above 1.0, but more testing and data would be required to confirm this. It was also observed that the 2x2 Rib pattern stretches more in the warp direction than in the weft direction, further differentiating it from others in the dataset.

Another interesting comparison is the total amount of stitches (weft x warp) required to produce the desired 300x300mm sample. A smaller total number of stitches indicates that the stitch composition produces more fabric with fewer stitches, and vice versa. From qualitative assessment, it was observed that the samples with lower total stitch amounts produced loose, flexible fabrics while samples with higher total stitch amounts produced tight, less flexible fabrics. Therefore, the global stretch of a knitted textile was observed to be related to the total stitch amount. Of the 2-Bed pattern group, Double Half Cardigan and Half Milano emerged as extremes with the lowest and highest stitch count respectively. In this case, Half Milano requires approximately 1.75 times the number of stitches than Double Half Cardigan to create a 300x300mm square. Close-up images of both textiles (Figure 50) reveal a visual difference in stitch tightness and density. Of the 1-Bed pattern group, Crepe and Mock Rib emerged as extremes. Mock Rib requires over 2 times the number of stitches than Crepe to create a 300x300mm square. Images of these patterns also reveal differences in density.

(A) Polo Pique at rest.

(B) Polo Pique stretches from 5cm to approx. 12cm in the warp direction.

(C) Polo Pique stretches from 5cm to approx. 9cm in the weft direction.

(D) Cross Miss at rest.

(E) Cross Miss stretches from 5cm to approx. 9cm in the warp direction.

(F) Cross Miss stretches from 5cm to approx. 9cm in the weft direction.

Figure 53. Of the 1-Bed pattern group, Polo Pique and Cross Miss maintain the lowest and highest weft/warp ratios of 0.26 and 0.68 respectively. In these images, both textiles were stretched to their perceived maximum point in the weft and warp direction within a 5x5cm area marked by pins. It is evident that Polo Pique stretches more in the warp direction than in the weft. For Cross Miss, which has a ratio closer to 1.0, the weft/warp stretch capacity is approximately equal.

2 Bed Pattern (Polyester)	X to Y Stitch Count	X/Y Ratio
Ripple Cardigan	92 / 424	0.22
Half Cardigan	113 / 424	0.27
Half Milano	144 / 360	0.40
Db. Half Cardigan	111 / 267	0.42
Milano	150 / 257	0.58
Cardigan	157 / 240	0.65
Rib Ripple	176 / 225	0.78
2x2 Rib	200 / 160	1.25

1 Bed Pattern (Polyester)	X to Y Stitch Count	X/Y Ratio
Polo Pique	103 / 400	0.26
Double Lacoste	109 / 400	0.27
Single Cross Tuck	100 / 327	0.31
Popcorn	116 / 360	0.32
Twill Effect	109 / 327	0.33
Long Tuck Stripe	107 / 300	0.36
Crepe	106 / 277	0.38
Double Cross-Miss	167 / 313	0.54
Mock Rib	200 / 313	0.64
Weft Lock	164 / 248	0.66
Cross-Miss	180 / 267	0.68

2 Bed Pattern (Polyester)	X * Y Stitch Count	Total Stitch Magnitude
Double Half Cardigan	111 x 267	29,637
2x2 Rib	200 x 160	32,000
Cardigan	157 x 240	37,680
Milano	150 x 257	38,550
Ripple Cardigan	92 x 424	39,008
Rib Ripple	176 x 225	39,600
Half Cardigan	113 x 424	47,912
Half Milano	144 x 360	51,840

1 Bed Pattern (Polyester)	X * Y Stitch Count	Total Stitch Magnitude
Crepe	106 x 277	29,362
Long Tuck Stripe	107x300	32,100
Single Cross Tuck	100 x 327	32,700
Twill Effect	109 x 327	35,643
Weft Lock	164 x 248	40,672
Polo Pique	103 x 400	41,200
Popcorn	116 x 360	41,760
Double Lacoste	109 x 400	43,600
Cross-Miss	180 x 267	48,000
Double Cross-Miss	167 x 313	52,271
Mock Rib	200 x 313	62,600

DOUBLE HALF CARDIGAN — FRONT — BACK

CREPE — FRONT — BACK

HALF MILANO — FRONT — BACK
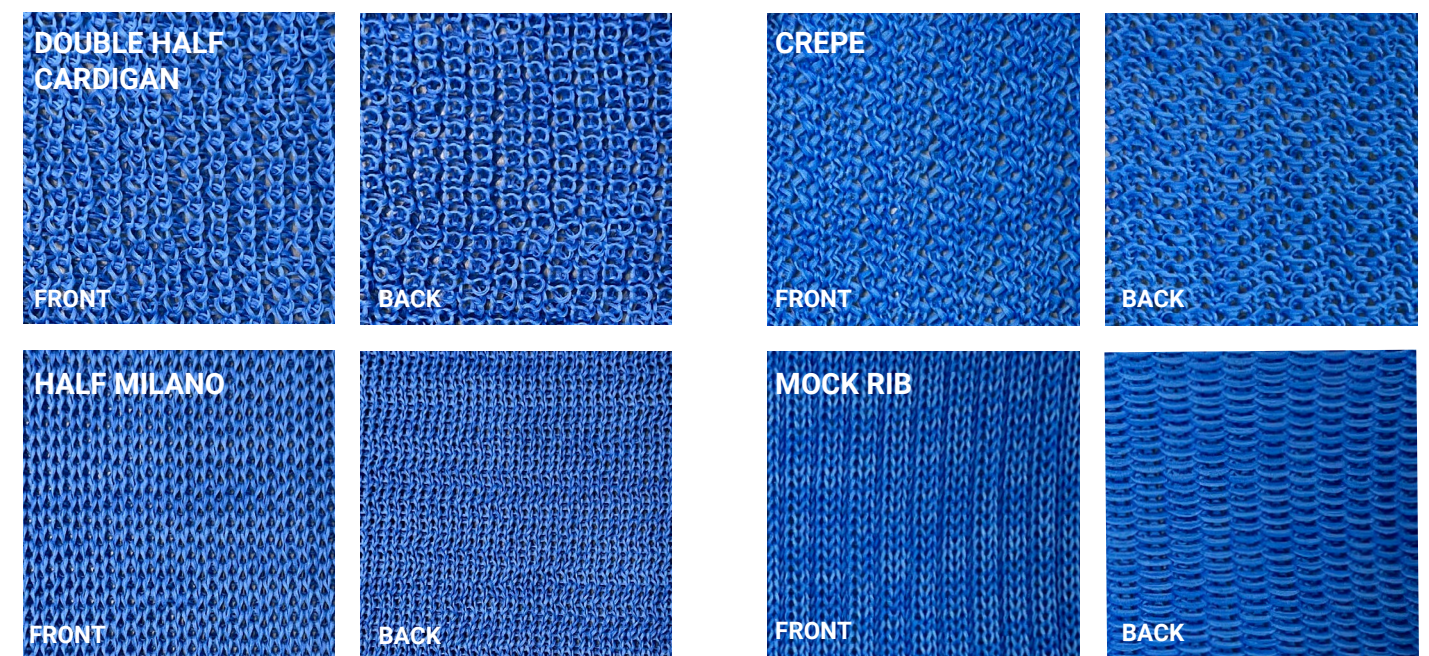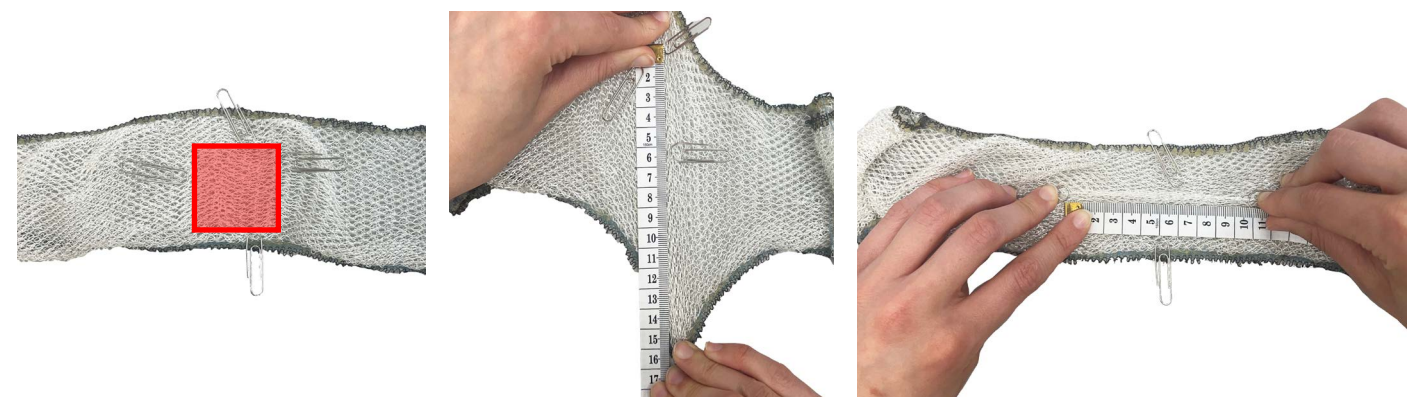
MOCK RIB — FRONT — BACK

Figure 54. (Top) 2-Bed and 1-Bed tables showing the weft/warp ratios for patterns knitted with polyester yarn. (Middle) 2-Bed and 1-Bed tables showing the total stitch magnitude for patterns knitted with polyester yarn. (Bottom Left) Close-Up images of 2-Bed patterns with the smallest (Double Half Cardigan) and largest (Half Milano) total stitch magnitude knitted in polyester yarn. (Bottom Right) Close-up images of 1-patterns with the smallest (Crepe) and largest (Mock Rib) total stitch magnitude knitted in polyester yarn.

The inclusion of the recycled PET yarn in addition to the 4-strand polyester yarn in the gauge testing provided insights into how yarn type affects the physical dimensions and properties of the knit patterns. Like Figure 50, the following tables describe the weft and warp stitch counts required to produce a 300x300 knitted sample using recycled PET yarn. It is evident from comparing the polyester to the recycled PET tables that the weft/warp ratios nor the total stitch magnitudes remain identical between the two yarn types. The exact ratios between these values are also not preserved, but certain extremes and approximate orders of magnitude remain consistent. For example, of the 2-Bed patterns, Double Half Cardigan maintains the lowest stitch magnitude across both yarn types, whereas Half Milano has the highest (polyester) and second highest (recycled PET) stitch count. Of the 1-Bed patterns, Mock Rib maintains the highest stitch magnitude across both yarn types, while Crepe, Long Tuck Stripe, and Single Cross Tuck consistently have the three lowest stitch counts. A comparison of the weft/warp ratios between the yarn types also reveals some consistent trends. For example, of the 2-Bed patterns, Half Cardigan and Ripple Cardigan maintain the two lowest ratios across both yarn types, while 2x2 Rib maintains the highest weft/warp ratio across both yarn types. It is also notable that, when knitted in PET yarn, the weft/warp ratio of the 2x2 Rib pattern is below 0.83. This shows that while most patterns with a ratio below 1.0 stretch more in the warp direction, this cannot be considered absolute. Of the 1-Bed patterns, Polo Pique and Double Lacoste retain the lowest ratios, while Weft Lock and Cross-Miss retain the highest ratios. It is also evident from the close-up photographs that the physical appearance of the knit patterns changes considerably when the yarn type is changed. Specifically, the polyester yarn exhibited much greater stitch definition in patterns with lower stitch magnitudes. A clear example is Double Half Cardigan; in the polyester swatch, each stitch can be easily identified and there is a clear difference between the front and back sides of the fabric. The same pattern knit in the recycled PET has a more obscure demarcation of stitches and shows almost no perceptible difference between the front and back sides when at rest.

2 Bed Pattern (Recycled PET)	X to Y Stitch Count	X/Y Ratio
Half Cardigan	106/514	0.21
Ripple Cardigan	100/424	0.24
Half Milano	120/400	0.30
Double Half Cardigan	103/327	0.31
Cardigan	138/288	0.48
Milano	136/267	0.51
Rib Ripple	150/248	0.60
2x2 Rib	200/240	0.83

1 Bed Pattern (Recycled PET)	X to Y Stitch Count	X/Y Ratio
Double Lacoste	88/514	0.17
Twill Effect	95/514	0.18
Polo Pique	88/450	0.20
Popcorn	100/400	0.25
Single Cross Tuck	95/288	0.33
Long Tuck Stripe	92/248	0.37
Crepe	113/300	0.38
Mock Rib	160/400	0.40
Cross Miss	144/327	0.44
Double Cross Miss	144/327	0.44
Weft Lock	150/240	0.63

2 Bed Pattern (Recycled PET)	X * Y Stitch Count	Total Stitch Magnitude
Double Half Cardigan	103x327	33,681
Milano	136x267	36,312
Rib Ripple	150x248	37,200
Cardigan	138x288	39,744
Ripple Cardigan	100x424	42,400
2x2 Rib	200x240	48,000
Half Milano	120x400	48,000
Half Cardigan	106x514	54,484

1 Bed Pattern (Recycled PET)	X * Y Stitch Count	Total Stitch Magnitude
Long Tuck Stripe	92x248	22,816
Single Cross Tuck	95x288	27,360
Crepe	113x300	33,900
Weft Lock	150x240	36,000
Polo Pique	88x450	39,600
Popcorn	100x400	40,000
Double Lacoste	88x514	45,232
Cross Miss	144x327	47,088
Double Cross Miss	144x327	47,088
Twill Effect	95x514	48,830
Mock Rib	160x400	64,000

(A) Double Lacoste at rest.

(B) Double Lacoste stretches from 5cm to approx. 15cm in the warp

(C) Double Lacoste stretches from 5cm to approx. 10cm in the warp direction.

(D) Weft Lock at rest.

(E) Weft Lock stretches from 5cm to approx. 10cm in the warp direction.

(F) Weft Lock stretches from 5cm to approx. 13cm in the weft direction.

Figure 55. Of the 1-Bed pattern group, Double Lacoste and Weft Lock maintain the lowest and highest weft/warp ratios of 0.17 and 0.63 respectively. In these images, both textiles were stretched to their perceived maximum point in the weft and warp direction within a 5x5cm area marked by pins. It is evident that Double Lacoste stretches more in the warp direction than in the weft. The Weft Lock textile stretches more in the weft direction than in the warp, identifying it as an outlier.

DOUBLE HALF CARDIGAN
FRONT — BACK

HALF CARDIGAN
FRONT — BACK

LONG TUCK STRIPE
FRONT — BACK

MOCK RIB
FRONT — BACK

Figure 56. (Top) 2-Bed and 1-Bed tables showing the weft/warp ratios for patterns knitted with PET yarn. (Middle) 2-Bed and 1-Bed tables showing the total stitch magnitude for patterns knitted with PET yarn. (Bottom Left) Close-Up images of 2-Bed patterns with the smallest (Double Half Cardigan) and largest (Half Cardigan) total stitch magnitude knitted in PET yarn. (Bottom Right) Close-up images of 1-patterns with the smallest (Long Tuck Stripe) and largest (Mock Rib) total stitch magnitude knitted in PET yarn.

(A) Half Cardigan at rest.

(B) Half Cardigan stretches from 5cm to approx. 15cm in the warp

(C) Half Cardigan stretches from 5cm to approx. 13cm in the warp direction.

(D) 2x2 Rib at rest.

(E) 2x2 Rib stretches from 5cm to approx. 14cm in the warp direction.

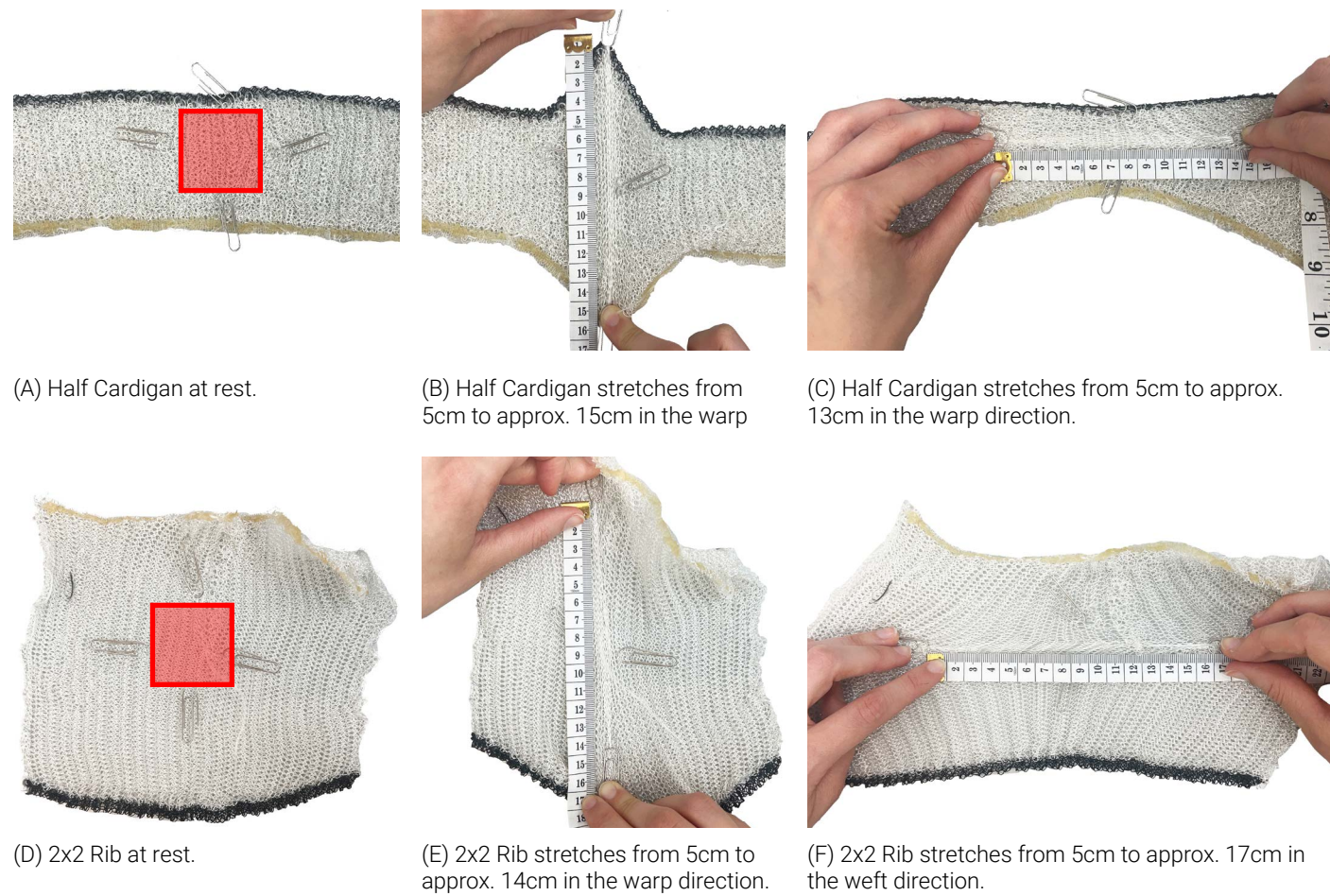(F) 2x2 Rib stretches from 5cm to approx. 17cm in the weft direction.

Figure 57. Of the 2-Bed pattern group, Half Cardigan and 2x2 Rib maintain the lowest and highest weft/warp ratios of 0.21 and 0.83 respectively. In these images, both textiles were stretched to their perceived maximum point in the weft and warp direction within a 5x5cm area marked by pins. It is evident that Half Cardigan stretches more in the warp direction than in the weft, and 2x2 Rib stretches more in the weft direction than in the warp.

The comparison of the total stitch magnitude and the weft/warp stitch count ratios across two yarn types reveals that despite some inconsistencies, the patterns which represent extreme values tend to remain at these extremes across both yarn types. While most of the data suggests that patterns with weft/warp stich count ratios below 1.0 stretch more in the warp direction, inconsistencies exist. For example, when knit with PET yarn, 2x2 Rib (ratio 0.83) and Weft Lock (ratio 0.63) stretch more in the weft direction. A more nuanced conclusion is that patterns with higher ratios (close to or above 1.0) tend to either stretch more equally in the weft in warp direction or stretch more in the weft direction. However, this conclusion cannot be taken as absolute to do the relatively small number of patterns tested and the certainty that the physical properties of each pattern will change in similar experiments where the yarn type, machine gauge, and/or tension are different. While the weft/warp stitch count ratio plays a role in the textile's behavior, an analysis of the micro-behavior stitch types (and their specific composition) would likely create a more accurate prediction of textile behavior, although this is beyond the scope of this thesis.

Therefore, this comparison underscores the need for physical prototyping and calibration to determine an accurate pattern gauge when changing the yarn type or other factors. This data can be interpreted as a general guide for understanding basic qualities and extremes of the specified knit patterns such as overall stretchiness, fabric density, or a greater stretch capacity in the weft or warp direction but should be verified through physical testing when applied in a different context.
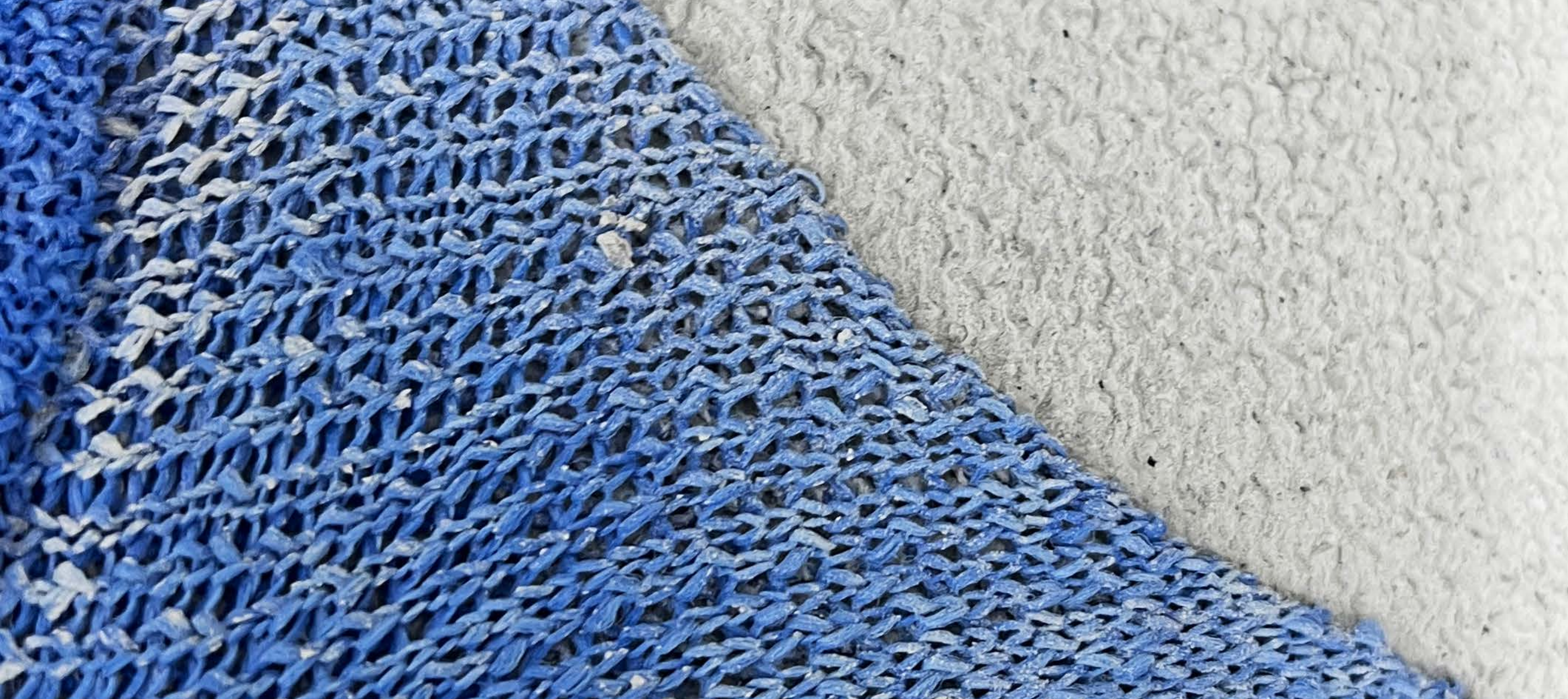
4.0 Determining Pattern-specific Curvature through Concrete Casting

Following fabrication and analysis, the knit patterns were tested as flexible formwork membranes to study their influence on deformation under loading and the resulting curvature of the cast forms. This chapter describes the experiment setup and methodology used to produce all 21 cast samples, findings from the fabrication process, and a pattern-specific curvature repository which visually and quantitatively documents the results of the casting process. Finally, a discussion and analysis identify trends and extremes and make relevant connections to the pattern repository in section 3.0. This body of research also forms the basis for the selective pattern combination performed in chapter 5.0.

Figure 58. Group of cast samples arranged from perceived smallest to largest deformation after casting.

4.1 Experiment Setup and Methodology

All 21 cast samples were performed on a 5-tier casting frame designed to accommodate five 300x300mm samples at one time. The square shape was chosen to create an even loading condition in both the X and Y directions, and, after some initial plaster tests, the 300x300 size with a 10mm thickness was determined to show enough curvature to generate data for a productive analysis. While all knitted patterns were sized to measure 300x300mm at rest, pre-tensioning was necessary to control deformation. This was accomplished by suspending sandbags from a steel rod threaded through channels on all four edges of the cruciform textiles. The degree of pre-tensioning was determined by weighing an initial hardened sample (approximately 2.6kg) and calibrating the eight suspended sandbags to apply an equal and opposite load. Theoretically, and assuming linear elastic behavior of the textile, this would create a state of equilibrium where there is zero net force acting on the textile. However, as knitted fabrics are anisotropic materials, the relationship between the applied force and the deformation is not strictly linear, which leads to deformation.

Figure 61 demonstrates the sequence of the casting process used to fabricate all 21 samples. This method was expanded on previous work performed in the Tailored Materiality Research group at TU Delft (Kariouh, 2023) involving a singular 500x500 frame. The process described in Figure 61 is as follows:

1. Supports are inserted into MDF receiving channels on the wood frame.

2. MDF panel is placed on supports and inserted into the wood frame.

3. Textile Pre-Tensioning: Cruciform textile is stretched over the frame, steel rods are inserted into textile's channels, and sandbag weights are suspended from the steel rods.

4. 10mm plastic edges define the boundary for the casting and help to create an even layer of concrete.

5. Concrete is applied directly to the textile and rests on the MDF panel until an even layer is attained.

6. The supports are removed and the MDF panel is released, allowing the textile to deform under the hydrostatic load from the concrete.

7. (Not pictured) The cast is covered with a plastic film and allowed to cure for 2-3 days before removal from the frame.

The concrete mix used in all pattern casts is adapted from previous research (Kariouh, 2023) but replaces the largest aggregate with the immediately smaller size and redistributes the volume. The mixing process is as follows: the cement and aggregate are measured and combined using an electric mixer set to a low speed for one minute. Then, on low speed, water is added gradually over 1 minute. The mix is then scraped down from the sides of the bowl and agitated by hand to ensure even mixing and release any aggregate or cement stuck to the bottom. Finally, the electric mixer is set to high speed and the concrete is mixed for 2 minutes. The workability, relatively uncomplicated mixing process, and weight of this mix worked well in showing pattern-specific curvature and deformation under loading but produced a rough surface texture and often formed surface cracking under more extreme deformation. The 10mm thickness helped to show deformation even in the stiffest of patterns, but likely could have been reduced. While experimenting with other mixes would add value to the research, it is beyond the scope of this thesis.

1 Liter	(kg)
Water	0.508
Cement CEM III / B 42.5 N	1.268
Fine Aggregates 0.125 - 0.25mm	0.176
Fine Aggregates 0.25 - 0.5mm	0.262
Fine Aggregates 0.5 - 1.0mm	0.526
Fine Aggregates 1.0 - 2.0 mm	1.908

Figure 59. Concrete mix matrix for 1 Liter adapted from Kariouh, 2023.

Figure 60. Highly deformed samples on the casting frame.

(01)

(02)

(03)

(04)

(05)

(06)
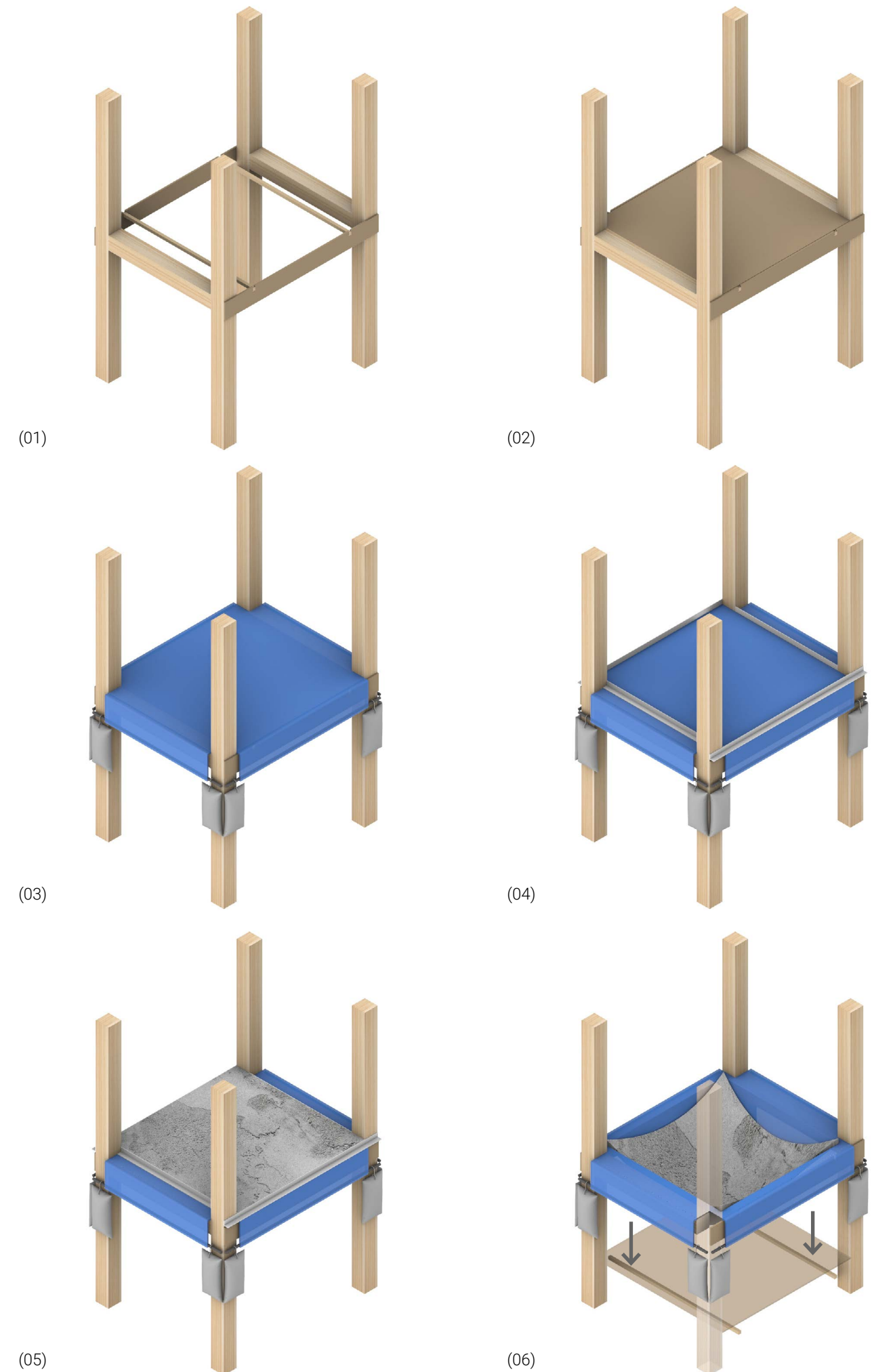
Figure 61. Diagram demonstrating the sequence of the casting process followed to fabricate all 19 samples.

Figure 62. (A) Casting frame prepared to receive concrete (B) Casting frame with deformed samples (C) Applying concrete directly to the textile (D) Evening the concrete to a consistent thickness with the help of plastic guides and a drywall spatula (E) Deformed sample after the supporting MDF panel is released.

This method was effective in quickly producing multiple pattern casts which provided data about each pattern's degree of deformation under concrete loading. However, certain imperfections in the setup and process influenced the forms of the pattern casts. Specifically, it was highly difficult to ensure uniform deformation across both the weft and warp axes respectively. This can be attributed to a few factors. First, the removal of the MDF stabilizing plates required some shimmying which may have caused uneven distribution of concrete in certain areas after the initial application, resulting in uneven deformation. In an idealized setup, the stabilizing plate would be removed in a completely uniform manner, which was not possible in this analog format. Further, the channels which held the steel rods ands suspended sandbag weights were stitched by hand to prevent shrinkage or distortion of the textiles due to the introduction of a new pattern. While every attempt was made to keep the channels completely straight, some imperfections may have caused the rods to be angled, rather than level, which would contribute to uneven deformation. Finally, the frame was likely not completely level due to imperfections in the frame construction and unevenness of the ground in the casting area; this would also influence uneven deformation of the concrete. Further research into this casting methodology should therefore explore how best to control deformation while the concrete is wet to ensure even deformation across the weft and warp axes respectively.

4.2 Pattern-specific Casting and Curvature Repository

This section documents the analysis method and results of the casting process. In the first section of this sub-chapter, the 3D scanning and Grasshopper script used to analyze the samples is introduced. The second section of this chapter contains the Curvature Repository, which synthesizes information about the physical properties of each sample and how each pattern performed during the casting and de-molding process.

4.2.1 Methodology for Extracting Curvature with 3D Scanning and Grasshopper
To best understand the curvatures created in each sample, 3D scanning offered an efficient solution to create detailed 3D mesh files that could be imported to Rhino 3DM. Each sample was placed on an identical setup of four bricks oriented longitudinally (which also corresponds to the direction of the warp axis) and scanned using the Photogrammetry function in Polycam. Lidar scanning was also tested, but in this scenario, photogrammetry scanning produced a more accurate scanned geometry likely due to the relatively small size of the samples. These scans were then downloaded as .obj files and imported to Rhino as meshes.

Figure 63. 3D scans of one sample showing the high degree of detail achieved through photogrammetry scanning.

Figure 64. Polycam interface showing an excerpt of the 19 3D scans.

Following 3D scanning and importation to Rhino, a Grasshopper script was developed to extract and quantify the principal curvatures of each sample in the weft and warp directions. The goal of the analysis is to understand if and how the principal curvatures of the cast samples are affected by the anisotropic behavior of the textiles observed in Chapter 3.0, specifically how the principal curvatures differ in the weft versus warp direction. The output of the script is a visual preview of the principal curvatures along with the corresponding magnitudes of their rise, span, and ratio of rise to span. The script also calculates the cast shapes' surface area and computes the difference from the original 300x300 square formed prior to deformation and shows a visual preview of the deformed shape in plan view. Throughout the workflow, it is assumed that the scanned geometry is imperfect due to errors made in the casting process. To set the foundation for a simplified analysis process, the script approximates an 'average' symmetrical warp and weft curvature that is as close as possible to the scanned form.

The script is activated by toggling between the meshes, which are organized in a single list where the index numbers correspond to the pattern number. Changing a number slider to the desired pattern prompts the script to generate the curvature and surface area for the corresponding mesh. The workflow is light and takes only a few seconds to calculate per mesh, although some mesh simplification was required to keep the script running efficiently, but this did not significantly affect the extracted curvatures. The script uses the logic described in Figure 65.
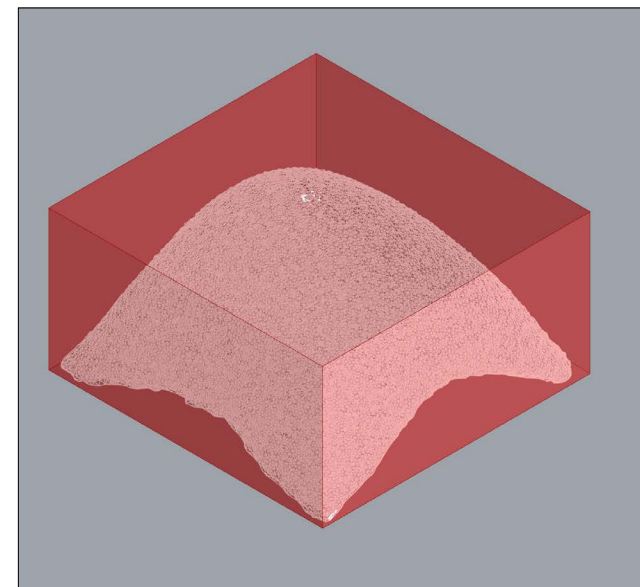
(02) Bounding Box is created around scanned mesh.

EXAMPLE PATTERN:
#4 Double Half Cardigan

START

(01) 3D scanned mesh is imported to Rhino.
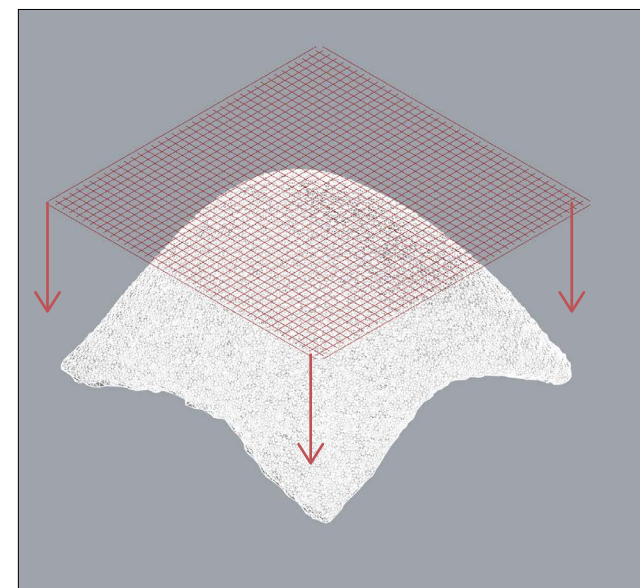
(03) Two intersecting arrays of lines in the X and Y direction are created by dividing the top surface of the bounding box.
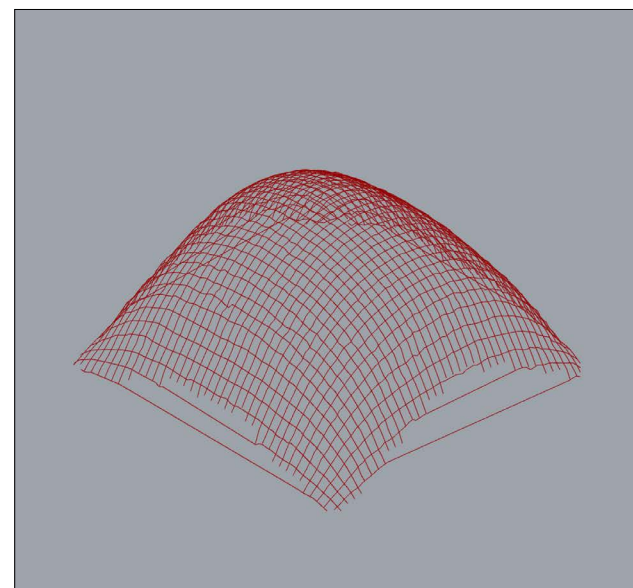
(04) Both arrays are projected onto the top surface of the scanned mesh.

WEFT DIRECTION
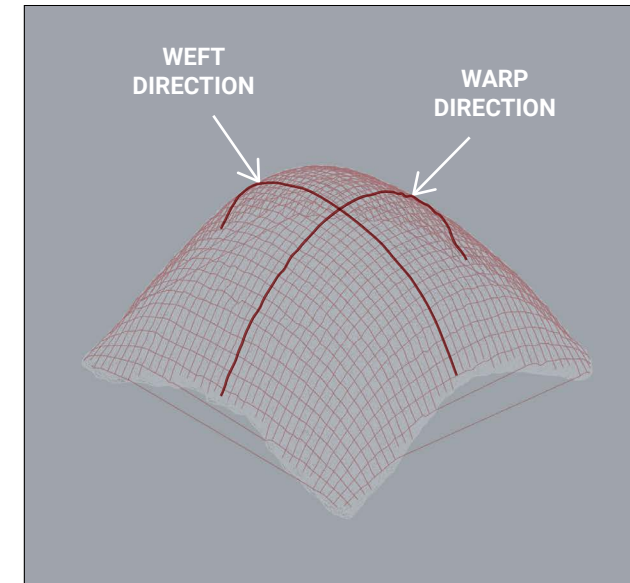
WARP DIRECTION

(05) The middle curve from both the X and Y curve sets is extracted to find the approximate middle point of the scanned edges.
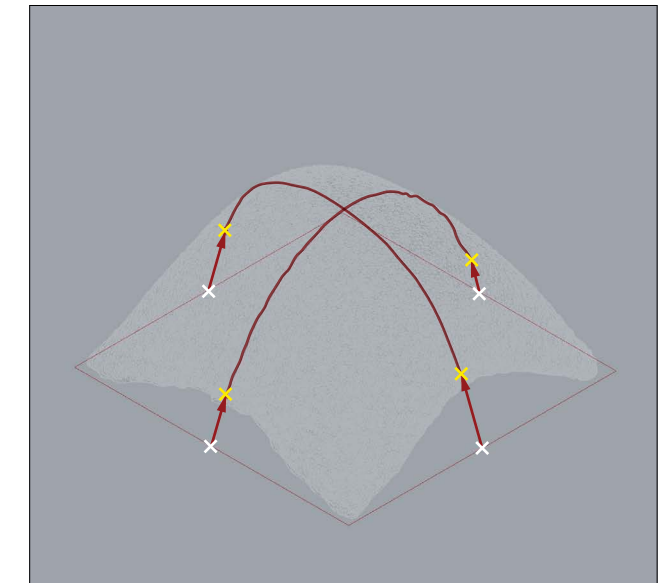
(06) Midpoints of the bounding rectangle are projected to the mesh following the vector direction between the midpoints of the bounding rectangle and the endpoints of the extracted curves.

MIRRORED CURVES

AVERAGE WEFT EDGE CURVE

AVERAGE WARP EDGE CURVE
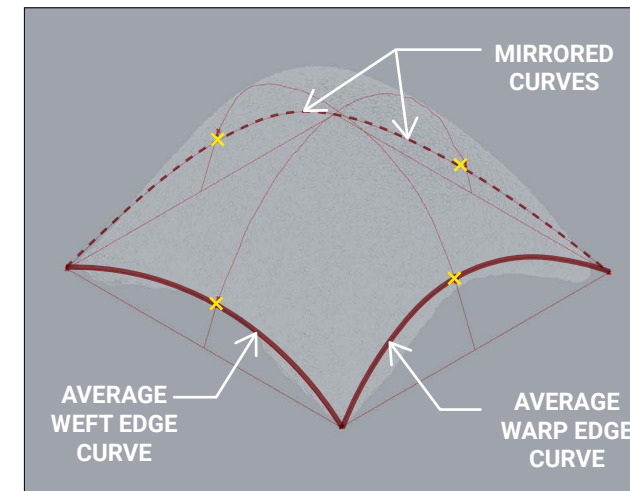
(07) The z-coordinate of the projected midpoints are averaged in the X and Y to produce 1 curve in the X and Y respectively that is mirrored to form a complete shape.
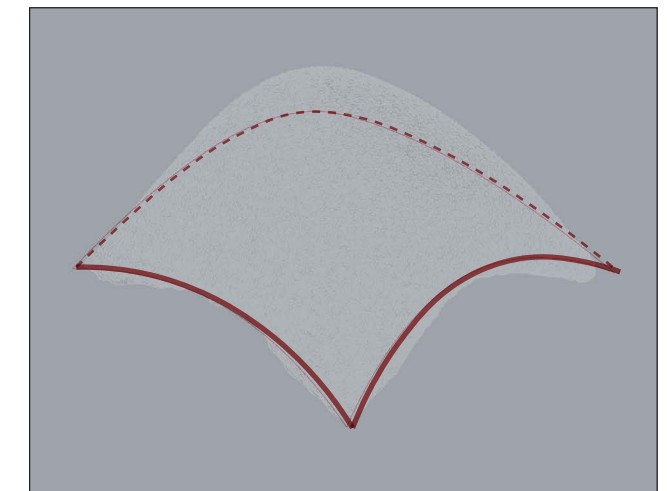
(08) All four edge curves are now averaged and extracted. The next step is to approximate the principal curvatures in the weft and warp direction.
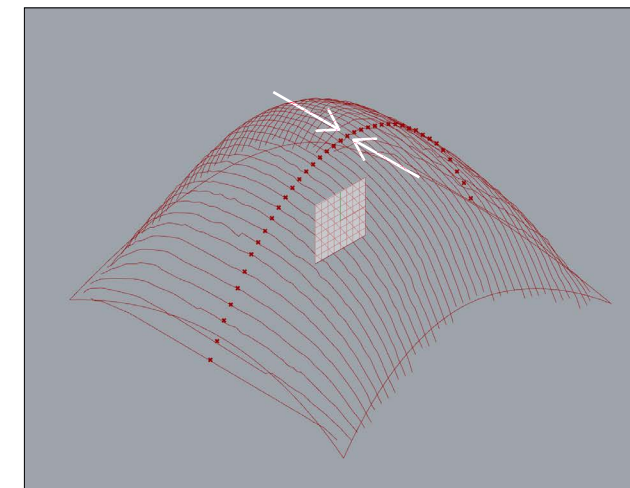
(09) Principal warp curvature extracted: the highest point on every projected curve in the weft direction is projected to the YZ plane to form the basis for the warp curve.
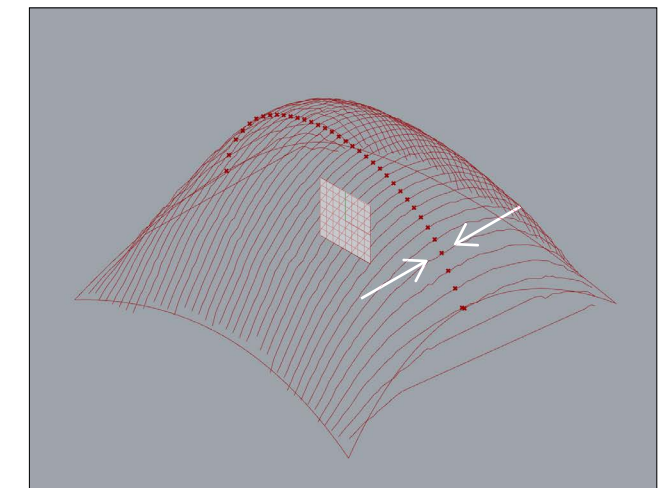
(10) Principal weft curvature is extracted: the highest point on every projected curve in the warp direction is projected to the XZ plane to form the basis for the weft curve.
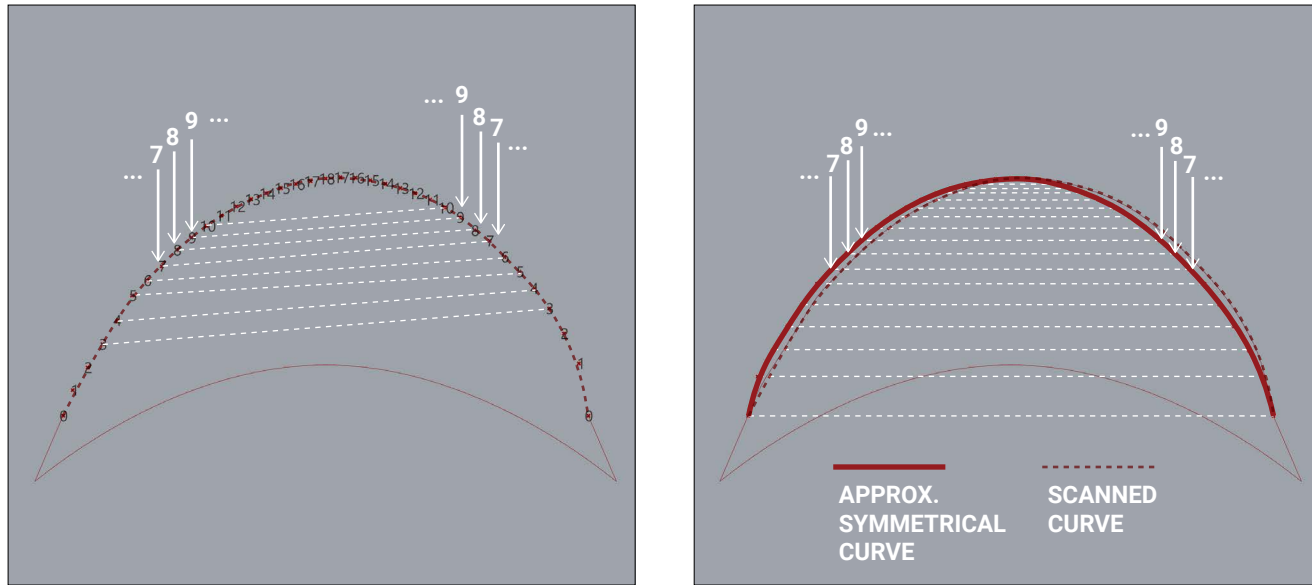
(11) To create a symmetrical curve from the extracted points, the list is split into two groups at the midpoint and corresponding relationships are established.

(12) The z-coordinates of the corresponding points are averaged to generate a symmetrical nurbs curve. Steps 11-12 are applied separately to the weft and warp directions.
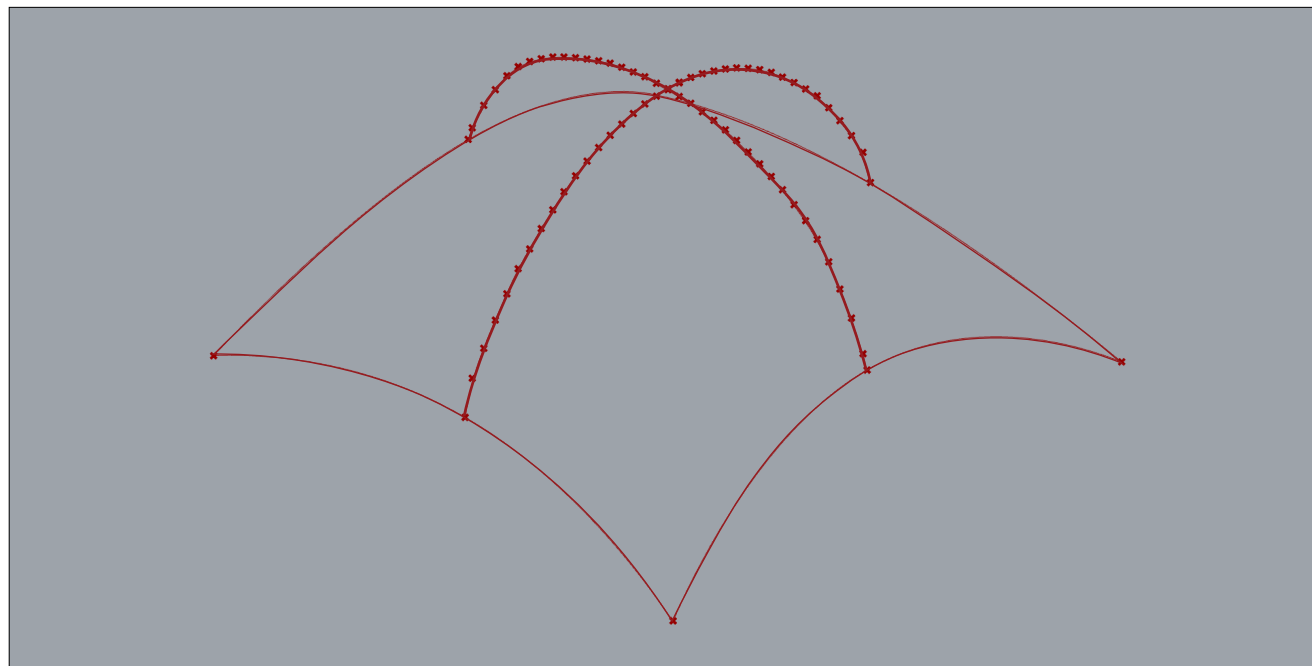
(13) The completed curves ready for further analysis.

shape area =92013.414255

warp span =242.690165
warp rise =109.29966

warp rise/span =0.450367
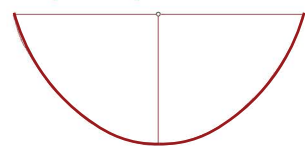
weft span =238.831309
weft rise =85.355392

weft rise/span =0.357388
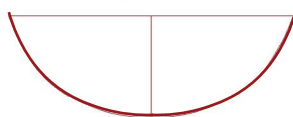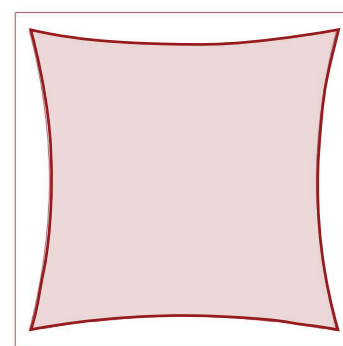
(14) The warp and weft curvatures along with the shape surface area are projected to the C-Plane and baked. This process is completed for all scanned shapes to form the basis of the curvature repository.

Figure 65. Grasshopper workflow diagram.
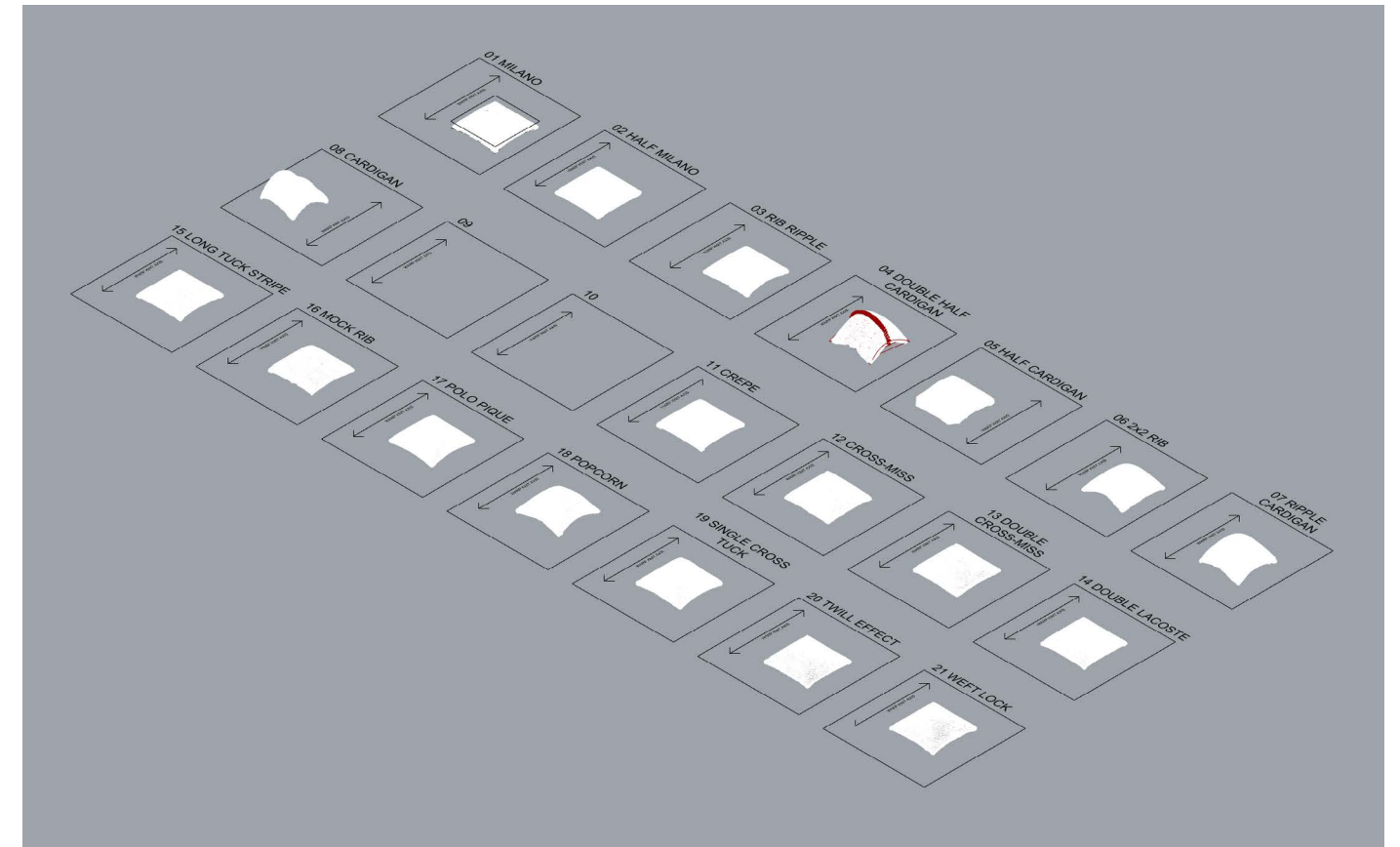
Figure 66. Complete Rhino file showing all 19 scanned patterns marked by warp orientation.

Figure 67. Excerpt of baked curvatures and corresponding surface areas and rise/span ratios.

4.2.2 Documentation of Pattern-specific Curvature

The following section forms a repository containing information about the curvature and surface area of each pattern cast, photographs following demolding, and fabrication-based findings such as the weight of the textile, the time required to remove the textile, damages to the textile following casting, and other notes specific to each pattern cast. All casts were performed on the 'right side,' or front of the knit textiles and used the 4-strand polyester yarn and the concrete mix described in Section 4.1. During demolding, all textiles were removed by the author and the removal process was timed. The timing was performed to create data that suggests a relative but replicable way to understand to what degree each pattern adheres to the textile. This information, along with the extent of damage to the textile, could support conclusions about the reuse potential of the textiles or inform pattern selections where strong adhesion is desirable, or vice versa. The pattern casts are presented in numerical order based on their assigned pattern number.

01 MILANO

SURFACE AREA

90,000 mm²
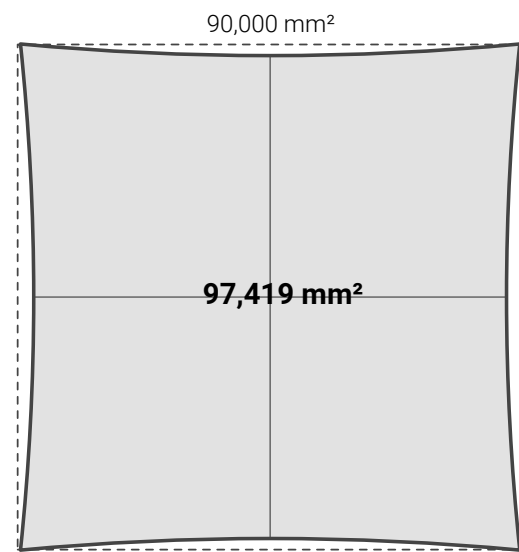
97,419 mm²

SURFACE AREA |Δ| = 7,419 mm²
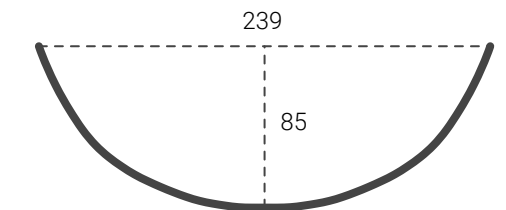

WARP CURVATURE
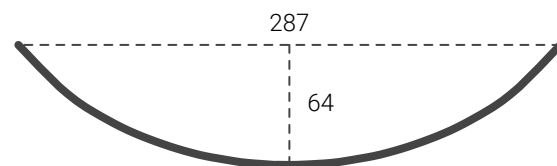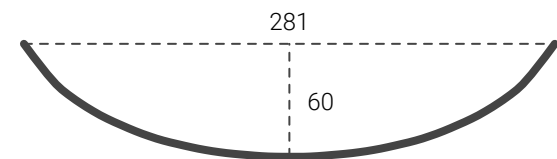
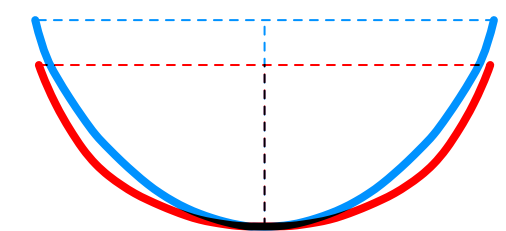Warp Rise / Span Ratio = 0.22

287

64

WEFT CURVATURE

Warp Rise / Span Ratio = 0.21

281

60

● WEFT / ● WARP CURVATURE OVERLAY
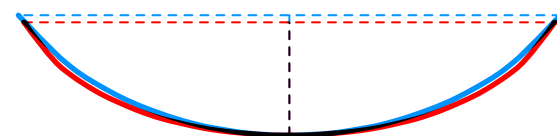
Casting Notes:

• Round bits of concrete remain in textile after demolding

• Some concrete coats edges after demolding

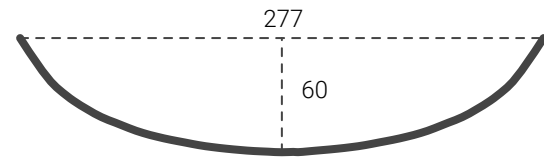Weight of Textile (300x300 sample) = 46.0g

Time to Remove = 02:00

Damage to textile : little to none
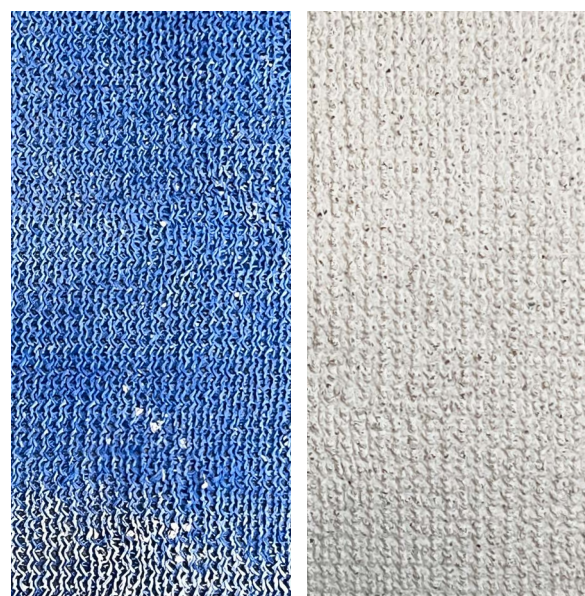
02 HALF MILANO

SURFACE AREA

90,000 mm²
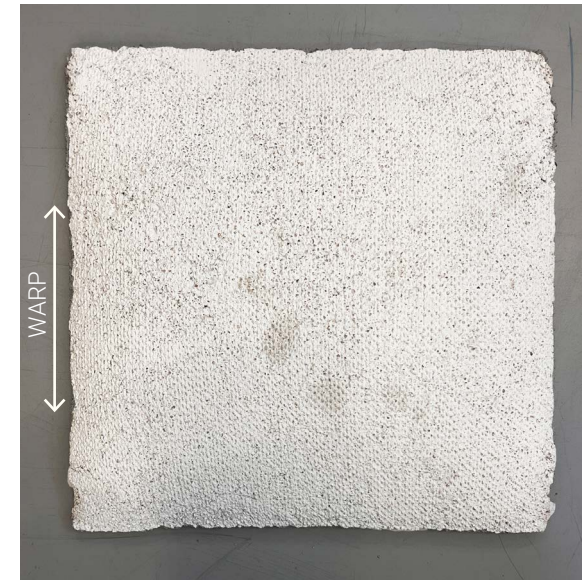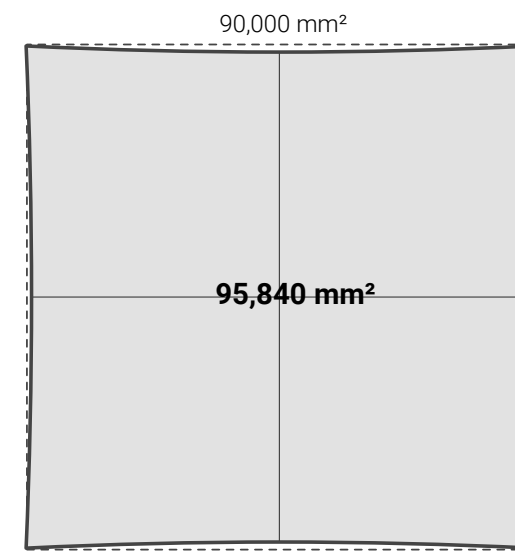
95,840 mm²

SURFACE AREA |Δ| = 5,840 mm²

WARP CURVATURE

Warp Rise / Span Ratio = 0.16
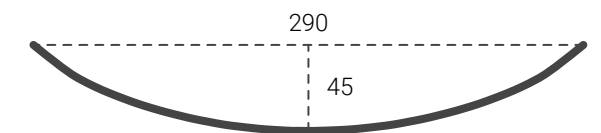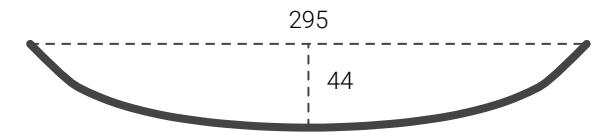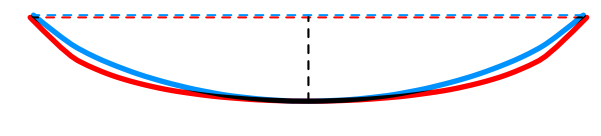
290

45

WEFT CURVATURE

Warp Rise / Span Ratio = 0.15

295

44

● WEFT / ● WARP CURVATURE OVERLAY

Casting Notes:

• Round bits of concrete remain in textile after demolding

• Some concrete coats edges after demolding

Weight of Textile (300x300 sample) = 52.0g

Time to Remove = 00:25

Damage to textile : little to none

03 RIB RIPPLE

SURFACE AREA

90,000 mm²
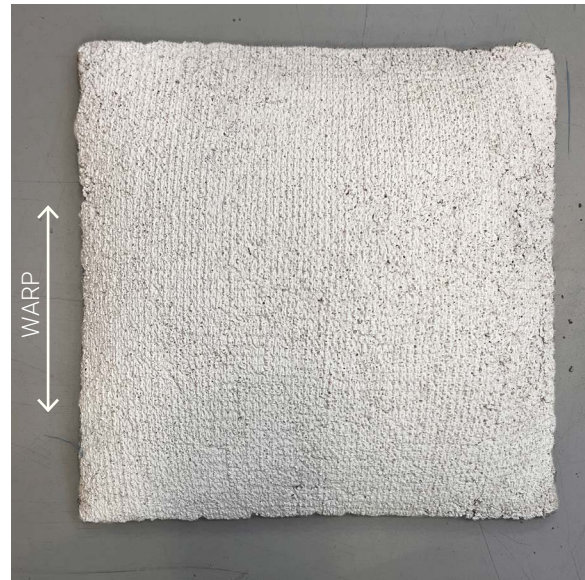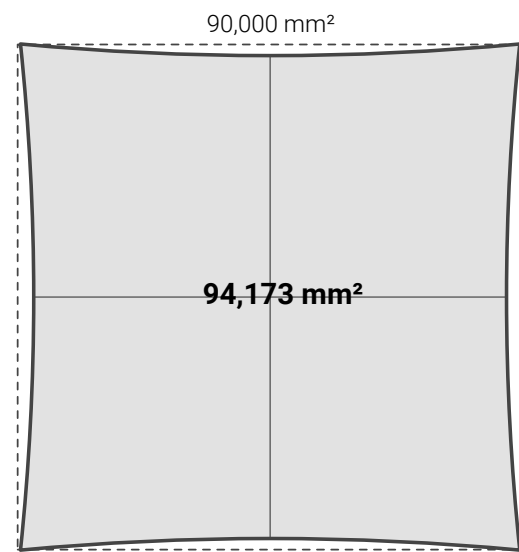
94,173 mm²

SURFACE AREA |Δ| = 4,173 mm²

WARP CURVATURE

Warp Rise / Span Ratio = 0.20

283

57

WEFT CURVATURE

Warp Rise / Span Ratio = 0.17

277

47
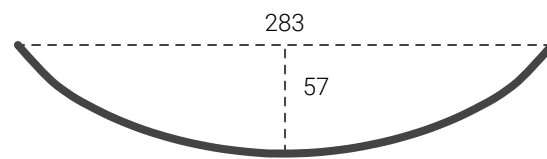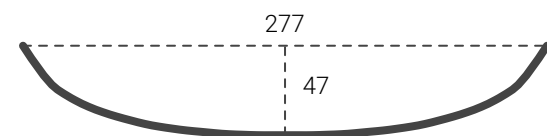
● WEFT / ● WARP CURVATURE OVERLAY
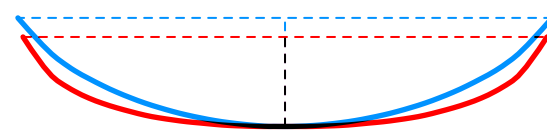
Casting Notes:

• Minimal ound bits of concrete remain in textile after demolding

• Thin layer of concrete coating remains in some areas

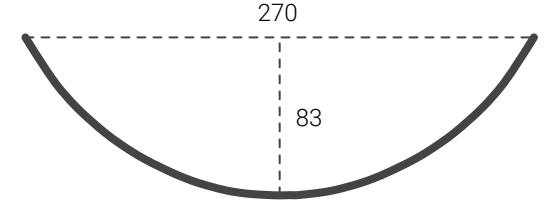Weight of Textile (300x300 sample) = 46.0g

Time to Remove = 00:25

Damage to textile : little to none

04 DOUBLE HALF CARDIGAN

SURFACE AREA

90,000 mm²
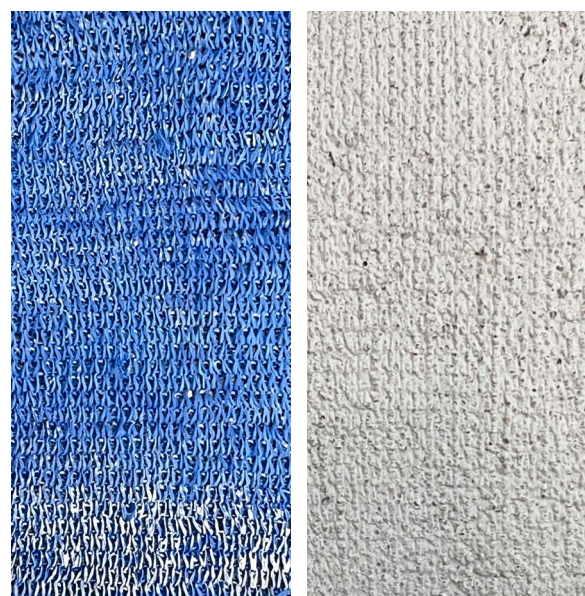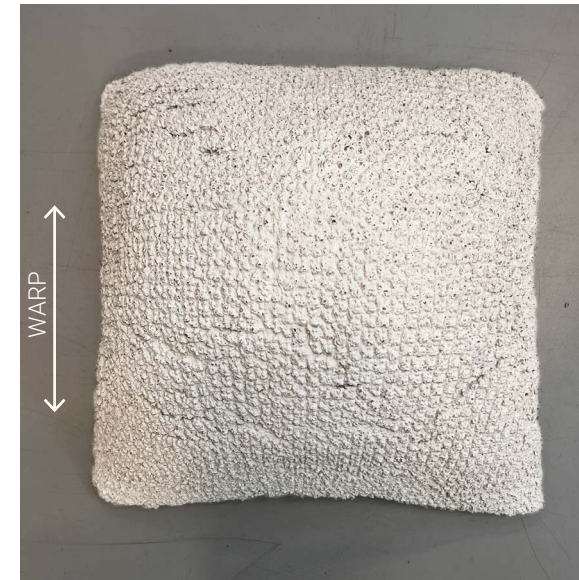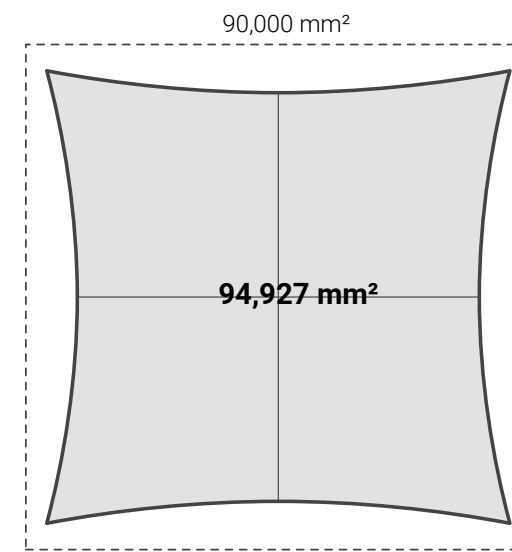
94,927 mm²

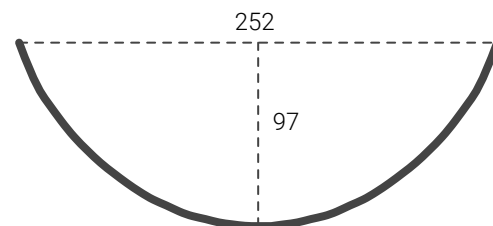SURFACE AREA |Δ| = 4,927 mm²

WARP CURVATURE

Warp Rise / Span Ratio = 0.45

243

109

WEFT CURVATURE

Warp Rise / Span Ratio = 0.36

239

85

● WEFT / ● WARP CURVATURE OVERLAY

Casting Notes:

• Round bits of concrete remain in textile after demolding at back side

• Thin layer of concrete coating remains throughout

• Some cracking during casting

Weight of Textile (300x300 sample) = 69.0g

Time to Remove = 02:30

Damage to textile = intermittent pulled threads
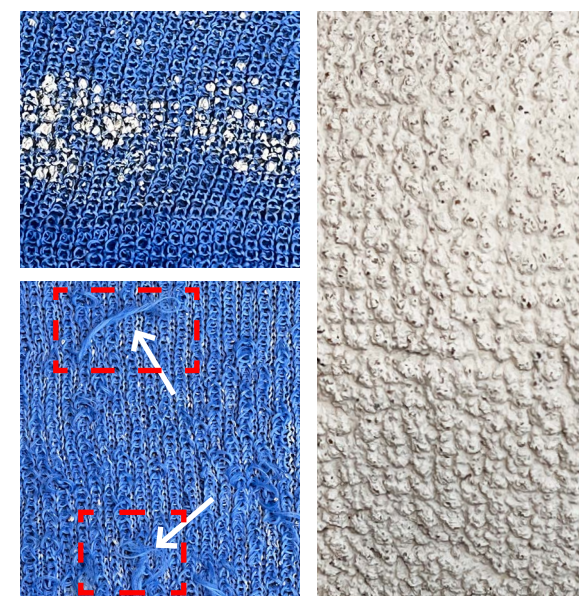
05 HALF CARDIGAN

SURFACE AREA

90,000 mm²
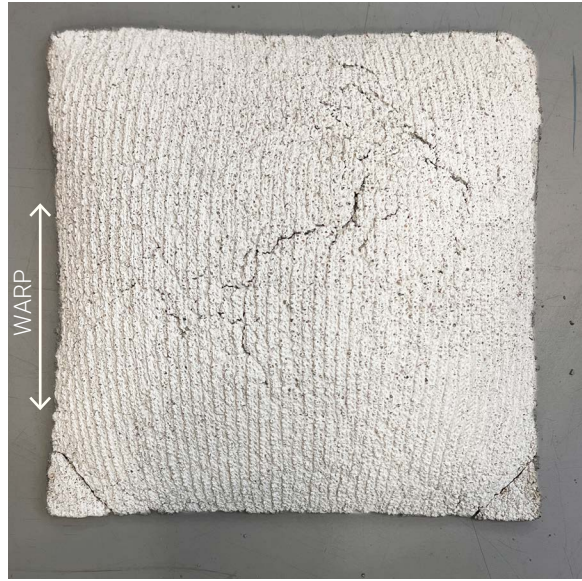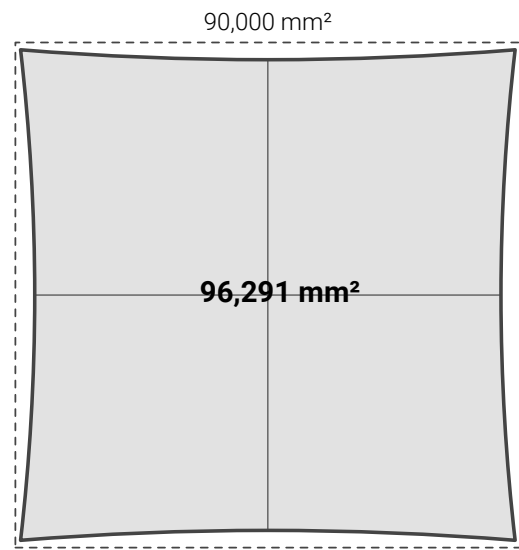
96,291 mm²

SURFACE AREA |Δ| = 6,291 mm²

WARP CURVATURE

Warp Rise / Span Ratio = 0.25
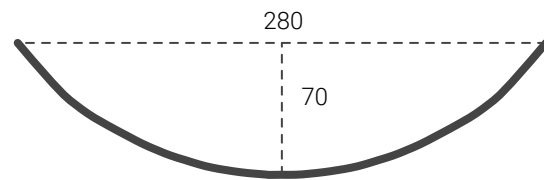
280

70

WEFT CURVATURE

Warp Rise / Span Ratio = 0.22

277

60

● WEFT / ● WARP CURVATURE OVERLAY
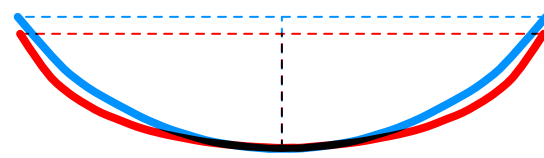
Casting Notes:

• Thin layer of concrete remains throughout

• Heavy cracking during casting

Weight of Textile (300x300 sample) = 69.0g

Time to Remove = 01:30

Damage to textile : pulled threads across entire textile
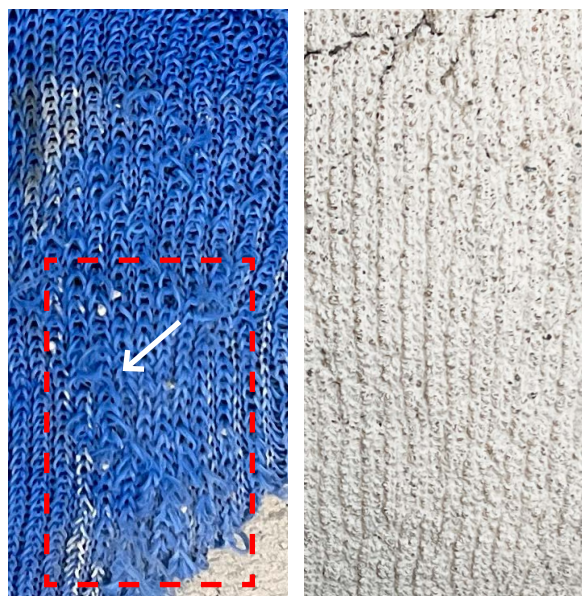
06 2x2 RIB

SURFACE AREA

90,000 mm²
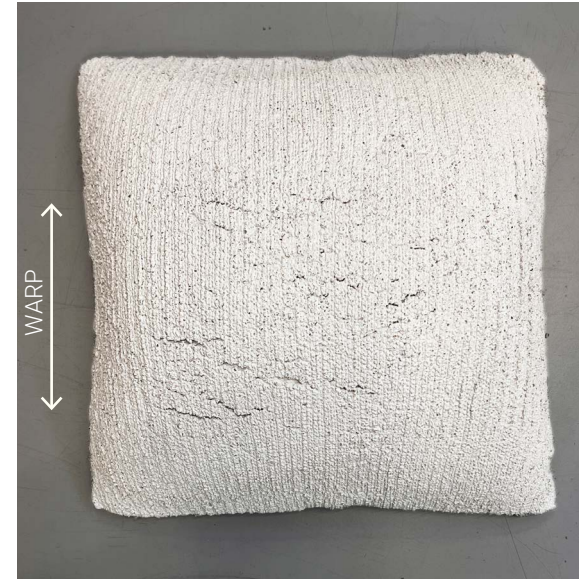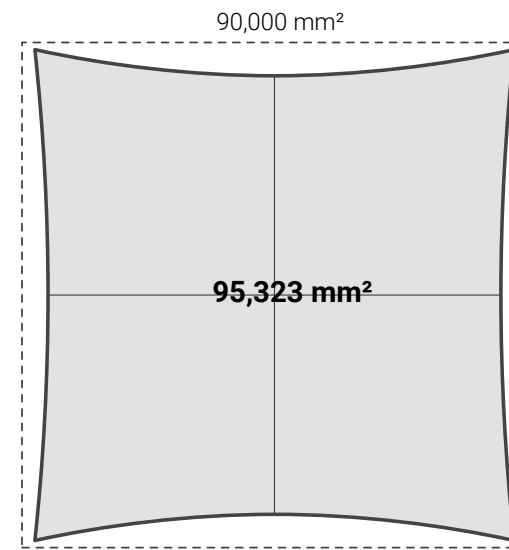
95,323 mm²

SURFACE AREA |Δ|= 5,323 mm²

WARP CURVATURE
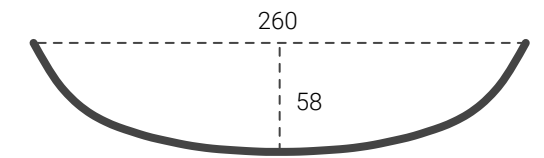
Warp Rise / Span Ratio = 0.22

260

58

WEFT CURVATURE

Warp Rise / Span Ratio = 0.31

270

83

● WEFT / ● WARP CURVATURE OVERLAY
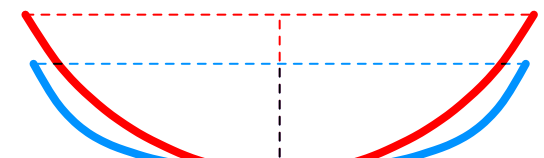
Casting Notes:

• Thin layer of concrete remains throughout

• Round bits of concrete remain in textile after demolding at front side

Weight of Textile (300x300 sample) = 46.0g

Time to Remove = 00:30

Damage to textile : little to none
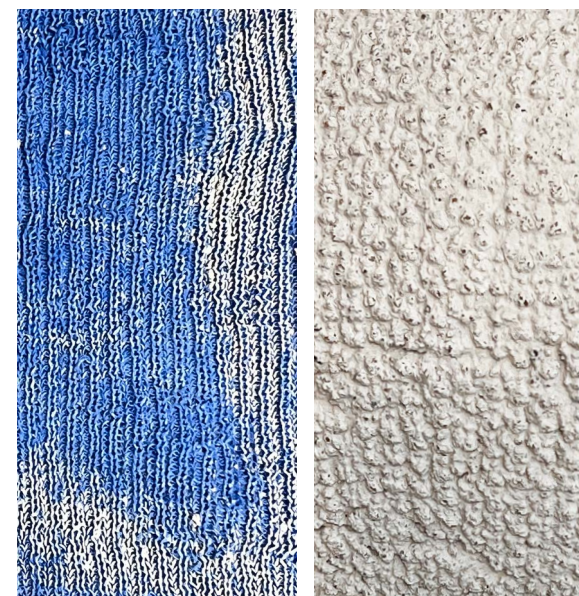
07 RIPPLE CARDIGAN

SURFACE AREA

90,000 mm²
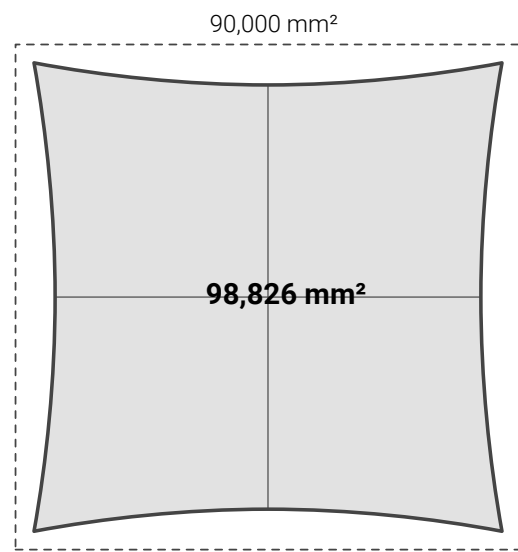
98,826 mm²

SURFACE AREA |Δ| = 8,826 mm²

WARP CURVATURE
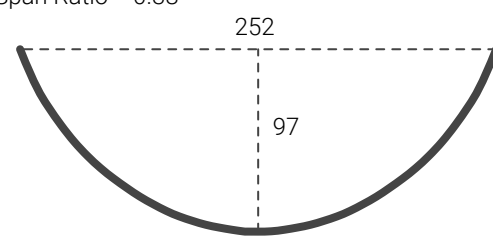
Warp Rise / Span Ratio = 0.38

252

97

WEFT CURVATURE

Warp Rise / Span Ratio = 0.38

252

97

● WEFT / ● WARP CURVATURE OVERLAY
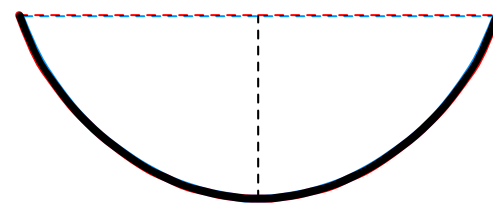
Casting Notes:

- Thin layer of concrete remains at edges
- Round bits of concrete remain in textile after demolding at front side
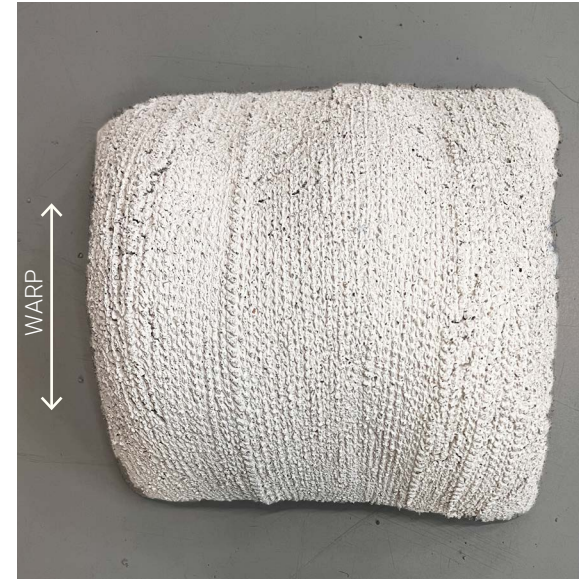
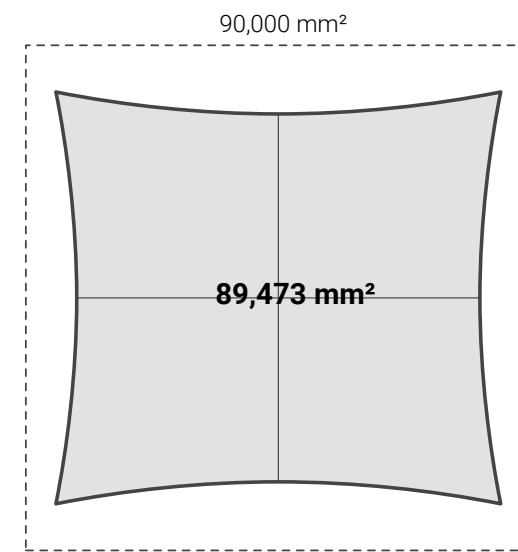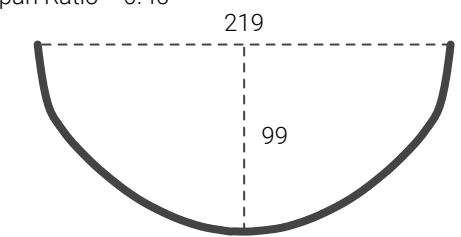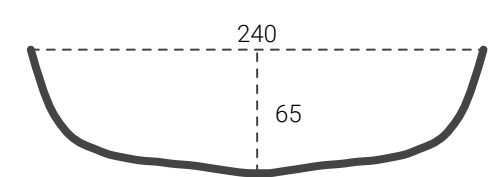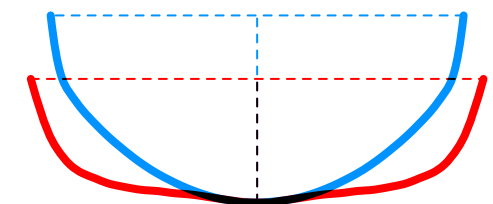Weight of Textile (300x300 sample) = 64.0g

Time to Remove = 01:00

Damage to textile : intermittent pulled threads

08 CARDIGAN

SURFACE AREA

90,000 mm²

89,473 mm²
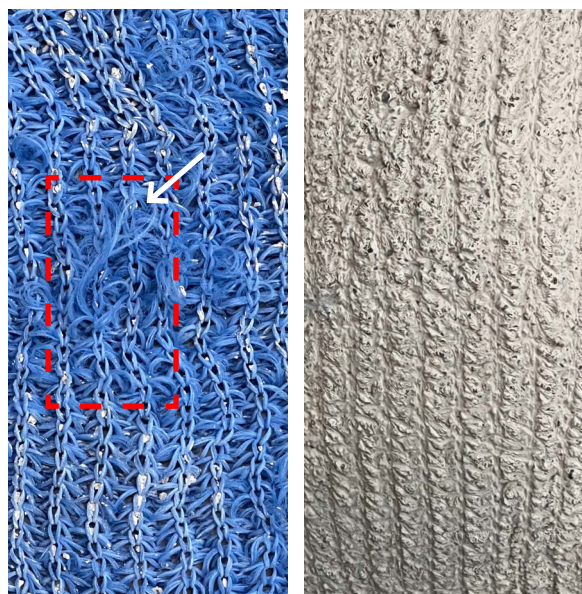
SURFACE AREA |Δ| = 527 mm²

WARP CURVATURE

Warp Rise / Span Ratio = 0.45

219

99

WEFT CURVATURE

Warp Rise / Span Ratio = 0.27

240

65

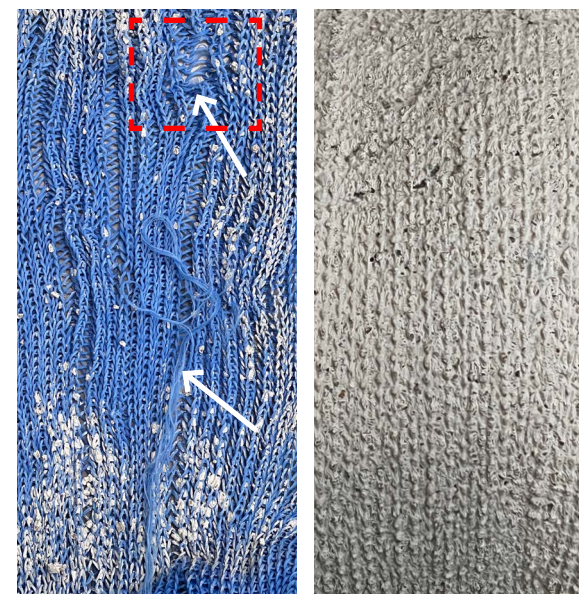● WEFT / ● WARP CURVATURE OVERLAY

Casting Notes:

- Thin layer of concrete remains at edges
- Round bits of concrete remain in textile after demolding at front side
- Textile is highly difficult to control during casting

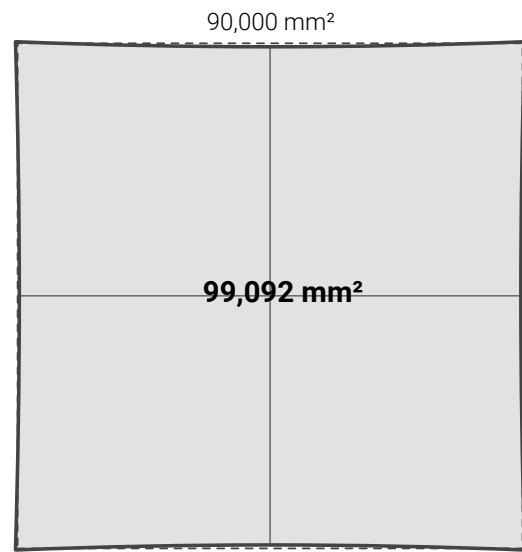Weight of Textile (300x300 sample) = 72.0g

Time to Remove = 00:50

Damage to textile : unraveling due to breakage during removal and pulled threads throughgout
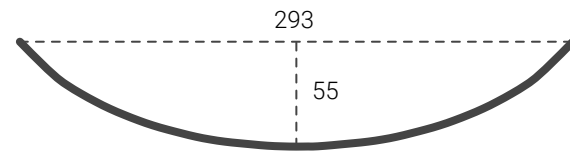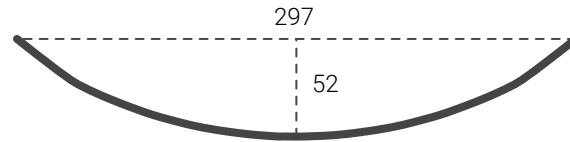
09 CREPE

SURFACE AREA

90,000 mm²

99,092 mm²

SURFACE AREA |Δ| = 9,092 mm²

WARP CURVATURE

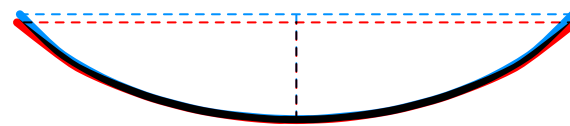Warp Rise / Span Ratio = 0.19

293
55

WEFT CURVATURE

Warp Rise / Span Ratio = 0.17

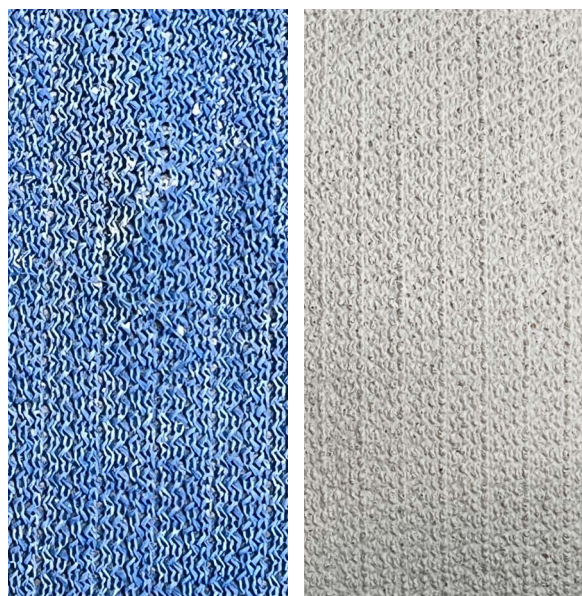297
52

🔴 WEFT / 🔵 WARP CURVATURE OVERLAY

Casting Notes:

• Thin layer of concrete remains throughout textile

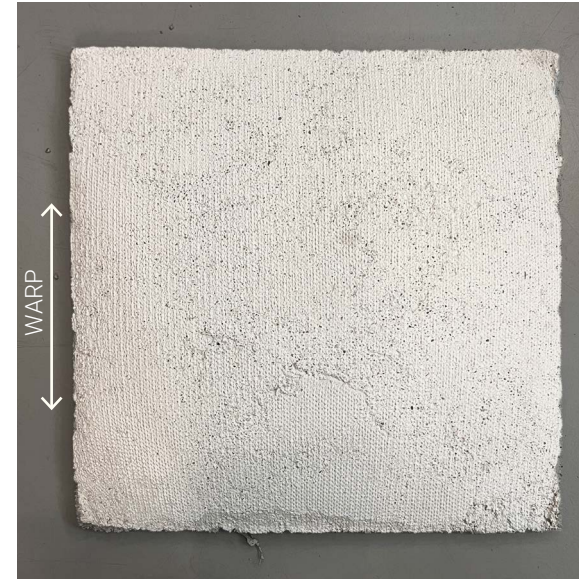• Minimal round bits of concrete remain at front side

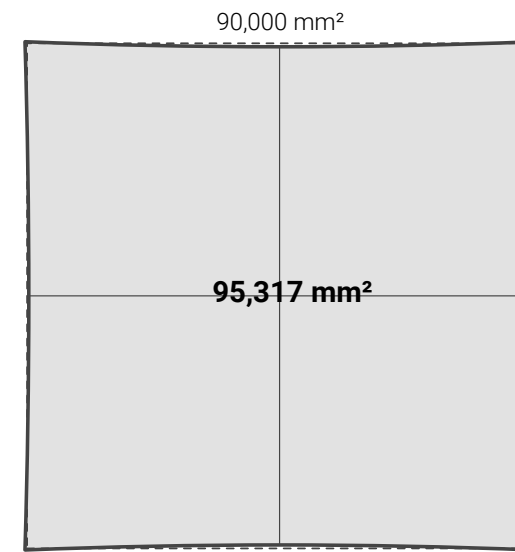Weight of Textile (300x300 sample) = 42.0g

Time to Remove = 00:45

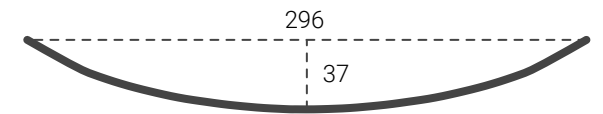Damage to textile : little to none

10 CROSS-MISS

SURFACE AREA

90,000 mm²

95,317 mm²

SURFACE AREA |Δ| = 5,317 mm²

WARP CURVATURE

Warp Rise / Span Ratio = 0.12

296
37

WEFT CURVATURE

Warp Rise / Span Ratio = 0.13

298
37

🔴 WEFT / 🔵 WARP CURVATURE OVERLAY

Casting Notes:

• Thin layer of concrete remains at edges

Weight of Textile (300x300 sample) = 34.0g

Time to Remove = 00:20

Damage to textile : little to none

11 DOUBLE CROSS MISS

SURFACE AREA

90,000 mm²

95,874 mm²
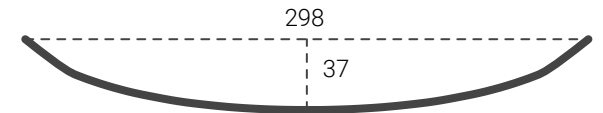
SURFACE AREA |Δ| = 5,874 mm²

WARP CURVATURE
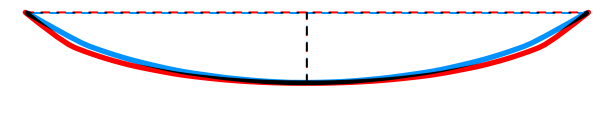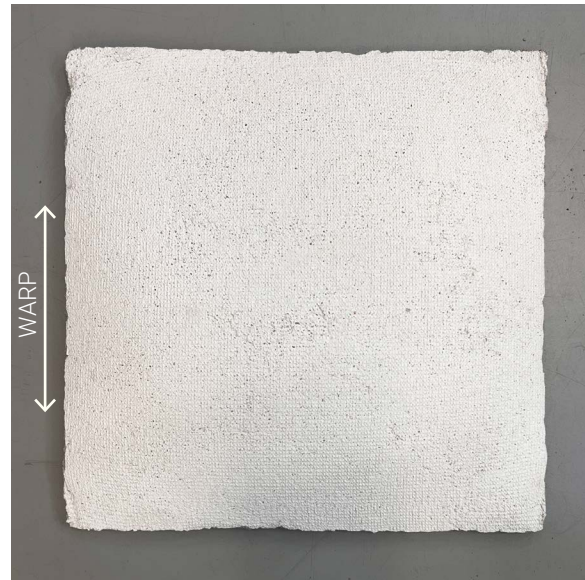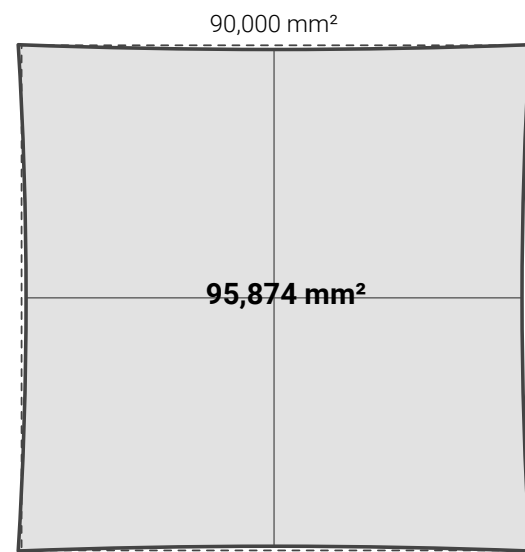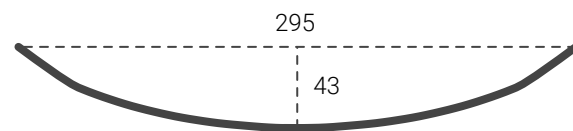
Warp Rise / Span Ratio = 0.15

295

43

WEFT CURVATURE

Warp Rise / Span Ratio = 0.13

295

39

● WEFT / ● WARP CURVATURE OVERLAY

Casting Notes:

• Thin layer of concrete remains throughout textile

Weight of Textile (300x300 sample) = 33.0g

Time to Remove = 00:25

Damage to textile : little to none

---
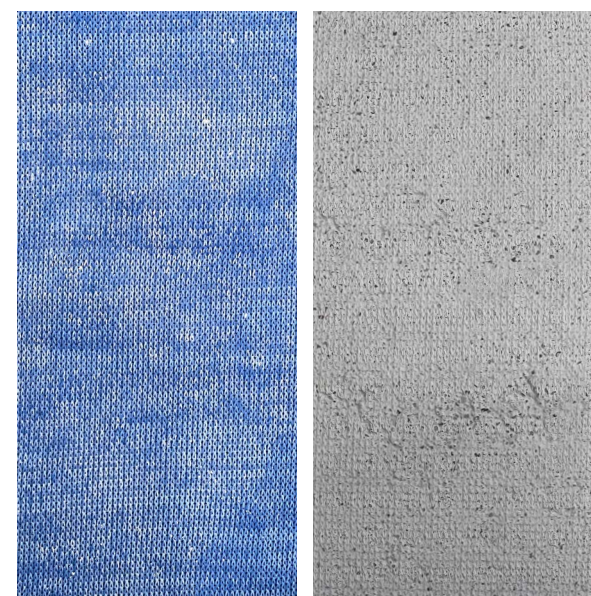
12 DOUBLE LACOSTE

SURFACE AREA

90,000 mm²
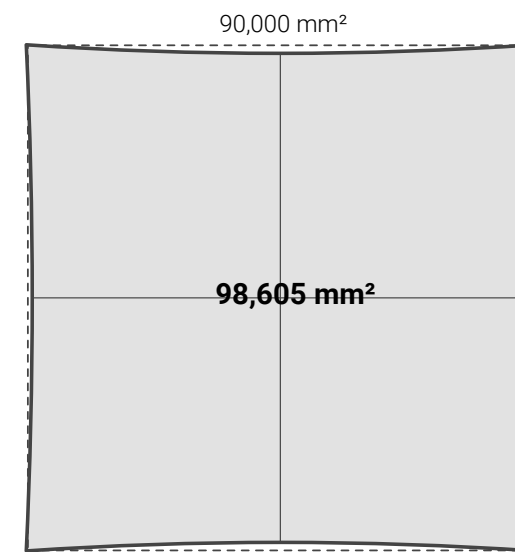
98,605 mm²

SURFACE AREA |Δ| = 8,605 mm²

WARP CURVATURE
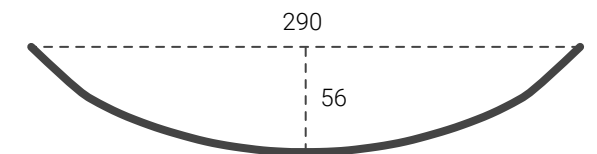
Warp Rise / Span Ratio = 0.19

290

56

WEFT CURVATURE

Warp Rise / Span Ratio = 0.17

295

51

● WEFT / ● WARP CURVATURE OVERLAY

Casting Notes:

• Thin layer of concrete remains throughout textile

• Minimal round bits of concrete remain at front side

Weight of Textile (300x300 sample) = 52.0g

Time to Remove = 1:30

Damage to textile : intermittent pulled threads

13 LONG TUCK STRIPE

SURFACE AREA

90,000 mm²
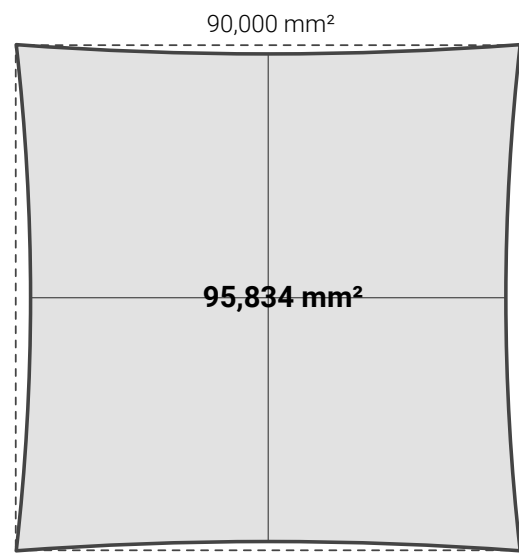
95,834 mm²

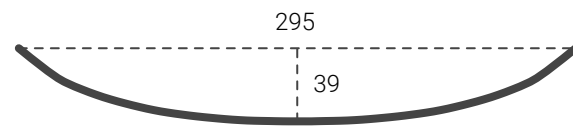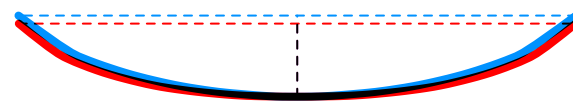SURFACE AREA |Δ| = 5,834 mm²

WARP CURVATURE

Warp Rise / Span Ratio = 0.21

290

60

WEFT CURVATURE

Warp Rise / Span Ratio = 0.18

282

51

● WEFT / ● WARP CURVATURE OVERLAY

Casting Notes:

• Thin layer of concrete remains at edges

• Minimal round bits of concrete remain at front side

Weight of Textile (300x300 sample) = 49.0g

Time to Remove = 00:30

Damage to textile : little to none

14 MOCK RIB

SURFACE AREA

90,000 mm²
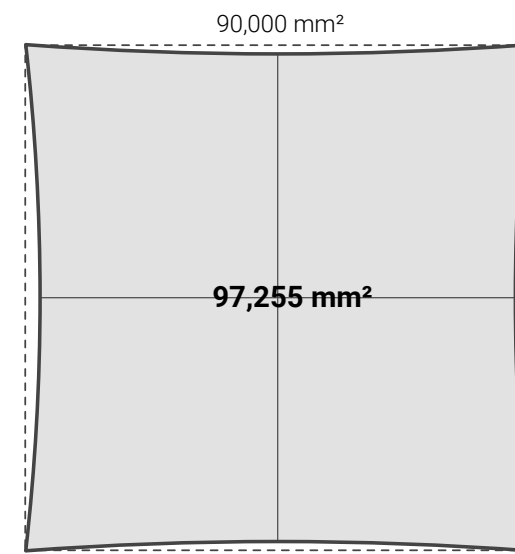
97,255 mm²

SURFACE AREA |Δ| = 7,255 mm²

WARP CURVATURE

Warp Rise / Span Ratio = 0.20

290

60

WEFT CURVATURE

Warp Rise / Span Ratio = 0.18

282

51

● WEFT / ● WARP CURVATURE OVERLAY

Casting Notes:

• Thin layer of concrete remains at edges

• Minimal round bits of concrete remain at front side

Weight of Textile (300x300 sample) = 36.0g

Time to Remove = 00:30

Damage to textile : little to none

## 15 POLO PIQUE

SURFACE AREA

90,000 mm²
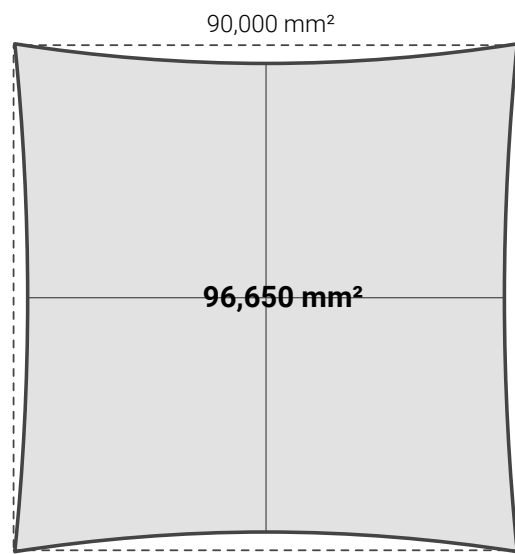
96,650 mm²

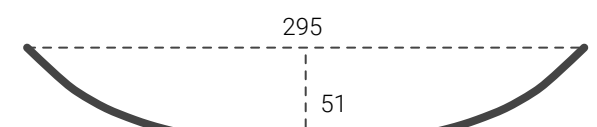SURFACE AREA |Δ| = 6,650 mm²

WARP CURVATURE

Warp Rise / Span Ratio = 0.24

279
66

WEFT CURVATURE

Warp Rise / Span Ratio = 0.22

283
62

● WEFT / ● WARP CURVATURE OVERLAY

Casting Notes:

- Thin layer of concrete remains at edges
- Minimal round bits of concrete remain at front side

Weight of Textile (300x300 sample) = 52.0g

Time to Remove = 01:50

Damage to textile : intermittent pulled threads

16 POPCORN

SURFACE AREA

90,000 mm²
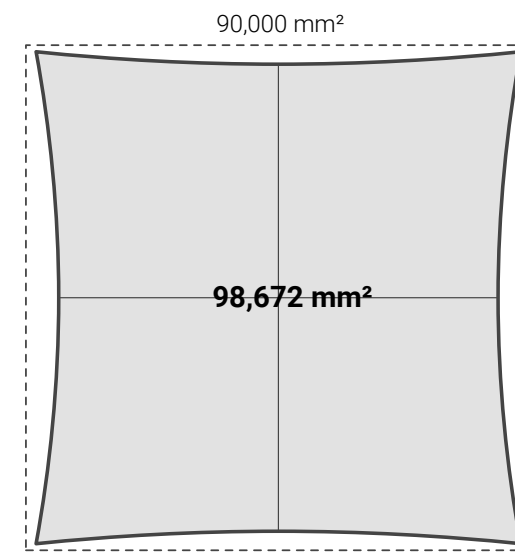
98,672 mm²

SURFACE AREA |Δ| = 8,672 mm²

WARP CURVATURE
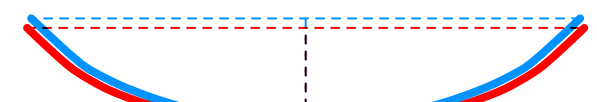
Warp Rise / Span Ratio = 0.31

277
86
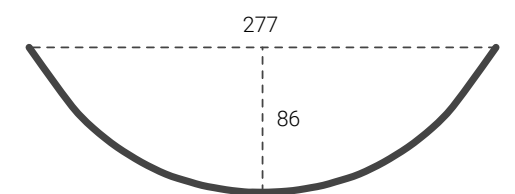
WEFT CURVATURE

Warp Rise / Span Ratio = 0.29

261
76
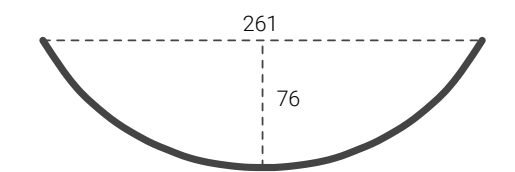
● WEFT / ● WARP CURVATURE OVERLAY
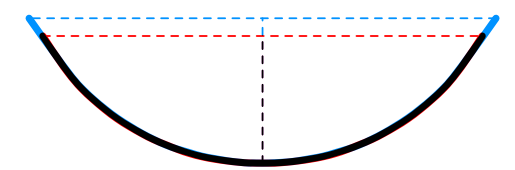
Casting Notes:

- Thin layer of concrete remains throughout
- Many round bits of concrete remain at front side

Weight of Textile (300x300 sample) = 50.0g

Time to Remove = 02:40

Damage to textile : intermittent pulled threads and some localized unraveling due to breakage during removal
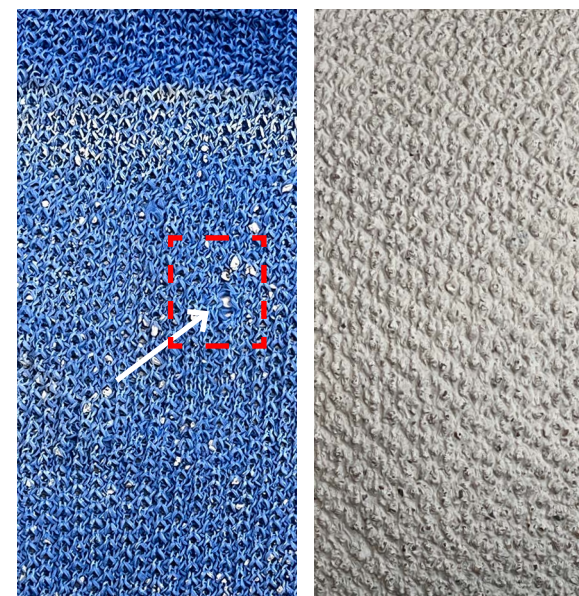
17 SINGLE CROSS TUCK

SURFACE AREA

90,000 mm²
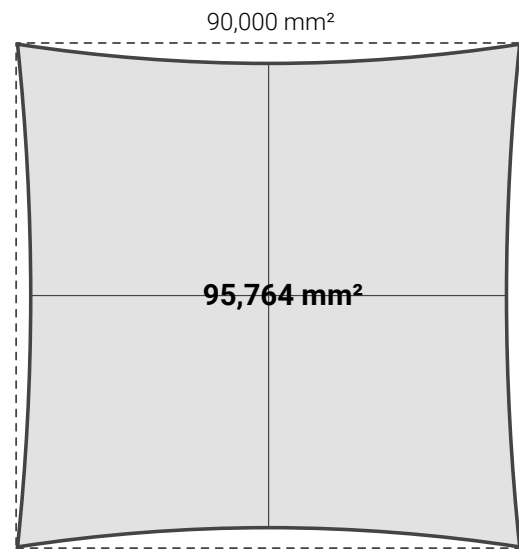
95,764 mm²

SURFACE AREA |Δ| = 5,764 mm²

WARP CURVATURE
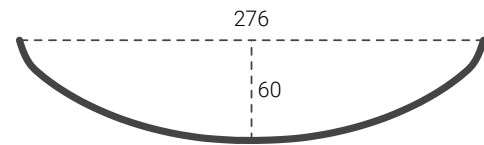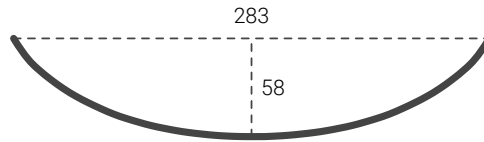
Warp Rise / Span Ratio = 0.22

276

60

WEFT CURVATURE

Warp Rise / Span Ratio = 0.21

283

58

● WEFT / ● WARP CURVATURE OVERLAY
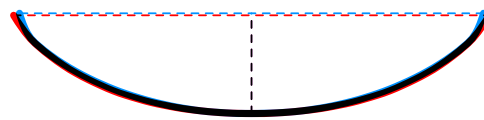
Casting Notes:

- Thin layer of concrete remains throughout textile
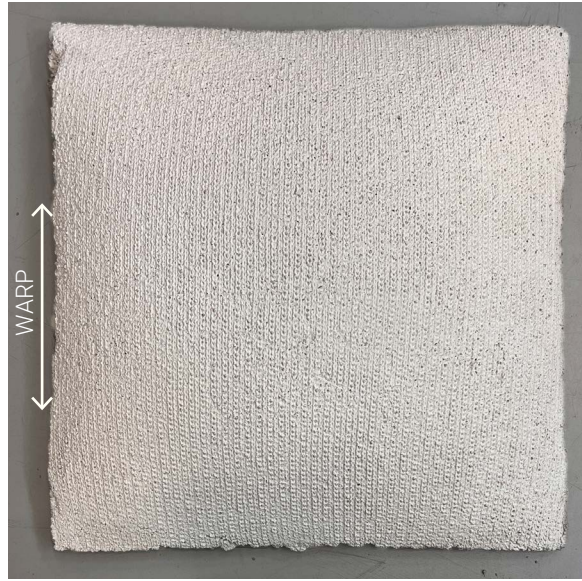- Minimal round bits of concrete remain at front side

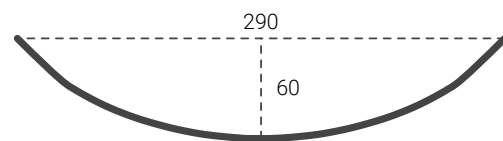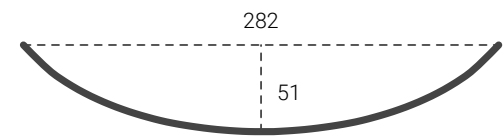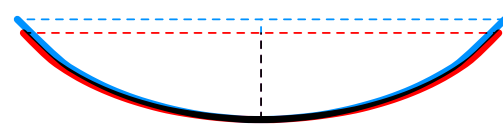Weight of Textile (300x300 sample) = 51.0g

Time to Remove = 00:20

Damage to textile : little to none
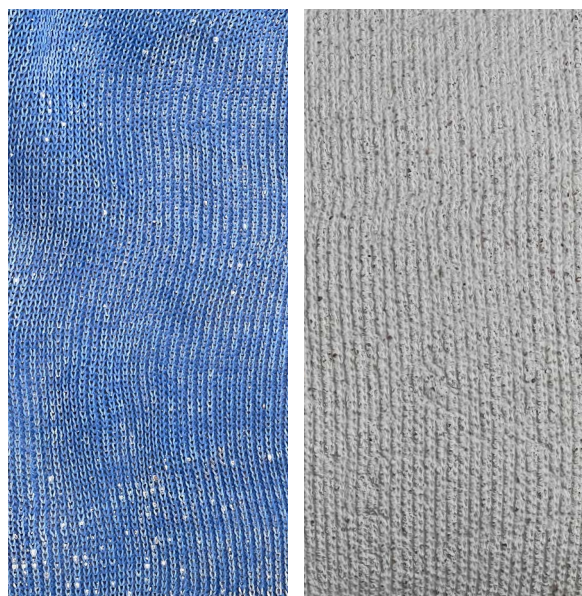
18 TWILL EFFECT

SURFACE AREA

90,000 mm²
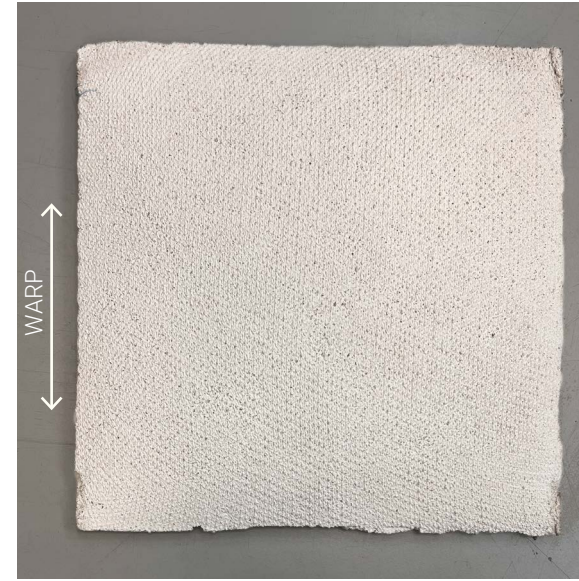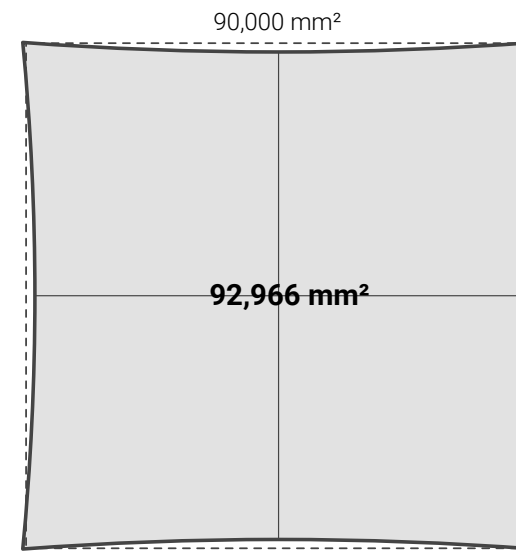
92,966 mm²

SURFACE AREA |Δ| = 2,966 mm²

WARP CURVATURE

Warp Rise / Span Ratio = 0.14
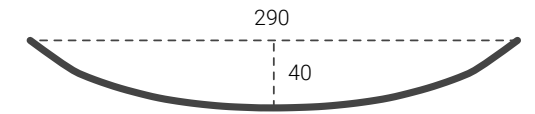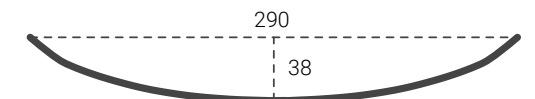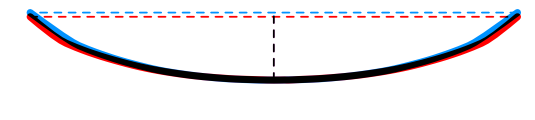
290

40

WEFT CURVATURE

Warp Rise / Span Ratio = 0.13

290

38

● WEFT / ● WARP CURVATURE OVERLAY

Casting Notes:

- Thin layer of concrete remains throughout textile
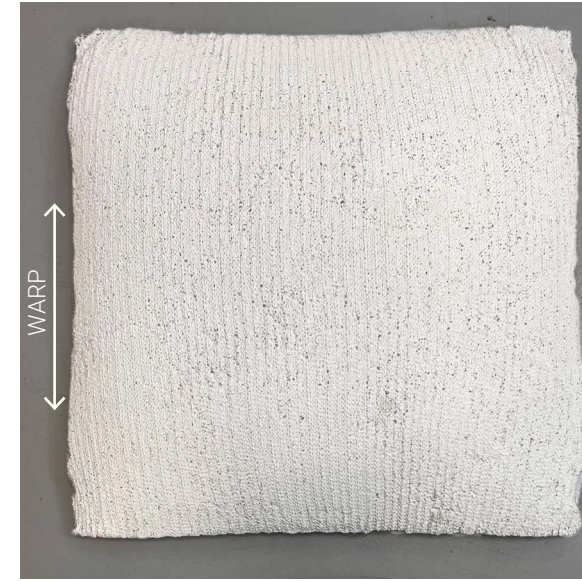- Minimal round bits of concrete remain at front side

Weight of Textile (300x300 sample) = 41.0g

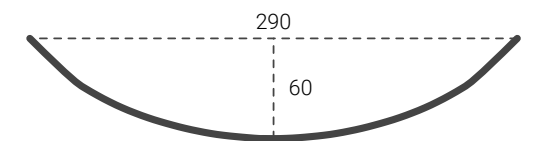Time to Remove = 00:45

Damage to textile : little to none

19 WEFT LOCK
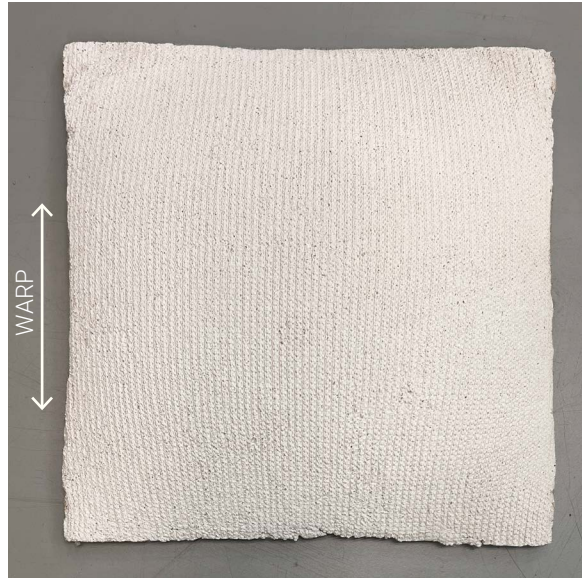
SURFACE AREA
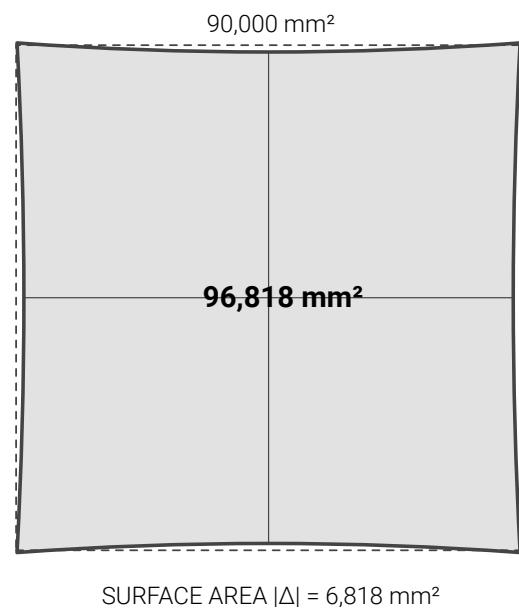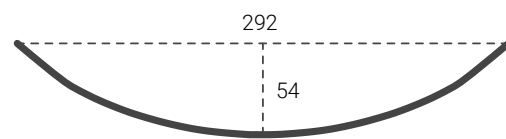
90,000 mm²

96,818 mm²

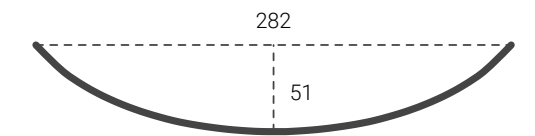SURFACE AREA |Δ| = 6,818 mm²

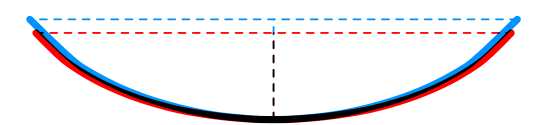### WARP CURVATURE

Warp Rise / Span Ratio = 0.19

292

54

WEFT CURVATURE

Warp Rise / Span Ratio = 0.17

291

50
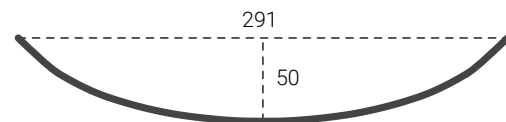
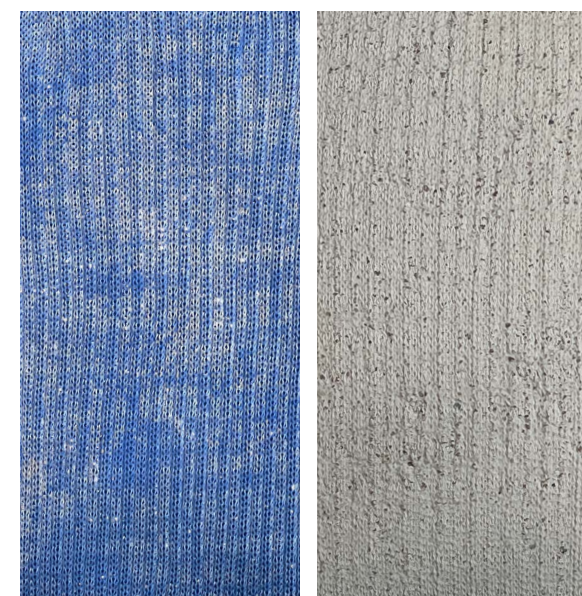● WEFT / ● WARP CURVATURE OVERLAY
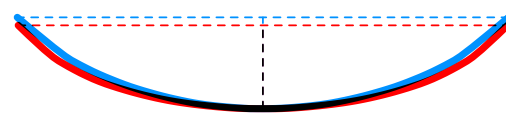
Casting Notes:

- Thin layer of concrete remains throughout textile
- Minimal round bits of concrete remain at front side

Weight of Textile (300x300 sample) = 45.0g

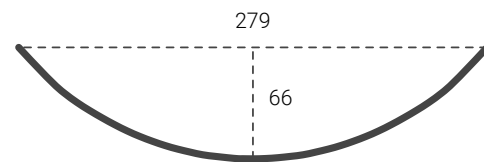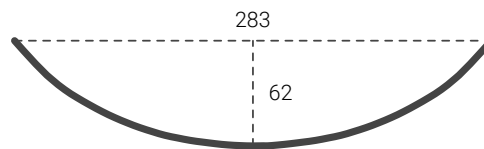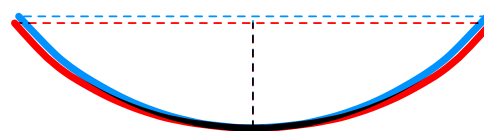Time to Remove = 00:20

Damage to textile : little to none

## 4.3 Discussion of Results: Curvature Repository and Casting Process

A comparison of the curvatures extracted in the previous section shows the influence of weft and warp properties on textile deformation.

Pattern	Max Rise (mm)	Warp Ratio (rise/span)	Weft Ratio (rise/span)	Srf Area (mm²)	Warp Curve	Weft Curve	Warp/Weft Overlay
(10) CROSS-MISS	37 (warp)	0.13	0.12	95,317			
(18) TWILL EFFECT	40 (warp)	0.14	0.13	92,966			
(11) DOUBLE CROSS-MISS	43 (warp)	0.15	0.13	95,874			
(2) HALF MILANO	45 (warp)	0.16	0.15	95,840			
(19) WEFT LOCK	54 (warp)	0.18	0.17	96,818			
(9) CREPE	55 (warp)	0.19	0.18	99,092			
(12) DOUBLE LACOSTE	56 (warp)	0.19	0.17	98,605			
(3) RIB RIPPLE	57 (warp)	0.20	0.17	94,173			
(16) MOCK RIB	57 (warp)	0.20	0.18	97,255			
(13) LONG TUCK STRIPE	60 (warp)	0.21	0.18	95,834			
(17) SINGLE CROSS TUCK	60 (warp)	0.22	0.20	95,764			
(1) MILANO	64 (warp)	0.22	0.21	97,419			
(15) POLO PIQUE	66 (warp)	0.24	0.22	96,650			
(5) HALF CARDIGAN	70 (warp)	0.25	0.22	96,291			
(6) 2X2 RIB	83 (*weft)	0.22	0.31	95,323			
(16) POPCORN	86 (warp)	0.31	0.29	98,672			
(7) RIPPLE CARDIGAN	97	0.38	0.38	98,826			
(8) CARDIGAN	99 (warp)	0.45	0.27	89,473			
(4) DBL. HALF CARDIGAN	109 (warp)	0.45	0.36	94,927			

Figure 68. Overall comparison of weft and warp curvatures arranged from lowest to highest deformation (rise).

4.3.1 Discussion of Curvature Results

Rise to Span Ratio

As shown in Figure 68, the warp curves tended to have higher rises and therefore higher rise to span ratios than the weft curvatures. With this information, and assuming isotropic behavior of concrete, hypothetical conclusions can be drawn about the stiffness of the cast shapes in the warp versus weft direction. This hypothesis is based on the intuition that a greater depth to span ratio generally leads to a stiffer cross-section due to increased area and moment of inertia. However, this is a simplified conclusion and does not capture the complexities of structural behavior and stiffness which would depend on the specific geometry, material properties, loading conditions, and support conditions among other factors. An actual determination of stiffness would necessitate a more detailed analysis which is beyond the scope of this thesis. Based on this intuitive assessment, the data suggests that, in general, stiffer curvatures are created in the warp direction than in the weft direction of a deformed knitted textile because the rise to span ratios are generally higher in the warp. However, there are some notable exceptions to this conclusion. First, 2x2 Rib shows an opposite relationship where the weft direction shows a higher rise and rise to span ratio than the warp. Another pattern, Ripple Cardigan, shows an identical rise to span ratio in the warp and weft direction.

$$I_y = \frac{wh^3}{12}$$

$$I_z = \frac{hw^3}{12}$$
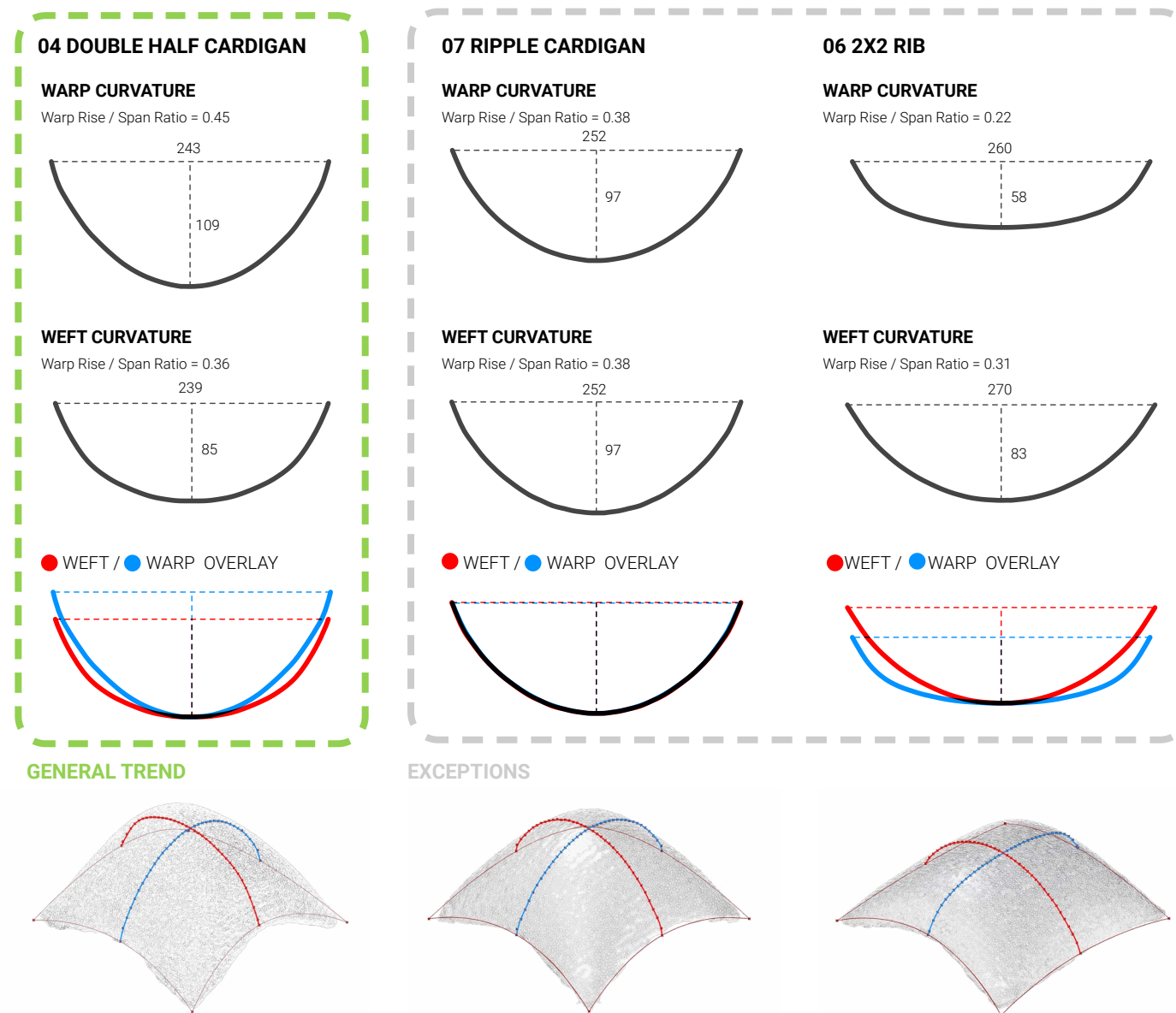
Curve Shape

In many patterns, the numerical difference in the weft versus warp rise to span ratios is small and may not provide enough information to draw hypothetical conclusions about stiffness. Therefore, another analysis strategy is to visually compare the shape of the weft and warp curves. Figure 70 demonstrates that most warp curves tend to have a more even, gradual curvature while some weft curves tend to be more angled at the ends and flatter at the mid-section. This discrepancy is most pronounced in patterns with higher deformations such as Half Cardigan and Double Half Cardigan but is also apparent in patterns with smaller deformations such as Half Milano. 2x2 Rib again shows the opposite condition of the general trend described in Figure 70. Other exceptional patterns include Crepe, Single Cross Tuck, Popcorn, and Ripple Cardigan which show almost identically shaped curves. The stiffness of a curve is closely related to the distribution of curvature along its length when considering structural elements that are subject to bending stress. Gradual, even curvature tends to distribute bending forces more uniformly along its length, resulting in a more consistent stiffness throughout the curve. Curvature with more abrupt changes, such as the weft curves described, would exhibit a varying stiffness along its length. The weft curves show higher curvatures at the ends and flatter curvatures at the midsection. This might indicate a concentration of higher bending forces at the ends as well as greater stiffness, whereas the midsection might exhibit lower bending forces and lower stiffness due to the flatter curvature.

Figure 69. Illustration of rise-to-span comparison findings. Double Half Cardigan represents a general trend where warp rise/span ratios tend to be higher than weft ratios. Ripple Cardigan and 2x2 Rib represent exceptions where the warp and weft curvatures are equivalent and the warp and weft curves show an opposite relationship to the general trend.
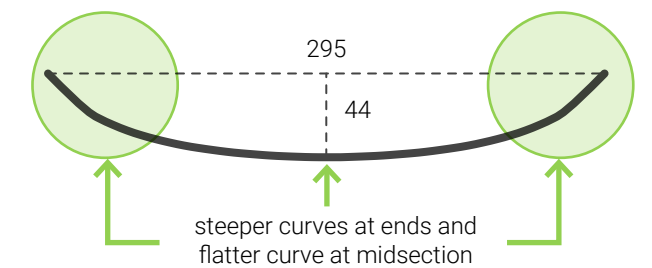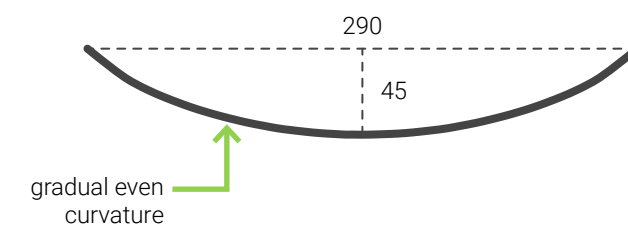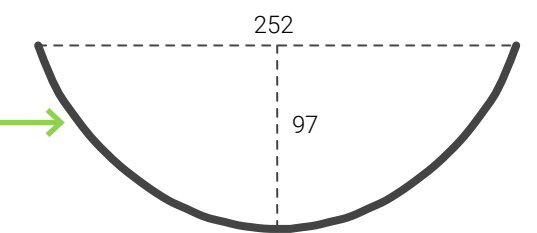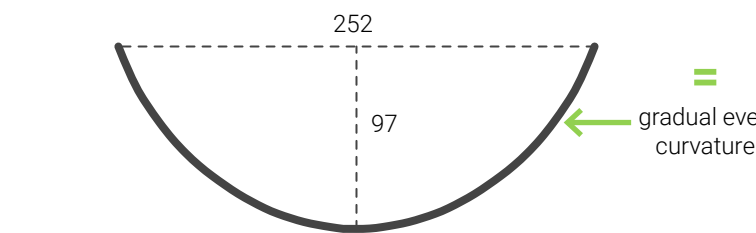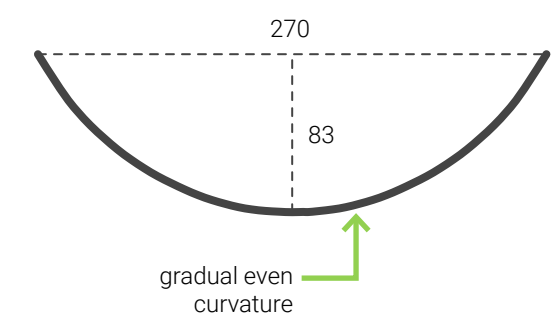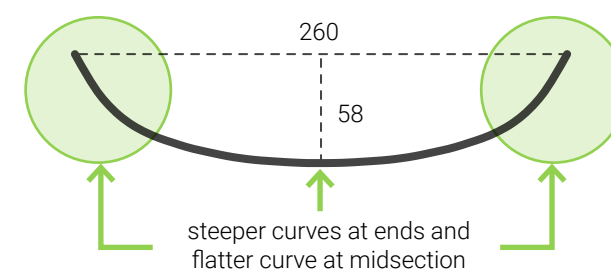
Figure 70. Comparison of warp and weft curve shapes for selected patterns.

Surface Area

It can also be seen in Figure 68 that the magnitude of the surface area does not directly correlate with the degree of deformation or the weft/warp ratios. For example, Cross-Miss, the pattern with the least deformation, shows a greater surface area than Double Half Cardigan, the pattern with the most deformation. The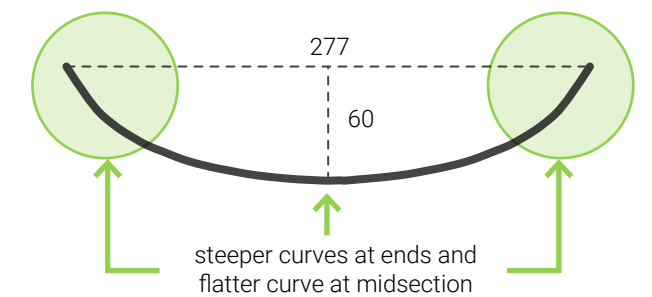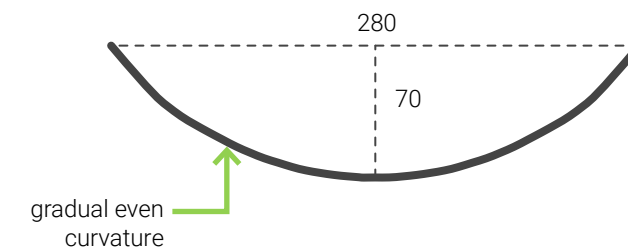 three patterns with the greatest surfaces areas, Crepe (99,092), Ripple Cardigan (98,826), and Popcorn (98,672) are also among the group of patterns showing almost identical weft and warp curves. The pattern with the lowest surface area (excluding Cardigan), Twill Effect (92,966), also shows relatively uniform warp and weft curves and a low deformation. For these cast shapes, the four edge curves, or boundary conditions, seem to play an important role in determining the surface area. For this type of shape, assuming a constant maximum deflection, the surface area decreases as the edge curves become more extreme. However, as the maximum deflection is not constant between patterns, it must be understood that the relationship between maximum deflection and boundary conditions might have more influence over the surface area of the shapes than the individual characteristics of the maximum deflection or edge curvatures.
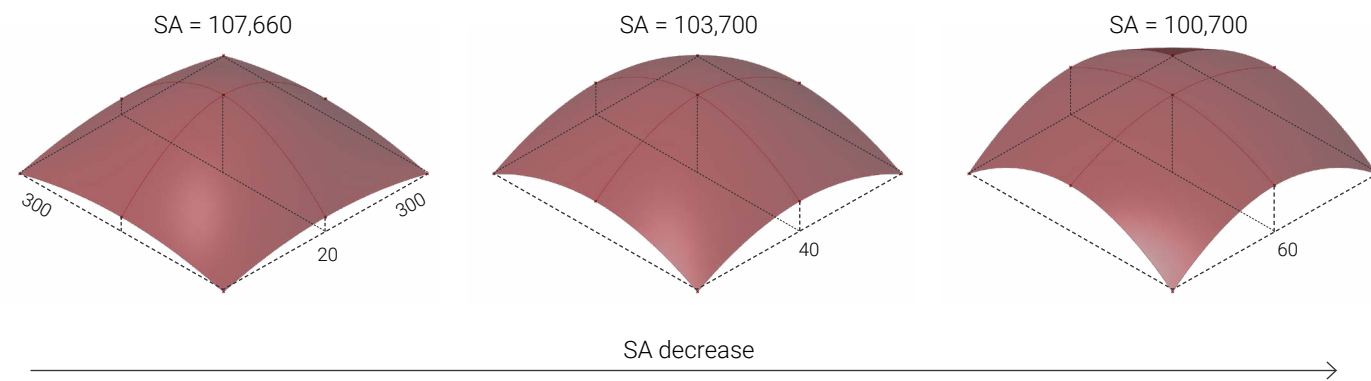
Figure 71. Theoretical shape demonstrating the effect of the edge curves on the overall surface area. Where the maximum deflection is constant, (100), the surface area decreases as the edge curvatures increase. This relationship is linear so long as the edge curvature deflection does not exceed the center maximum deflection. However, when the center deflection changes and the edge curvature deflections are not equivalent, this relationship is no longer linear, as demonstrated in the cast samples.
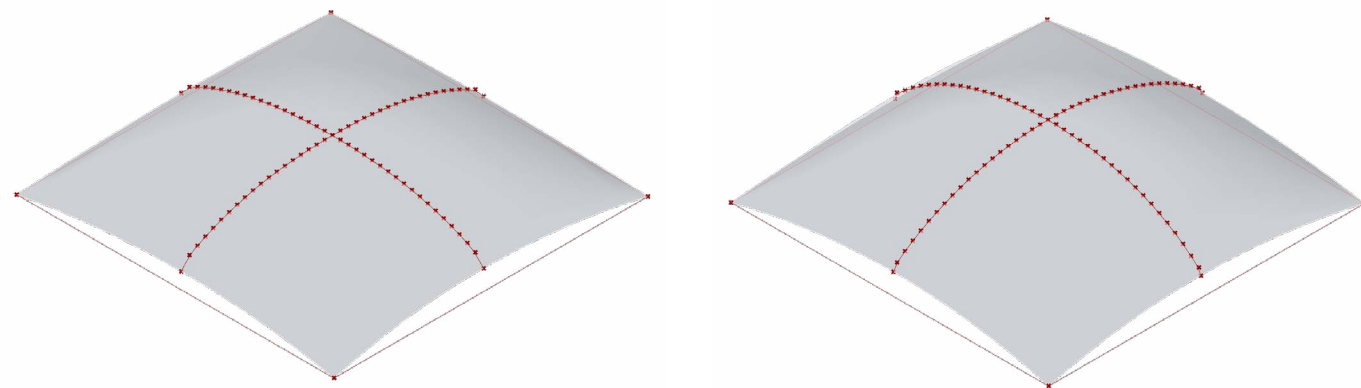
Figure 72. (Left) Twill Effect, pattern with lowest surface area of 92,966 mm2 (Right) Crepe, pattern with highest surface area of 99,092 mm2

Principal Stress Lines

A basic analysis of the principal stress lines in the pattern casts performed with Karamba suggests that the nature of the warp and weft curvature influences how stress is distributed. Most of the cast forms appear to square, which would initially suggest a uniform and symmetrical stress distribution within the form. However, in most cases, the warp and weft curves have a different shape and therefore a different length. If these curves were flattened and the lengths maintained, they would form a rectangle rather than a square. This might explain why in most patterns the principal stress lines resemble a rectangular form rather than a square. In patterns which showed identical or highly similar warp and weft curvatures, the principal stress lines resemble a square, as expected. Figure 73 explains this concept in more detail. While these findings are

valuable insofar as they suggest that different patterns will show different structural behavior, and that the warp and weft direction within one pattern might behave differently, they are limited to this body of research. An actual determination of principal stress is dependent on the actual geometry, load case, supports, among other factors. In addition, the combination of patterns would further complicate this discussion.

A consistent outlier in this discussion is the Cardigan pattern which shows a curve with almost vertical end conditions in the warp and a slightly ribbed curve in the weft direction. This pattern is highly irregular when manipulated at rest and requires a great deal of pre-tensioning to create even behavior in the textile. While the curvature shown reflects what was cast, it should be noted that this curvature might be circumstantial based on the way the textile was arranged at the moment of casting. Nonetheless, because of its extreme flexibility and perceived randomness, this pattern shows potential for more exploratory applications.

07 RIPPLE CARDIGAN **04 DOUBLE HALF CARDIGAN**
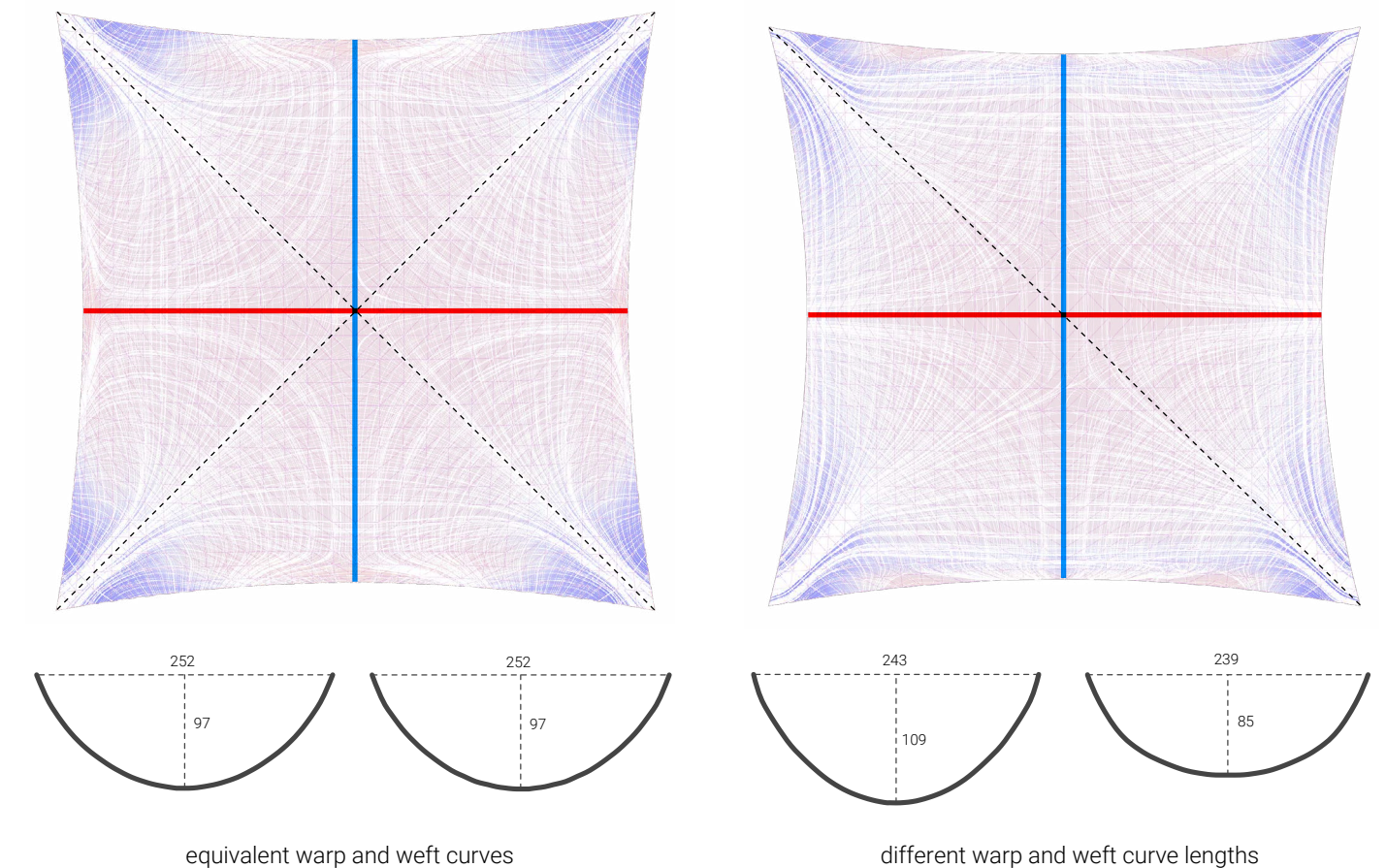
equivalent warp and weft curves   different warp and weft curve lengths
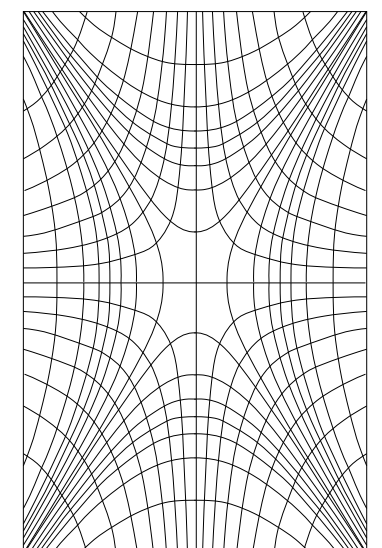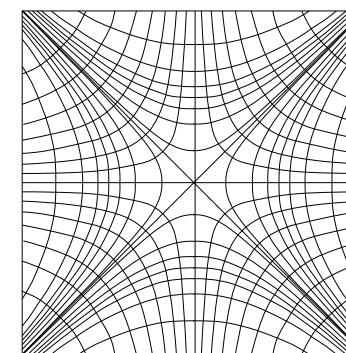
Figure 73. Comparison of principal stress line pattern between Ripple Cardigan and Double Half Cardigan. While Ripple Cardigan shows a symmetrical square stress line distribution, Double Half Cardigan shows a stress line distribution closer to that of a rectangular shape likely due to the differences in warp and weft curve lengths. This observation is relevant insofar as it suggests that these pattern-reliant forms, while similar in shape, might be structurally different.

4.3.2 Relationship to Pattern Repository Data
The following was noted in Section 3.4:

Most patterns across both yarn types with a ratio below 1.0 showed more stretch in the warp direction than in the weft…From observations of the selected pattern group used in this research, it can be inferred that lower ratios (higher warp stitch counts) tend to indicate greater stretch in the warp direction, while higher ratios (higher weft stitch counts) tend to indicate either less discrepancy between in the stretch in the weft and warp directions or greater stretch in the weft direction.

When this statement is compared to the data produced by the cast samples, certain consistencies and contradictions emerge. First, most samples showed greater deformation in the warp direction, which is consistent with the statement made in section 3.4 where the textiles are shown to stretch more in the warp than in the weft. However, some samples showed almost identical deformation in the weft and warp directions despite having been observed to show varying stretch in the weft versus warp. A notable example is Ripple Cardigan, which was identified as the 2-bed pattern with the lowest weft/warp stitch count ratio (0.22) and observed to stretch more in the warp direction. However, Ripple Cardigan also showed the most uniform deformation out of all the samples, producing identical warp and weft curves. Half Cardigan, the pattern with the second-highest weft/warp stitch count ratio (0.27) showed higher warp deformation and a more pronounced difference in warp/weft curvature. At the other end of the extreme, 2x2 Rib, which was identified as the 2-bed pattern with the highest weft/warp stitch count ratio (1.25) produced a sample that deformed more in the weft direction, which is consistent with statements made in Section 3.4.

07 RIPPLE CARDIGAN

WARP CURVATURE + STRETCH

WARP/WEFT OVERLAY

WEFT CURVATURE + STRETCH
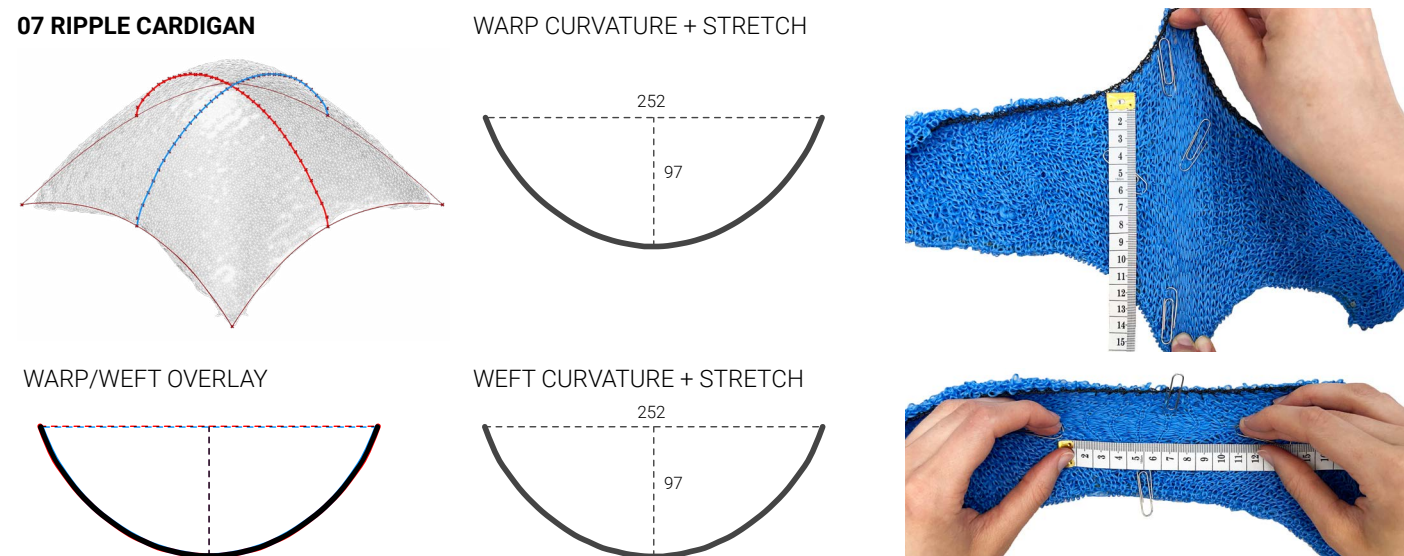
Figure 74. Ripple Cardigan stands in contradiction to the statement made in section 3.4. While the deformation showed equivalent warp and weft curves, the textile itself was showing to stretch significantly more in the warp direction than in the weft, suggesting that the relationship between the warp and weft properties has significant influence over the deformation characteristics rather than the individual warp and weft behaviors of the textile.

Of the 1-bed patterns, Polo Pique was identified as the pattern with the lowest weft/warp stitch count ratio (0.26) and was shown to deform more in the warp. At the other end of the extreme, Cross-Miss, the 1-bed pattern with the highest weft/warp stitch count ratio (0.68) also deformed more in the warp but showed a less pronounced difference in the weft versus warp curvatures. This is consistent with the observation that patterns with weft/warp stitch count ratios closer to 1.0 tend to show less discrepancy between the amount of stretch in the weft versus warp direction.

Despite some consistent trends, it must be noted that weft to warp stitch count ratios is not an accurate prediction of how a textile will behave under loading. This is evident through the example of Ripple Cardigan, among others such as Popcorn and Single Cross Tuck which all showed almost uniform deformation despite differing properties in the weft and warp direction of the textile. This supports a conclusion drawn in Section 3.4 that a more accurate prediction of how textiles will behave under loading might stem from a deeper analysis of individual stitch behavior and how that impacts the global deformation of the textile. While it is relatively simple to understand how a pattern deforms when pulled in one direction, it is more complicated

to understand the impact that the warp and weft properties have on each other when stressed multiaxially. While this kind of analysis is beyond the scope of this thesis, the research presented uses physical prototyping to set a basis of understanding for how various patterns might behave under loading.

10 CROSS MISS

WARP CURVATURE + STRETCH

WARP/WEFT OVERLAY

WEFT CURVATURE + STRETCH
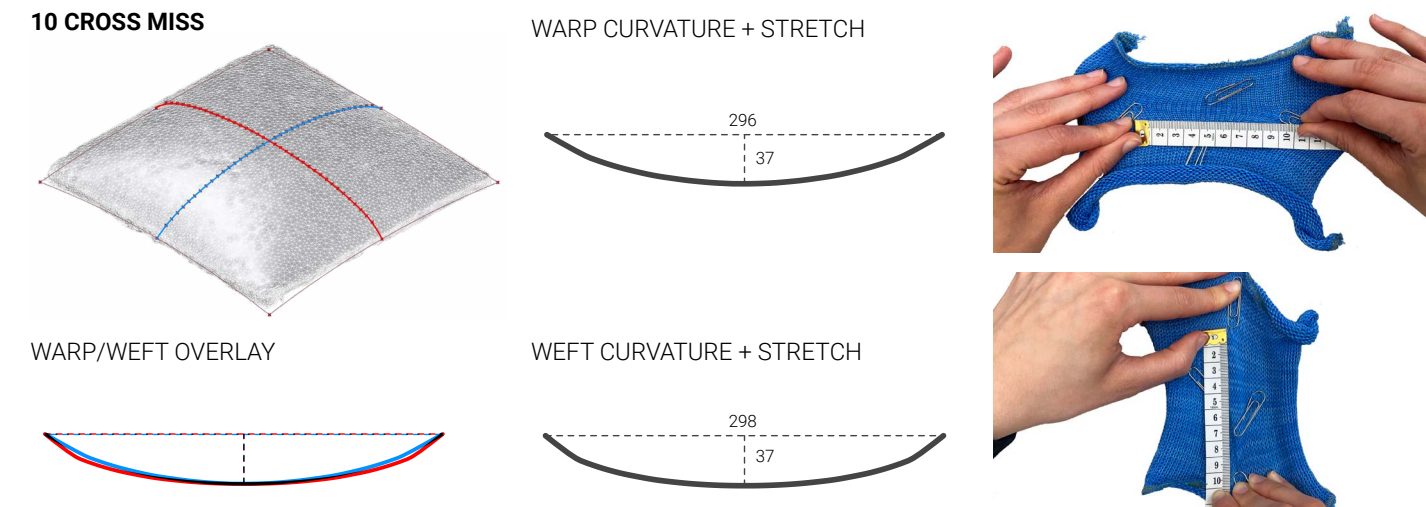
Figure 75. The similar deformation in the warp and weft direction shown by Cross Miss is consistent with the observation that patterns with weft/warp stitch count ratios closer to 1.0 show less discrepancy between the amount of stretch in the weft versus warp.

4.3.3 Discussion of Textile Removal
To create a basis for discussion, the removal of all textiles was recorded and comments were made on the time and damage state. Most patterns showing low removal times (00:20-00:30) also showed little to no damage to the textile, indicating limited adhesion to the concrete. Patterns with higher removal times (01:00-02:00+) showed more damage to the textile, indicating stronger adhesion to the concrete. These patterns also tended to show more pronounced surface textures with layered or loose stitches. In some cases, the loops formed anchor-like bonds with the concrete, making the adhesion stronger but also creating irreparable pulls in the textile when removed. A notable exception is Milano, which required 02:00 to remove but showed little to no damage to the textile. Figure 76 organizes the patterns from lowest to highest removal time, which may indicate which patterns do or do not adhere strongly to the concrete and could form the basis of selection for situations where either condition is desired. In all the textiles, a thin layer of concrete remained, while in some of the more textured patterns, small round bits of concrete remained scattered throughout. All casts were made using the 4-strand polyester yarn. The degree of damage and removal time would also likely change were the yarn type or concrete mix to be altered.

Pattern	Removal Time
Single Cross Tuck	00:18
Cross Miss	00:20
Weft Lock	00:22
Double Cross Miss	00:25
Half Milano	00:25
Rib Ripple	00:25
2x2 Rib	00:30
Long Tuck Stripe	00:30
Mock Rib	00:30
Crepe	00:44
Twill Effect	00:46
Cardigan	00:50
Ripple Cardigan	01:00
Half Cardigan	01:30
Double Lacoste	01:30
Polo Pique	01:50
Milano	02:00
Double Half Cardigan	02:30
Popcorn	02:40
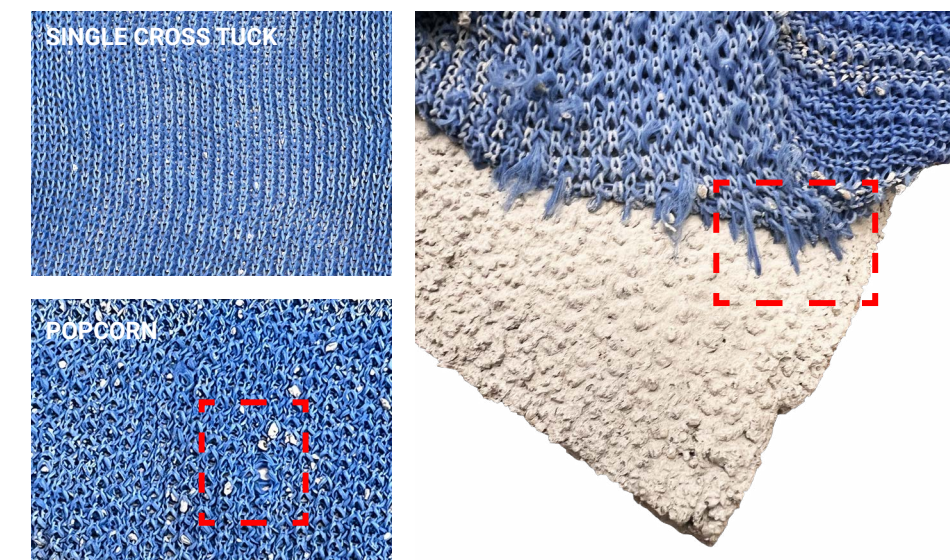
Figure 76. (Left) Pattern list organized from lowest to highest removal time. (Middle) Single Cross Tuck and Popcorn show significant differences in pattern texture and degree of damage following removal, where Single Cross Tuck showed no damage and Popcorn showed tearing and unraveling. (Left) Double Half Cardigan shows a representative example of the stitch anchoring as described in this section.

5.0 Pattern Combinations

In this phase of the research, 2 of the 19 patterns were chosen for combination in a variety of formations. Pattern combinations were designed based on diagrammatic sketches, translated to Model 9, and were knit using the recycled PET yarn. This section documents the resulting forms and describes the methodology behind the specific pattern selections. It also provides insight into sources of inspiration that informed the way the 2 patterns were arranged together in one textile.

5.1 Selecting Patterns for Combination

Of the 21 patterns tested, Cross Miss and Double Half Cardigan emerged as extremes with the lowest and highest deformation respectively. These patterns were selected as a starting point because they were expected to show extreme contrast in deformation behavior and would effectively demonstrate the impact of combining different pattern behaviors. In addition to deformation behavior, a critical aspect to consider when combining patterns is the weft and warp stitch count required to form a similarly sized textile. Considering an example situation where two patterns are knit side-by-side in the same textile, the warp stitch count has a great impact on the knit textile. For instance, if one pattern requires 100 stitches in the warp to knit 50mm of length, and another pattern requires 200 stitches in the warp to knit the same length, the resulting textile will be warped or buckled because the warp stitch count can only be one value, which will result in two different lengths within the same pattern. The same issue applies to the weft direction if textile width were under consideration. Essentially, when combining patterns, it is ideal for the weft or warp stitch counts (depending on the situation) to be equivalent or at least not extremely different. Equivalent or similar stitch counts will prevent rippling and distortion of the knit textile.

Figure 77. Diagrammatic explanation of the impact of incompatible warp stitch counts on a knit textile.
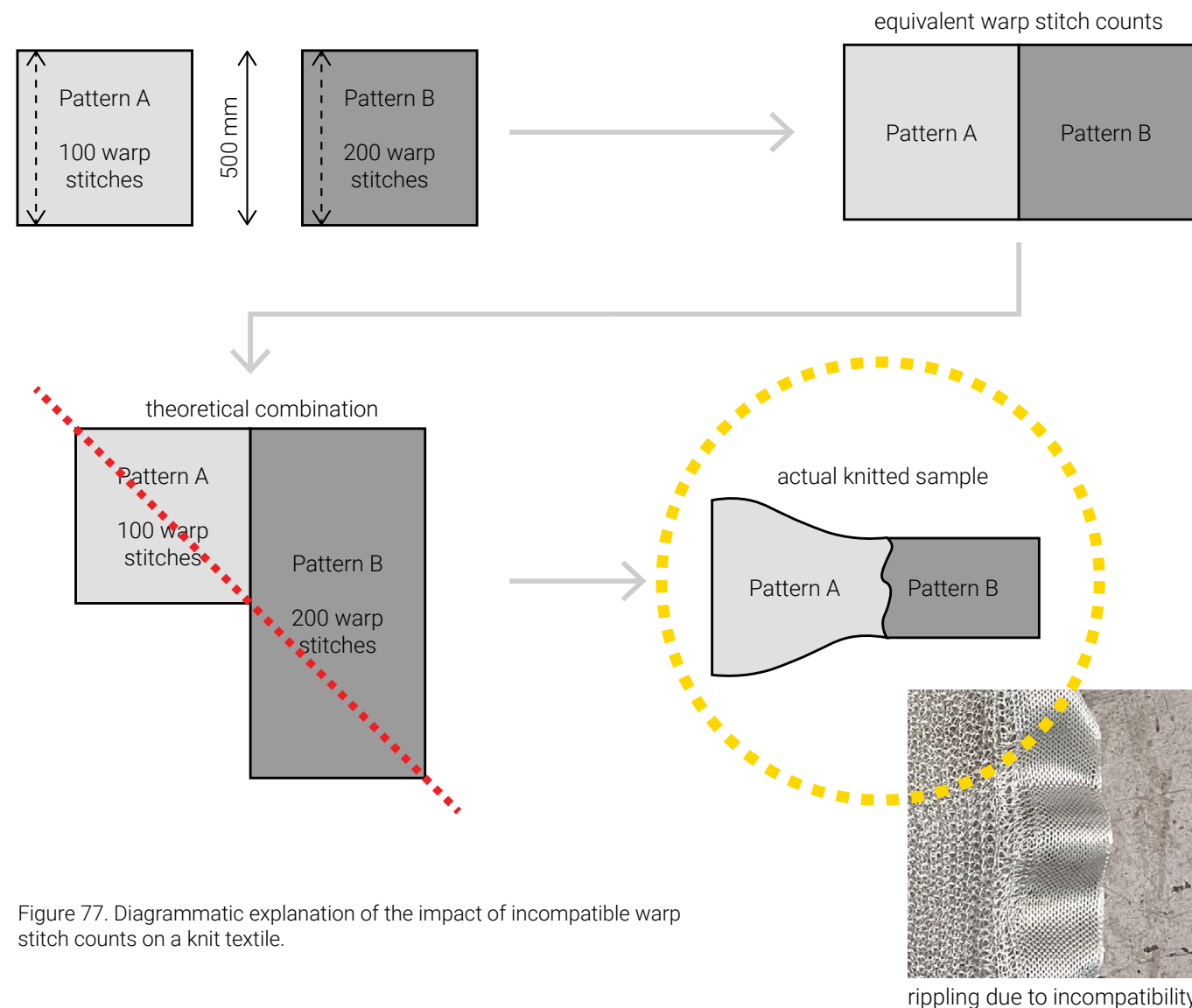
It is likely coincidental that Cross-Miss and Double Half Cardigan have identical warp stitch counts in both the polyester and recycled PET yarn, but this coincidence is significant in that it allowed for the combination of the two most extreme patterns in terms of deformation behavior. Figure 78 identifies other pattern combinations that share significant deformation variation and equivalent stitch counts: Twill Effect (low deformation) and Double Lacoste (high deformation) or Half Cardigan (high deformation) as well as Mock Rib (low deformation) or Half Milano (low deformation) and Popcorn (high deformation). In this research, only Cross-Miss and Double Half Cardigan were combined but future research should include other patterns.

Pattern	Measured Width (mm) 120x120 Sample	Measured Height (mm) 120 x 120 Sample	Adjusted Stitch Count Weft 300x300 Sample	Adjusted Stitch Count Warp 300x300 Sample
(4) Double Half Cardigan	350	110	103	327
(10) Cross Miss	250	110	144	327
(12) Double Lacoste	410	70	88	514
(5) Half Cardigan	340	70	106	514
(18) Twill Effect	380	70	95	514
(16) Popcorn	360	90	100	400
(14) Mock Rib	225	90	160	400
(2) Half Milano	300	90	120	400

Figure 78. Chart of selected patterns which showed both significant deformation variation and equivalent warp stitch counts using the recycled PET yarn. Darker colors indicate higher deforming patterns whereas lighter colors indicate lesser deforming patterns. Three sets of combinations (green, blue, orange) are identified. It is clear from the chart that patterns within these groups showed equal measured length in the 120x120 samples and therefore produced equivalent warp stitch counts when scaled to a 300x300 sample.

Another aspect that was considered during pattern selection is the compatibility of pattern motives. It is generally not possible to place one pattern motive next to another in the pattern generation file within Model 9 and expect the machine to knit without error. In combining Cross-Miss with Double Half Cardigan, certain operations were required to transition between the patterns, involving basic actions of transferring stitches between two sides of the needle bed as demonstrated in Figure 79. This process could become more involved as the complexity of the patterns increase, but in this case, the transition stitches were placed manually. This could likely be automated for more complicated situations through advanced scripting.
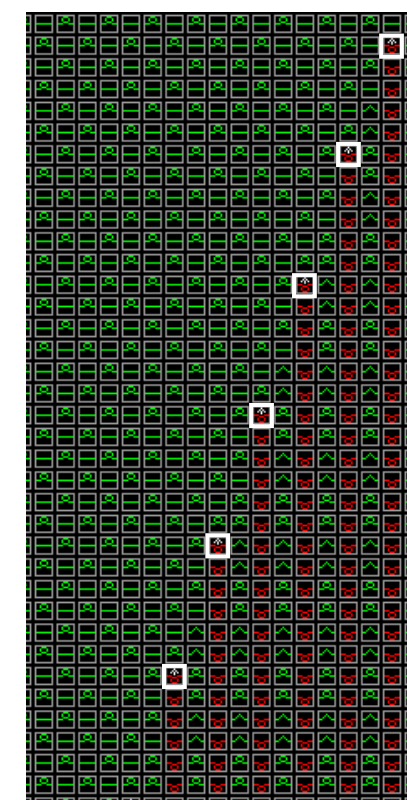
Figure 79. Transition stitches are placed manually to create transfers between Double Half Cardigan and Cross Miss.
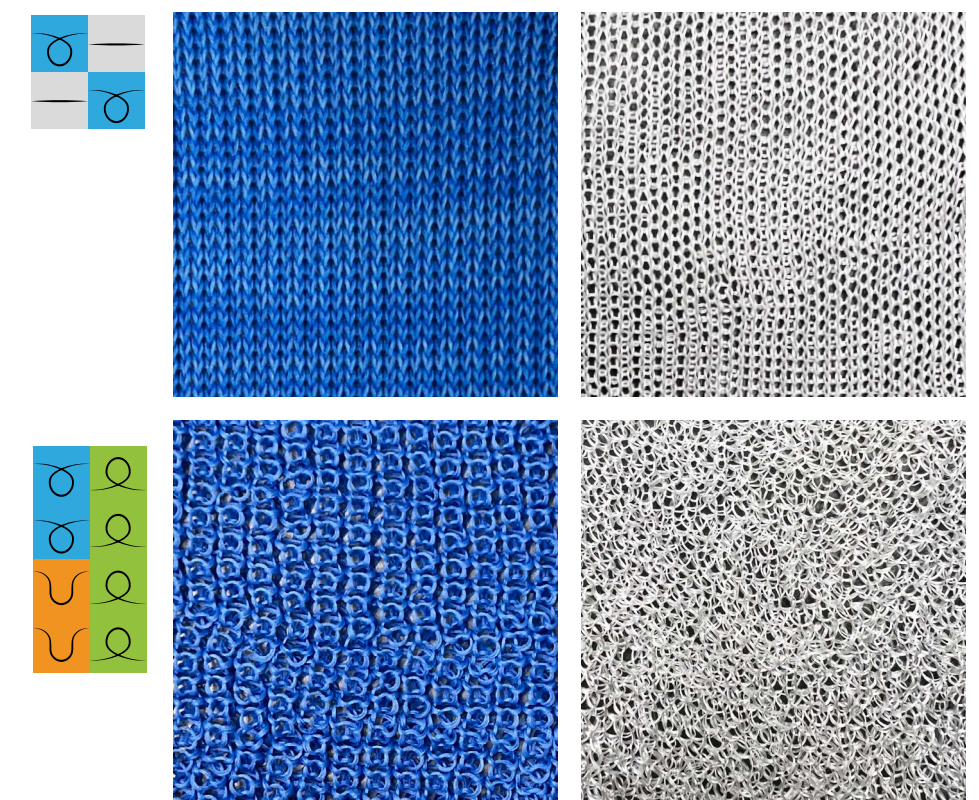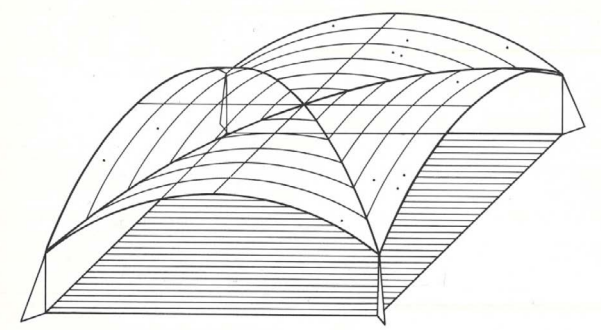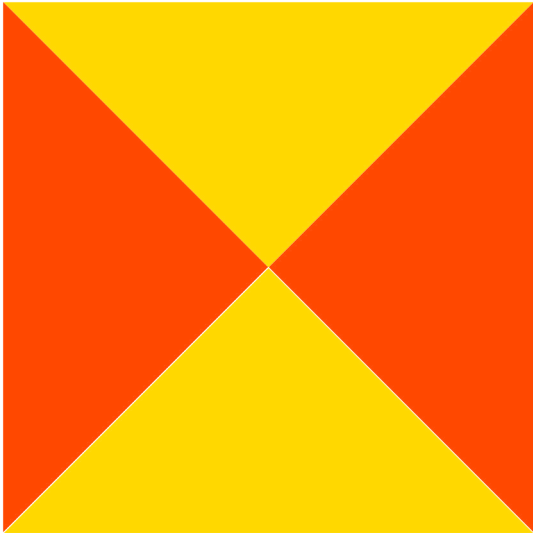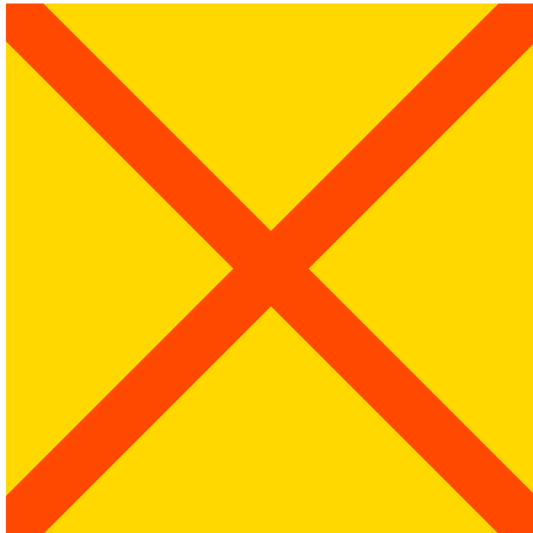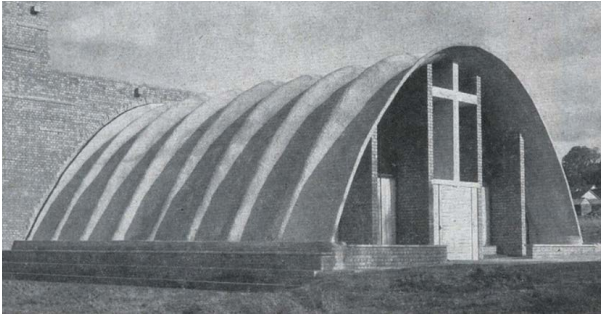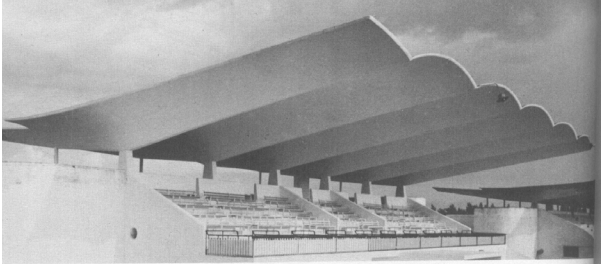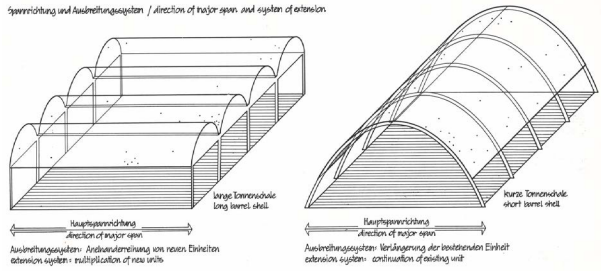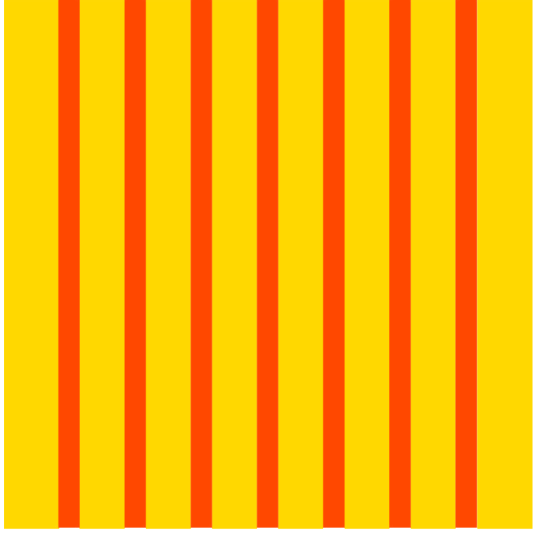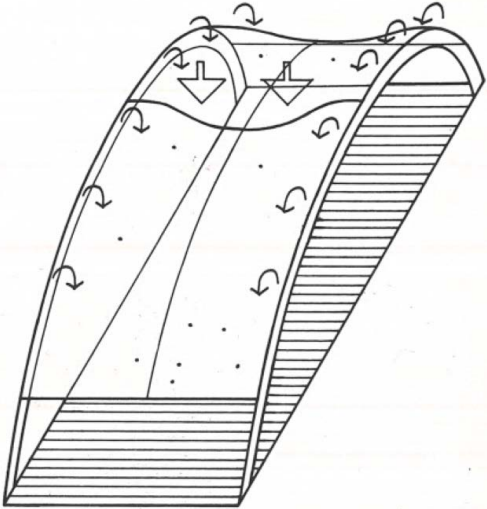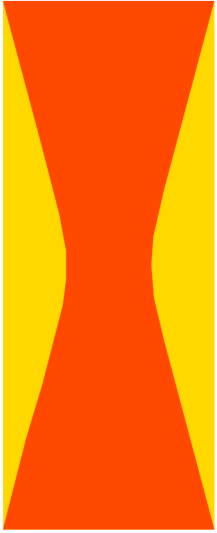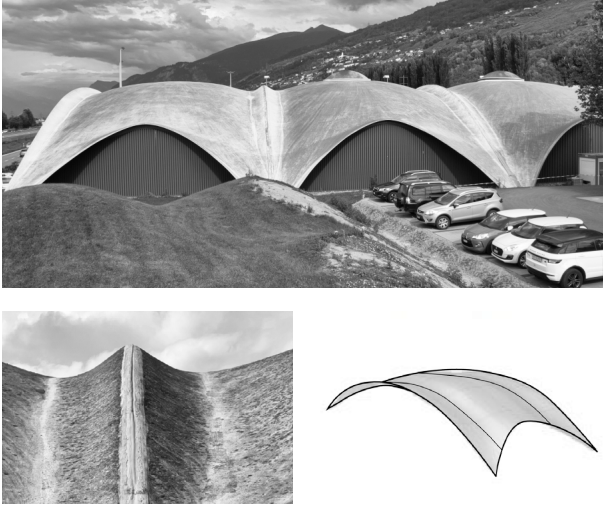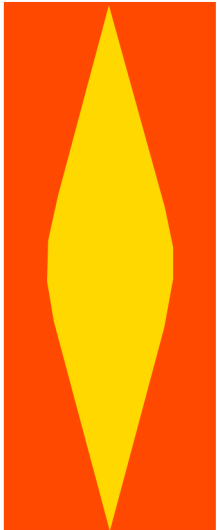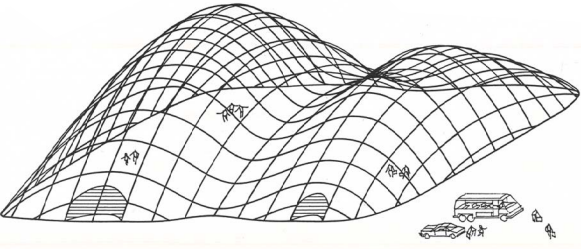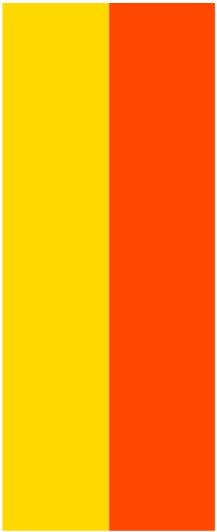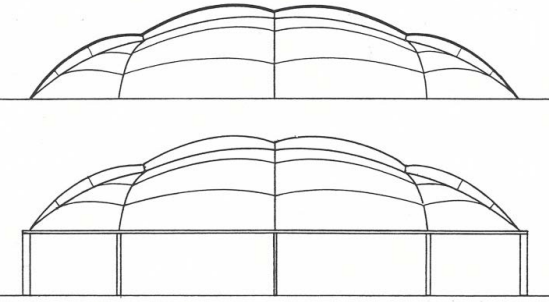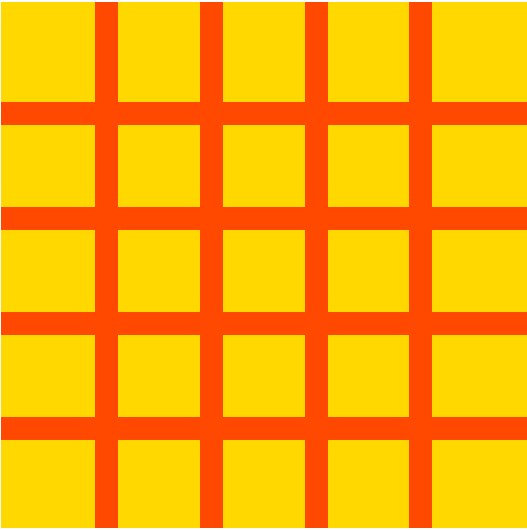
Figure 80. (Top) Cross Miss pattern in polyester and recycled PET yarn (Bottom) Double Half Cardigan pattern in polyester.and recycled PET yarn with accompanying motives.

5.2 Inspiration from Existing Shell Structures and Other Forms

Once the selected patterns were established, the next step in the research necessitated the design of pattern templates where the two patterns are arranged specifically within one textile. The design process involved the review of notable shell structures and various basic shell forms (Engel, 1967). The pattern templates were designed to mimic or reflect certain forms extracted from this literature review. This method was purely exploratory in that certain intuitive predictions were made about how the pattern templates would behave under hydrostatic loading based on the information developed in previous phases. To establish the general sizing and stitch count, the pattern gauge excel sheet mentioned in previous chapters was used, although this method proved to be a relatively imprecise way to size combination patterns and will be discussed in a later section. The following chart demonstrates the relationships between the target geometries and the designed pattern templates.

Shell Geometry	Pattern Template(s)
	= High Deformation = Low Deformation
Cross Vault Figure 81. Bacardi Bottling Plant by Felix Candela (Source: LUNA Image Collections) Figure 82. Illustration of a cross vault (Engel, 1967).	4-Quadrant and X-Shape Patterns

Shell Geometry	Pattern Template(s)
Ribbed Arch or Ribbed Ceiling Shell Figure 83. Ctesiphon Shell, a ribbed catenary arch, by James Waller (Source: Flickr via ArchiDave) Figure 84. Zarzuela Hippodrome (Source: MetaLocus) Figure 85. Illustration of ribbed roof system (left) and ribbed catenary vault (right) (Engel, 1967).	Alternating Stripe Pattern
Double Curved Vault / Arch Figure 86. Illustration of a short barrel shell (Engel, 1967).	Hourglass Pattern

Shell Geometry	Pattern Template(s)
Flared Shell Figure 87. Bruhl Sports Center, 1982 (Top) Series of repetitive shells (Bottom) Close-up of flared seams between repetitive shells (Source: Structurae)	Diamond Pattern
Variable Curvature Shell Figure 88. Illustration of thrust lattice system defined by surface indentation (Engel, 1967).	Half-Half Pattern
Variable Curvature Shell Figure 89. Illustration of a variable shell structure (Engel, 1967).	Grid Pattern

5.3 Documentation of Results

The following section describes and documents the results of each pattern template. All casts were performed on a 500x500mm frame with a removable stabilizing plate. The method of casting used is fundamentally the same as the method described in section 4.1 but uses a cement paste coating instead of the previous mix described. The cement paste mix was chosen for its general stability when applied to extreme curvatures which is likely due to the inclusion of PVA fibers which hold the material together. The previous mix showed heavy surface cracking in more extreme curvatures and a more workable consistency which raised concerns about slumping. Unlike the previous casts which maintained a thickness of 10mm, the combination casts have a 5mm thickness to highlight the potential for minimal thickness of the cast forms. The cement paste mix proved to be highly effective for the desired intent and showed limited cracking and no slumping.

In addition to the casting process and results of these tests, this section also documents the number of calibration attempts performed to achieve an appropriately sized textile for each pattern template. This information is included to demonstrate the unpredictable impact of pattern combination on the overall dimensions of a knit textile. In some cases, multiple versions of a single pattern template were knitted until the desired effect was achieved.

1 Liter	(g)
Water	584
Cement CEM III / B 42.5 N	1580
Limestone Powder	1580
Superplasticizer	3.195
PVA Fibers	39
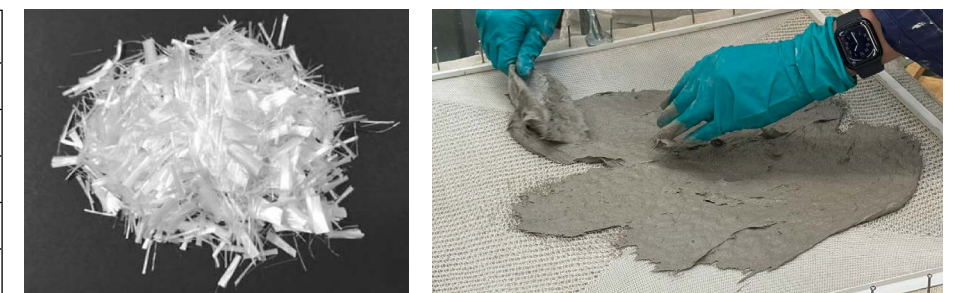
Figure 90. (Left) PVA fiber mix used for the combination pattern casts, (Middle) PVA Fibers (Source: Nycon), (Right) PVA Fiber mix being applied to a combination pattern textile.

Figure 91. 4-Quadrant (Alt Supports) pattern before casting (left) and after casting (right). A 500x500 casting frame was used for the pattern combination tests and followed the same methodology described in Section 4.1.

4-Quadrant

The design of the 4-Quadrant pattern template is inspired by cross vault forms such as the Bacardi Rum Bottling Plant by Felix Candela. This pattern template places Cross-Miss and Double Half Cardigan in four alternating quadrants within one textile. During casting, the textile was supported on all four sides of the casting frame. As expected, the result shows a significant difference in curvature between the two types of quadrants, where Double Half Cardigan deforms considerably whereas Cross-Miss visibly restricts the material. The form shows an undulating curvature with noticeable but more gradual transitions between the curvatures. The defined lines shown in the bottling plant ceiling would only be possible to fabricated with textile if stiffening elements were inserted.

During the gauging process, three versions of the 4-Quadrant pattern were knitted until a textile was created which fit as desired on the 500x500 casting frame (Figure 91). The main issues observed included too much warp length, not enough weft width, and some distortion at the intersection point of all four quadrants. The length and width dimensions were solved through trial and error, while the center point distortion was solved by adding stitches above and below the intersection, so the patterns did not touch at a sharp angle. Intense curling of the Cross-Miss edges also posed a problem for the general workability of the textile. To address this, a few rows of Double Half Cardigan, which has almost no curling tendencies, were added to the Cross Miss edges to reduce its tendency to curl. This method was somewhat effective but might require more rows of a non-curling pattern to cause the curled pattern to lie flat.

Figure 92. (Left) Desired pattern template shape, (Middle) Representation of actual bitmap pattern used to knit the sample, (Right) Appropriately sized 4-Quadrant pattern attached to frame and supported on all four sides by nails.

Figure 93. Side view of 4-Quadrant casting result after removal from frame.
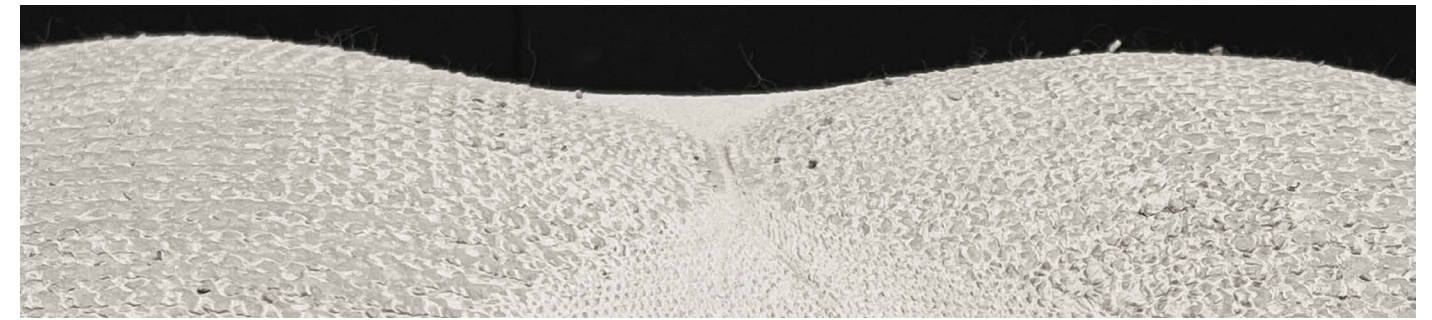
Figure 94. Close-up view of resulting surface texture following removal of textile.

Figure 95. (Left) Perspective view of 4-Quadrant casting result after removal of textile, (Right) Close-up view of surface texture prior to removal of textile.

Figure 96. (Left) Top view of 4-Quadrant casting result after removal of textile, (Right) Removing the combination pattern textile.

4-Quadrant (Alternative Supports)

Following removal, the 4-Quadrant template described above was re-used to demonstrate the potential of creating different shapes with the same textile. In this case, the 4-Quadrant textile was suspended on the casting frame and only supported at the two Cross-Miss edges while the Double Half Cardigan edges were allowed to deform unsupported. This resulted in a similar but more dramatic curvature in these quadrants. Another alternative could involve supporting the textile only at the four end points and allowing all edges to deform unsupported.
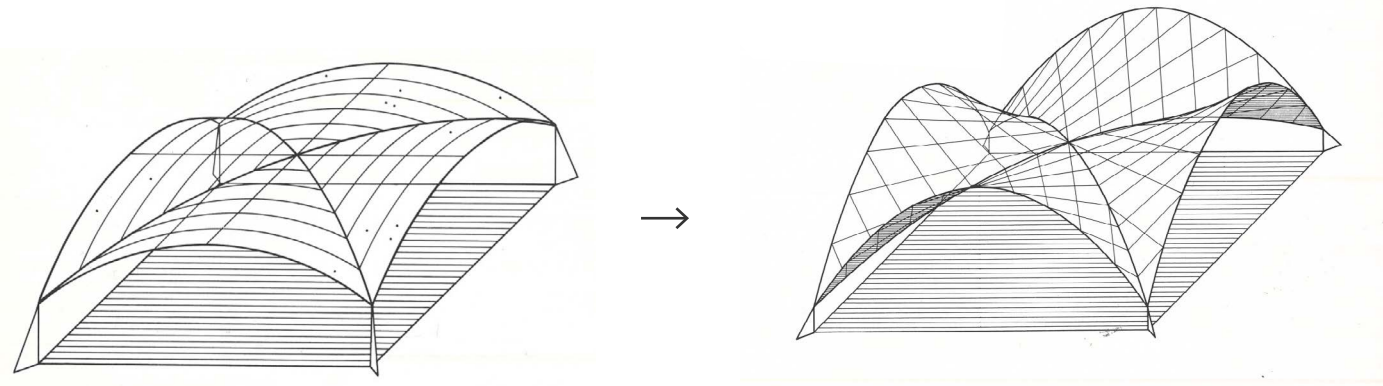
Figure 97. By releasing two of the four edges of the textile, specifically the edges with a higher deforming pattern, more dramatic curvatures like those shown on the right were achieved on two edges.

Figure 98. (Left) 4-Quadrant pattern textile after removal from the first version of this cast form, (Right) 4-Quadrant Alt-Supports on the casting frame showing high deformation at the released edges.

Figure 99. Side view of 4-Quadrant (Alt Supports) casting result after removal of textile.

Figure 100. Close-up view of cross-sectional curvature and surface texture prior to the removal of the textile.

Figure 101. Side view of 4-Quadrant (Alt Supports) casting result prior to textile removal.

Figure 102. (Left) Plan view of 4-Quadrant (Alt Supports) casting result, (Right) Close-up view of high curvatures.

X-Shape

Like the 4-Quadrant template, this combination was initially developed to mimic a cross-vault shape. The placement of the Cross-Miss pattern in thin diagonal strips produced more defined but still gradual delineations between the two patterns. While the pattern tested was supported on all four edges, a more dramatic curvature like a hypar shell (Figure 97) could likely be created by only supporting the four corners of the Cross-Miss diagonal strips.

The X-Shape template only required two attempts to fabricate an appropriate size for the casting frame. This is possibly due to the small area of Cross-Miss in relation to the area of Double Half Cardigan which may have had a lesser distorting impact on the overall textile.
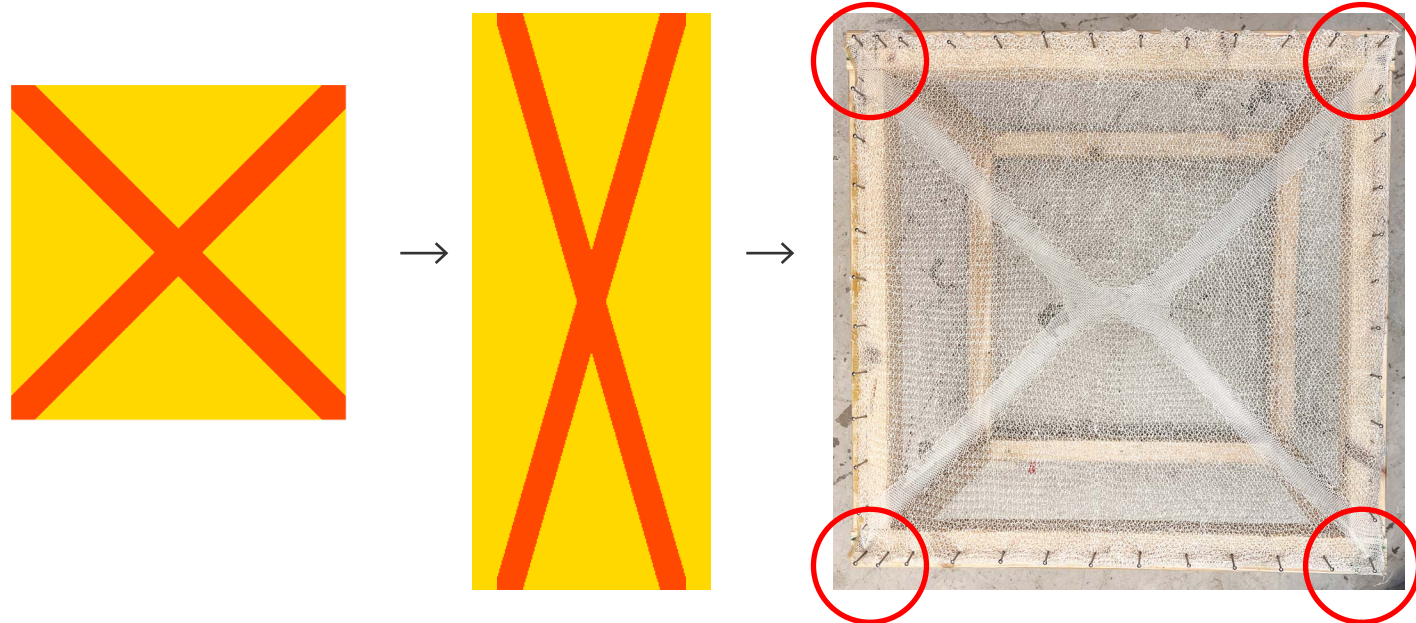
Figure 103. (Left) Desired pattern template shape, (Middle) Representation of actual bitmap pattern used to knit the sample, (Right) Appropriately sized X-Shape pattern attached to frame and supported on all four sides by nails. If the sample were to be supported at the four corners marked within red circles, it is likely that the cast shape would take on a more dramatic curvature.

Figure 104. Side view of X-shape cast sample.

Figure 105. Close-up view of X-shape sample curvature.

Figure 106. (Left) X-Shape pattern textile after removal showing limited damage or distortion, (Right) Close-up view of concrete texture after textile removal.

Figure 107. (Left) Plan view of X-shape cast sample, (Right) Close-up view of pattern texture.

Grid

The Grid template was developed to test the feasibility of creating a ribbed or waffle-like shell structure. As expected, the pattern zones showed a significant difference in curvature and deformation, where the Double Half Cardigan zones bulged considerably around the Cross- Miss zones under the weight of concrete. While casting, this pattern was supported on all four edges and allowed to deform freely. Due to the size of the textile, the application of support at the edges did not cause much pre-tensioning to occur, so the overall shape shows high deformation. In future experiments, greater control should be placed over deformation where there is more global pre-tensioning but also concentrated supports at every grid line. This could support the fabrication of a waffle-like floor/ceiling plates or other shell structures.
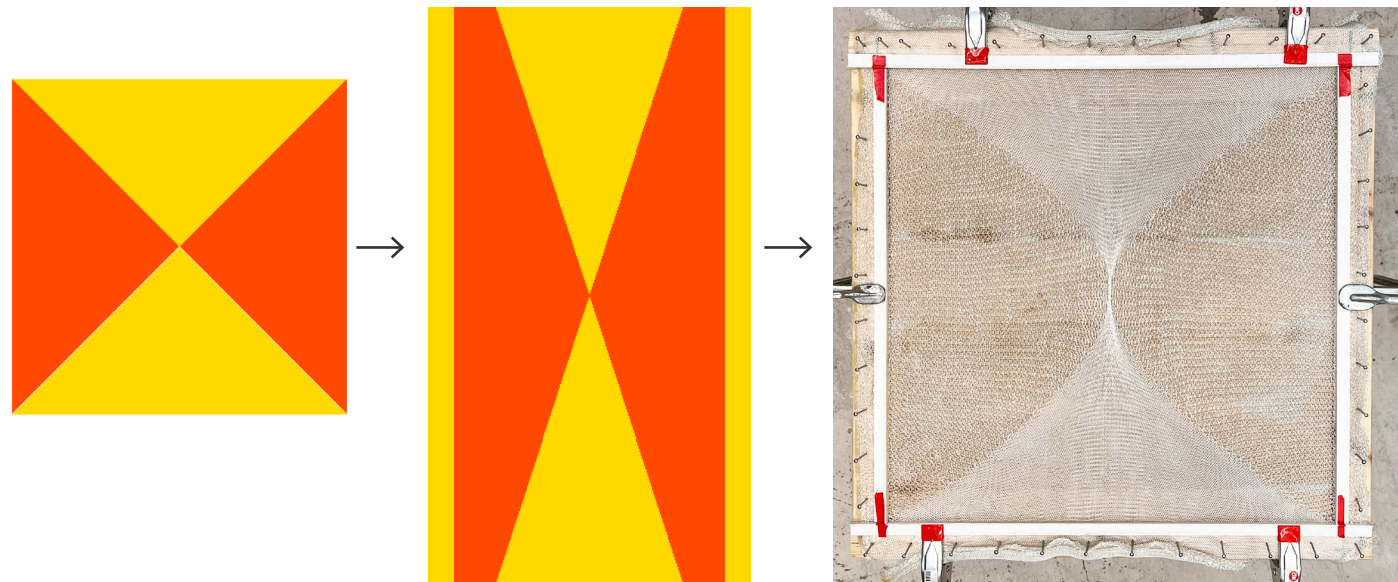

Figure 108. (Left) Desired pattern template shape, (Middle) Representation of actual bitmap pattern used to knit the sample, (Right) Appropriately sized Grid pattern attached to frame and supported on all four sides by nails.

Figure 109. Front view of Grid casting result.
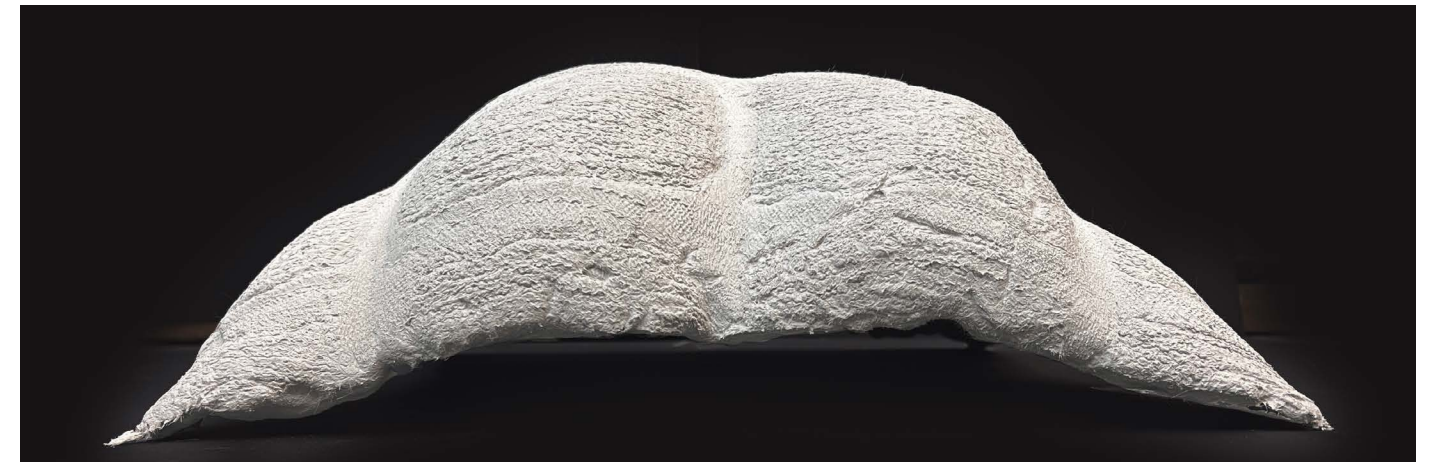
Figure 110. Side view of Grid casting result after textile removal.

Figure 111. (Left) Perspective view of Grid casting result after textile removal, (Right) Close-up view of Grid pattern texture.

Figure 112. (Left) Top view of Grid casting result, (Right) Close-up view of Grid pattern texture.

Hourglass

The initial motivation of the Hourglass pattern was to create a barrel vault-like structure. However, physical prototyping of the pattern template suggested that a more expressive curvature might be possible by narrowing the width of the Cross-Miss strip at the center of the pattern. By supporting the pattern only two edges, the areas of Double Half Cardigan were allowed to deform significantly while constrained at one edge by the Cross-Miss, which showed much less deformation. This resulted in an extreme double curved vault-like form. By changing the support conditions, for example supporting the pattern only at the four corners, there could be significant variety within this type of form.

Figure 113. (Left) Desired pattern template shape, (Middle) Representation of actual bitmap pattern used to knit the sample and the finished textile, (Right) Hourglass textile immediately after casting showing extreme curvature when supported only at two ends.
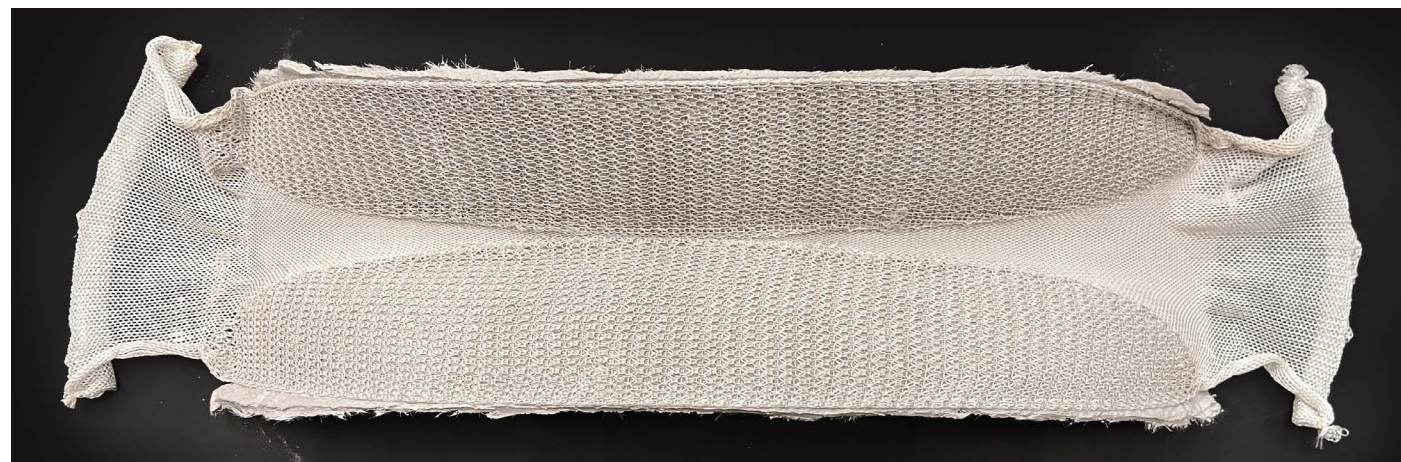
Figure 114. Top view of Hourglass casting result.
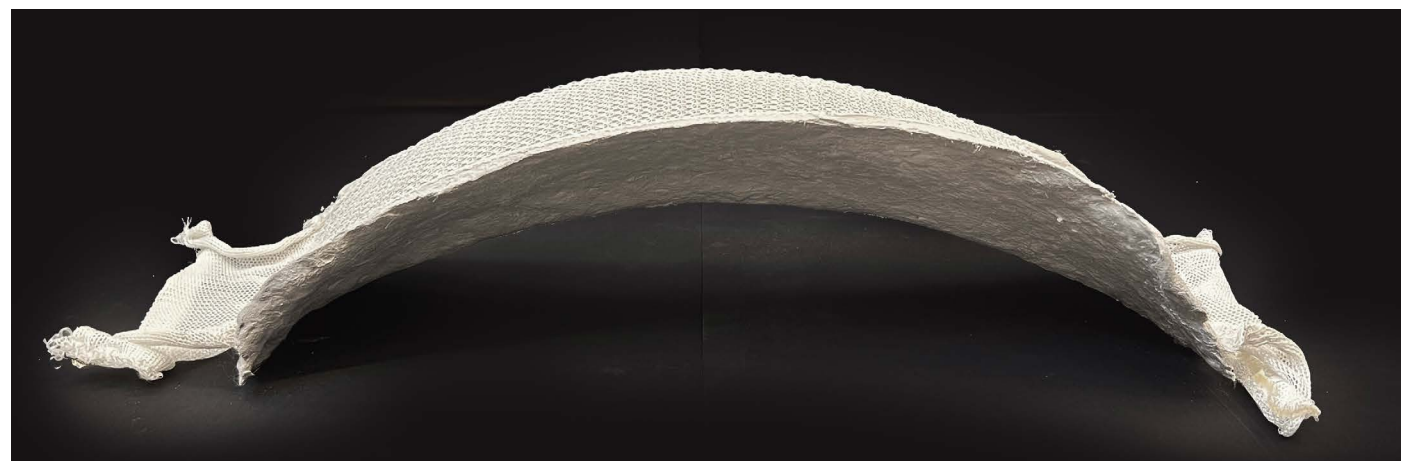
Figure 115. Side view of Hourglass casting result.

Figure 116. Overall view of Hourglass casting result.

Figure 117. Close-up images of Hourglass curvature and pattern texture.

Alternating Stripe

The Alternating Stripe pattern was generated to test the feasibility of creating a ribbed arch form like the Ctesiphon shells developed by James Waller in the 1950s. The combined pattern alternates between longitudinal strips of Double Half Cardigan and Cross-Miss to create distinct zones of varying stretch. The textile was hung from the casting frame and supported only at two ends, which resulted in ribbed arched form. Additional point supports in the Cross-Miss zone might have created a more pronounced ribbed effect, but the potential is clear from the existing prototype. A significant increase in pre-tensioning of the Cross-Miss zones coupled with an increase in overall pre-tensioning might result in a form closer to the Zarzuela hippodrome, where there is no arching action. However, the Cross-Miss zones would need to be significantly rigidified for this to be achieved.

Figure 118. (Left) Desired pattern template shape, (Middle) Actual knit textile, (Right) Alt Stripe textile immediately after casting showing significant deformation and ribbing.

Figure 119. Top view of Alternating Stipe casting result.

Figure 120. Side view of Alternating Stripe casting result.

Figure 121. Perspective view of Alternating Stripe casting result.

Figure 122. (Left) Close-up view of Alternating Stripe surface texture, (Right) Head-on view of Alternating Stripe casting result showing ribbed cross section with the greatest deformation at the center rib.

Diamond

The Diamond pattern was first developed as an exploratory exercise with no clear goal form. Fitting this pattern to the casting frame where the entire oval, or diamond, is encapsulated within the 500x500 boundary required multiple calibration tests which will be discussed in the following section. The textile was then hung from the casting frame and supported at two edges. This resulted in an undulating form with a flared cross section that is reminiscent of the repetitive shells of the Bruhl Sports Center. A different support condition, where the textile is suspended only from the four corners, would yield a shape that is formally closer to the Bruhl Sports Center.
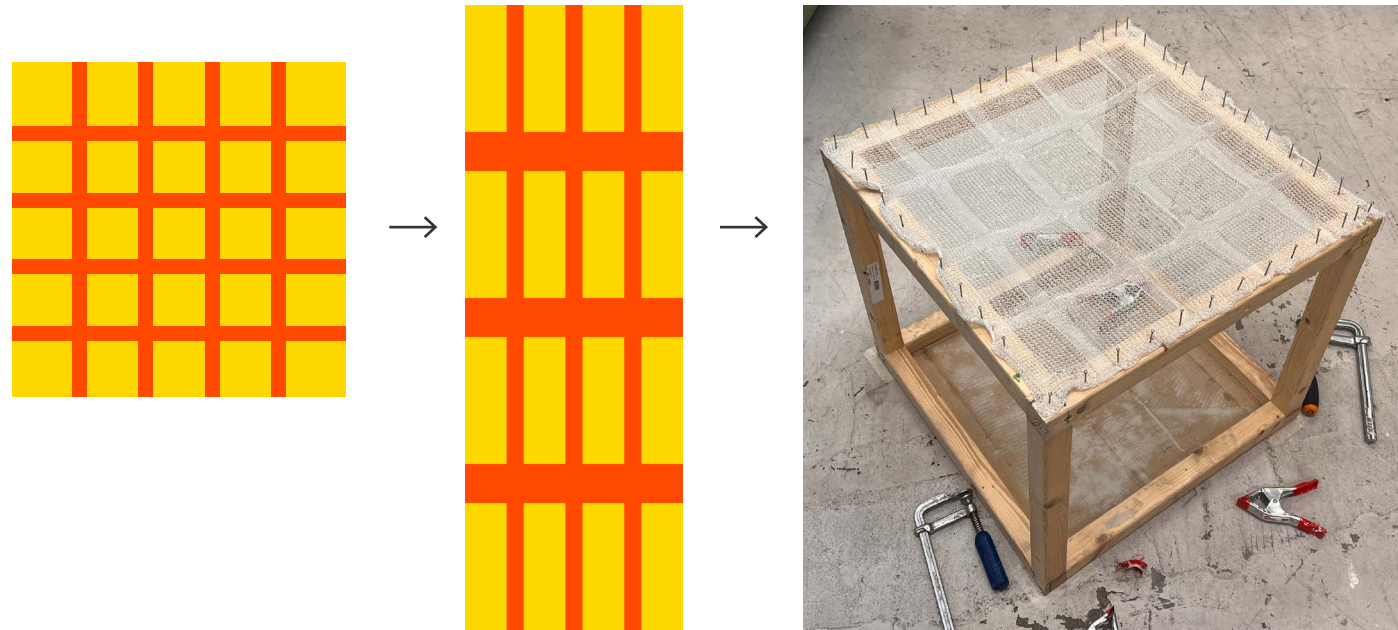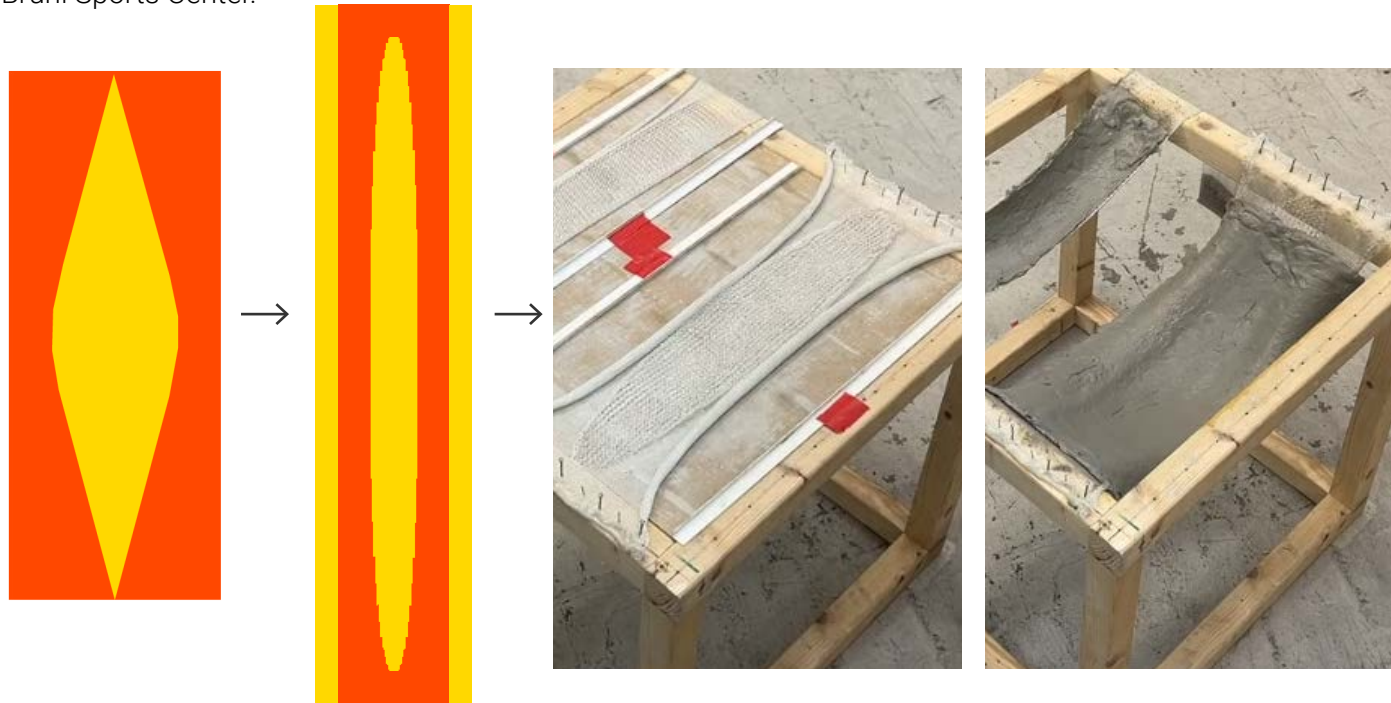

Figure 123. (Left) Desired pattern template shape, (Middle) Representation of actual bitmap pattern used to knit the sample, (Right) Diamond textile before and after casting.
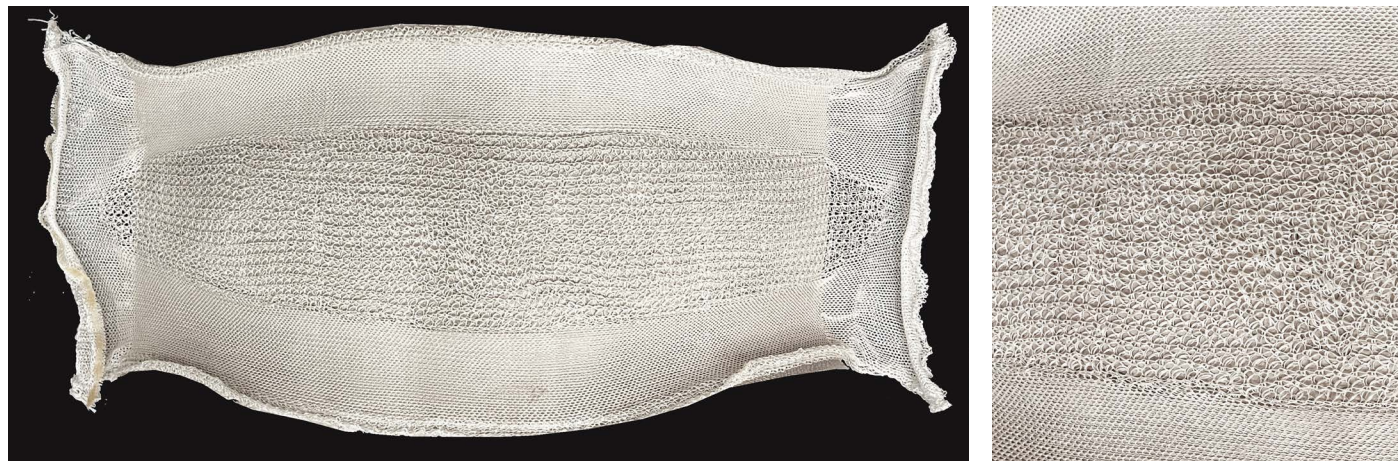
Figure 124. (Right) Top view of Diamond casting result, (Left) Close-up view of Diamond pattern's surface texture.

Figure 125. Side view of Diamond casting result.

Figure 126. Perspective view of Diamond casting result.
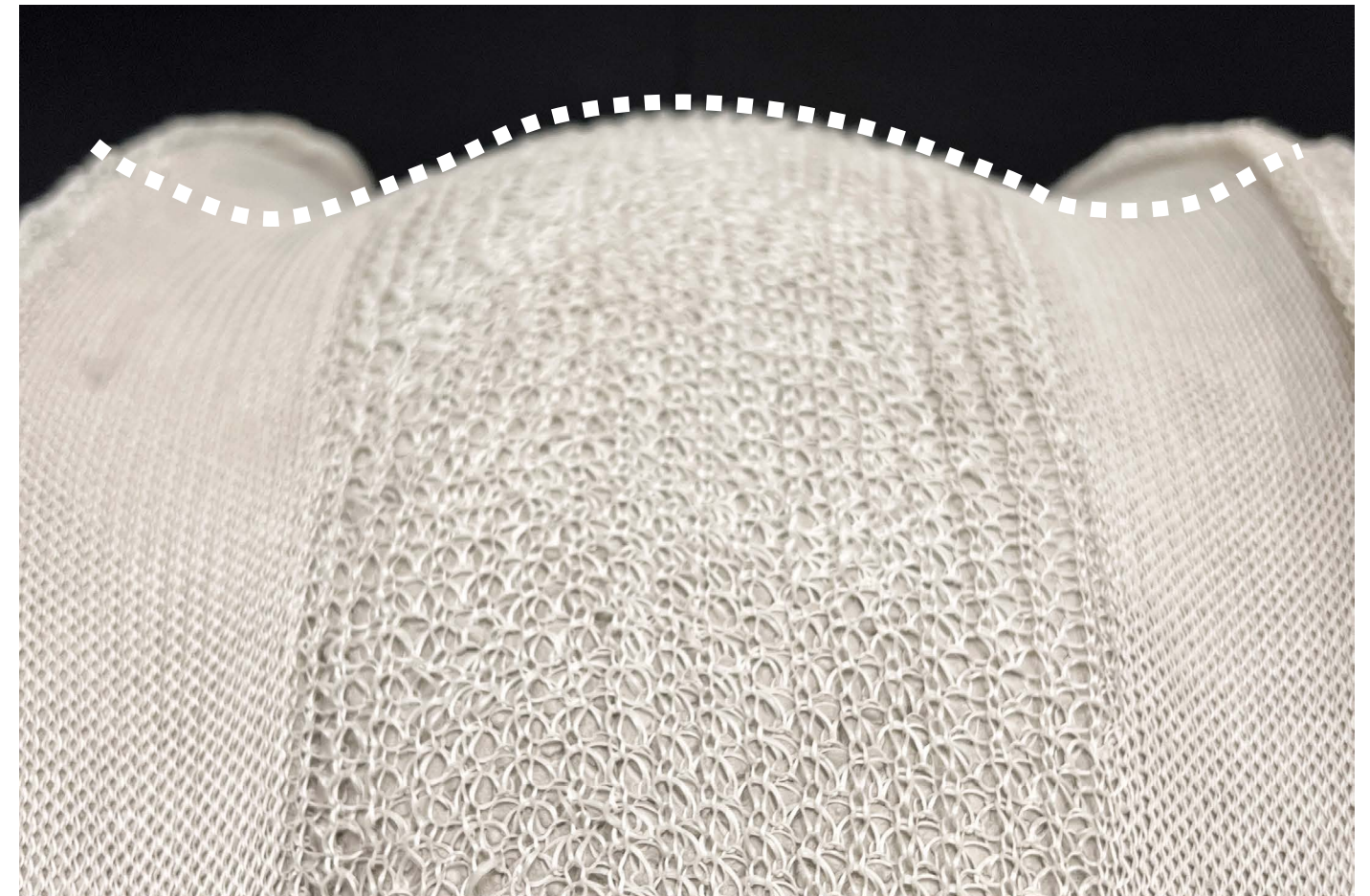
Figure 127. Close-up view of Diamond casting result showing undulating cross section with flared ends.

Half-Half

The Half-Half pattern was also developed as a purely exploratory exercise. Two vertical zones of Double Half Cardigan and Cross-Miss are placed next to each other with the same number of weft stitches. The expected outcome was a double curved form with clearly defined pattern-specific curvature zones. Instead, the result showed a relatively smooth double curvature with no clear delineation between the pattern zones. The cross section begins with a relatively steep curvature and appears to taper slightly when transitioning between Double Half Cardigan and Cross-Miss. A more intentional calibration of the pattern zones could allow for specific cross-section curvatures, while the widening of the Cross-Miss zone might show more of a delineation of curvature between the zones.
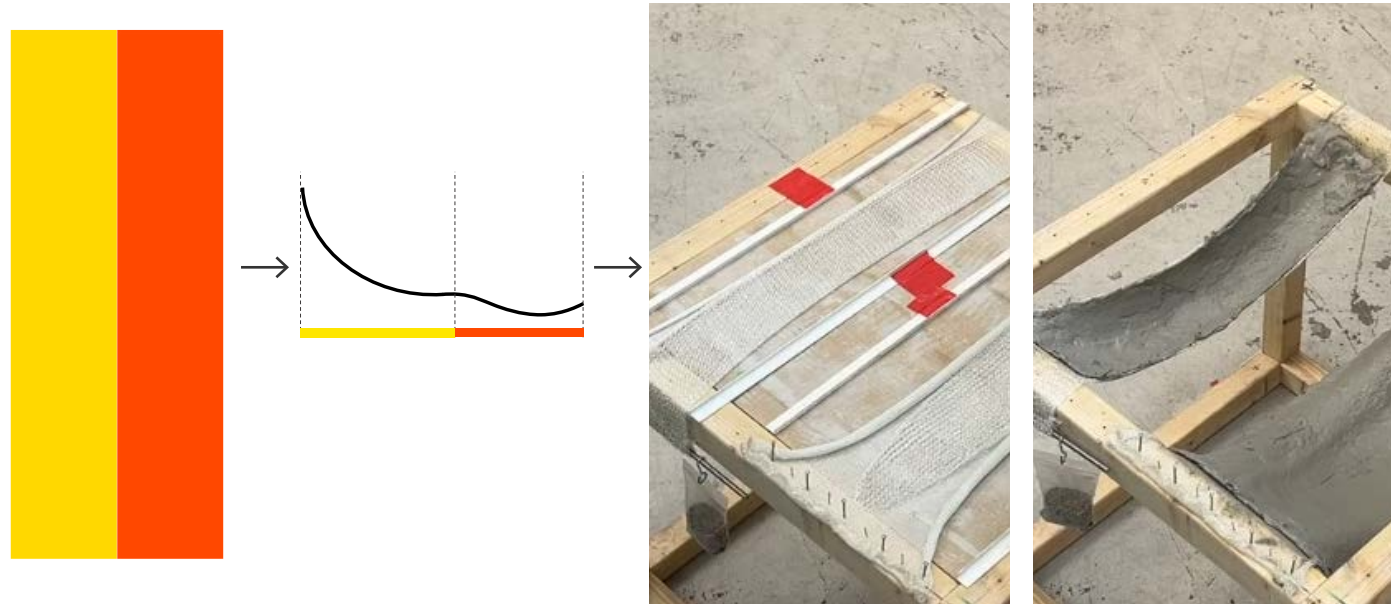
Figure 128. (Left) Desired pattern template shape, (Middle) Expected cross-section, (Right) Half-Half textile before and after casting.

Figure 129. Perspective view of Half-Half casting result.

Figure 130. Top view of Half-Half casting result.

Figure 131. Side view of Half-Half casting result looking from the Cross-Miss edge.
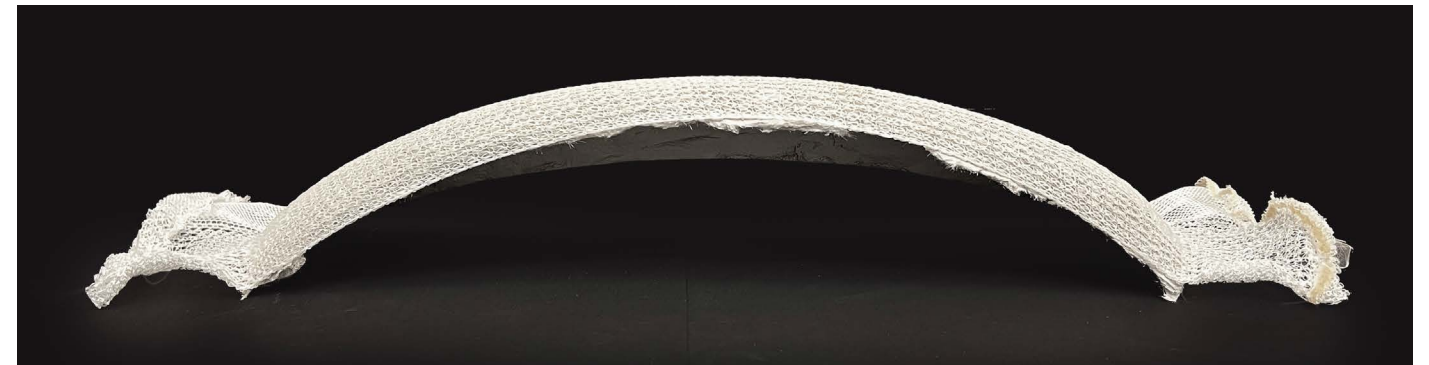
Figure 132. Side view of Half-Half casting result looking from the Double Half Cardigan edge.

Figure 133. Close-up view of the Diamond casting result pattern texture.

5.4 Discussion: Pattern Combination Results

The research reveals the enormous potential of pattern combinations to fabricate a wide range of shell forms with varying degrees of curvature and deformation. However, there are several limitations to consider.

Dimensional Changes in Combined Patterns

Through the combination process, it was observed that combining patterns often alters their dimensions, complicating the reliance on the previously developed pattern gauge system. The interaction between different stitch types and deformation behaviors means that the final dimensions of the combined textile can differ from those predicted. Specifically, the warp dimension of the combined textiles consistently was measured to be longer than desired. This was especially evident in the Grid pattern template where an increase in weft stitches created a dimensional increase in both the weft and warp direction. Although no stitches were added in the warp direction, the addition of stitches in the weft produced an overall increase in dimension of the textile. While the cause of this is unknown, it could be related to the overall weight of the textile, the yarn type, or an inconsistency in the knitting machine.

Figure 134. Two versions of the Grid pattern were knitted during the calibration process. The 4x4 grid shown on the left was too small in the weft direction for the casting frame, so another column was added to create the 5x4 grid shown on the right. Although no additional stitches were added in the warp, the addition of this column created an increase in both the weft and warp directions.

This underscores the unpredictability of pattern combinations and therefore the need for physical prototyping. No clear method was developed to negotiate this besides knitting multiple versions of the same pattern template where stitches were added or subtracted until the desired effect was achieved. Therefore, this necessitates a more nuanced approach to developing these textiles which considers the combined effects of multiple patterns. This might be approached by developing a dataset from physical prototypes of combination knits which measures and catalogues the influence of one pattern on the other in the weft and warp direction. A combination of three or more patterns would also require significant calibration and study which could be performed in a similar manner.

Figure 135. (Left) Three attempts were made to calibrate the 4-Quadrant pattern, (Right) Five attempts were made to calibrate the Hourglass pattern.

Challenges in Achieving Uniform Deformation

Another significant challenge encountered during the casting process is achieving uniform deformation under gravity loading, especially with a manual setup. While combining patterns with contrasting deformation behaviors effectively demonstrates the impact of this method, most combination textiles did not deform uniformly, making it difficult to understand the ideal uniform condition of the cast forms. Potential errors in the setup include irregular pre-tensioning, uneven applications of cement paste, and the sudden removal of the stabilizing plate. The consistency of uneven deformation also raises concerns about applying this method to larger scale applications where non-uniformity could lead to unpredictable structural behavior.

Figure 136. The manual nature of the casting process likely contributed to uneven deformations in the samples. (Left) Concrete paste is applied manually to the textile, (Right) The removal of the stabilizing plate often caused some areas of the textile to be released before others which might contribute to uneven deformation.
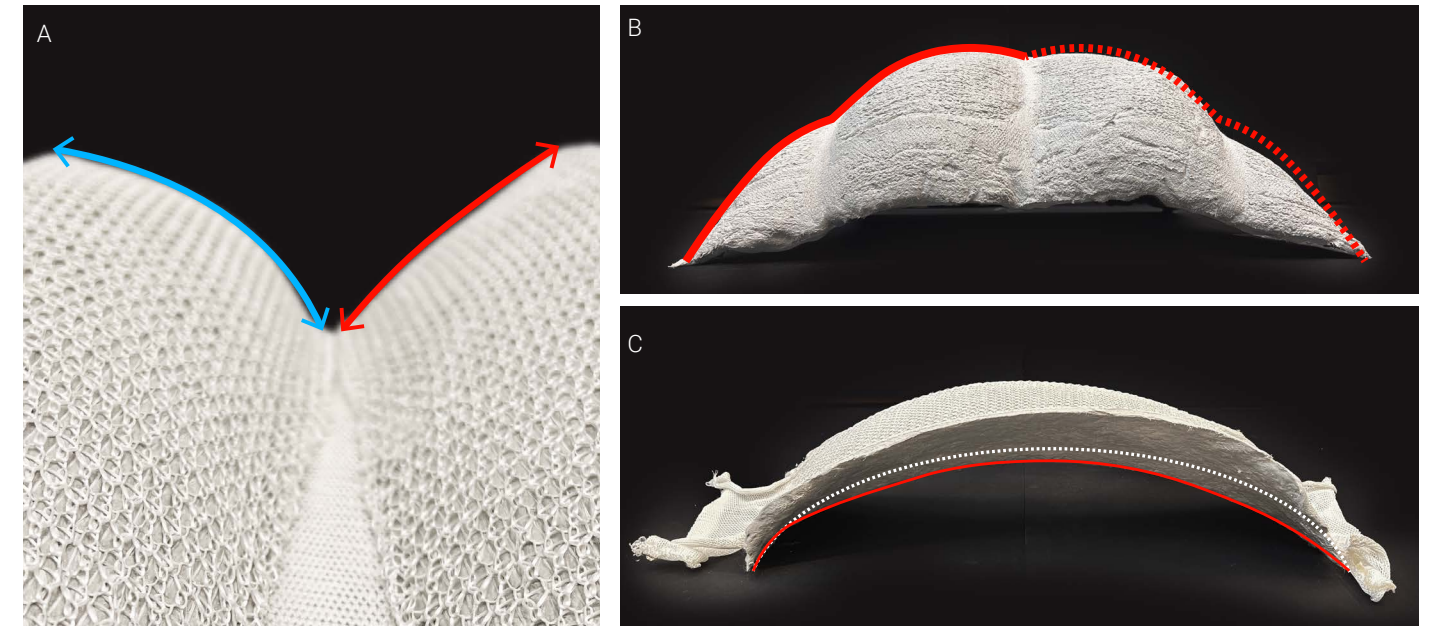
Figure 137. Examples of uneven deformations in the samples. (A) The Hourglass casting result showed different curvatures in its winged edges, (B) The Grid casting result did not show symmetrical deformation across its main axis, (C) The overall arching form of the Hourglass shape did not achieve a symmetric arch (white dashed line).

Future Research into Pattern Combinations

Despite these challenges, the potential for creating innovative architectural forms through pattern combinations remains. Future research should aim to address these limitations by automating transitions between patterns during generation, refining predictive models for more precise sizing, developing automated approaches to avoid uneven deformation, and by exploring more pattern combinations besides Cross Miss and Double Half Cardigan. By addressing these limitations, it would be possible to harness the full potential of CNC knitted flexible formwork in innovative architectural designs.

5.5 Imagining Future Applications

Adapting the Form to a Design

Any of the pattern combinations described in Section 5.3 could be adapted to the design of a building element. The high degree of customization and opportunities for variation provided by this technology present countless ways these forms could be calibrated, shaped, or combined. In this section, the casting result of the 4-Quadrant (Alternate Supports) pattern was selected for a basic design exploration. This exercise is meant to demonstrate both the exciting design potential and the significant construction challenges of CNC-knit flexible formwork technology.

Figure 138. The 4-Quadrant (Alt Supports) pattern was 3D scanned and parametrically rebuilt as a mesh in Grasshopper. This allowed for manipulation of the edge and center curve heights as shown in Figure 139.

It is relatively simple to imagine each of the pattern combinations scaled to the size of a free-standing, independent shell structure. While this is an exciting prospect, the feasibility of fabricating a shell of this scale using the methodology laid out in this thesis is questionable. First, scaling the overall dimension of a cast form exponentially increases the weight of the concrete, while the physical properties of a knit textile remain the same. This might cause unexpected deformations and make uniform deformation even harder to achieve. However, the more limiting factor of this methodology is the need to flip the cast forms after removal from the casting frame. Consequently, fabricating large shell structures with this method such as the form shown in Figure 139 would likely be impossible.
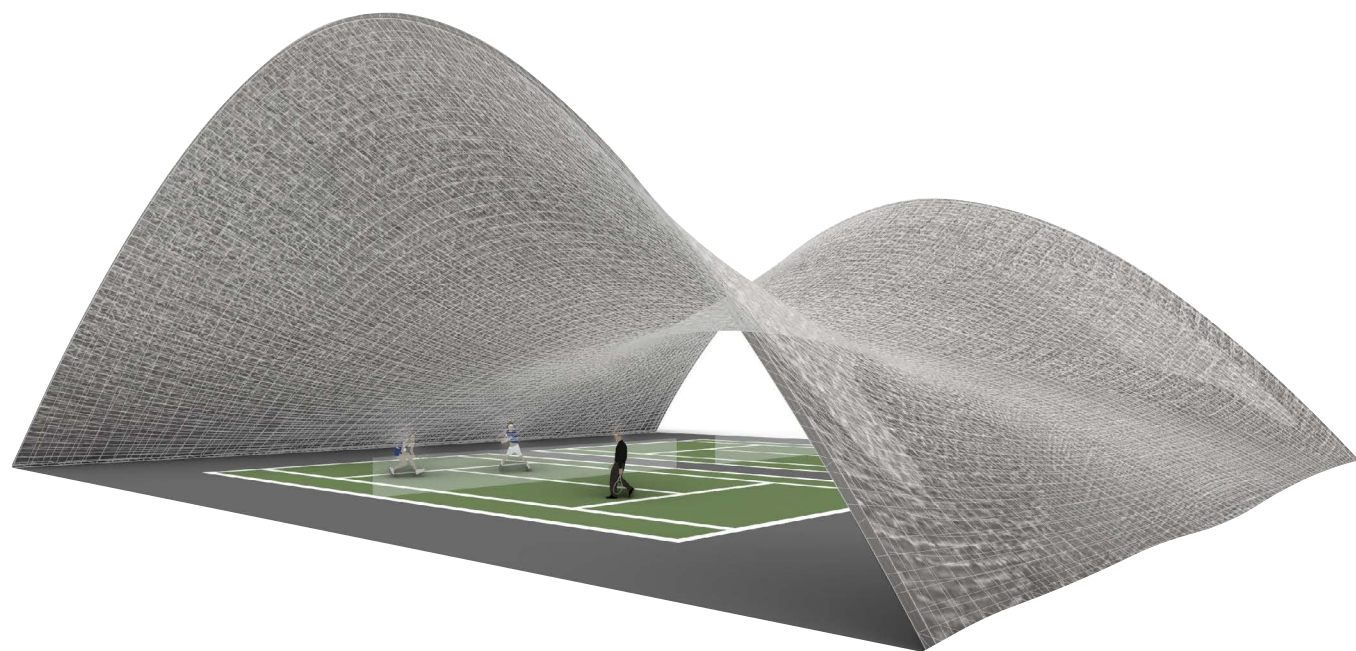
Figure 139. Hypothetical scaling up of the 4-Quadrant (Alt Supports) pattern to a stand-alone shell. While this is an exciting proposition, fabrication constraints would likely make this impossible to construct given the proposed methodology.

As this technology is clearly limited by size, a more realistic approach would consider each element as part of a repetitive system that makes up a larger structure. The 4-Quad (Alt Supports) pattern lends itself easily to a standalone covering supported at the two flat ends, or when aggregated in the X and Y direction, a barrel-vault ceiling punctuated by ovular openings.
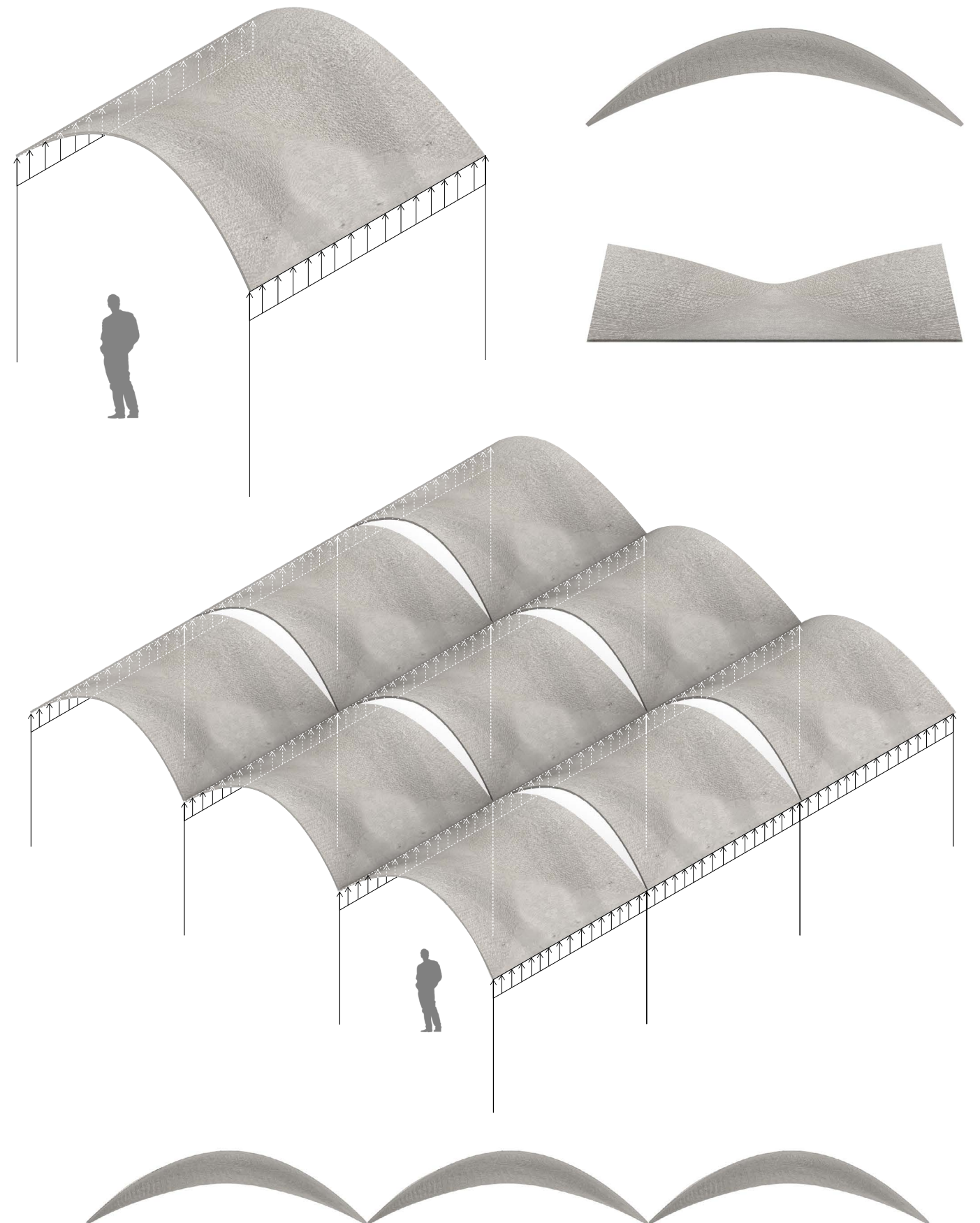
Figure 140. Aggregation option where the cast form is repeated in the X and Y direction to form a series of barrel vaults.

An alternative aggregation method, shown in Figure 141, could be to invert every other panel to form a corrugated roof structure. Although this would be more complicated to support than a simple barrel vault, it would allow for an increased cross section and function well as an outdoor shelter.

A key consideration of discrete-element systems is the connection strategy between elements. The conceptual proposals for roof structures shown in Figures140 and 141 would require a precise connection to resolve the diminishing intersection points the individual elements meet. While there are many ways to design this connection, a straightforward approach would integrate orthogonal supports at the two straight ends of the form. However, this would require some adjustments to the casting setup. Achieving exact replicability in multiple flexibly formed elements, especially those formed under their own self-weight, is likely impossible. That said, the precise integration of rigid formwork only where necessary could strategically negotiate this problem. This might be achieved in the process described in Figure 142.
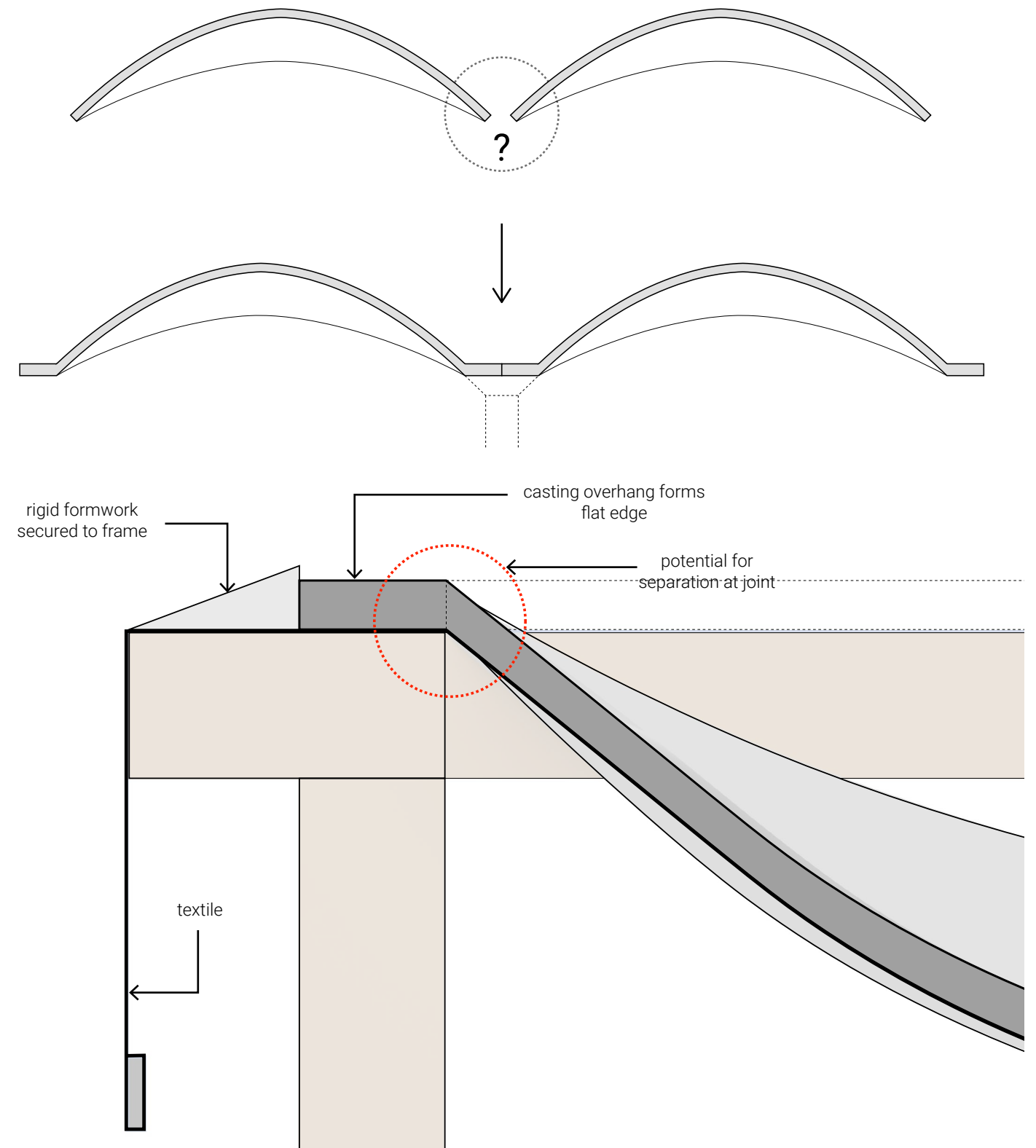
Figure 142. Proposed resolution of cast edges where rigid formwork is introduced in specific areas to ensure that the connections between the pieces are consistent. A hard edge is placed at the ends of the frame to create orthogonal tabs at either end. While this design has potential, some initial issues might involve separation between the rigid and flexible parts of the cast during deformation.

Figure 141. Aggregation option where every other cast form is inverted to form a corrugated roof shell.

Fabrication: Controlling Deformation, Connections, and Flipping the Cast Form

In the casting methodology described throughout this research, concrete is applied by hand and deformation is activated by manually removing a stabilizing plate. The small size of the samples also allows for manual inversion. At the scale of a building, casting errors would have greater consequences and therefore necessitates a more advanced setup. Besides achieving uniform deformation, the lifting, inversion, and transportation of the cast element is likely the most challenging aspect of this methodology. In response, the process described in Figure 143 proposes a strategy which combines lifting and inversion and eliminates the need for transportation to the construction site.
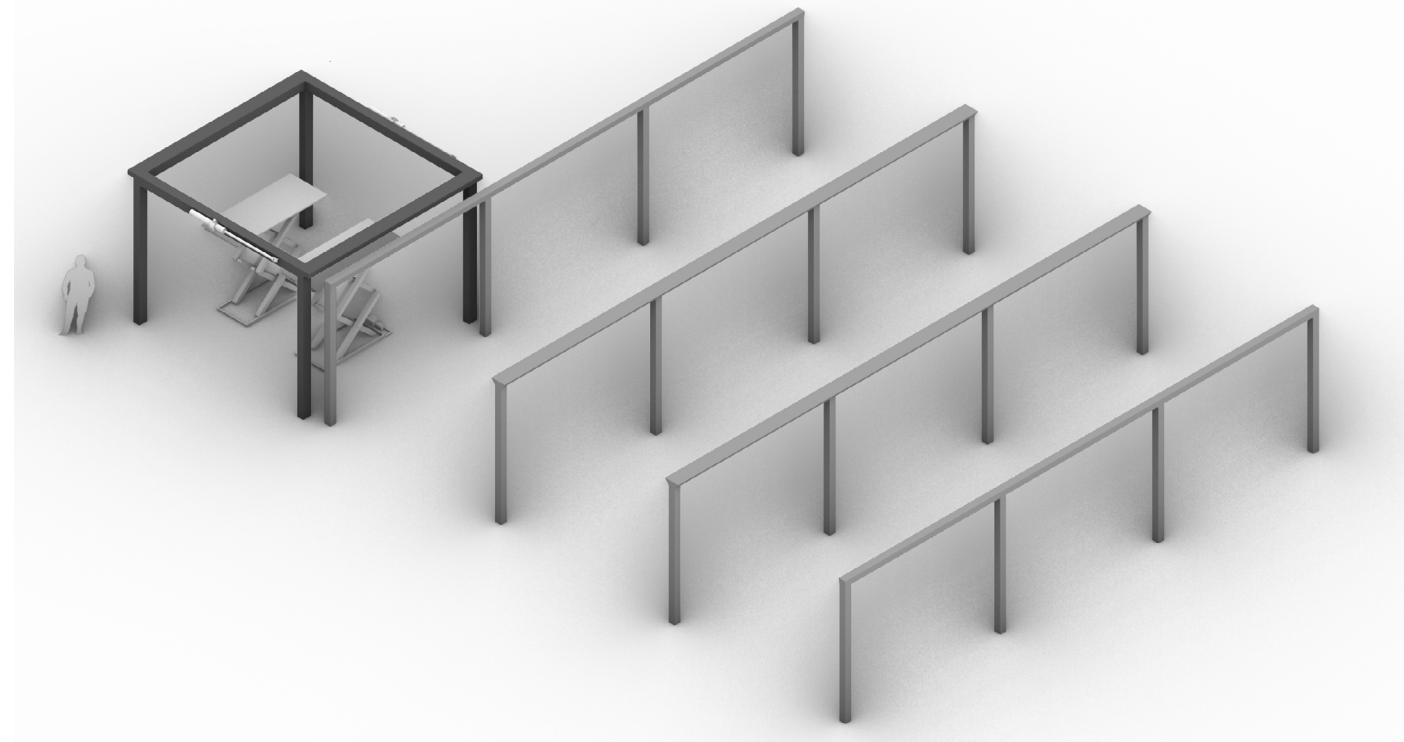
Figure 143. (A) A casting frame is erected next to the pre-fabricated column grid shown in the diagram. Each form is fabricated in the auxiliary frame and lifted onto the structural frame. This eliminates the need for packing or transportation.
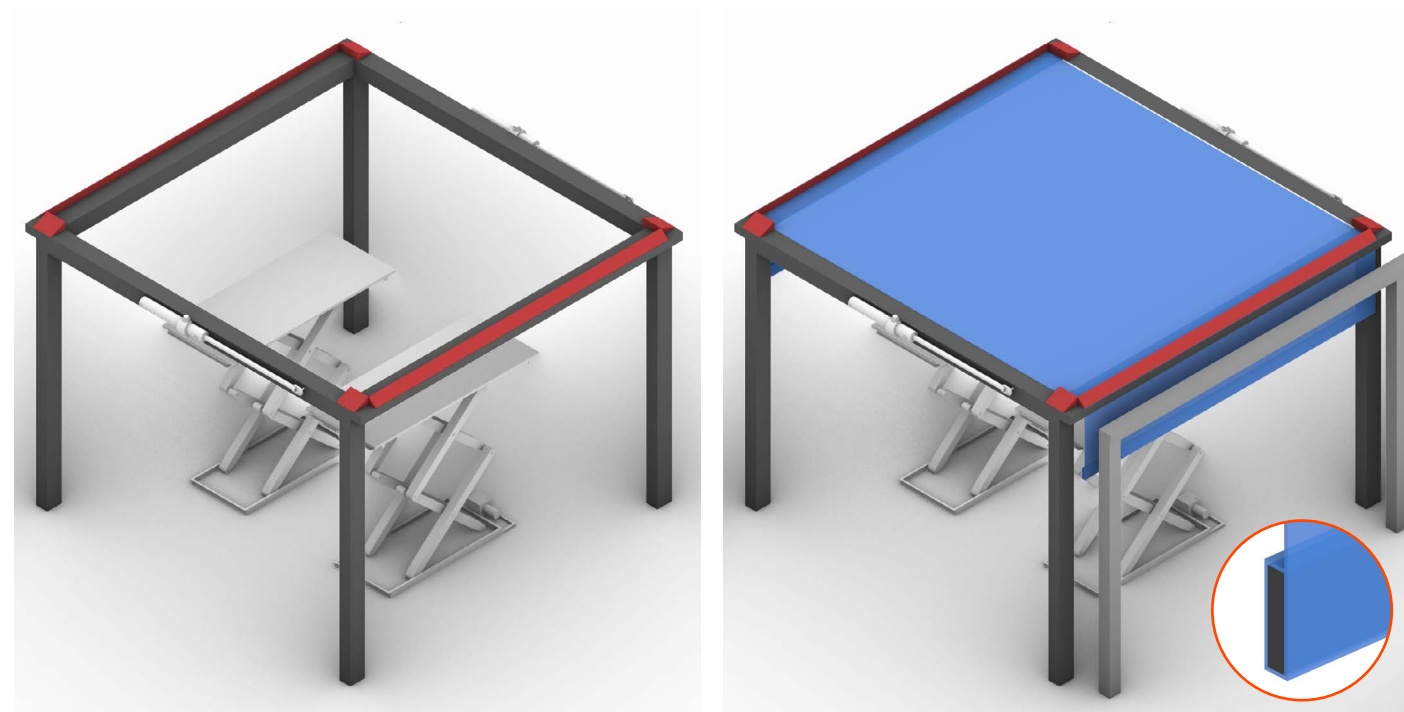
(B) Hydraulic lifts are placed under the frame to support even lowering of the stabilizing plate. The textile is hung over the frame and pre-tensioning by a weight bar encapsulated in a channel. Rigid formwork is placed as the edges of the frame.
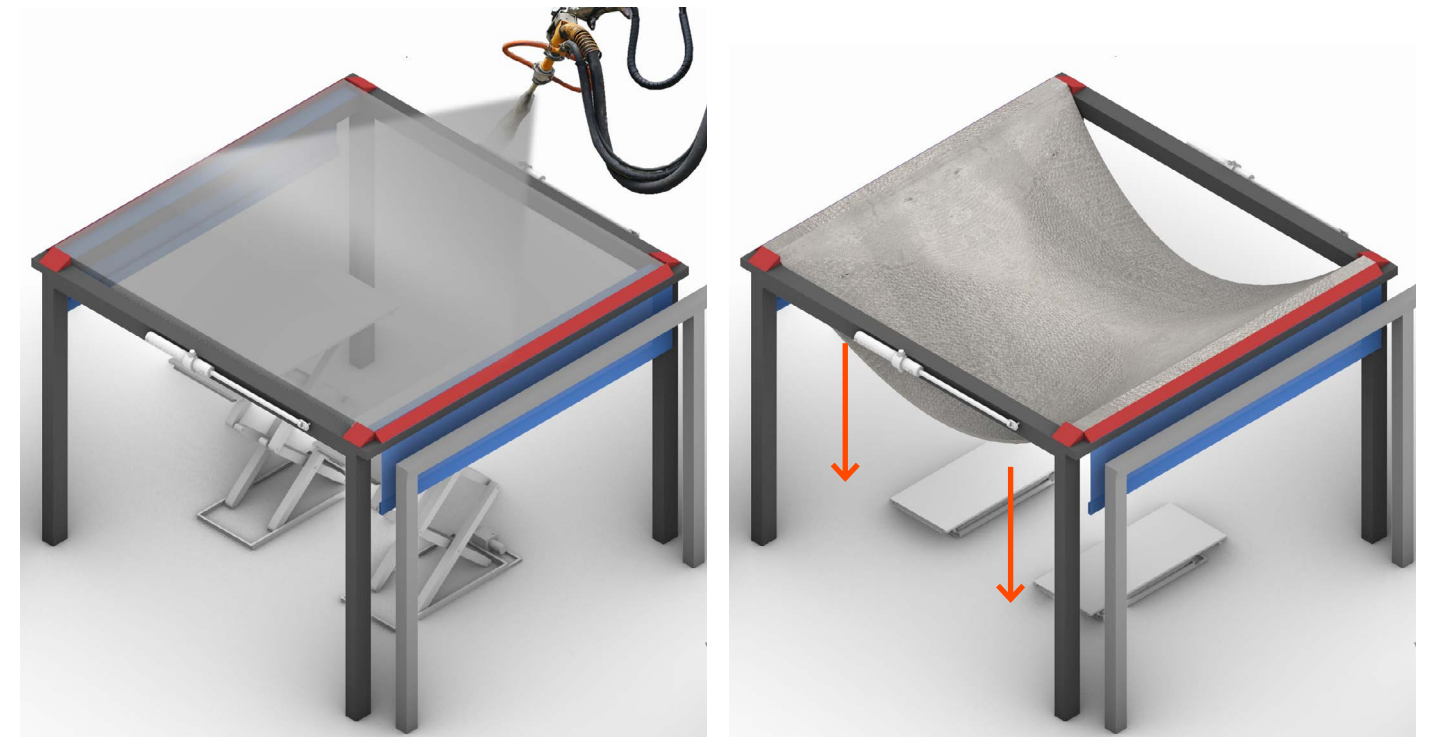
(C) An even layer of concrete is applied using a Shotcrete machine to ensure consistency. (D) The stabilizing panel is removed slowly by the hydraulic lifts and the textile deforms under the weight of the concrete.

(1)

(2)
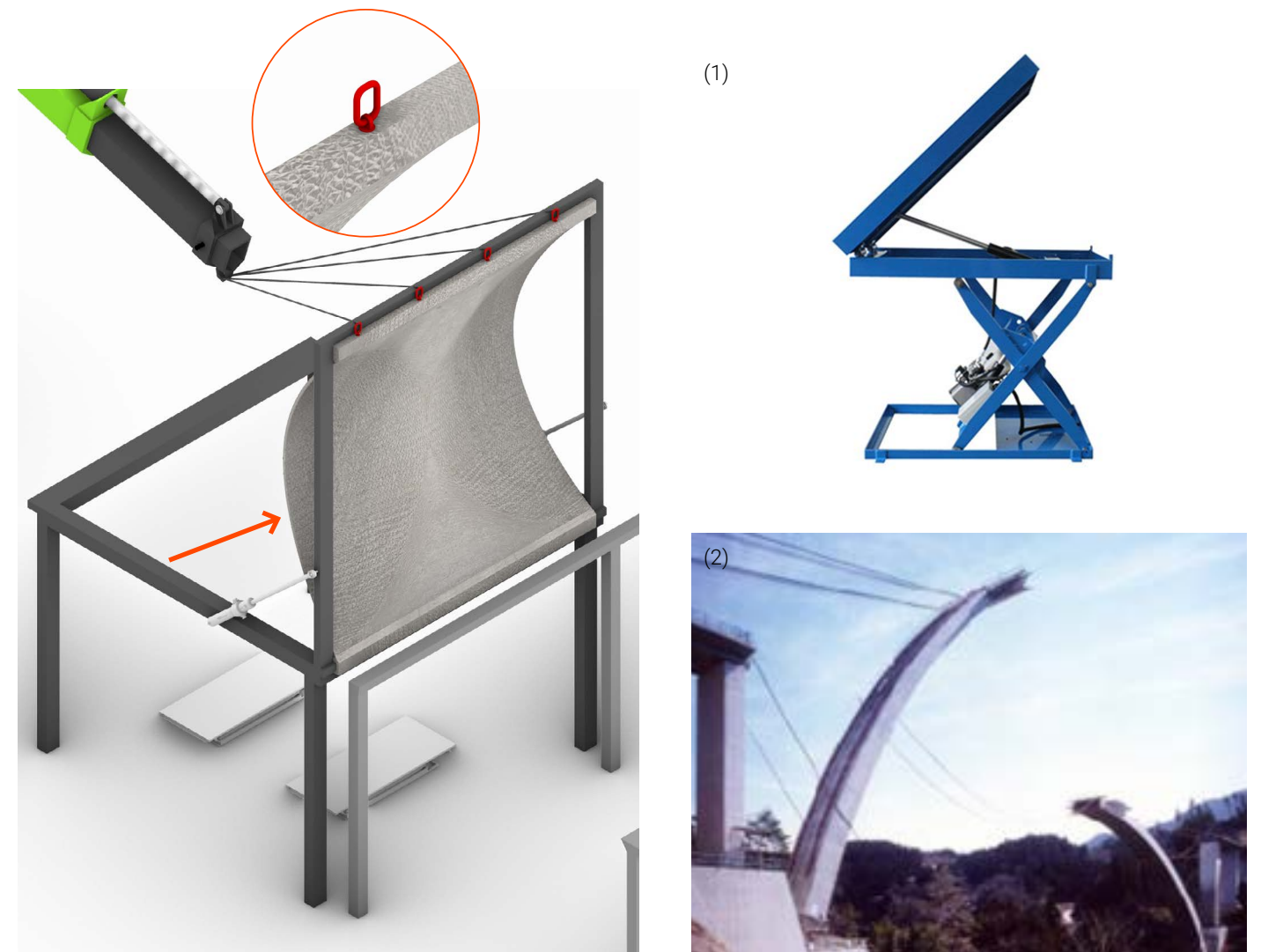
(E) The proposed system of lifting and inversion draws inspiration from two commonplace construction techniques: the flipping table and a lowering technique used mainly in bridge construction. The casting frame itself could be rotated by 90 degrees using hydraulic lifts on either end of the frame, and which point a crane would lower the piece by connecting to pre-cast anchors embedded during the casting process. (Image Sources: (1) Industries D. Labonte, (2) Oriental Shiraishi Corporation
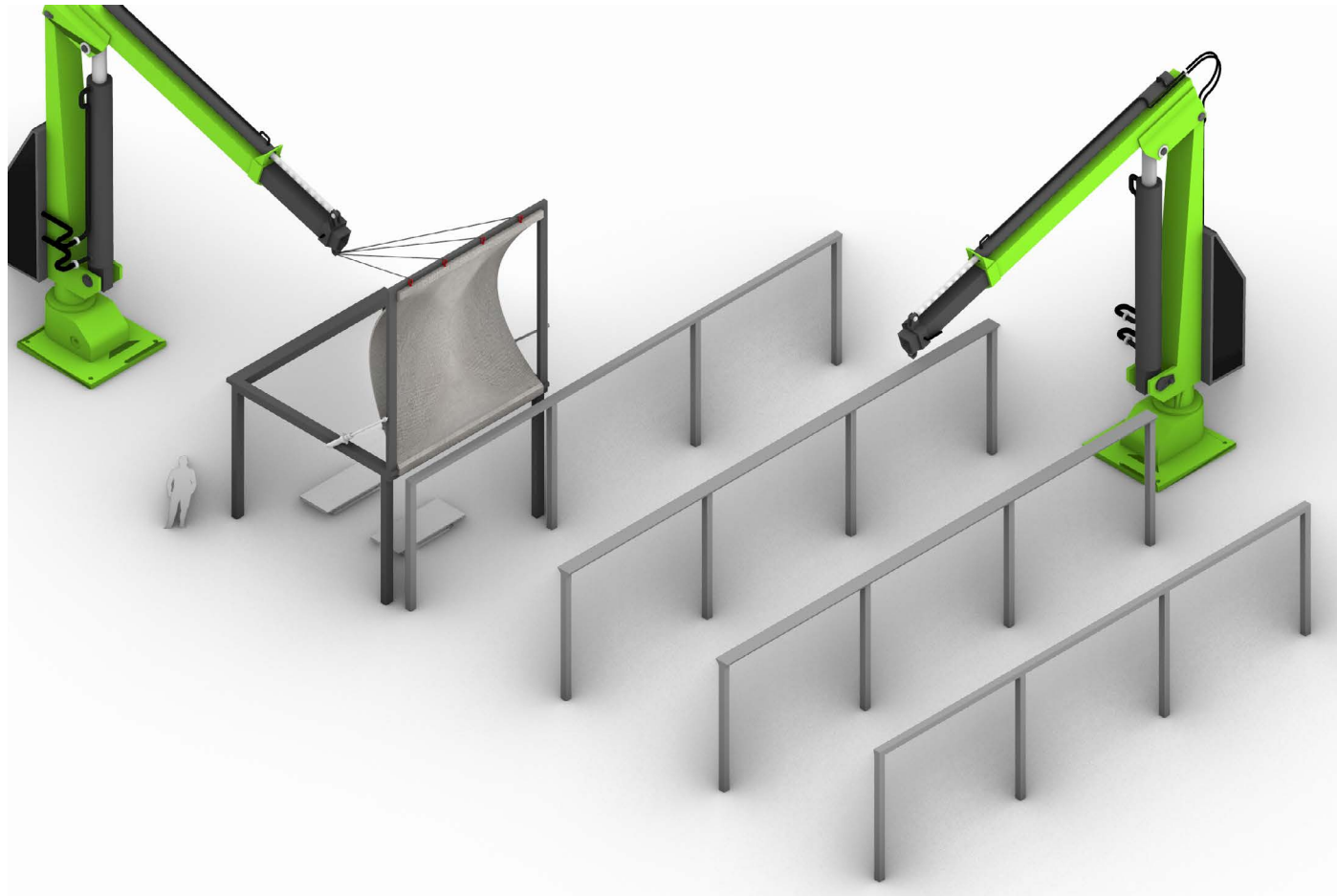
(F) A crane stabilizes the form at 90 degrees and prepares to lower it onto the structural frame.
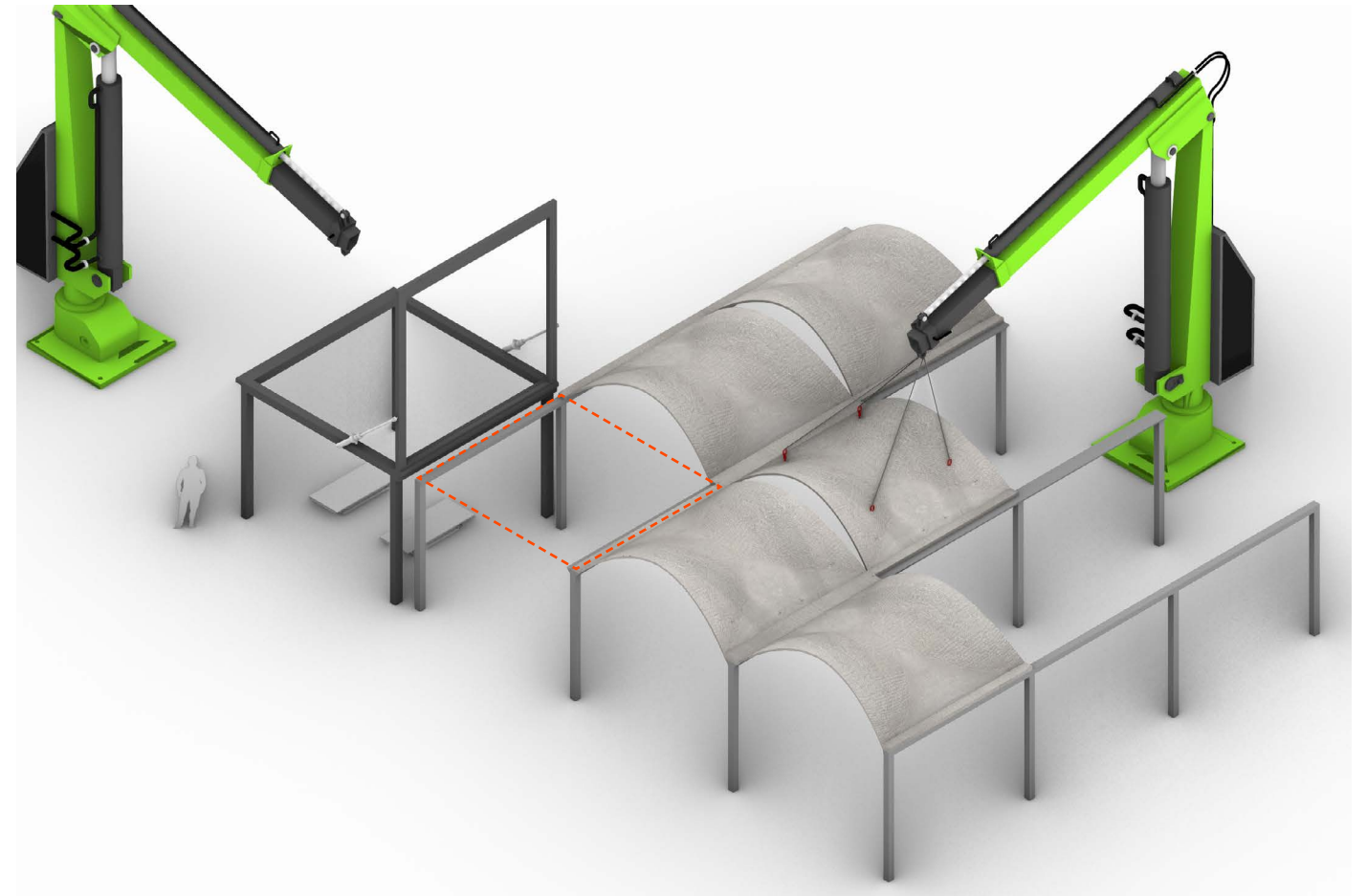
(H) The process of casting, rotating, and picking up each form continues.
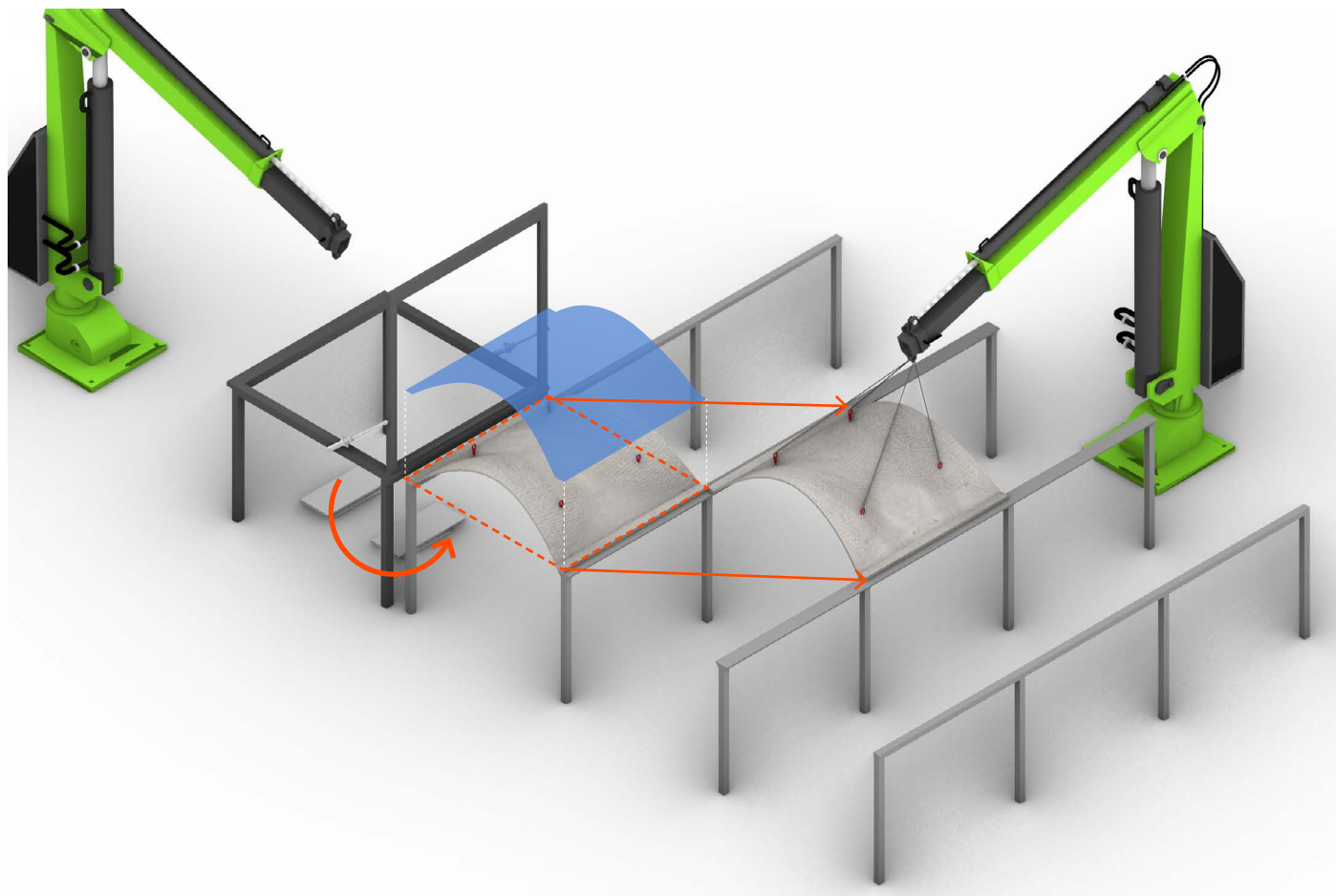
(G) The crane lowers the form onto the structural frame and the textile is removed. Additional lifting anchors are then installed which allows another crane to lift each form to its proper place within the frame. The corner of the structural grid closest to the casting frame acts as a pickup point for all cast forms.

(I) The completed roof shell structure.

6.0 Conclusion & Reflection

6.1 Research Goals and Method

The objective of this research is to develop a pattern-specific knowledge base that supports designers in fabricating new and innovative architectural forms with CNC-knitted flexible formwork. Through understanding the implications of pattern selection, flexible formwork designs can be more carefully calibrated to a specific outcome. Knitted textile formwork holds extraordinary potential to efficiently create complex forms, but it is highly unpredictable and often difficult to control. This research contributes to a greater understanding of the uncertain behavioral tendencies of knit textiles through the careful documentation and analysis of selected knit patterns.

The research process combined information-based and inspiration-based design research to answer the research questions and to demonstrate the potential of pattern combination. The investigation began with the development of a comprehensive pattern repository, followed by rigorous testing of these patterns under concrete loading to understand their deformation and resulting principal curvatures. Finally, the study examined the potential of combining different patterns to create complex and architecturally innovative forms. The sequential process followed in the thesis methodology where theoretical information was translated to physical prototyping was successful in generating the appropriate data for further analysis of the cast forms. The analysis method whereby weft and warp curvatures were compared by rise to span, general shape, surface area, and stress line distribution was also effective in revealing consistent differences in weft versus warp properties, as well as notable exceptions. Negotiation between the computer-based patterns and the physical prototypes played a significant role in the research approach. This revealed a basic truth about working with knitted textiles which is that, despite extensive theoretical planning, calibration through physical prototyping is an essential part of the process to achieve the desired result. The work presented in Chapter 5.0 shows that multiple versions of each pattern combination were knitted before the desired effect was achieved, even after the comprehensive calibration of knit patterns in the previous chapters. The process and methodology, while successful in answering the research questions, showed that there is still much to be learned about how knitted textiles behave, especially when multiple patterns are combined.

6.2 Key Findings

Fundamentally, the research shows that pattern selection is likely the most important factor in designing CNC-knitted flexible formwork. The deformation analysis revealed that different patterns exhibit quite distinct behaviors under hydrostatic loading which influence the resulting concrete forms' structural and aesthetic properties. Specifically, most patterns deformed more in the warp direction than in the weft, with some notable exceptions. The warp curvatures were generally more gradual and even, while the weft curvatures exhibited more irregular forms, also with some exceptions. This understanding of directional deformation is crucial for predicting and controlling the final shapes of concrete elements.

The research and process also highlighted the challenges of controlling deformation, in that precise calibration is required to manage the behavior of the textile formwork. This was particularly evident in the manual experiments conducted, which underscored the need for more advanced or automated setups to achieve consistent results. While studying the behavior of one pattern was relatively straightforward, the combination of knit patterns proved to be more complex. Once combined, patterns cannot be expected to behave as they did in isolation. This interplay between patterns can affect the overall behavior of the formwork in ways that are not yet fully understood in the context of this research. Further, the basic design exploration where a specific form was adapted to a building component sparked more questions about general feasibility. While the fabrication method described worked well in the context of small experiments, the process becomes more complicated when applied at a larger scale. Finding strategic ways to integrate rigid formwork elements which can facilitate easy aggregation and reconcile irregularities along with methods of lifting and inverting the hardened form are all key considerations.

Another significant finding is the potential for CNC-knit textiles to be reused. In this research, reuse potential was defined by the degree of adhesion of the textile to the concrete which was qualified by timing each removal process and noting if significant damage occurred. Unsurprisingly, textiles with a more raised or defined surface texture adhered more to the concrete and sustained more damage. This suggests that these particular patterns might be more suitable in situations where removal does not occur, and strong adhesion is desired. The impact of repetitive use on a single textile to create multiple identical shapes was not addressed in this research but is a valuable avenue of investigation for future research.

6.3 Reflection and Future Research

By answering the research questions outlined in Section 1.3, this study has shown that CNC-knit textile formwork has the potential to transform concrete construction and shift the industry toward lighter and more innovative structures. The flexibility in pattern design enables the creation of customized and efficient building elements that can be calibrated to follow the natural force flows of the material, simultaneously reducing material waste and construction cost. The exploration of pattern combinations has created new possibilities for architectural innovation and complex, expressive forms that were previously unattainable with traditional formwork methods.

Contributions

This research makes contributions to the field of architectural engineering and construction technology. First, it advances the understanding of how CNC-knit textile patterns behave under hydrostatic loading, providing a foundational knowledge base for future studies on flexible formwork. The deformation analysis, particularly the differentiation between warp and weft behaviors, adds to the theoretical framework necessary for designing precise and effective textile formwork. Further, the phased research approach, encompassing the pattern repository development, concrete tests, and pattern combination experiments, provides a comprehensive and replicable strategy for future work by others. The methodology also highlights the interdisciplinary nature of this research which combines textile engineering, material science, and architectural design. This approach encourages collaboration across these fields, fostering innovation and providing opportunities for practical applications.

Limitations

Despite its exciting potential, CNC-knit formwork has some limitations. First, the process of designing knit patterns for a specific situation is not yet automated and requires significant time and iterations. Currently, specialized knowledge is required to design and fabricate CNC-knit textiles, which makes integrating this technology into mainstream construction practices difficult. Further, traditional building practices are deeply ingrained in the construction industry, which is often resistant to change. This makes it challenging to introduce and standardize new technologies such as CNC-knit flexible formwork. Control and calibration of knit textile formwork presents another major challenge when considering elements of a larger scale. Advanced and automated processes are required to control deformation precisely, but even with these technologies, a degree of unpredictability remains. In a situation where multiple identical elements are required, for example a series of beams, exact replication would be difficult and maybe impossible. Therefore, this technology is more suited to cases where some variation is acceptable, but the constant issue of unpredictability remains the key limitation for CNC-knit formwork.

The fabrication challenges outlined in Section 5.5 also present a significant limitation for this technology. The reality of scaling this fabrication process presents major issues like resolving the connections between flexibly formed elements as well as inverting the cast forms. While the process shown in Section 5.3 presents some initial ideas, much more work is required to develop this methodology for actual applications.

Future Work

The insights gained from this research lay the groundwork for the continued development of this transformative technology in the architectural, engineering, and construction fields. Future work could focus on optimizing knitting patterns for specific structural requirements, enhancing the understanding of per-stitch behavior within a single pattern, investigating the reuse potential of the textiles, or exploring larger scale applications. Addressing the identified limitations will also be crucial for advancing the adoption of this technology and realizing its full potential to support sustainable, efficient, and innovative building practices.

CNC-knitted flexible formwork represents a significant advancement in the architecture and construction industries. This research provides a robust foundation for future exploration and development of this efficient, sustainable, and exciting building technology.

References

About Cement & Concrete. (2023). GCCA. https://gccassociation.org/our-story-cement-and-concrete/

Acharekar, A., & Savoikar, P. (2019). *FABRIC AS FLEXIBLE FORMWORK*. https://ukiericoncretecongress.com/ucc2019/files/Proceedings/pdf/UCC-2019-303.pdf

Ahlquist, S. (2016). Sensory material architectures: Concepts and methodologies for spatial tectonics and tactile responsivity in knitted textile hybrid structures. *International Journal of Architectural Computing*, *14*(1), 63–82. https://doi.org/10.1177/1478077115625525

Anishchenko, M. (2023). *Performance-based design of bespoke non-uniformly knitted textiles for architectural projects*. https://doi.org/10.13140/RG.2.2.34985.16488

Araya, R. (2014, July 31). Fabric Formed Slab cantilever—Arro Design. *Arro Design - Architecture and Construction*. https://www.arrodesign.com/projects/fabric-formed-slab-cantilever/

Block, P., Schlueter, A., Veenendaal, D., Bakker, J., Begle, M., Hischier, I., Hofer, J., Jayathissa, P., Maxwell, I., Echenagucia, T. M., Nagy, Z., Pigram, D., Svetozarevic, B., Torsing, R., Verbeek, J., Willmann, A., & Lydon, G. P. (2017). NEST HiLo: Investigating lightweight construction and adaptive energy systems. *Journal of Building Engineering*, *12*, 332–341. https://doi.org/10.1016/j.jobe.2017.06.013

Block, P., Van Mele, T., Rippmann, M., Ranaudo, F., Calvo Barentin, C., & Paulson, N. (2020). Redefining structural art: Strategies, necessities and opportunities. *The Structural Engineer*, *98*(1), 66–72. https://doi.org/10.56330/UJFI2777

C.A.S.T. (2010). *Precast slab New Women's Hospital C.A.S.T. - ronniearaya*. https://ronniearaya.com/Precast-slab-New-Women-s-Hospital-C-A-S-T

Engel, H. (1967). *Tragsysteme (Structure Systems)* (6th ed.). Hatje Cantz Verlag.

Faber, C. (1963). *Candela / The Shell Builder*. Reinhold Publishing Corporation.

Farrar, D., Forbes, D. J. C., & Marriott, H. T. G. (1937). *Construction of roofs, floors, ceilings, and the like* (United States Patent US2096629A). https://patents.google.com/patent/US2096629A/en?oq=US2096629

Fearn, R. (2024). *Fast-Tube Overview*. https://www.fab-form.com/fast-tube/fast-tubeOverview.php

Fisac, S. M. (1975). *Flexible Form für Beton oder Gußmörtel* (Germany Patent DE2404852A1). https://patents.google.com/patent/DE2404852A1/en?assignee=fisac+miguel&oq=fisac+miguel

Flatt, R. J., Roussel, N., & Cheeseman, C. R. (2012). Concrete: An eco material that needs to be improved. *Journal of the European Ceramic Society*, *32*(11), 2787–2798. https://doi.org/10.1016/j.jeurceramsoc.2011.11.012

Hawkins, W. J., Herrmann, M., Ibell, T. J., Kromoser, B., Michaelski, A., Orr, J. J., Pedreschi, R., Pronk, A., Schipper, H. R., Shepherd, P., Veenendaal, D., Wansdronk, R., & West, M. (2016). Flexible formwork technologies – a state of the art review. *Structural Concrete*, *17*(6), 911–935. https://doi.org/10.1002/suco.201600117

Jiang, Y., Zegard, T., Baker, W., & Paulino, G. (2018). Form-finding of grid-shells using the ground structure and potential energy methods: A comparative study and assessment. *Structural and Multidisciplinary Optimization*, *57*. https://doi.org/10.1007/s00158-017-1804-3

Kariouh, A. (2023). *Flexibly formed concrete: Exploiting the deformation behaviour of weft-knitted formworks caused by concrete pressure*. https://repository.tudelft.nl/islandora/object/uuid%3A66c69dfc-fc8a-4d2c-bf45-f74fbc60eaa0

Kersavage, J. A. (1975). *Method for constructing a tensile-stress structure and resultant structures* (United States Patent US3927496A). https://patents.google.com/patent/US3927496A/en?oq=US3927496

Kreiger, E. L., Kreiger, M. A., & Case, M. P. (2019). Development of the construction processes for reinforced additively constructed concrete. *Additive Manufacturing*, *28*, 39–49. https://doi.org/10.1016/j.addma.2019.02.015

Lee, M., Mata-Falcón, J., & Kaufmann, W. (2021). Load-deformation behaviour of weft-knitted textile reinforced concrete in uniaxial tension. *Materials and Structures*, *54*(6), 210. https://doi.org/10.1617/s11527-021-01797-5

Lee, M., Mata-Falcón, J., Popescu, M., & Kaufmann, W. (2023). Thin-walled concrete beams with stay-in-place flexible formworks and integrated textile shear reinforcement. *Structural Concrete*, *24*(4), 4960–4977. https://doi.org/10.1002/suco.202200648

Lilienthal, L. W. G. (1899). *Fireproof Ceiling* (United States Patent US619769A). https://patents.google.com/patent/US619769A/en?oq=US619769

Liu, Y., Hua, C., & Yuan, P. (2021). *Knitted Composites Tower: Design Research for Knitted Fabric Reinforced Composites Based on Advanced Knitting Technology*. https://doi.org/10.52842/conf.caadria.2020.1.055

Milne, K., Pedreschi, R., & Richardson, L. (2015, August 16). Tailoring Fabric Formwork. *Proceedings of the International Society of Flexible Formwork Symposium*.

Nader, G., Han Quek, Y., Chia, P. Z., Weeger, O., & Yeung, S.-K. (2021). KnitKit: A flexible system for machine knitting of customizable textiles. *ACM Transactions on Graphics*. https://doi.org/10.1145/3450626.3459790

Nawab, Y., Hamdani, S. T. A., & Khubab, S. (2017). *Structural Textile Design: Interlacing and Interlooping*. CRC Press, Taylor & Francis Group.

Nervi, P. L. (1956). *Structures*. F.W. Dodge Corporation.

NG, T. Y., Ahlquist, S., Filipov, E. T., & Weisman, T. (2023). *Knit formwork casting* (United States Patent US20230399777A1). https://patents.google.com/patent/US20230399777A1/en

Orr, J. J., Darby, A., Ibell, T., & Evernden, M. (2014). Design methods for flexibly formed concrete beams. *Proceedings of the Institution of Civil Engineers - Structures and Buildings*, *167*(11), 654–666. https://doi.org/10.1680/stbu.13.00061

Owen-Burge, C. (2022, March 30). *Cement and Concrete industry launches Net Zero Accelerators at MENA Climate Week*. Climate Champions. https://climatechampions.unfccc.int/cement-and-concrete-industry-launches-net-zero-accelerators-across-the-world/

Parker, S. A. (1971). *Concrete building* (United States Patent US3619959A). https://patents.google.com/patent/US3619959A/en?oq=US3619959

Pedreschi, R. (2011). The use of fabrics as formwork for concrete structures and elements. *Textiles Composites and Inflatable Structures V: Proceedings of the V International Conference on Textile Composites and Inflatable Structures*, 421–431. https://upcommons.upc.edu/bitstream/handle/2117/186224/MEMBRANES_2011-38_The%20use%20of%20fabrics%20as%20formworks.pdf

Popescu, M. A. (2019). *KnitCrete: Stay-in-place knitted formworks for complex concrete structures* [Doctoral Thesis, ETH Zurich]. https://doi.org/10.3929/ethz-b-000408640

Popescu, M., Reiter, L., Liew, A., Van Mele, T., Flatt, R. J., & Block, P. (2018a). Building in Concrete with an Ultra-lightweight Knitted Stay-in-place Formwork: Prototype of a Concrete Shell Bridge. *Structures*, *14*, 322–332. https://doi.org/10.1016/j.istruc.2018.03.001

Popescu, M., Reiter, L., Liew, A., Van Mele, T., Flatt, R. J., & Block, P. (2018b). Building in Concrete with an Ultra-lightweight Knitted Stay-in-place Formwork: Prototype of a Concrete Shell Bridge. *Structures*, *14*, 322–332. https://doi.org/10.1016/j.istruc.2018.03.001

Popescu, M., Rippmann, M., Liew, A., Reiter, L., Flatt, R. J., Van Mele, T., & Block, P. (2021). Structural design, digital fabrication and construction of the cable-net and knitted formwork of the KnitCandela concrete shell. *Structures*, *31*, 1287–1299. https://doi.org/10.1016/j.istruc.2020.02.013

Popescu, M., Rippmann, M., Van Mele, T., & Block, P. (2020). *KnitCandela—Challenging the construction, logistics, waste and economy of the concrete-shell formworks*. 194–201. https://doi.org/10.14324/111.9781787358119

Rolex Learning Center | SANAA. (n.d.). Archello. Retrieved 12 January 2024, from https://archello.com/project/rolex-learning-center-2

Sanders, E. (2005). *Information, Inspiration and Cocreation*.

Scheder-Bieschin, L., Bodea, S., Popescu, M., Mele, T., & Block, P. (2023). A bending-active gridshell as falsework and integrated reinforcement for a ribbed concrete shell with textile shuttering: Design, engineering, and construction of KnitNervi. *Structures*, *57*, 105058. https://doi.org/10.1016/j.istruc.2023.105058

Scheder-Bieschin, L., Bodea, S., Popescu, M., Van Mele, T., & Block, P. (2023). A bending-active gridshell as falsework and integrated reinforcement for a ribbed concrete shell with textile shuttering: Design, engineering, and construction of KnitNervi. *Structures*, *57*, 105058. https://doi.org/10.1016/j.istruc.2023.105058

Stappers, P., & Giaccardi, E. (2014). *Research through Design*. Interaction Design Foundation - IxDF. https://www.interaction-design.org/literature/book/the-encyclopedia-of-human-computer-interaction-2nd-ed/research-through-design

Tamke, M., Sinke Baranovskaya, Y., Monteiro, F., Lienhard, J., La Magna, R., & Ramsgaard Thomsen, M. (2020). Computational knit – design and fabrication systems for textile structures with customised and graded CNC knitted fabrics. *Architectural Engineering and Design Management*, *17*(3–4), 175–195. https://doi.org/10.1080/17452007.2020.1747386

Tamke, M., Šinke, Y., Deleuran, A., Monteiro, F., Fangueiro, R., Stranghöner, N., Uhlemann, J., Schmeck, M., Gengnagel, C., & Thomsen, M. (2016). *Bespoke materials for bespoke textile architecture*.

The Project Gutenberg eBook of Ten Books on Architecture, by Vitruvius. (n.d.). Retrieved 15 January 2024, from https://www.gutenberg.org/files/20239/20239-h/20239-h.htm

Thomsen, M., & Hicks, T. (2008). *To Knit a Wall, knit as matrix for composite materials for architecture* (p. 115).

Thomsen, M. R., Tamke, M., Deleuran, A. H., Tinning, I. K. F., Evers, H. L., Gengnagel, C., & Schmeck, M. (2015). Hybrid Tower, Designing Soft Structures. In M. R. Thomsen, M. Tamke, C. Gengnagel, B. Faircloth, & F. Scheurer (Eds.), *Modelling Behaviour: Design Modelling Symposium 2015* (pp. 87–99). Springer International Publishing. https://doi.org/10.1007/978-3-319-24208-8_8

United Nations Environment Programme. (2022). 2022 Global Status Report for Buildings and Construction. *UNEP - UN Environment Programme*. http://www.unep.org/resources/publication/2022-global-status-report-buildings-and-construction

Veenendaal, D., West, M., & Block, P. (2011). History and overview of fabric formwork: Using fabrics for concrete casting. *Structural Concrete*, *12*(3), 164–177. https://doi.org/10.1002/suco.201100014

Waller, J. H. W., & Aston, A. C. (1953). Corrugated concrete shell roofs. *Proceedings of the Institution of Civil Engineers*, *2*(4), 153–182. https://doi.org/10.1680/ipeds.1953.12308

Warrenne, W. J. H. (1934). *Method of building with cementitious material applied to vegetable fabrics* (United States Patent US1955716A). https://patents.google.com/patent/US1955716A/en?oq=US1955716

Warrenne, W. J. H. (1952). *Method of molding in situ concrete arched structures* (United States Patent US2616149A). https://patents.google.com/patent/US2616149A/en?oq=US2616149

West, M. (2017). *The Fabric Formwork Book: Methods for Building New Architectural and Structural Forms in Concrete*. Routledge.